Investigations into the effect of nucleoside modifications on the physicochemical properties and biological function of DNA and RNA

Dissertation
zur Erlangen des Grades

„Doktor der Naturwissenschaften“

im Promotionsfach Pharmazie

am Fachbereich Chemie, Pharmazie und Geowissenschaften
der Johannes Gutenberg-Universität
in Mainz

vorgelegt von Olwen Charlotte Domingo
geb. in Mossel Bay, Südafrika

Mainz, den 04. September 2013

Dekan:

1. Berichterstatter:

2. Berichterstatter:

Tag der mündliche Prüfung: 18.10.2013

I Corinthians 10:31

Whatever you do, do it all to the glory of God.

Acknowledgements

Abstract

This thesis explores the effect of chemical nucleoside modification on the physicochemical and biological properties of nucleic acids. Positional alteration on the Watson-Crick edge of purines and pyrimidines, the "C-H" edge of pyrimidines, as well as both the Hoogsteen and sugar edges of purines were attempted by means of copper catalyzed azide-alkyne cycloaddition. For this purpose, nucleic acid building blocks carrying terminal alkynes were synthesized and introduced into oligonucleotides by solid-phase oligonucleotide chemistry.

Of particular interest was the effect of nucleoside modification on hydrogen bond formation with complementary nucleosides. The attachment of propargyl functionalities onto the N^2 of guanosine and the N^4 of 5-methylcytosine, respectively, followed by incorporation of the modified analogs into oligonucleotides, was successfully achieved. Temperature dependent UV-absorption melting measurements with duplexes formed between modified oligonucleotides and a variety of complementary strands resulted in melting temperatures for the respective duplexes. As a result, the effect that both the nature and the site of nucleoside modification have on base pairing properties could thus be assisted.

To further explore the enzymatic recognition of chemically modified nucleosides, the oligonucleotide containing the N^2-modified guanosine derivative on the 5'-end, which was clicked to a fluorescent dye, was subjected to knockdown analyses of the eGFP reporter gene in the presence of increasing concentrations of siRNA duplexes. From these dose-dependent experiments, a clear effect of 5'-labeling on the knockdown efficiency could be seen. In contrast, 3'-labeling was found to be relatively insignificant.

Zusammenfassung

Derivatisierungen von Nukleinsäuren haben deutliche Effekte auf deren Strukturen und Funktionen. Diese Arbeit befasst sich mit der Untersuchung der Auswirkung chemischer Modifikationen von Basen auf die physikochemischen und biologischen Eigenschaften von DNA und RNA. Insbesondere wurden eine positionsspezifische Derivatisierungen der Watson-Crick-Edge von Purinen und Pyrimidinen, der „C-H"-Edge von Pyrimidinen, sowie der Hoogsteen- und der Sugar-Edge von Purinen durchgeführt. Terminale Alkine wurden an verschiedenen Positionen der Nukleoside eingeführt, um CuAAC-Reaktionen zu ermöglichen. Der Effekt von Nukleosidmodifikationen auf die Wasserstoffbrückenbildung zu komplementären Nukleosiden wurde betrachtet. Ein Propargylrest wurde am N^2 von Guanosin bzw. N^4 von 5-Methylcytosin eingebracht und die modifizierten Basen nachfolgend in Oligonukleotidsynthesen verwandt. Der Einfluss der Guanosinmodifikation am 5'-Ende eines siRNA-Strangs, sowie des Cytosinderivats an verschiedenen Positionen eines DNA-Stranges wurde hinsichtlich der Basenpaarungseigenschaften evaluiert. Schmelzpunkte von Duplexen mit verschiedenen komplementären Strängen haben gezeigt, dass die Guanosinmodifikation am 5'-Ende keinen deutlichen Einfluss auf Thermostabiliät des Duplexes hat. Dagegen hat die Anwesenheit der Methylgruppe an Position fünf des Cytidinderivats einen signifikanten Einfluss auf dessen Basenpaarungsverhalten, auch wenn die eigentliche Modifikation sich an Position vier befindet.

Zur Eruierung der enzymatischen Erkennung chemisch modifizierter Nukleoside wurde zusätzlich ein Oligonukleotid, welches das N^2-modifizierte Guanosinderivat am 5'-Ende enthält und mit einem Fluoreszenzfarbstoff markiert wurde, einer Knockdown-Analyse bzgl. des eGFP–Reportergens unterzogen. Basierend auf diesen Experimenten konnte bei der 5'-Markierung, im Gegensatz zur 3'-Markierung ein deutlicher Effekt auf die IC_{50}-Werte festgestellt werden.

Table of contents

List of figures

List of tables

List of schemes

1. Introduction

Enzymatic modification of nucleotides is ubiquitous as well as crucial in all domains of life, mainly due to the variety of functions that modified nucleotides can perform. Especially in the field of RNA[1], much effort has thus far been invested into the discovery and further analysis of naturally occurring nucleotide modifications. These structural deviations from the four main canonical bases, *i.e.* adenosine, guanosine, cytidine and uridine/thymidine, are mainly a result of post-transcriptional processing[2] and are known to influence both nucleic acid structure and function.

Simple methylations are the most common example of post-transcriptional nucleoside modifications[3]. The presence of a methyl group, especially on hydrogen bond donor and/or acceptor sites, is expected to have a dramatic impact on the hydrogen bonding properties of the given base. In some cases, post-transcriptional methylation is a natural mechanism in certain organisms to prevent undesirable interactions with the given base[4]. Depending on its position and orientation, methylation may also lead to additional stabilization of the tertiary structure as a result of base-stacking interactions of the hydrophobic methyl group[5].

Similarly, whether intentional or unintentional, non-natural modification of nucleosides should also have a clear impact on the physicochemical properties of nucleobases. In recent times, the combination of organic chemistry with nucleoside biology has found a variety of applications in molecular biology and therapeutic sciences. Unless the purpose of modification was to alter chemical interactions between nucleosides, the effect of such modifications to the RNA or DNA, particularly its influence on Watson-Crick base pairing, should preferably be kept to a minimum.

1.1 The chemical modification of DNA and RNA

The major progress in the chemical synthesis of RNA and DNA over the last decade now enables the incorporation of modifications into oligonucleotides in a site-specific manner, whether directly at the base, on the sugar, at the end of the chain, or at the phosphate backbone. As a result, such chemical modification of RNA and DNA can feature as tool in a variety of biochemical procedures. In addition to enhancing certain standard biological properties, such as hybridization or cellular uptake, chemical modifications can also serve to introduce a completely new physical and/or chemical property to the nucleic acid. The introduction of fluorescent probes and other reporter groups for studying structure-function relationships, the attachment of chemically reactive groups, such as for the formation of

disulfide bridges for locking RNA molecules in a particular tertiary fold and groups promoting intermolecular interactions (*e.g.* biotin and streptavidin) are but a few examples of the latter[6].

There are currently two well-known and more commonly used methods for the introduction of such modifications to oligonucleotides. The phosphoramidite method, which utilizes the chemical synthesis of modified building blocks, involves the direct and site-specific incorporation of the desired modification during oligonucleotide synthesis *via* a solid support based procedure. On the other hand, the convertible nucleoside approach allows the substitution of a common modification in the oligonucleotide with the desired functionality, following the solid phase synthesis by means of the phosphoramidite method. The convertible nucleoside approach has the advantage that a single oligonucleotide synthesis with the convertible nucleoside may eventually result in differently labeled oligonucleotides, since the substituting group can be chosen from a number of possibilities, such as a variety of alkylamines.

A more recent technique, the functionality transfer by oligodeoxynucleotides (FTODN), allows the site-specific and cytosine- and guanosine-selective modification of RNA molecules. By means of the formation of a DNA/RNA hybrid between the target RNA and a previously functionalized DNA strand, a base-to-base transfer of the functionality from the DNA strand is made possible by the close proximity between the two molecules.

1.1.1 The phosphoramidite method in solid phase oligonucleotide synthesis (SPOS)

A nucleoside phosphoramidite is an orthogonally protected derivative of a DNA or RNA monomer used in the chemical synthesis of short DNA and/or RNA chains. First introduced by Beaucage and Caruthers in 1981[7], phosphoramidite chemistry has come a long way since. A number of major developments over the years made it possible to complete an oligonucleotide synthesis within only a few hours. This is indeed a major leap from the pioneering work done by Khorana in 1979[8], where a few years were invested into the total synthesis of a particular DNA sequence.

A typical DNA phosphoramidite contains an acid labile protecting moiety on its 5'-hydroxyl group (*e.g.* 4,4'-dimethoxytrityl/DMT), a phosphite triester on the 3'-hydroxyl (*e.g.* 2-cyanoethyl-*N*,*N*-diisopropylphosphoramidite/CEP) and, in the case of adenine, cytosine and guanine, a base sensitive protection group (*e.g.* benzoyl/Bz, isobutyryl, phenoxyacetyl/pac[9] or 4-*t*-butylphenoxyacetyl/tac[10]) on any of the exocyclic amines (see figure 1.1 A). Because of the sensitivity of the phosphite group in the phosphoramidite to oxidation, it is typical to

introduce the trityl group first and to perform the phosphitylation step last. The primary 5'OH has a higher nucleophilicity than the 3'OH and because the trityl group is introduced first, it is rather contained on the 5'-position of the nucleoside. As a result, the chemical synthesis of oligonucleotides thus proceeds in the direction of the 5'-end. The general procedure towards the synthesis of phosphoramidites will be discussed in detail in chapter 3 (see 3.3.2).

1.1.1.1 General procedures for the chemical synthesis of DNA, using phosphoramidite chemistry

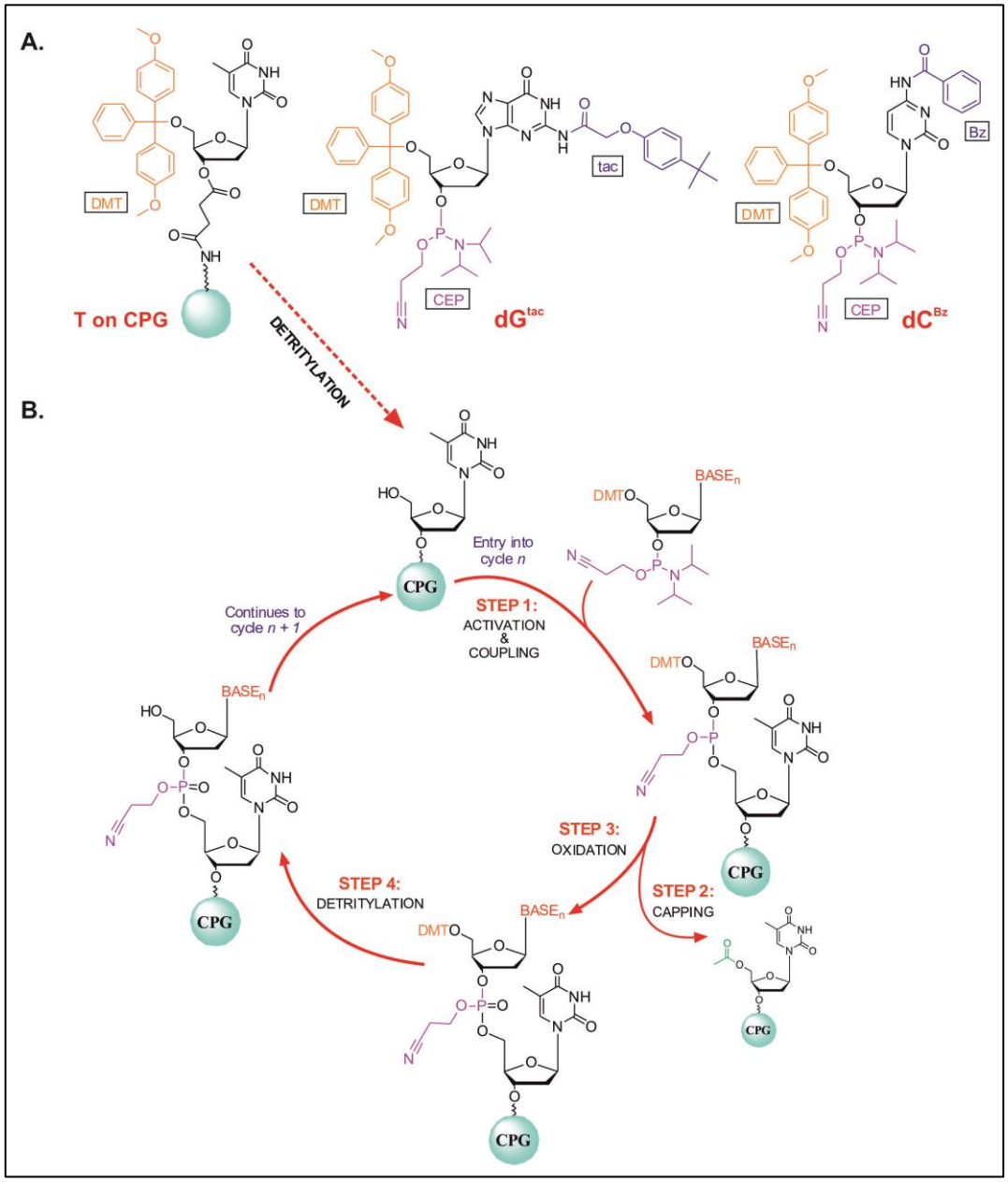

Fig. 1.1 A. 5'-*O*-Dimethoxytritylthymidine attached to a solid support *via* a succinyl linkage (T on CPG), 5'-*O*-dimethoxytrityl-N^2-(*tert*butylphenoxyacetyl)-3'-*O*-(β-cyanoethyl-*N,N*-diisopropylphosphoramidite)deoxyguanosine (dG^{tac}) and 5'-*O*-dimethoxytrityl-N^4-benzoyl-3'-*O*-(β-cyanoethyl-*N,N*-diisopropylphosphoramidite)deoxycytidine (dC^{Bz}) as examples of typical building blocks for solid phase oligonucleotide synthesis. **B.** Solid phase oligonucleotide synthesis cycle.

As the name indicates, the solid phase synthesis of oligonucleotides takes place on a solid support, to which the 3'-terminal nucleoside is attached, usually *via* a long succinyl linkage to allow accessibility of the attached molecules during the synthesis procedure. The development of solid supports over the years made it possible to render this synthesis procedure as automated. Among the most commonly used solid supports for oligonucleotide synthesis is controlled pore glass (CPG).

With the very first base attached to the CPG *via* its 3'-OH, the synthesis thus starts from the 3'-end and, in contrast to biological nucleic acid syntheses, proceeds in the direction of the 5'-terminus. The chain is elongated one nucleotide per cycle, starting with the removal of the DMT-group from the first base (also known as detritylation) in the presence of either dichloro- or trichloroacetic acid in a non-aqueous solvent, such as. dichloromethane. The DMT cation has an absorption maximum at 498 nm, which can be used to monitor the coupling efficiency of each step. Prior to coupling with the following base, an activation step occurs, during which the incoming phosphoramidite is mixed with a coupling reagent. Conventional 1*H*-tetrazole[7], or 5-(benzylthio)-1*H*-tetrazole (BTT) in case of steric hindrances[11], can be used as mild proton donor in the activation step. After the coupling step, the free 5'OH of all uncoupled chains are reacted with acetic anhydride/2,6-lutidine and *N*-methylimidazole in THF (see figure 1.1 B - capping). This acetylation step is to minimize the formation of shorter, unwanted chains during subsequent SPOS cycles.

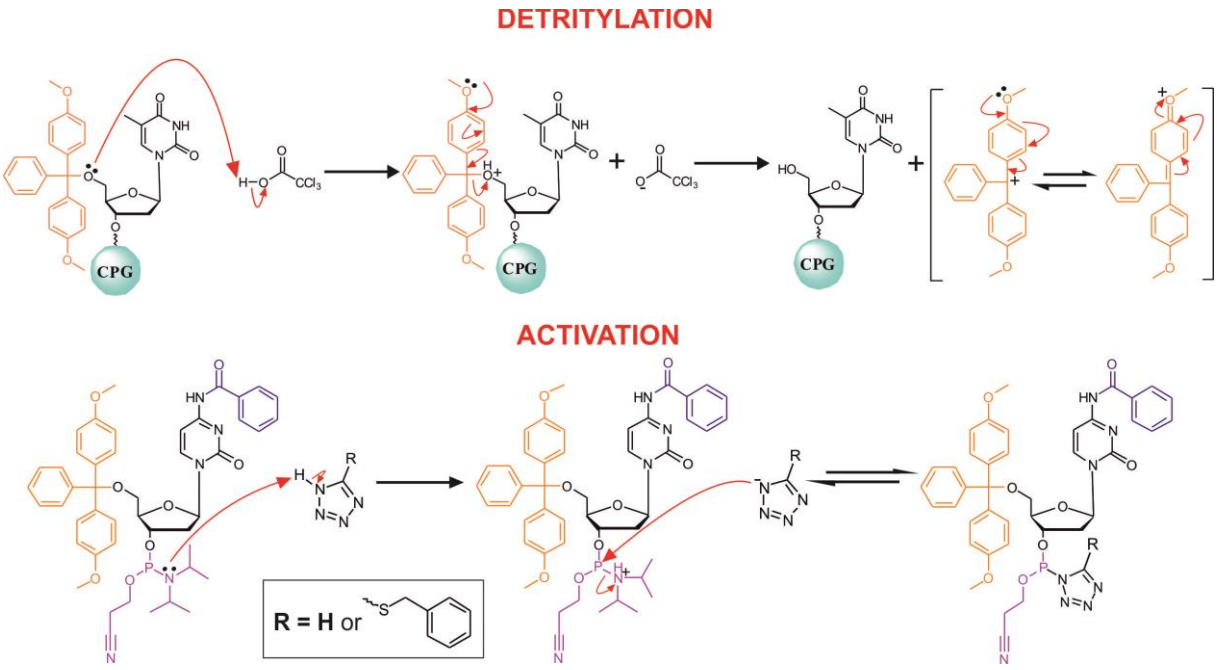

Fig. 1.2 Reaction mechanisms involved in the detritylation and activation steps of the SPOS.

In 1984 Sinha *et al.*[12] introduced the use of β-cyanoethyl groups for the protection of the phosphate as improvement in the phosphite triester approach, which was first introduced by Tener almost two decades earlier[13]. The activation of the β-cyanoethyl group is based on the ability of aminophosphines to be protonated in the presence of acidic species[14]. Important to consider, though, is that the acid should be weak enough, so as to not cause a premature cleavage of the 5'-*O*-dimethoxytrityl group. 1*H*-tetrazole fulfills this requirement. After activation and condensation with the incoming base, an oxidation step with iodine in THF/water is added to the cycle to generate the tetracoordinated internucleotide phosphotriester linkage. The liberated hydrogen iodide is neutralized by the addition of pyridine and 2,6-lutidine.

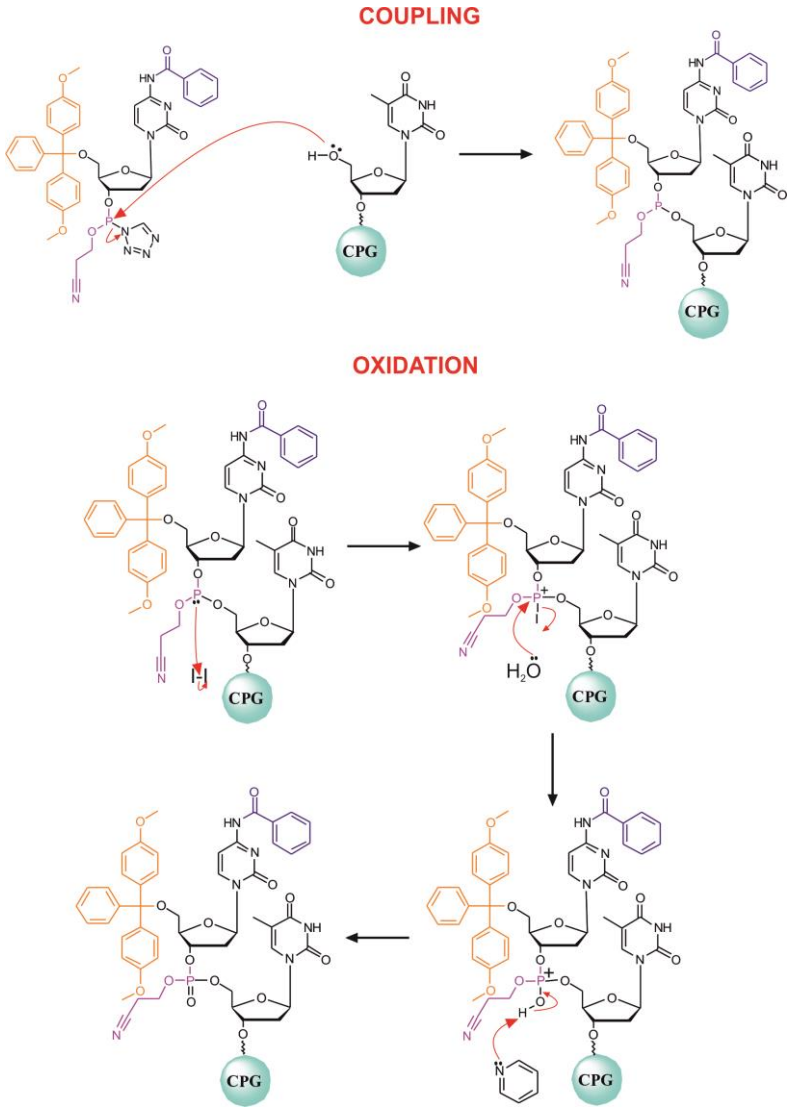

Fig. 1.3 Reaction mechanisms involved in the coupling and oxidation steps of the SPOS.

The synthesis cycle is repeated until the desired oligonucleotide length is achieved. The total yield of the synthesized strand is, of course, highly dependent on its length, as well as the

synthesis scale. Depending on the scale, a 20mer synthesis typically produces coupling yields around 99%. With an increase in oligonucleotide length, the yield automatically drops.
The 2-cyanoethyl group, which still remains intact after the oxidation step, is removed during the post-synthesis work-up of the oligonucleotide. In a one-step treatment of the synthesized oligonucleotide with ammonia or similar base at elevated temperatures, a β-elimination reaction for removal of the cyanoethyl, an *N*-deacylation for removal of the exocyclic amino protection groups, as well as cleavage of the oligonucleotide from the solid support takes place.

1.1.1.2 Solid phase oligonucleotide synthesis of RNA, using phosphoramidite chemistry

Apart from longer coupling times for RNA due to weaker accessibility of reactive groups, the synthesis procedure for oligoribonucleotides as compared to that for oligodeoxynucleotides is very similar. One of the few exceptions is that the extra hydroxyl group on the ribose of RNA requires an additional orthogonal protective group in their phosphoramidites. There are currently three major variants of solid-phase RNA synthesis chemistry, based on the choice of protective group on the ribose 2'OH. All three are ether protecting groups, of which the most typical variant is *tert*butyldimethylsilyl (TBDMS)[15]. One of the major drawbacks of the TBDMS-group is its tendency to migrate from the 2'-*O* to 3'-*O*-positions under weak basic conditions, leading to the potential formation of isomeric RNA that include 2'-5'-phosphodiester linkages during oligonucleotide synthesis. The development of a structurally related derivative with an acetal structure resulted in a more stable protecting group[16]. TOM, or triisopropylsilyloxymethyl, is also sterically less demanding than TBDMS and subsequent coupling yields are improved with TOM.
The third variant, *bis*(2-acetoxyethoxy)methyl (ACE), is a highly specialized method and is not compatible with normal DNA synthesizers[17]. Whereas the silyl based protection groups require different deprotection conditions from the 5'-*O*-dimethoxytrityl ether, ACE is also cleaved under mildly acidic conditions in the presence of water. This characteristic thus requires replacement of the commonly used DMT group for 5'-*O*-protection with a different temporary protection group and hence the inventors made use of a silyl ether instead for protecting the 5'-OH.
Especially in the case of TBDMS, the additional protection group on the 2'OH of ribonucleoside phosphoramidites may act as steric hindrance during the SPOS activation step. A slightly better hydrogen donating agent is thus required as activator of the phosphite group.

Froehler and Matteucci[18] evaluated the use of tetrazoles of enhanced acidity and discovered that 5-phenyltetrazoles can act as improved activators in phosphoramidite procedures. Currently, 5-(benzylthio)-1*H*-tetrazole (BTT) is the activator of choice during chemical RNA syntheses.

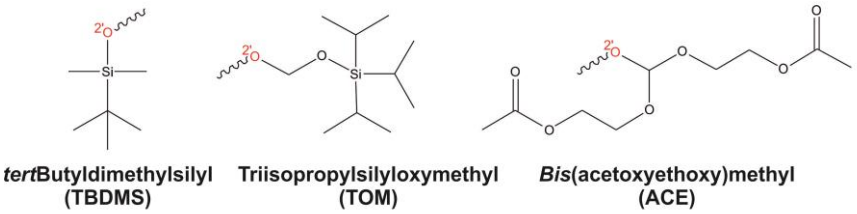

Fig. 1.4 Commonly used 2'*O*-protecing groups for the chemical synthesis of RNA.

Following the sequential assembly of the ribonucleosides on the solid support in an RNA synthesis, the strand is cleaved from the solid support, with a simultaneous cleavage of all exocyclic amino protection groups. The presence of the additional hydroxyl group on the RNA ribose causes it to be more prone to chain cleavage than its deoxyribonucleotide counterpart. The premature removal of the 2'-silyl group, which occurs during deprotection procedures usually applied to oligodeoxynucleotides, may lead to an attack of the liberated hydroxyl on the adjacent phosphodiester group and ultimately result in strand breakage. To prevent this, the use of concentrated aqueous ammonia for cleavage and deprotection of oligoribonucleotides has been replaced with anhydrous ethanolic ammonia[19,20] or methylamine[21]. Additionally, protection groups for exocyclic amines that are more prone to aminolysis, such as phenoxyacetal[16], dimethylformamidine[22] or 4-*t*-butylphenoxyacetyl [10], are used in combination with RNA phosphoramidites in order to reduce and minimize deprotection times after oligonucleotide synthesis.

A second deprotection step for RNA is necessary to remove the 2'-*O*-protection. Bu_4NF and *tris*(hydrofluoride) are typical desilylation reagents, whereas the orthoester 2'-*O*-ACE groups can be removed by incubating the solid support cleaved oligoribonucleotides in an acidic environment.

1.1.1.3 Post-synthetic purification of oligonucleotides

After cleavage from the solid support, the desired oligonucleotide is likely to be contaminated with protected or unprotected abortive sequences, as well as various reagents used during the course of the nucleobase or 2'OH deprotections. As a result, at least one purification step is required to obtain the desired oligonucleotide in good quality. Alcohol-based precipitation,

ion exchange and reversed phase chromatography, phase tags, as well as polyacrylamide gel electrophoresis are commonly used post-synthetic purification methods for oligonucleotides. These methods are usually used in combination with one another to obtain oligonucleotides of good purity[23–26].

(i) Reversed phase HPLC (RP-HPLC)

Reversed phase chromatography separates according to differences in lipophilicity and when eluting with a polar mobile phase, typically an ammonium acetate buffer combined with acetonitrile, the components should elute in order of increasing lipophilicity. As the mobile phase is made less polar, partition should no longer favor the stationary phase for the least lipophilic molecules. By gradually increasing the acetonitrile content, the polarity decreases and as a result, both separation time and band broadening can be minimized[27].

RP-HPLC is also one of the two most common techniques in the purification of synthetic oligonucleotides by means of HPLC[28]. Although the other variant, anion exchange chromatography, is more predictable, RP-HPLC has the advantage that the elution of the desired oligonucleotide can be adjusted by chemically changing its hydrophobicity. During the solid phase synthesis of oligonucleotides, one has the choice of either removing or retaining the DMT group of the very last monomer attached to the chain. By retaining the 5'-terminal trityl group a much better resolution of the full-length oligonucleotide from the shorter, non-DMT abortive products can be obtained due to its now higher affinity for the hydrophobic matrix. After this separation, a detritylation can be done of the HPLC purified oligonucleotide by means of acidification and the free trityl group, together with salts present can simply be removed by means of manual size exclusion chromatography, such as Nap columns.

This so-called DMT-ON technique works well for oligonucleotides of up to 20 bases long, but starts losing its applicability as soon as the oligonucleotide becomes lengthy or if additional internal lipophilic modifications are present. The possibility of premature cleavage of the DMT-group, even under neutral conditions, exists and may lead to lower synthesis yields.

(ii) Anion exchange HPLC

The affinity of the oligonucleotide for the solid phase in anion exchange chromatography is mainly based on differences in charge between the full-length oligonucleotide and smaller fragments. This gives the anion exchange chromatographic method an advantage to RP-HPLC

in that it allows the reliable separation of oligonucleotides according to their chain length. Anion exchange chromatography is thus the superior chromatographic method for separating longer oligonucleotides.

In this technique quaternary ammonium columns generally serve as stationary phase in combination with a salt-gradient solution (*e.g.* alkali perchlorate salts with acetonitrile) as elution mixture. Traces of heavy metals that could otherwise cause degradation of especially RNA can be removed by complex formation with EDTA.

(iii) Affinity tag chromatography

An approach comparable to the trityl-ON technique is followed during affinity phase tagging. The general strategy of phase tags is based on traditional solid phase oligonucleotide synthesis, followed by purification using a 5'-terminal phase tag. Only the full-length oligonucleotide would thus contain the tag and after the tagged oligonucleotide is attached to the solid support, the unwanted sequences are washed off and the pure oligonucleotide is cleaved from the solid support again. Among the affinity tags used for oligonucleotide purification are biotin, histidine tags and fluorous affinity tags as functional groups.

The high affinity between biotin and streptavidin has made this combination a common application in non-radioactive DNA/RNA labeling techniques[29]. For application in oligonucleotide purification, the biotin moiety can be introduced to the full-length oligonucleotide either directly during the solid phase oligonucleotide synthesis, using a biotinyl phosphoramidite[30–32], enzymatically with biotinylated nucleoside triphosphate analogs[33], or by means of post-synthetic modification techniques[34]. For release from the solid support, techniques, such as photocleavable biotin[35] or the introduction of chemically cleavable spacer arms[36–38] have been developed.

A slightly more complicated technique involves the initial use of a 5'-hexahistidine tag, which, after strand purification, is exchanged for a biotin group[39]. The histidine tag is attached to the oligonucleotide *via* its reaction with an aldehyde functionality, previously incorporated into the oligonucleotide during SPOS. Purification is made possible by the affinity of the tag for a nickel resin solid phase. This method has the disadvantage that it is only applicable to oligonucleotides where 5'-biotinylation is a requirement, such as in the use of biotin as affinity tag in biological experiments[40]. In addition to this, two purification steps are necessary before the final 5'-biotinylated oligonucleotide is obtained.

Finally, the use of fluorous affinity tags is based on their affinity for perfluorinated solvents or solid phases[41,42]. The advantage of this technique is that this type of reaction is strong and

well distinguishable from other affinity interactions, such as lipophilicity, and thus allows successful solid-phase extraction of the desired product.

The introduction of the tag takes place *via* the dimethoxytrityl functionality, attached to the 5'-most monomer. In order to ensure a minimal effect of the electronegative perfluoroalkyl group on the chemistry of the dimethoxytrityl group, the perfluoroalkyl group is insulated from the DMT nucleus *via* a propyl or ethyl group. Following SPOS and post-synthesis work-up, the crude mixture of oligonucleotides is subjected to a perfluorinated surface, to which only the fluorous-tagged molecules should attach. Release of the desired oligonucleotide is made possible by on-column detritylation with trifluoroacetic acid.

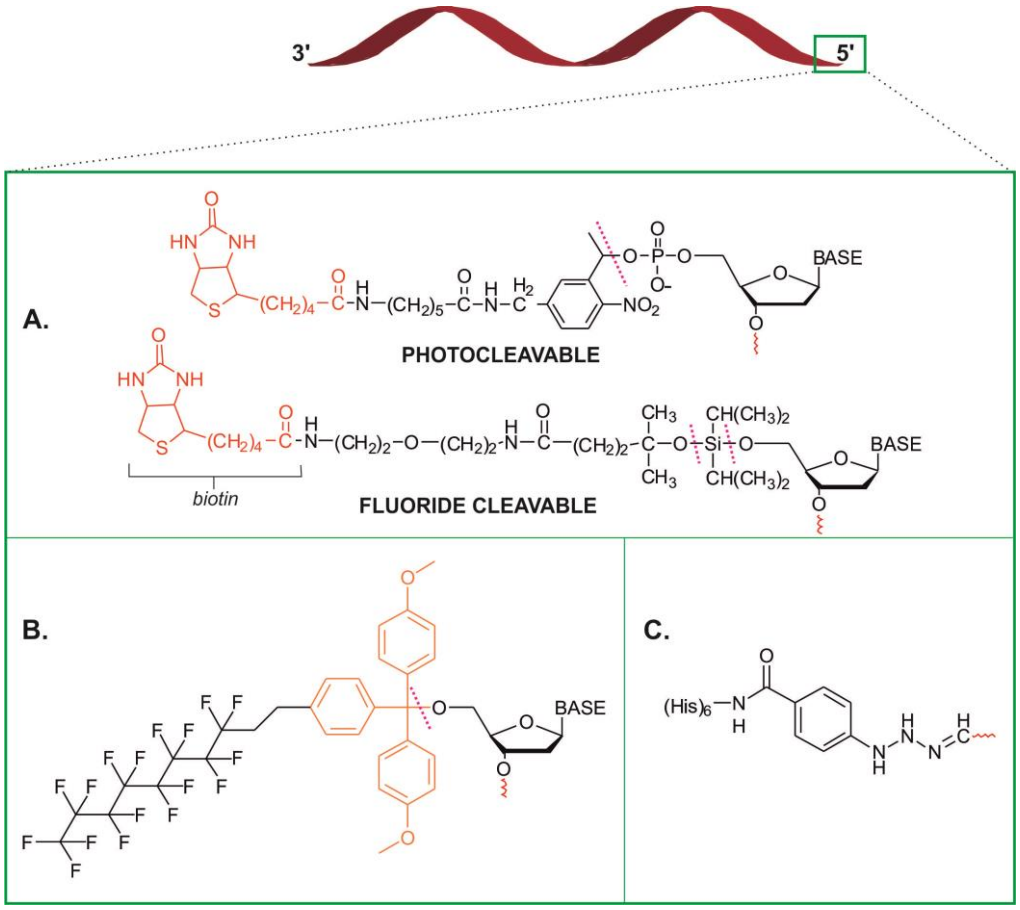

Fig. 1.5 Examples of affinity tags used in the purification of oligonucleotides. The pink lines show the positions of cleavage after purification: **A.** biotin, **B.** fluorous and **C.** histidine affinity tags.

Once again, premature detritylation may result in lower yields. However, due to the effect of the substituent, the fluoro-containing trityl group is removed slightly slower than the unfluorinated trityl group. As a result, premature detritylation occurs less frequently with these molecules[43].

(iv) Polyacrylamide gel electrophoresis (PAGE)

The differences in unit charge and molecular weight of oligonucleotides of different length results in their separation during denaturing gel electrophoresis. After the electrophoresis procedure the bands developed are visualized by means of UV shadowing and the bands of interest are excised. This is followed by elution of the product from the gel matrix and its precipitation, usually from ethanol. Especially the gel elution step usually leads to a significant loss in material and for this reason PAGE is usually the purification technique of choice only when product of high purity is a requirement for its further use.

1.2 Current techniques for the chemical modification of oligonucleotides

The chemical synthesis of nucleic acids, as described above, allows the incorporation of naturally occurring and artificial nucleobases, as well as a variety of labeling and other functional moieties, into an RNA and/or DNA strand. In contrast to biological synthesis procedures, the SPOS makes it possible to introduce these modifications at any particular, predetermined site within the strand. In addition to the synthetic duplication of naturally occurring nucleosides for the study of their effect on DNA and RNA structure and behavior[25,44,45], a number of motives exist for modifying these biological entities chemically. As an example, chemical alterations are brought about to nucleosides to purposefully alter the thermodynamic stability of duplexes formed[46,47]. Their biological stability, on the other hand, can also be altered, whether it is to make the strand resistant to or even a particular target for enzymes. Especially in therapeutic applications of RNA, as is the case with antisense nucleotide therapy, the ribose sugar or phosphate backbone is modified in such a way that the enzyme responsible for strand degradation does not recognize it as target, thus leading to RNA that is biologically stable for longer periods of time. In contrast, pre-fluorophores, *i.e.* molecules that require a particular chemical or biological reaction to become fluorescent, are an example of chemical entities attached to oligonucleotides designed as enzyme targets.
Other applications include the attachment of functionalized tethers to DNA and RNA to allow cross-linking with other biological entities[46,48], fluorescent labeling, especially for diagnostic applications[49], the attachment of affinity tags, such as biotin or antibodies[40] and a whole range of conjugation reactions with chemical units to change the biological behavior of the oligonucleotide, *e.g.* cellular uptake.

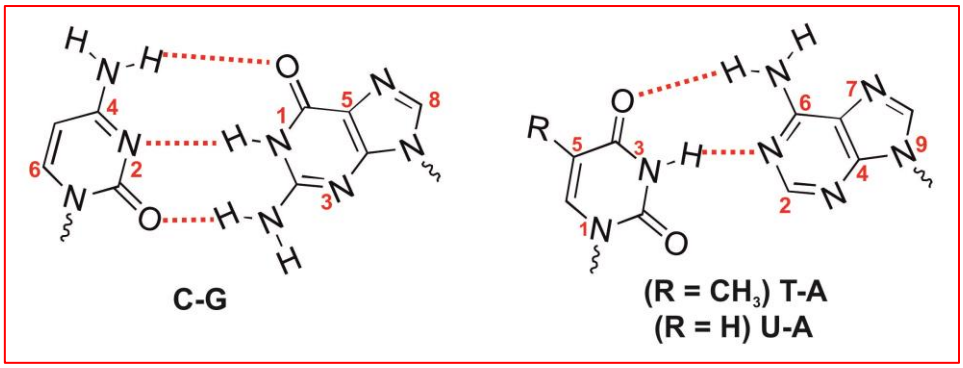

Fig. 1.6 Typical Watson-Crick base pairing between nucleic acid bases.

The exact position of the modification within the strand may vary, depending on its purpose. Typical positions for modifying oligonucleotides are their terminal ends, *i.e.* 5'- and/or 3'-terminal, the base itself, the sugar moiety and even the internucleotide linkages. Generally and with a few exceptions such as with the incorporation of locked or unlocked nucleic acids, modifications to the end and backbone of the biopolymer are achieved easier synthetically. The chemistry involved during base and ribose modifications is, however, more challenging. In addition to this, because the natural functionalities on the bases are responsible for interactions with other strands, careful consideration should be taken during attachment of modifications to the nucleobase, so as to not disrupt hydrogen bond formation.

As discussed earlier, there are mainly three methods available for chemically modifying synthesized oligonucleotide strands, among which the functionality transfer by oligodeoxynucleotides is the slightly more biological approach. The chemically more appealing method, however, involves the incorporation of the modification directly during strand synthesis. This method of functionalization will be discussed first.

1.2.1 Incorporation of modifications during oligonucleotide synthesis

The incorporation of modifications and conjugates directly during the oligonucleotide synthesis cycle is the most rigorous approach towards the chemical alteration of nucleic acid chains. With the exception of some internucleotide modifications, the modifier is attached directly onto the monomer during phosphoramidite synthesis, ensuring that modification at the position of choice takes place to completion. This is not always the case for post-synthetic labeling techniques. However, disadvantages associated with this method include the possible challenges posed during the synthesis and purification of the building blocks prior to oligonucleotide synthesis. Due to the reactivity of the functional groups on nucleosides, the preparation of modified monomers for incorporation into oligonucleotides usually requires the

attachment of temporary protection groups, followed by their deprotection after the modification has been introduced. Here, the manipulation of multiple protecting groups is usually necessary and does not yet even include the installation of the usual orthogonal protection groups for phosphoramidite synthesis. The phosphoramidite method will be discussed in detail in a later section.

In an attempt to circumvent these efforts and to avoid temporary protecting groups for the synthesis of the phosphoramidite of 5-hydroxymethyldeoxycytidine[50], Hansen *et al.*[44] considered an early introduction of a 5'-DMT protecting group. This step not only avoided the need for temporary 5'-protection, but also simplified the purification and identification of the now less polar product. Provided the chemistry of the modification to be introduced would not jeopardize the stability of the 5'-DMT group, this technique could be applied to other phosphoramidite syntheses of modified nucleosides to make them easier accessible.

As mentioned before, artificial changes can be made at any position within the nucleic acid chain, meaning either on the terminal ends, on the nucleobase, the phosphate backbone or the ribose sugar. Examples of ribose modifications incorporated directly during oligonucleotide synthesis include 2'*O*-alkyl[51,52], 2'-amino-2'-deoxy[53,54], 2'-deoxy-2'-fluoro[55], 2'-deoxy-2'-methylseleno[56] and locked[57] and unlocked nucleic acids[58] (LNAs and UNAs). LNAs are an example of artificial ribose modifications, in which the 2'-oxygen and the 4'-carbon atoms are linked *via* a methylene bridge. This locks the ribose in the structurally rigid C3'-*endo* conformation. In contrast, unlocked nucleic acids are highly flexible structures. This is due to the absence of the bond joining the 2'- and 3'-carbons on the sugar (see figure 1.7).

The most common practices in backbone modifications are the replacement or blockage of the negative charge on the oxygen atom. Not all of these modifications are, however, accessible *via* the standard phosphodiester oligonucleotide synthesis method. Among the phosphate containing internucleotide modifications are the methylphosphonates[59], the phosphotriesters[60,61], phosphorothioates[62,63], phosphoramidates[64–67] and boranophosphates[68].

The synthesis of phosphorothioates, in which the non-bridging oxygen of the phosphodiester is replaced with a sulfur atom, is pretty straightforward and is also applicable to normal phosphoramidite chemistry. The synthesis procedure simply involves the replacement of the normal iodine/H_2O oxidation step during the SPOS cycle with a sulfurizing reagent[69], resulting in a chiral phosphorous center. This modification has the advantage that it is the closest to the natural nucleotide in terms of structure and charge density, seeing that the negative charge of the phosphate is retained and the size of the sulfur atom is only slightly higher than that of the oxygen atom (1.5 *vs.* 1.8 Å). Interestingly, it was discovered in 2007

that phosphorothioate linkages are in fact a natural modification present in the DNA of certain bacteria[70].

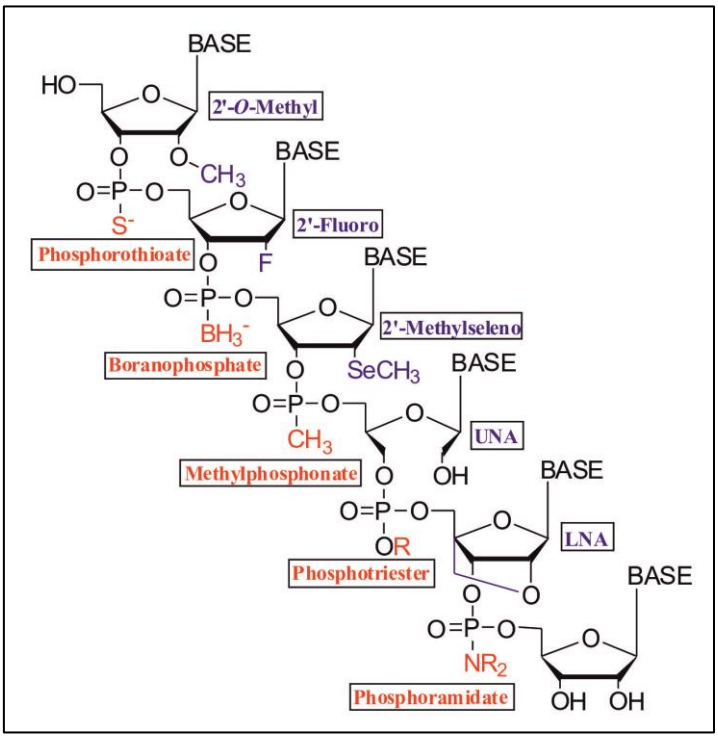

Fig. 1.7 Examples of ribose (as indicated in blue) and internucleotide (indicated in red) modifications in synthetic oligonucleotides.

In methylphosphonates the non-bridging oxygen of the phosphate group is replaced by an alkyl (typically methyl) or aryl group, resulting in an uncharged internucleoside linkage. Special nucleoside amidites, known as methylphosphonamidites[71], are required during the production of methylphosphonate linkages. Following their synthesis, special deprotection chemistry has to be applied before obtaining the final oligomer.

Internucleotide linkages where the hydroxyl on the phosphate is replaced by an amino group are referred to as phosphoramidates or phosphoramidic acids[64,66,67]. An appealing feature of this type of modification is the possibility to introduce a diverse range of amines, thus offering a great opportunity for structural variation at this position.

The synthesis and application of non-phosphate internucleoside linkages have also been investigated. However, the development of these types of compounds is still in a relatively early stage[72,73].

Even with the wide variety of internucleotide and ribose based modifications of synthetic oligonucleotides, the synthesis of nucleobase modified oligonucleotides is by far the most widely studied. Even the complete omission of the canonical nucleobases in synthetic oligomers has been explored. These positions, which are naturally occurring mutations, are

referred to as abasic sites. They are formed by the hydrolysis of the *N*-glycosidic bond, or by oxidation of sugar moieties in DNA nucleotides[74]. Most methods in synthetic oligonucleotides for the generation of such abasic sites depend on chemical modifications that develop a positive charge on the nucleic base, thus weakening the glycosidic bond and leading to its cleavage.

Moreover, chemical modifications on the base have found wide applications in molecular biology as well. Because changes on the base itself have the most influence on the physicochemical properties of the oligomer, mainly because of the hydrogen bonding edges' role in base pairing, these positions are also mostly the points of interest for introducing changes. Here, purines and pyrimidines offer different sites for functionalization and in literature essentially all available base positions have been explored for this purpose. For pyrimidines, positions three, four and five are usually preferred. Typical targets for chemically modifying purines include the nitrogen atoms on positions one[45], two[45], three and seven[75,76]. Examples of such modifications include the replacement of the nitrogen atom by a methine (CH) group, such as is the case with 7-deaza-guanine and 3-deaza-adenine. Methylation reactions, as is often the case in naturally occurring nucleosides, have also been explored at these *N*-positions[45].

N^7-methylguanosine, as an example, has the distinct property that it emits fluorescence upon excitation with light. Other naturally occurring modified bases that show intrinsic fluorescence are 4-thiouridine, N^4-acetylcytidine and the so-called Y-bases or wybutosine derivatives. The advantages of fluorescent nucleic acids, such as the sensitivity associated with fluorescence measurements, has led to the application of naturally occurring fluorescent base analogs in many studies on detection and analyses of structure and dynamics of biopolymers. However, when incorporated into polynucleotides, the fluorescence quantum yields of these molecules are considerably reduced. This and the rarity of such natively fluorescent bases necessitated the development of non-natural nucleobase analogs with optimized fluorescence properties. These are usually designed in such a way as to resemble the naturally occurring purine and pyrimidine structures, so as to not alter their biological activity to a large extent.

Some of the simplest synthetic alterations to natural nucleobases to render them fluorescent include an extension of their Π-electron system, usually by fusion of aromatic rings to the natural base[77–79]. Other examples include the conjugation of the base to already fluorescent aromatic moieties, thus using fluorescently tagged phosphoramidite building blocks in the oligonucleotide synthesis[80,81].

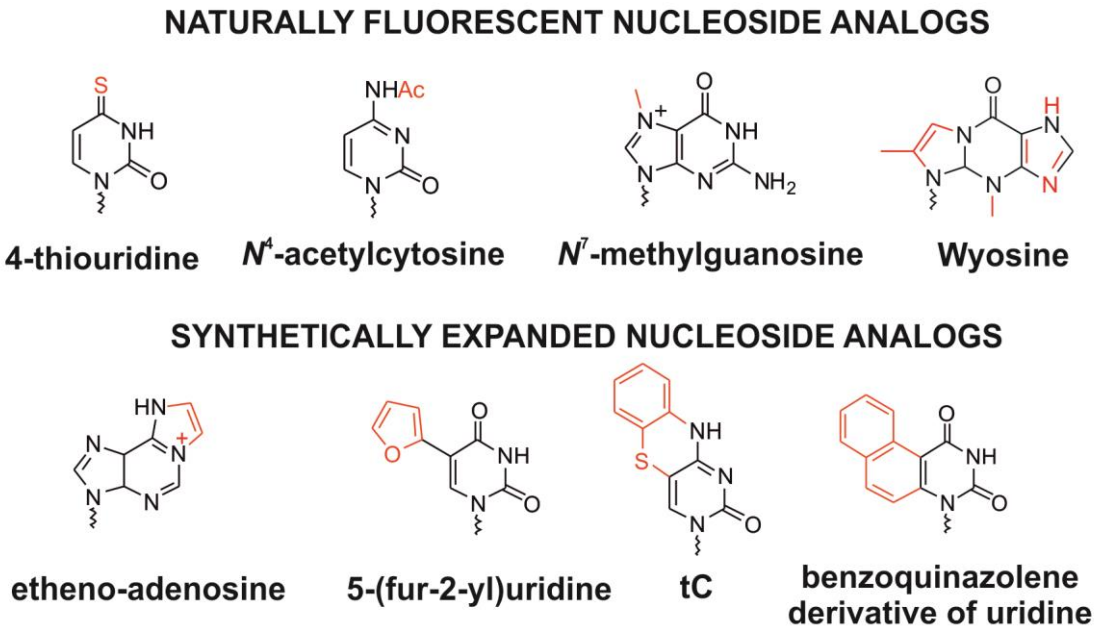

Fig. 1.8 Examples of natural and synthetic fluorescent nucleobases.

In some cases, even the complete substitution of the nucleobase for the fluorophore has been done[82]. Fluorophores are, however, not the only examples of non-nucleotides that have been converted to phosphoramidites to allow their incorporation into DNA and RNA strands. Other such examples include cholesterol[83], reporter groups, such as biotin[35], 1-substituted 1*H*-1,2,3-triazoles[84], as well as nucleophilic linker groups that provide binding sites for the attachment of conjugates after the completion of the oligonucleotide synthesis procedure[85,86].

Clearly, especially with the constant developments in molecular biology, there is an increasing need for the introduction of not only fluorescent moieties, but also various other modifications at different positions of the nucleotide. This, however, increases the chances for an incompatibility between the functional groups of the potentially large and complex labels with synthesizer chemistry. To circumvent this problem, various research groups are now making use of the introduction of a small reactive anchor during oligonucleotide synthesis *via* phosphoramidite chemistry, to attach the modifier itself post-synthetically. As a result, solid phase synthesis modification can thus be combined with post-synthetic labeling to optimize the functionalization of nucleic acids and to overcome some obstacles posed during direct SPOS labeling techniques.

1.2.2 Post-synthetic labeling of oligonucleotides

The post-synthetic labeling of oligonucleotides has the advantage that it requires less effort than the preparation of reagents for incorporation during standard automated oligonucleotide synthesis. This method, however, does suffer from other disadvantages. Due to the polyanionic and labile nature of nucleic acids, post-synthetic transformations are required to take place in an aqueous environment and at low temperatures, which already excludes a number of organic reactions for the conjugation step. Another problem that may further restrict the possibilities of synthetic chemistry reactions is the likely occurrence of unwanted reactions at many internal sites within the oligonucleotide, thus requiring ligation reactions with entities that are chemically unreactive towards the relevant biomolecules.

There is currently a selection of chemical reactions used in site-selective bioconjugation with synthetic oligonucleotides. Among these, the Sonogashira cross-coupling reaction[87–89] and the different variations of click chemistry[90], *i.e.* the copper catalyzed azide alkyne cycloaddition reaction (CuAAC)[91,92], Staudinger ligation, the Diels Alder reaction and strain promoted click (SPAAC), have received particular attention in recent years. Other common and slightly older bioconjugation reactions include the derivatization of artificial amino groups to produce thiourea linkages with isothiocyanates, or amide bonds with *N*-hydroxysuccinimide (NHS) esters[93].

1.2.2.1 Click chemistry in post-synthetic bioconjugation reactions with oligonucleotides

Click chemistry refers to a term developed by the group of Sharpless[90] to describe a set of chemical reactions that make possible the conjugation of organic molecules in a simple manner, while obtaining consistently high yields under mild conditions. Reaction work-up and purification following the reaction should also not be complicated. An interesting concept of click reactions is that they proceed most rapidly in water as solvent. This is mainly due to the exothermic character of these types of reactions and water being the best heat-sink for handling the heat output, especially when the reactions are performed in large scale. Another advantage of water as solvent is that its presence prevents interference from simple protic functional groups, such as alcohols[91]. This role of water is all the more reason to make click chemistry ideal for bioconjugation reactions.

(i) The copper(I) catalyzed azide alkyne cycloaddition reaction (CuAAC)

The Cu^{I} catalyzed [3+2] cycloaddition reaction between azides and terminal acetylenes (CuAAC reaction) is currently the method of choice for DNA click chemistry[94,95]. Due to the instability, as well as the insolubility of the Cu^{1} species, it is often preferred that it is formed *in situ* by the addition of a reducing agent, such as sodium ascorbate, in combination with a copper(II) salt (*e.g.* $CuSO_4 \bullet 5H_2O$). The CuAAC has the advantage that the regioselective 1,4-substituted 1,2,3-triazole, which forms during the reaction is not only extremely stable, but also non-toxic. In addition to this, the functional groups required for the reaction, *i.e.* azides and terminal alkynes, are relatively easy to install and unreactive towards most other functional groups.

Nonetheless, until very recently, a major challenge in phosphodiester SPOS was the incorporation of an azido functionality to allow CuAAC post-synthesis functionalization of nucleic acids. Prior to the publication of the Micura group[96] in 2011, nucleoside modification for this variant of click functionalization of oligonucleotides formed *via* the phosphodiester approach was mainly limited to the incorporation of terminal alkynes during phosphoramidite syntheses[95,97]. The reason for this is the high activity between the phosphor(III) species and the azide, which results in a Staudinger reaction and a subsequent reduction of the azide moiety[98]. The phosphotriester approach for oligonucleotide synthesis[99,100], where the internucleotide phosphate is protected and thus not susceptible to react with the azide, was applied by Polushin *et al*[101] in 1996. However, some difficulties were encountered where a stretch of nucleosides were incorporated, of which each carried the azide. Additionally, the phosphoramidite or phosphodiester method still remains the most common and convenient approach towards DNA and RNA solid phase synthesis.

During their experiments, Aigner *et al.*[96] from the Micura group discovered that the Staudinger side reaction only took place at very high concentrations of the azido modified phosphoramidite. This observation led them to consider the possibility that strand assembly by phosphoramidite chemistry might still be feasible, provided the phosphoramidite concentrations are reasonable. Similar to the work done by Polushin *et al.*[101], the azido functionalized building blocks were converted into phosphodiesters (see scheme 1.1), making their incorporation into oligonucleotides possible *via* phosphotriester coupling. The rest of the strand assembly followed standard phosphoramidite chemistry.

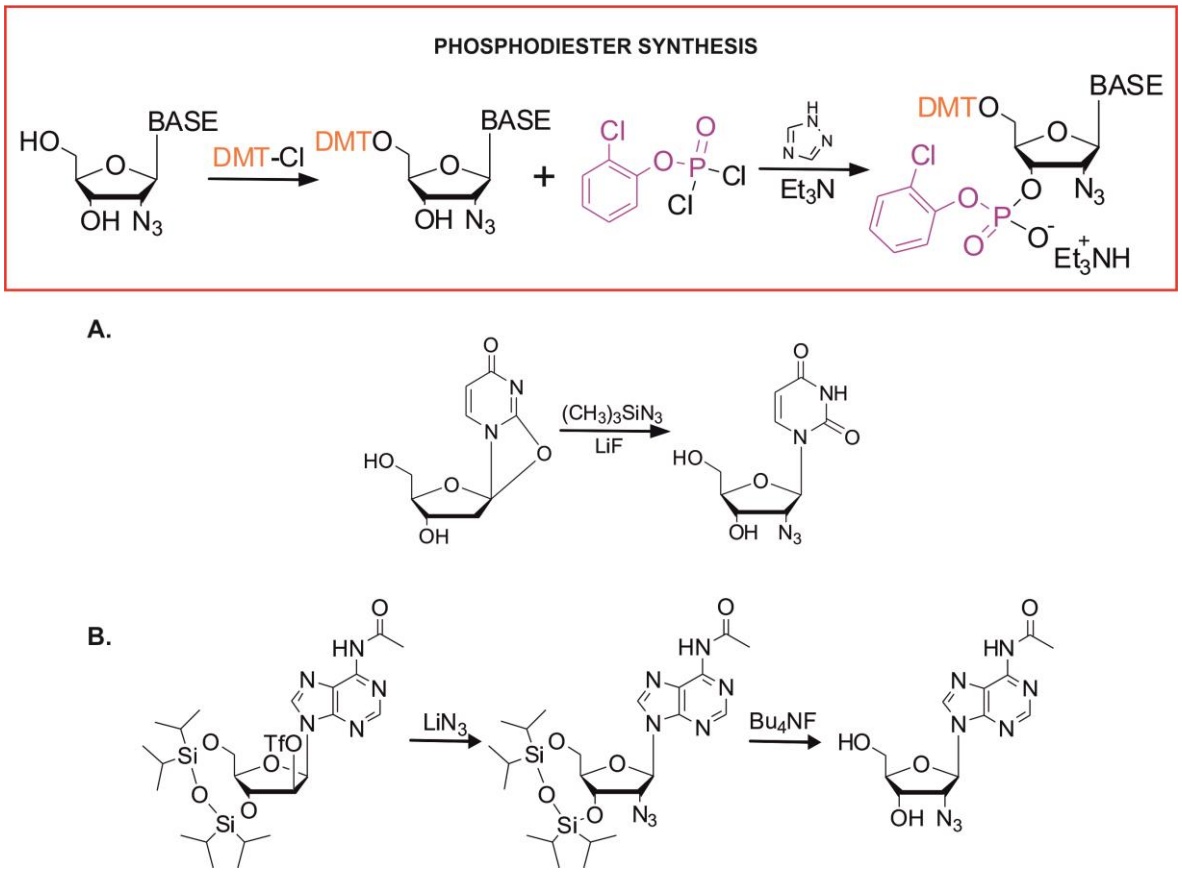

Scheme 1.1 Synthesis of the 2'-azido functionalized phosphodiesters of **A.** deoxyuridine and **B.** deoxy-adenosine for solid phase oligonucleotide synthesis[102,103].

(ii) Strain-promoted alkyne-azide cycloaddition (SPAAC)

The incompatibility of azides with synthesizer chemistry is not the only problem associated with the CuAAC reaction. The use of copper ions in biological systems causes strand breaks due to its toxic effect on DNA and RNA[104]. This led to the development of a newer, uncatalyzed version of the cycloaddition reaction, where azides can be reacted with cyclic alkynes in the absence of copper, resulting in the same 1,2,3-triazoles as products. The 160 ° bond angle of the sp-hybridized alkyne in cyclooctyne becomes distorted toward the transition state of the cycloaddition reaction and thus causes a dramatic acceleration of the reaction rate. The strain in the cyclic ring, therefore, provides the necessary energy as driving force for the reaction and hence also the designation strain-promoted azide-alkyne cycloadditions (SPAAC) for this type of conversion. Assuming that the reaction takes place between the highest occupied molecular orbital (HOMO) of the azide and the lowest unoccupied molecular orbital (LUMO) of the alkyne, the reaction kinetics could be further enhanced by lowering the LUMO of the latter. This could be achieved by withdrawing electron density from the bond, *e.g.* by the addition of an electron withdrawing group, such as fluorine[105]. This

causes a three-fold increase in reaction rate constant[106], which was even further improved with a second fluorine atom[107]. This copper-free click ligation has since been applied to conjugation reactions of ribonucleotides in various functionalization reactions, showing that the SPAAC is indeed amenable in biological systems[108,109].

(iii) Inverse electron demand Diels-Alder cycloaddition (iEDDA)

Another example of metal-free click chemistry is the inverse electron demand Diels-Alder cycloaddition reaction (iEDDA). This reaction typically takes place between a diene, such as the tetrazines and a dienophile (*e.g.* olefins or alkynes) to yield a pyridazine as product[110]. The first step in the reaction sequence, which is a Diels-Alder [4+2] cycloaddition reaction, results in the formation of a highly strained bicyclic adduct, as can be seen in figure 1.9. Upon release of nitrogen, this intermediate is converted to the corresponding 4,5-dihydropyridazine which, in turn, undergoes a 1,3-prototropic isomerization reaction. The stable 1,4-dihydro-isomer is thus formed[111], which, in the presence of an oxidant (*e.g.* nitrous gases or H_2O_2), results in the formation of the final pyridazine. This step is, however, absent when alkynes act as dienophiles and the final product is formed without the necessity of an oxidation reaction. Because this reaction is likely to take place between the $HOMO_{dienophile} - LUMO_{diene}$ gap, the placement of electron-withdrawing substituents at positions 3 and 6 of tetrazine would lower the LUMO of the diene and thus accelerate the reaction rate. In the same manner, electron-rich substituents would naturally raise the HOMO of the dienophile and therefore result in a similar effect[112].

The iEDDA reaction features several characteristics that can qualify it as 'click-like'. Its versatility and orthogonality with other types of click reactions were confirmed by the Jäschke group in 2012, when they performed a one-pot reaction of tetrazines with *trans*-cyclooctenes (TCOs) for iEDDA[111] and an azide with terminal alkynes for CuAAC[26]. The one-pot reaction delivered a site-specific double modification of an oligonucleotide without the need to protect or purify the relevant functional groups. Karver *et al.*[113] and Patterson *et al.*[114], respectively, took this one step further and combined the inverse electron demand Diels-Alder reaction with strain promoted, copper-free click (SPAAC), allowing the orthogonal reactions to proceed in the absence of toxic copper ions.

(iv) Staudinger ligation

A minor modification to the very side reaction that occurs when incorporating an azido functionality into a phosphoramidite also counts as one of the newer click-type reactions. Of course, this side reaction limits its use in SPOS *via* phosphodiester chemistry. The Staudinger ligation, which involves the reduction of azides with phosphines[98], was modified by Bertozzi[115] in 2011. Under normal circumstances, the intermediate aza-ylide undergoes spontaneous hydrolysis in the presence of water and, as a result, a primary amine and the corresponding phosphine oxide are formed. Bertozzi and co-workers steered this reaction in a different direction, by designing a phosphine that would allow rearrangement of the water-unstable aza-ylide to form a stable covalent adduct. An electrophilic trap (a methyl ester) within the phosphine structure would contribute to the stabilization of the intermediate product by means of intramolecular cyclization. This process, in turn, would ultimately produce a stable amide bond, rather than the products of aza-ylide hydrolysis (see figure 1.9).

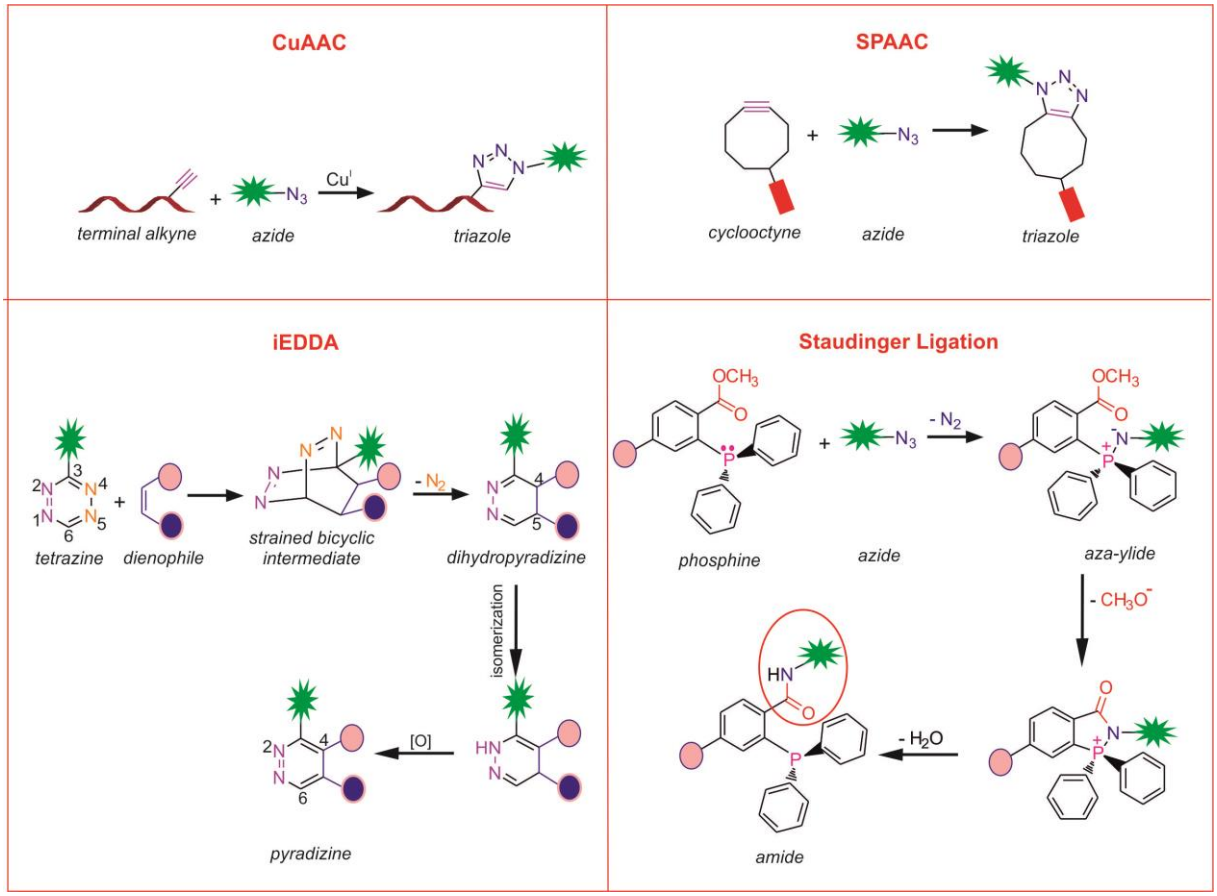

Fig. 1.9 Typical click reactions used for bioconjugations today: Copper catalyzed azide-alkyne (CuAAC); Strain promoted azide-alkyne (SPAAC); Inverse electron demand Diels-Alder cycloaddition reactions (iEDDA) and Staudinger ligation.

Despite the challenges associated with the use of both functional groups (phosphines and azides) of the Staudinger ligation in oligonucleotide synthesis, Wang *et al.*[116] explored the use of this reaction in post-synthetic labeling with DNA. A linker containing a terminal amino group was incorporated into the oligonucleotide which, after synthesis, was converted into an azido active ester. This was followed by the successful labeling of the oligonucleotide by means of the Staudinger ligation reaction.

Clearly, the CuAAC and other click reactions have received a considerable amount of attention in bioconjugation reactions with synthetic DNA and RNA. Even with the enormous pace at which this field continues to evolve the post-synthetic labeling of oligonucleotides still suffers from one or two major shortcomings. Whether it involves the older types of synthetic chemistry such as amine and maleinimide couplings, or the reinvented click-type reactions, the incompatibility of the functional groups with SPOS still result in low yields.

The groups of Verdine[117,118] and Xu[119,120] have independently developed a post-synthetic modification technique to introduce a common leaving group into oligonucleotides, which is then replaced by functionalized nucleophiles that carry the final modification. Today, this method is commonly known as the convertible nucleoside approach.

1.2.2.2 The convertible nucleoside approach

The introduction of a temporary leaving group (*i.e.* convertible nucleoside) during SPOS allows the attachment of a desired functionalized tether (*e.g.* primary amine) to the nucleic acid polymer by means of a nucleophilic substitution reaction after strand elongation. The schematic representation of this concept can be found in figure 1.10.

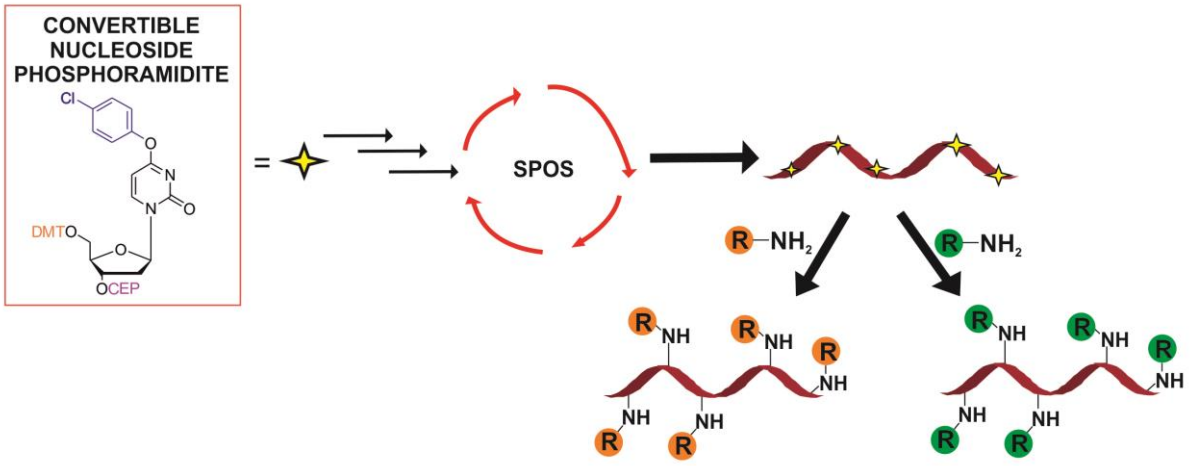

Fig. 1.10 Schematic representation of the convertible nucleoside approach.

The convertible nucleoside approach is ideal for the functionalization of the exocyclic amines of A, C and G residues in both RNA and DNA. Typical positions for attaching the convertible groups are position four for the pyrimidines, position six for adenosine and position two for guanosine (see figure 1.11). The post-synthetic conversion of T or U residues to cytidine analogues is thus possible without the necessity of introducing a temporary protecting group on the exocyclic amine on position four (N^4). This route also enables the synthesis of a wide variety of functionalized tethered oligonucleotides (FTOs), all carrying the same convertible nucleoside, but which can be reacted with different amines after their solid phase synthesis. A single precursor oligonucleotide can thus be used for the functionalization with different types of primary amines, without the need to repeat the oligonucleotide synthesis. Other advantages of this approach are the stability of these temporary groups to automated DNA or RNA synthesis – often in contrast to the final tether – and the ability of FTOs to undergo clean aminolysis reactions, together with the simultaneous cleavage of the oligonucleotides from the solid support in the same step.

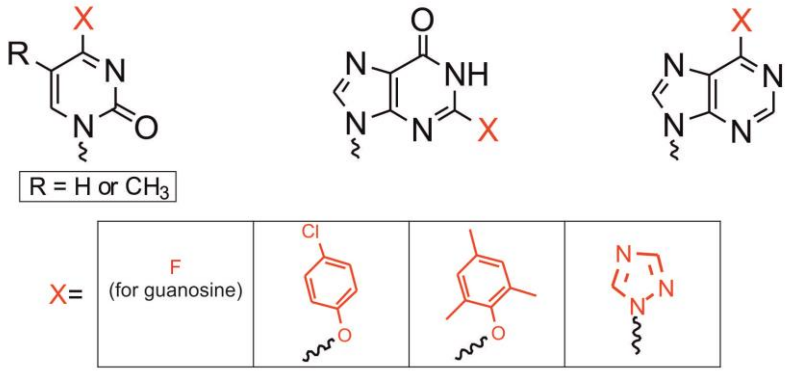

Fig. 1.11 Typical examples of functional groups used as temporary tethers in the convertible nucleoside approach.

These reactions are, however, not so well tolerated in RNA as in deoxyribonucleotide strands. As discussed previously, a premature cleavage of the 2'-*O*-protection groups after oligonucleotide synthesis, usually as a result of treatment with concentrated solutions of a base, result in hydrolysis of the more labile RNA strand[20]. This effect can be reduced when alcoholic, instead of aqueous amines, are used for the deprotection and aminolysis step.

1.2.3 Functionality transfer by oligodeoxynucleotides (FTODN)

A much more recent method for the modification of RNA molecules was introduced by Ali *et al.*[121] in 2004. Their strategy is based on a site-specific functional group transfer reaction within a hybridized complex. Initially using nitric oxide (NO) as transfer molecule, *S*-nitroso

deoxythioguanosine was applied as source of the functional group in an oligodeoxynucleotide strand. Mainly due to the efficient proximity between the two relevant bases in the duplex, the NO was transferred to an imino tautomer of cytosine in the opposing DNA strand in a highly selective manner. This reaction was accompanied by a hydrogen transfer from N^3 of cytosine to N^1 of thioguanine.

In succeeding reports, the group expanded this application to the transfer of different functionalities from correspondingly functionalized *S*-vinyl deoxythioguanosines to form 4-amino-modified cytidine derivatives, in both DNA and RNA as opposing strand[122,123]. An increase in pH from 7 to 9.6 surprisingly caused the selectivity of this reaction to shift from cytidine to the 2-amino group of the guanine base, thus increasing the application of the FTODN method for the functionalization of oligonucleotides[124]. It was postulated that the *syn* conformation of the *S*-functionalized thioguanosine base may be included in the reaction of the *anti* conformation of G in the target RNA.

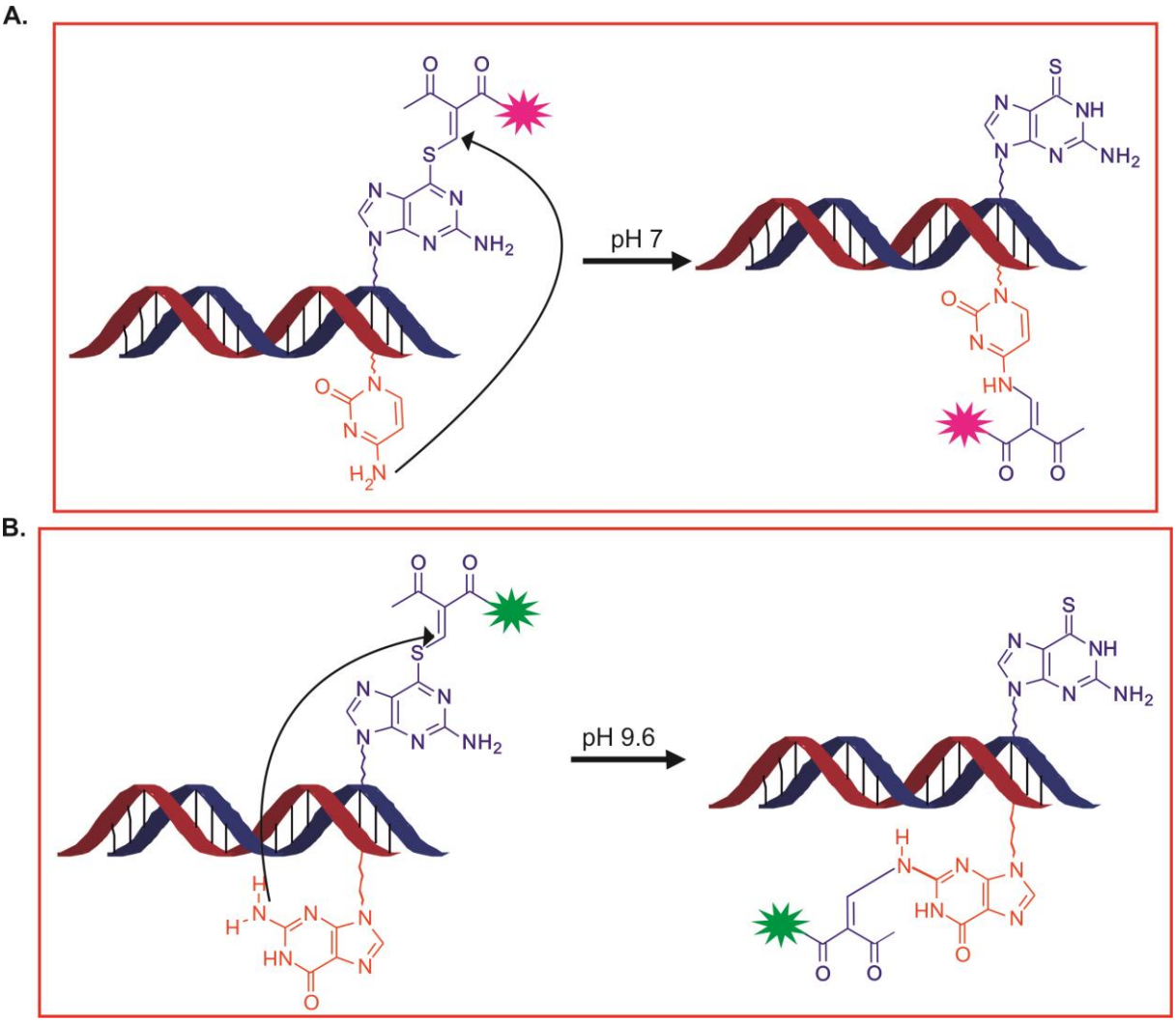

Fig. 1.12 FTODN reactions between functionalized *S*-vinyl deoxyguanosine and **A.** cytidine, or **B.** guanosine in the opposing strand.

This sequence and base-specific delivery can be applied to a variety of other molecules, such as fluorescent labeling groups or tagging molecules. The modification site of RNA can also be controlled and varied between C and G by changing the pH between 7 and 9.6.

1.3 The effect of chemical modifications on nucleoside properties

As mentioned earlier, the modification of nucleic acids, whether natural or synthetic, has the potential to cause major changes to their biological and physicochemical properties. Of particular interest is the impact on the hybridization properties, biological stability or cell uptake of the given biopolymer. More often than not, the main idea behind introducing the chemical modification is to purposefully alter these characteristics of oligonucleotides. However, mainly due to the influence of the modification on base pairing, some of the resulting effects may be unintentional and the results even undesired. For this reason, it is of utmost importance to carefully consider not only the nature, but also the position of chemical modifications to be brought about to DNA and RNA.

1.3.1 The thermodynamic stability of nucleic acids

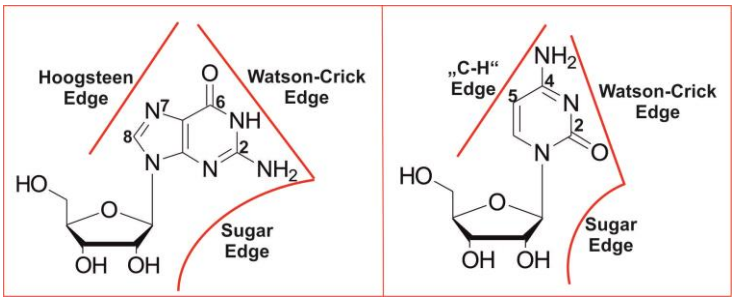

Fig. 1.13 Hydrogen bonding edges for purines and pyrimidines in RNA (Adapted from Leontis and Westhof[125]).

The very famous discovery by Watson and Crick in 1953[126], which describes the intrinsic pairing capabilities of the nucleotide bases, is what mainly governs structure and function of DNA and RNA. This so-called Watson-Crick base pairing is what results in the self-assembly of nucleic acid strands, of which the stability is critically important in their function.

Watson-Crick base pairing is, however, only one of four edge-to-edge H-bonding interactions between nucleosides. Others include the Hoogsteen edge for purines, or the equivalent ‘CH’-edge for pyrimidines, as well as the sugar edge in the case of ribonucleic acids (see figure 1.13), as described by Leontis and Westhof in 1998[125]. The presence of the additional hydroxyl group on the 2’-position of the ribose in RNA does not only provide an additional

site for hydrogen bonding, but also causes steric hindrances and a more labile sugar ring. This 2'OH is also what contributes to the altered backbone in RNA, leading to a slightly different double helical structure (A- *vs.* B-form geometry for RNA and DNA, respectively) and a higher duplex stability than DNA.

Forces other than these that contribute to duplex stability in both DNA and RNA include interactions of the biopolymer with the solvent, hydrophobic or stacking interactions between the bases, as well as destabilizing, repulsive forces of the charged phosphate backbone. The latter can be influenced by high salt concentrations in the solution, which may neutralize the negative charge on the backbone, thus resulting in more stable duplexes.

However, even with this variety of other interactions that contribute to duplex stability, the edge-to-edge interactions still play a much higher role in the specificity and directionality of binding. As a result, particular care should be taken when chemical modifications to the nucleoside involve these planes, so as to not influence base pairing within the double helix.

1.3.1.1 Temperature dependent UV-absorption measurement

Among the number of biophysical techniques available for assessing the stability of double stranded nucleic acid structures, the spectrophotometric measurement of nucleic acids in dependence of temperature is one of the most commonly applied. This method is based on the characteristic ultraviolet absorption spectrum of purines and pyrimidines, with an absorption maximum at 260 nm. The absorption intensity of native DNA is much lower than the spectrum calculated from its constituent nucleotides and, following dissociation of a duplex, a strong increase in absorbance can be observed. This effect is also referred to as a hyperchromic shift in the absorption spectrum and results from the unstacking of the nucleotide bases[127].

These findings led to the development of the temperature-dependent UV-absorption measurement to determine the stability of DNA and RNA duplexes. Here, the absorption of the nucleic acids at 260 nm is monitored as a function of temperature. A typical S-shaped curve is obtained, of which the midpoint of transition is referred to as the melting temperature (T_m) of the duplex.

Among the factors influencing the melting temperature of a duplex, are the sequence, the length and the fidelity of base pairing. The latter can, of course, be influenced by the addition of chemical moieties by means of synthetic modifications.

1.3.1.2 The effect of chemical modification on duplex stability

The chemical modification of nucleic acids may have a variety of effects on the structure of a duplex. Depending on the nature of the modification, stacking interactions, H-bonding or steric effects may be influenced.

When modifying pyrimidine nucleic acid bases, the C5 of uridine[97,128,129] and N^4 of cytosine[130–133] are usually the easiest positions to manipulate. Position five is on the 'CH'-edge of the pyrimidine ring and substitution at this position is not expected to diminish base pairing. In fact, the simple addition of a methyl group to C5 is known to cause an increase in base-stacking due to its hydrophobicity[134]. This is confirmed by the function of the methyl group in 5-methylcytosine (m^5C), which is to stabilize the secondary structure of tRNA. m^5C was the first nucleobase modification to be detected in DNA[134].The opposite effect is observed when the bulkiness of the substituent at the 5-position is increased, possibly due to hindrance of duplex solvation[135].

Another example of a post-transcriptional modification that increases the chemical diversity of nucleotides is the methylation of guanosine's exocyclic amine[1,136]. Studies performed on the effect of such methylation on the sugar edge of guanosine showed that a mono-alkylation has a minimal impact on duplex stability[23,137]. A single substitution on N^2 would still allow base pairing with the opposing base, depending on whether the rotamer is in the *s-cis* or *s-trans* confirmation. However, upon removal of both hydrogen atoms on the nitrogen by means of a double methylation, base pairing at this position is completely abolished and secondary nucleic acid structure influenced substantially[138,139]. The same could be observed when N^1 of guanosine was methylated[139].

Similar studies with 4-methylcytosine (m^4C) also suggest that rotamers of this structure exist that would still allow base pairing, albeit stability was slightly diminished[139]. In the free nucleoside the *cis*-rotamer is favored. However, the substituent adapts the thermodynamically less stable *anti*-rotamer about the C4-N^4 bond to be able to form Watson-Crick base pairs. The effect on duplex stability is, however, still not major. Even with the single attachment of the more bulky fluorescein moiety onto N^4 of cytidine *via* a linker, the stability of the duplexes was not influenced. However, in the absence of a linker, duplex stability was altered[140], which suggests a steric hindrance of the chromophore with Watson-Crick base pairing. This effect is even more pronounced with bulkier substituents[141]. As is the case with N^2,N^2-dimethylguanosine, a double methylation on position 4 of cytosine also disrupts Watson-Crick base pairing completely[130].

Even ribose modifications have an influence on duplex stability. However, since modification on the 2'-position are generally well-tolerated in oligonucleotide duplexes, this position is widely used to attach a large variety of substituents. 2'-*O*-Methyl-oligoribonucleotides are known to be more stable in binding complementary DNA or RNA than are oligodeoxyribonucleotides. The reason for this is that the 2'-*O*-methyl sugar adopts a C3'-*endo* ribose confirmation. For the same reason, locked nucleic acids also form more stable duplexes.

These and similar chemical modifications are being applied to research, diagnostic and therapeutic systems, in order to purposefully change characteristics such as biostability, cellular uptake, fluorescence or cellular distribution of synthetic oligonucleotides. Because this field is so broad, the next section will focus on one of the most recent and highly researched fields, *i.e.* RNA interference.

1.3.2 RNA interference (RNAi) and nucleoside modification in siRNA

Gene silencing was first described by Jørgensen and co-workers in 1990[142]. It describes the process by which the expression of a certain gene is switched off by a mechanism that blocks translation of messenger RNA. It was, however, not until 1998 that clear evidence was published for the role of double stranded RNA in this process[143] and in 2001 it was established that synthetic 21-nucleotide siRNAs could trigger RNA interference (RNAi) in mammalian cells[144]. Ever since, there has been an ongoing focus on the biological function and synthetic production of small RNAs, particularly due to the therapeutic potential of these duplexes in RNAi.

Seeing that siRNA-based drugs are synthetic in nature, it became relatively easy to manipulate their structure, in order to overcome therapeutic challenges, such as their instability in the bloodstream[145,146], unwanted off-target effects, toxicity and pharmacokinetic or pharmacodynamic problems, like tissue delivery and cellular uptake[145]. In recent years a stream of publications has been issued that address these and similar matters. However, the chemical modification of siRNA is not only applied for the optimization of its therapeutic use. Studies of the various mechanistic aspects of RNAi also require their chemical modification and typically, the attachment of fluorescent tags to the double stranded RNA is a common practice in such studies[23,147–149].

However, for the rational design of siRNA, whether for therapeutic or diagnostic purposes, both the position and character of the novel functionality should be carefully considered. Not only could the synthetic modification of the duplex influence its thermodynamic stability, but,

especially due to the dependence of the mechanism of RNAi on such hybridization properties, modification could either enhance or impede its eventual gene silencing potential.

The antisense strand in the RNA duplex plays a particularly important role in gene silencing. Its sequence is complementary to the target mRNA and its 5'-end determines the position of target RNA cleavage[144]. However, it is the stability of the respective terminals of the duplex that determines which of the two strands will act as antisense (guide) strand in the gene silencing process[150]. It is hypothesized that the RNA strand with the least stable 5'-end in the duplex is the one which will be chosen as antisense[151]. For this reason, it is of particular importance that oligonucleotide modification does not alter duplex stability in an undesired fashion. In fact, chemists have purposefully designed siRNA duplexes in such a way to reduce thermodynamic stability at the 5'-end of the antisense strand, so as to increase the gene silencing effect of the resulting duplex[152].

Another factor to consider when designing an siRNA duplex is that, because modifications from the 5'-end towards the center of the antisense strand may interfere with mRNA cleavage, they are rarely tolerated. Also, general duplex stability will decrease when DNA residues are incorporated. However, the presence of a few deoxyribose residues may even be tolerated at the target cleavage site[153].

2. Goal of the work

Developments in the chemical synthesis of nucleic acids, in combination with bioconjugation reactions, such as click chemistry, have made it possible to manipulate DNA and RNA structure for research and diagnostic purposes. Of particular interest in molecular biology investigations is the use of click chemistry to fluorescently label synthetic oligonucleotides. In the present study, it was envisaged to modify both deoxy- and ribonucleic acids to allow the copper catalyzed azide-alkyne cycloaddition (CuAAC) reaction after their incorporation into synthetic nucleic acid strands.

However, the replacement of a natural nucleoside by any chemical congener may cause fundamental changes in stacking interactions, hydrophobicity and van der Waals interactions, but more particularly, on the base pairing properties of the nucleoside. Especially due to the major role that secondary and tertiary structure of nucleic acids plays in their biological function, it is thus important to consider that such chemical modifications do not hinder the thermodynamic stability of the nucleotides involved. Despite the small structure of the alkyne and azide functionalities involved in CuAAC, their exact position both on the nucleoside, as well as in the nucleic acid strand may determine the extent of compromise on stability brought about by the modification. For this reason, a series of oligonucleotides – both DNA and RNA – have been synthesized, that contain differently alkyne labeled nucleosides. For determining the effect of the particular modification on the Watson-Crick base pairing properties of the relevant nucleoside, temperature dependent UV-absorption melting experiments were carried out for duplexes.

This thesis also briefly addresses the possible influence of artificial modifications on biological systems, such as enzyme recognition of the modified DNA and RNA.

3. Results and Discussion

3.1 Overview

The chemical modification of nucleobases has found several applications in diverse fields of research, including diagnostics, detection and therapeutics of RNA and DNA. In particular, the conjugation of fluorescent labels to nucleic acids forms a crucial part of current chemical modification experiments with nucleosides. The first covalent labeling technique of DNA was recorded in 1924 and involved the reaction of Schiff reagents with aldehyde groups engendered in the deoxyribose molecules by HCl hydrolysis[154]. Nucleic acid labeling has since advanced to the now famous variant of click chemistry, the copper catalyzed azide alkyne cycloaddition (CuAAC) reaction between azides and terminal alkynes[90]. However, the involvement of organic chemistry in molecular biology techniques continues to evolve and a number of reactions are currently known that can be classified as 'click'. Among these, the strain promoted cycloaddition reaction between cyclic alkynes and azides (SPAAC), which allows triazole formation in the absence of copper ions[108,109], the Staudinger ligation between azides and modified phosphines[115,116] and the inverse electron demand Diels-Alder reaction (iEDDA) between dienes and dienophile functionalities[26,110–114] are some of the favorites and their use in biological chemistry (also in combination) continues to develop at a fast pace. However, in a recent review by El-Sagheer and Brown, the authors still described the CuAAC reaction as the click reaction of choice in molecular biology techniques[155]. Despite the incompatibility of the azide functionality in SPOS, both the azide and alkyne functional groups are small, which is very advantageous in bioconjugation reactions. For this very reason, my thesis will focus on CuAAC for labeling of DNA and RNA.

Even though the attachment of azides and alkynes to nucleic acids should not necessarily disturb their biophysical properties greatly, it should still be taken into account to what extent such modifications influence the behavior of modified DNA and RNA as compared to their native counterparts. From a different perspective, the question also arises whether unexpected effects brought about by nucleoside modification could be used to our advantage in the molecular biology research of nucleic acids.

For these reasons, 'clickable' nucleosides – both RNA and DNA - have been synthesized (see figure 3.1), followed by studies on the influence of these modifications, as well as dye labeling *via* click chemistry, on the nucleoside properties.

There is a current rise in the use of click chemistry, particularly CuAAC, in RNA and DNA modifications and literature shows that the incorporation of both azides and alkynes into their

building blocks has recently been explored greatly. For the purpose of the chemical incorporation of 'clickable' nucleosides into synthetic RNA and DNA strands, the scope of such modifications is, however, more limited. As discussed in a previous chapter, the most common problem here is the incompatibility of azides with synthesizer chemistry, caused by their high reactivity with the phosphines on the 3'OH[98] and has thus, until recently[96], limited such modifications to alkyne containing phosphoramidites for solid phase oligonucleotide synthesis (SPOS). For this reason, the current studies mainly include the functionalization of nucleobases with terminal alkynes, to allow the post-synthetic labeling of the DNA and RNA oligonucleotides *via* the CuAAC reaction.

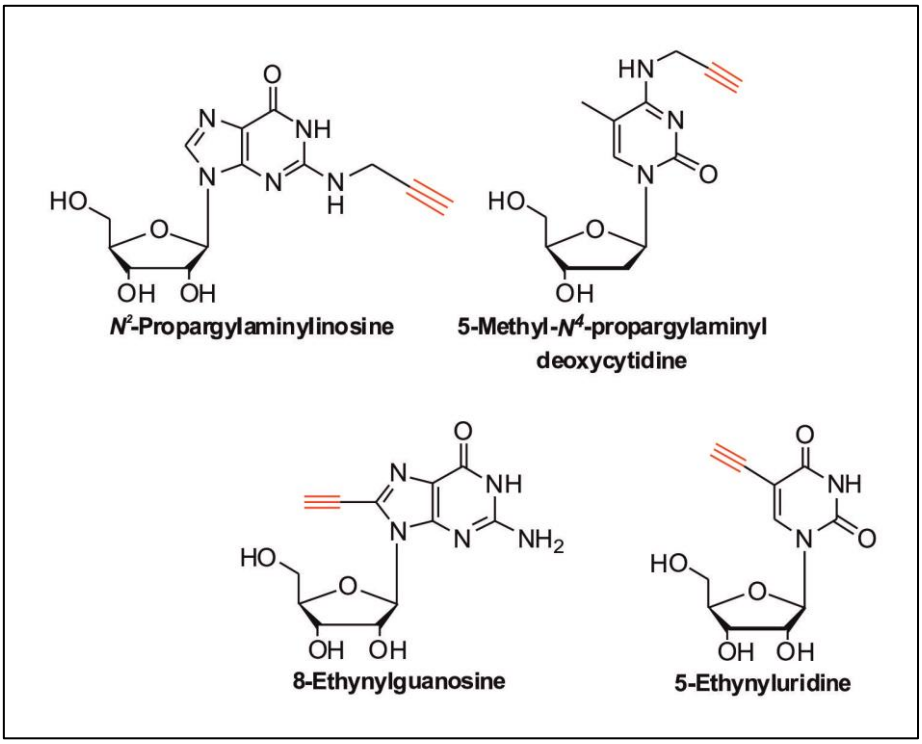

Fig. 3.1 Modified nucleosides envisaged for synthesis.

In nucleobase modifications, the 5-position of pyrimidines and the 7- or 8-positions of purines are commonly considered as labeling points directly on the base. This strategy was applied to the pyrimidine base, uridine, as well as to the purine base, guanosine. Their labeling positions would allow the investigation of the effect of Hoogsteen edge and "C-H"-edge labeling, respectively, on the physicochemical properties of nucleic acids (figure 3.2).

Other labeling positions were also explored in this study, including position 4 for the attachment of a propargyl moiety onto cytidine, as well as the exocyclic amine of guanosine on position 2. Seeing that these modifications are positioned on the "C-H"- and Watson-Crick edges of cytidine and on the Watson-Crick and sugar edges of guanosine (see figure 3.2),

respectively, it was anticipated that structure and function of the oligonucleotides in which they occur, may be influenced. Among other methods of analysis, absorbance melting measurements of synthesized oligonucleotide strands, hybridized to a variety of complementary oligonucleotides, provided the necessary information to analyze the thermal stability of the duplexes, as compared to unmodified strands. The structural impact of such labeling on the physicochemical, as well as functional properties of the relevant nucleosides could thus be investigated.

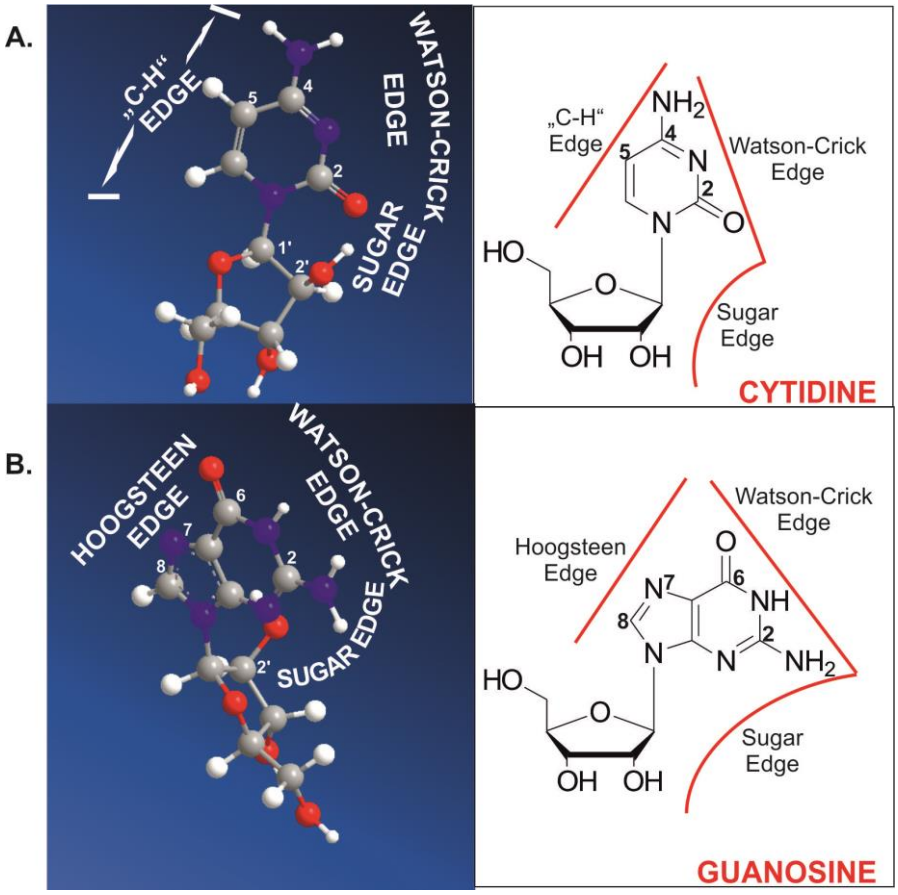

Fig. 3.2 H-bond interacting edges for **A.** pyrimidines and **B.** purines, as shown for cytidine and guanosine, respectively. Adapted from Leontis and Westhof[125].

Different methods are currently available for incorporating functionalized nucleosides into nucleic acids and include their enzymatic incorporation by means of *in vitro* transcription, feeding functionalized nucleobases to cells during their transcription or translation phases, as well as the solid phase oligonucleotide synthesis technique. Even though, during the course of this thesis, some experiments were conducted with the biosynthetic incorporation of ethynyluridine into both prokaryotic and eukaryotic cells, the solid phase oligonucleotide synthesis of DNA and RNA was still the labeling method of choice.

3.2 Synthesis of a water-soluble ligand for the CuAAC reaction with DNA and RNA

3.2.1 Synthesis of *tris*-(3-hydroxypropyltriazolylmethyl)amine (TPTA)

The CuAAC reaction usually proceeds in the presence of a chelating ligand, of which the function is to stabilize the reduced form of copper (Cu^{I}) and thus protect it from oxidation. Among the polytriazoles that act as ligands for the CuAAC reaction, TPTA is the water soluble member of this family, thus making it ideal for bioconjugation reactions involving azides and alkynes.

The polytriazoles contain a propargylamine core and are, themselves, synthesized *via* the copper(I)-catalyzed ligation of azides and alkynes. Since the azido counterpart in this reaction, the 3-azido-1-propanol, was not commercially available at the time of TPTA synthesis, it had to be synthesized from 3-bromo-1-propanol in an azidation reaction with NaN_3[156]. Tripropargyl amine was the source of both the propargylamine core and the terminal alkyne functionality in the synthesis of TPTA[157].

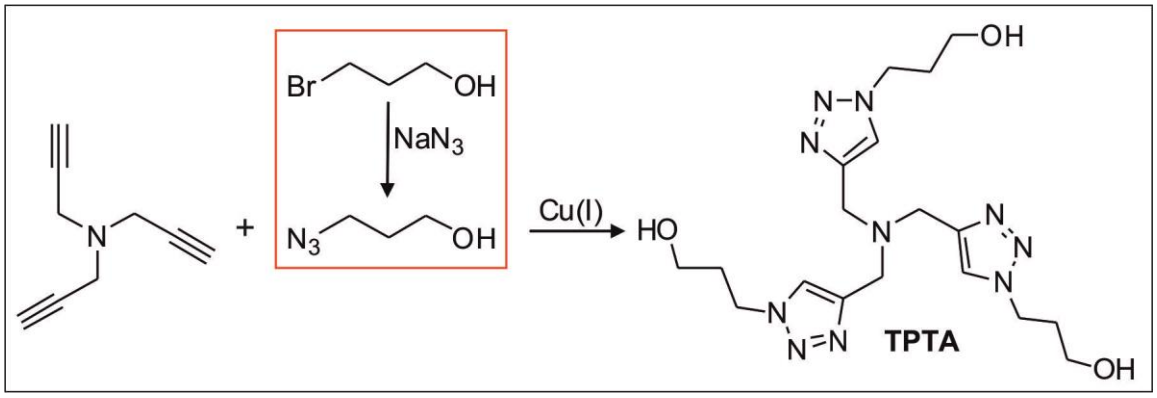

Scheme 3.1 Synthesis of *tris*-(3-hydroxypropyltriazolylmethyl)amine (TPTA).

The final yield of TPTA after two steps was 36%. This fairly low yield may be attributed to the additional formation of both mono- and disubstituted hydroxypropyltriazolylmethyl amine products, which complicated the final purification step. On the other hand, only nano- to micromol amounts of material are used in molecular biology techniques, making the low yields in organic syntheses insignificant in this regard. In the meanwhile, TPTA has also become available commercially.

3.3 Phosphoramidite synthesis for ribonucleic acid bases

3.3.1 Synthesis of the phosphoramidite of 5-methyluridine (m^5U)

5-Methyluridine, or ribothymidine, is the RNA counterpart to deoxythymidine. The methylation at position 5 is one of the well-known posttranscriptional modifications of RNA and the phosphoramidite synthesis of such modified bases, which precedes their incorporation into synthetic RNA, forms an important part of studies into understanding the structural and functional contributions of natural RNA modifications in general.

Phosphoramidite chemistry allows the site-specific incorporation of nucleosides into DNA and RNA strands and thus requires the orthogonal protection of the ribose hydroxyl groups, as well as the protection of the exocyclic amines in the case of all bases, excluding thymidine and its RNA counterpart, uridine. The presence of the additional OH-group on the ribose sugar of RNA makes their phosphoramidite syntheses slightly more complicated than that of DNA.

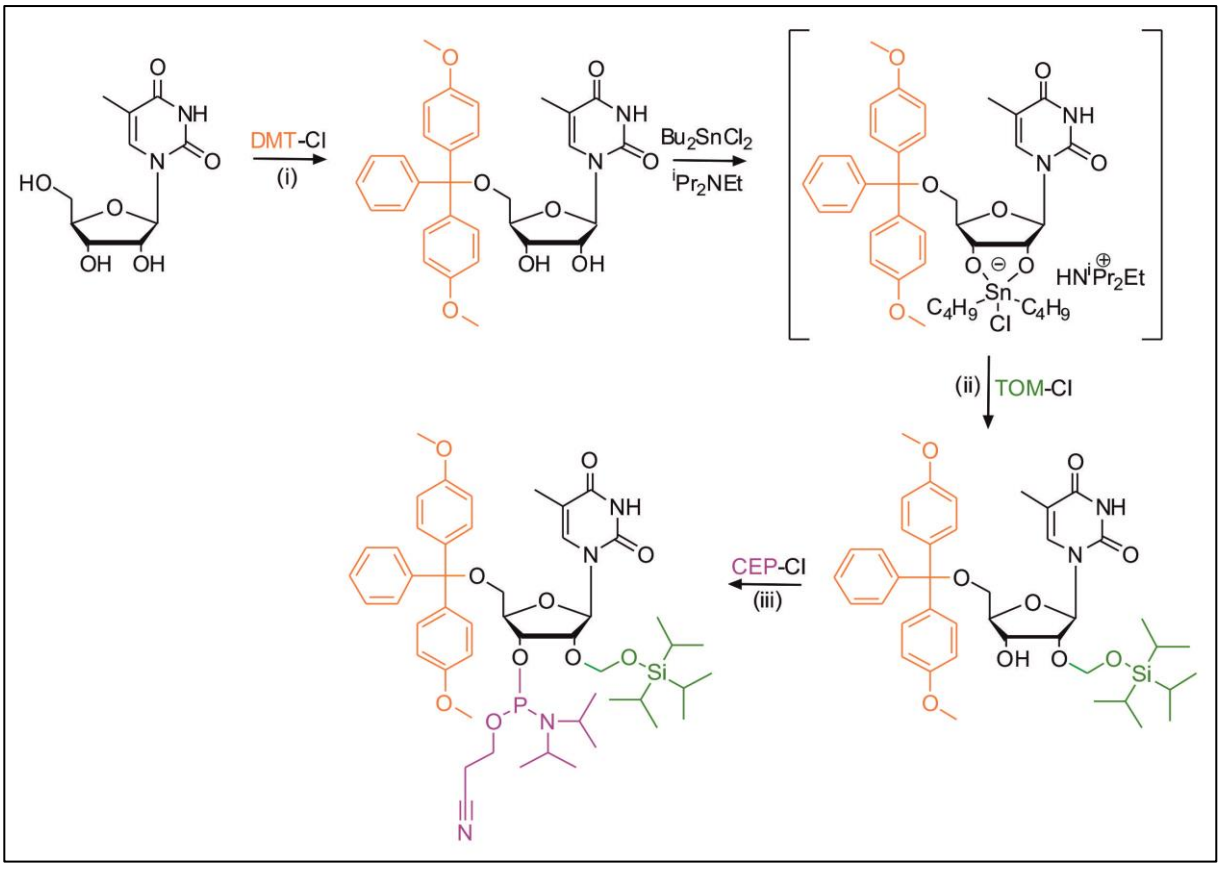

Scheme 3.2 Standard procedure for the synthesis of the m^5U phosphoramidite: *(i)* Tritylation of 5'OH, *(ii)* 2'*O*-protection with TOM-Cl and *(iii)* phosphitylation of the 3'OH.

The general procedure for phosphoramidite synthesis involves, firstly, the 5'*O*-protection of the given nucleoside with the acid labile 4,4'-dimethoxytrityl (DMT) group[158]. In the case of RNA nucleosides, this step is usually followed by protection of the 2'OH with a fluoride labile group, of which *tert*butyldimethylsilyl (TBDMS) is the most widely applied[159]. In 2001, Pitsch *et al.*[160] introduced a more sterically hindered moiety for 2'OH protection, thus eliminating a common problem associated with the use of TBDMS, *i.e.* the migration between the 2'*O*- and 3'*O*-positions under strongly basic conditions. The new fluoride labile protecting group, [(triisopropyl)oxy]methyl or TOM, was used in the synthesis of the m^5U phosphoramidite and was introduced to the 5'*O*-DMT protected nucleoside *via* the formation of a 2',3'-*O*-dibutylstannylidene intermediate (scheme 3.2). The resulting alkylation reaction with TOM-Cl resulted in a mixture of 2'*O*- and 3'*O*-TOMilated nucleosides (in favor of 2'*O*-TOM), of which the desired and first eluting isomer was purified *via* silica gel column chromatography. The presence of Et_3N in the elution mixture prevented the detritylation of the 5'-protecting group in the presence of the acidic silica gel.

The 2'*O*-TOM protected intermediate was phosphitylated on the 3'-position with 2-cyanoethyl diisopropylphosphoramidochloridite, to deliver the m^5U phosphoramidite in a final yield of 24%.

This three step synthesis would form the basis for future phosphoramidite syntheses of modified bases during my PhD thesis. The phosphoramidite synthesis of 2'-deoxynucleosides, as well as bases where the exocyclic amines were substituted with 'clickable' functionalities, required a slightly less complicated procedure than normal.

3.4 Modification of guanosine for click functionalization on the sugar edge and its incorporation into siRNA

Post-transcriptional modifications to RNA nucleotides increase their chemical diversity. N^2,N^2-dimethylguanosine ($m^2{}_2G$) counts as one of the naturally occurring modifications of guanosine and can be found in a wide variety of RNAs. The possible functions of the various modifications to the four basic nucleotides have been under intense investigation and with the additional methyl groups of $m^2{}_2G$ on the sugar edge of the nucleoside, it was envisaged that it may play a role in the modulation of stability in RNA structures. In a study on the effects of $m^2{}_2G$ on RNA structure[138], it was discovered that such a modification completely alters the pairing behavior of the base, thus supporting the hypothesis that guanosine methylation serves a structural purpose in RNA.

However, single substitution at the exocyclic amine of guanosine has no significant effect on duplex stability. By replacing N^2-methylguanosine (m_2G) by G in G-C Watson-Crick pairs and G•U wobble pairs within RNA duplexes, a slight stabilizing effect (possibly due to hydrophobic interactions) for an internal m_2G•U pair could be observed, but otherwise no energetic difference was observed at all[137]. In this case, the N^2-function still has the ability to donate in hydrogen bonding and pairing behavior is thus not altered.

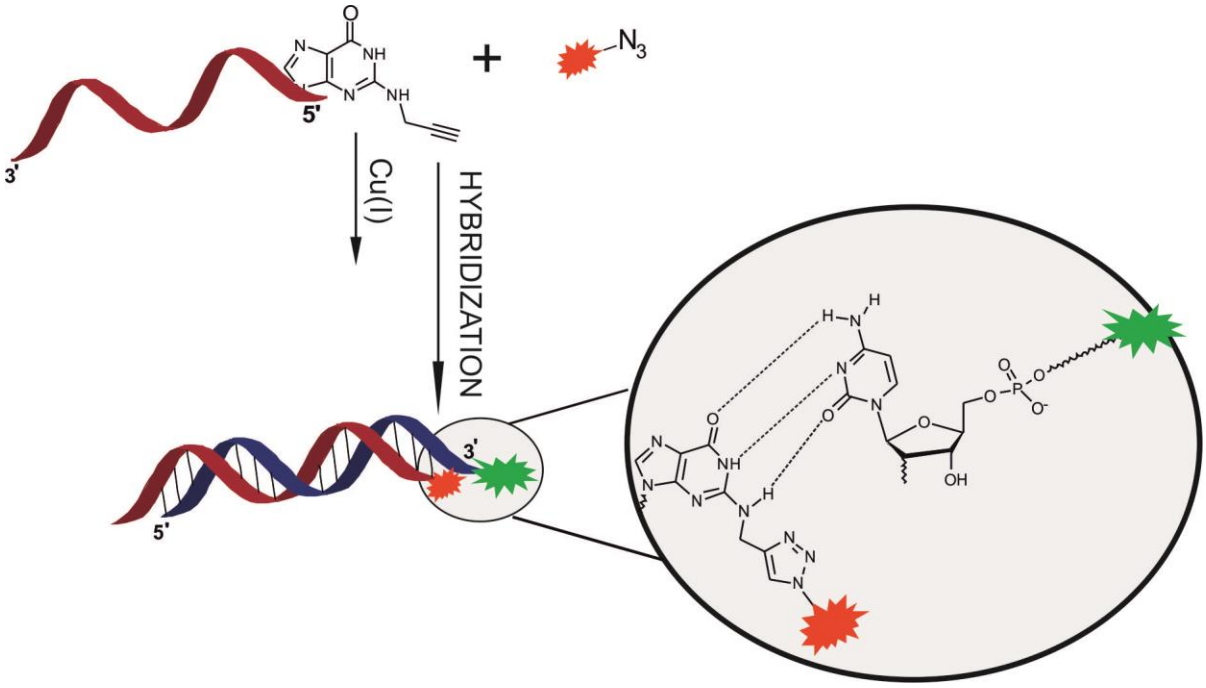

Fig. 3.3 Click reaction between the alkyne functionalized oligonucleotide and the azide dye, followed by a hybridization step with the 3'-labeled complementary strand, showing reserved base pairing between the modified G and the C on the sense strand.

In the current studies, a similar modification was done to guanosine, but one that would allow a click-ligation onto the nucleobase sugar edge. Just as is the case with m_2G, it was thought that Watson-Crick base pairing with the complementary base (figure 3.3) should still be possible after incorporating an N^2-propargyl modified derivative of guanosine into an oligonucleotide strand. Even after reacting the incorporated propargyl group with an azido dye, the remaining free electron pair on N^2 would still enable hydrogen bond formation.

3.4.1 Guanosine modification and phosphoramidite synthesis

Earlier studies on the methylation of guanosine on N^2 have shown that the alkaline reaction conditions for direct alkylation led to imidazole ring opening, mainly due to a preferred attack at position 7 of the purine ring[161]. As a result, different alternative preparation possibilities

had to be considered, of which the direct introduction of an alkylamino group – in their case methylamino and dimethylamino, respectively – seemed to be the most promising option. Seeing that position 6 of guanosine would be more susceptible to nucleophilic attack, the oxygen of the amide function at this position was masked by NPE as protecting group and as a result, the purine ring was also rendered more aromatic for substitution at position 2. Nevertheless, the introduction of a better leaving group at this position was still required to ensure substitution by the alkyl amine. Fluorine was incorporated during a diazotization reaction with $NaNO_2$ and HBF_4, where the latter acted both as acid and source of the fluoride ion. The consequent reaction with the suitable alkyl amine under mild reaction conditions resulted in the desired N^2-alkylated compound.

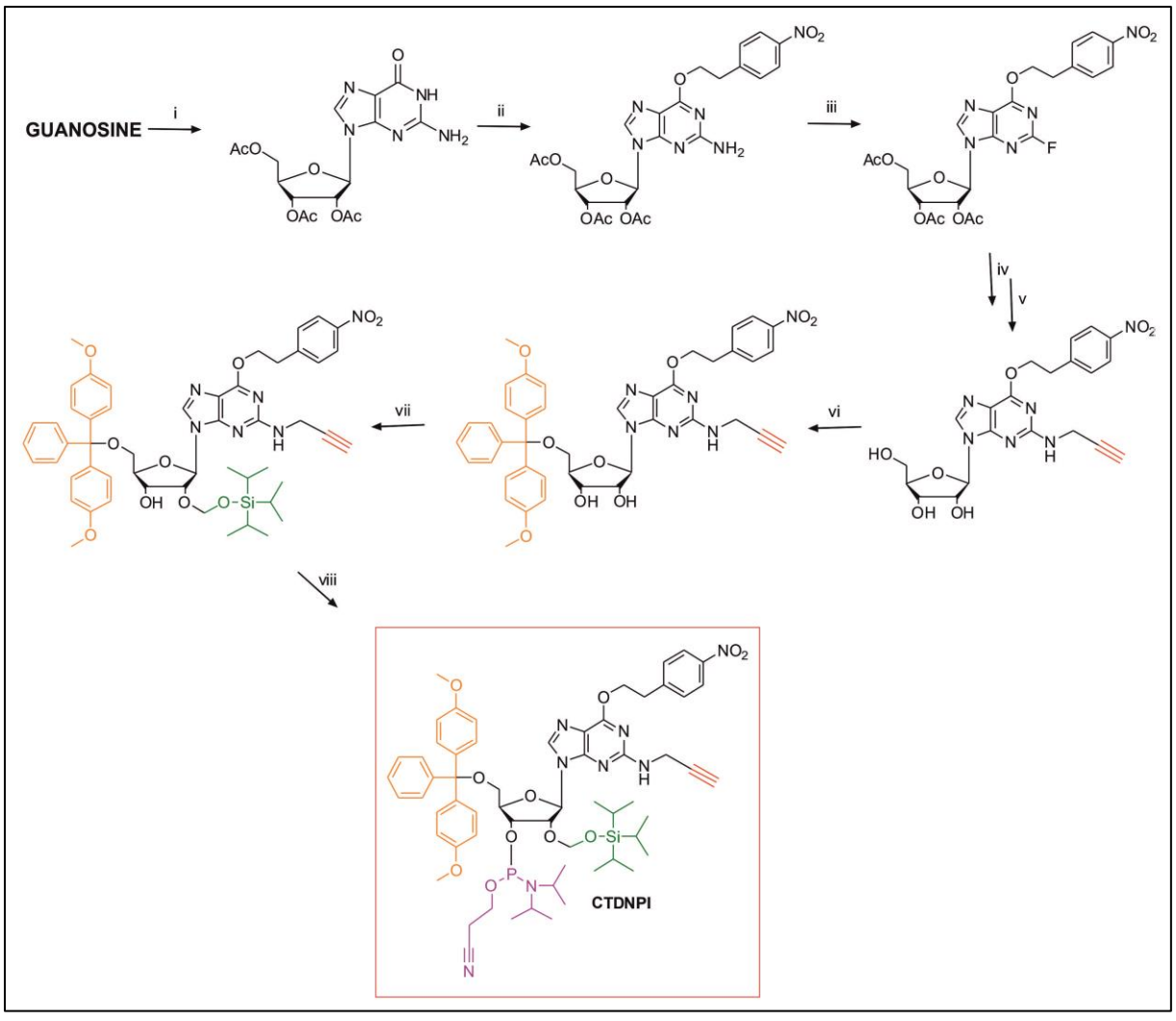

Scheme 3.3. Eight step synthetic route to the final alkyne functionalized phosphoramidite of guanosine (**CTDNPI**): *(i)* peracetylation of guanosine, *(ii)* ether synthesis *via* the Mitsunobu reaction, *(iii)* diazotization of the aromatic amine and nucleophilic substitution by the fluoride ion, *(iv)* nucleophilic substitution of the fluoride ion by propargylamine and concomitant hydrolysis, followed by the *(vi-viii)* three-step phosphoramidite synthesis.

For the synthesis of the propargyl containing guanosine derivative, a similar synthetic route was followed as was published for the chemical synthesis of the m^2G synthon[161]. Following the Mitsunobu reaction of the oxygen on position 6 of guanosine, the exocyclic amine on position 2 was targeted for a diazotization reaction, as described above. This intermediate was converted to the 2-fluoride derivative by means of a nucleophilic substitution reaction with HBF_4. Finally, for the introduction of the terminal alkyne, propargylamine was used as nucleophilic substituent for fluoride to produce O^6-nitrophenyl-2-propargylaminylinosine (Scheme 3.3, steps *i*-*v*).

With the aim of incorporating the modified nucleobase into a synthetic RNA strand during solid phase oligonucleotide synthesis (SPOS), the phosphoramidite of O^6-nitrophenyl-2-propargylaminylinosine was synthesized (steps vi-viii in scheme 3.3). The O^6-4-nitrophenylethyl protection group would be susceptible to cleavage by β-elimination at the end of the oligonucleotide synthesis and would thus be removed during the standard deprotection steps after SPOS. [(Triisopropyl)silyloxy]methyl (TOM)-chemistry was preferred for 2'-protection of the RNA phosphoramidite, due to the tendency of the common 2'-protecting agent, *tert*butyldimethylsilyl (TBDMS), to migrate from the 2'- to the 3'-position. This side reaction commonly occurs for TBDMS during the phosphitylation step of the phosphoramidite synthesis, whereas TOM is stable in this regard. Additionally, as compared to TBDMS, the TOM group also has a reduced steric demand during internucleotide bond formation, and as a result allows for higher coupling yields in oligonucleotide syntheses.

3.4.2 Incorporation of the propargyl containing guanosine phosphoramidite into an siRNA strand

The chemical synthesis of oligonucleotides makes it possible to site-specifically incorporate both natural and artificial nucleoside modifications into RNA and/or DNA. It has thus far proven to be a useful tool for biochemical and biophysical investigations of nucleic acid structure and function. The role of synthetic antisense oligonucleotides in gene silencing is such an example.

Not only have chemical modifications aided the clinical application of siRNA, but also the search for a deeper understanding of the mechanism that underlies RNAi. Here, molecular imaging techniques serve as powerful tools to track cellular siRNA *in vivo*, as well as to monitor siRNA activity[162]. Fluorescence microscopy has always been valuable to investigate complicated biological processes and, thus far, various fluorescent analogues have been

explored as spectroscopic tags for the investigation of subcellular distribution patterns of siRNA[163].

More recently, fluorescent resonance energy transfer (FRET) between dyes that are attached to the two respective strands of an siRNA double strand has made it possible to successfully trace the structural integrity of the RNA duplexes inside cells[162,164,165]. In our laboratory the Atto 488 dye, together with Atto 590 - both attached to the two opposing strands of the siRNA duplex directed against the enhanced green fluorescence protein (eGFP) - has proven to be a favorable combination for FRET applications[165]. The Atto 488 dye, which acts as donor dye during FRET, is attached to the 3'-end of the sense strand, whereas the 5'-end of the antisense strand carries the Atto 590 dye as acceptor. This dye combination has made it possible to estimate the spatial proximity between two siRNA strands and both RNA distribution and its degradation can thus be followed inside cells.

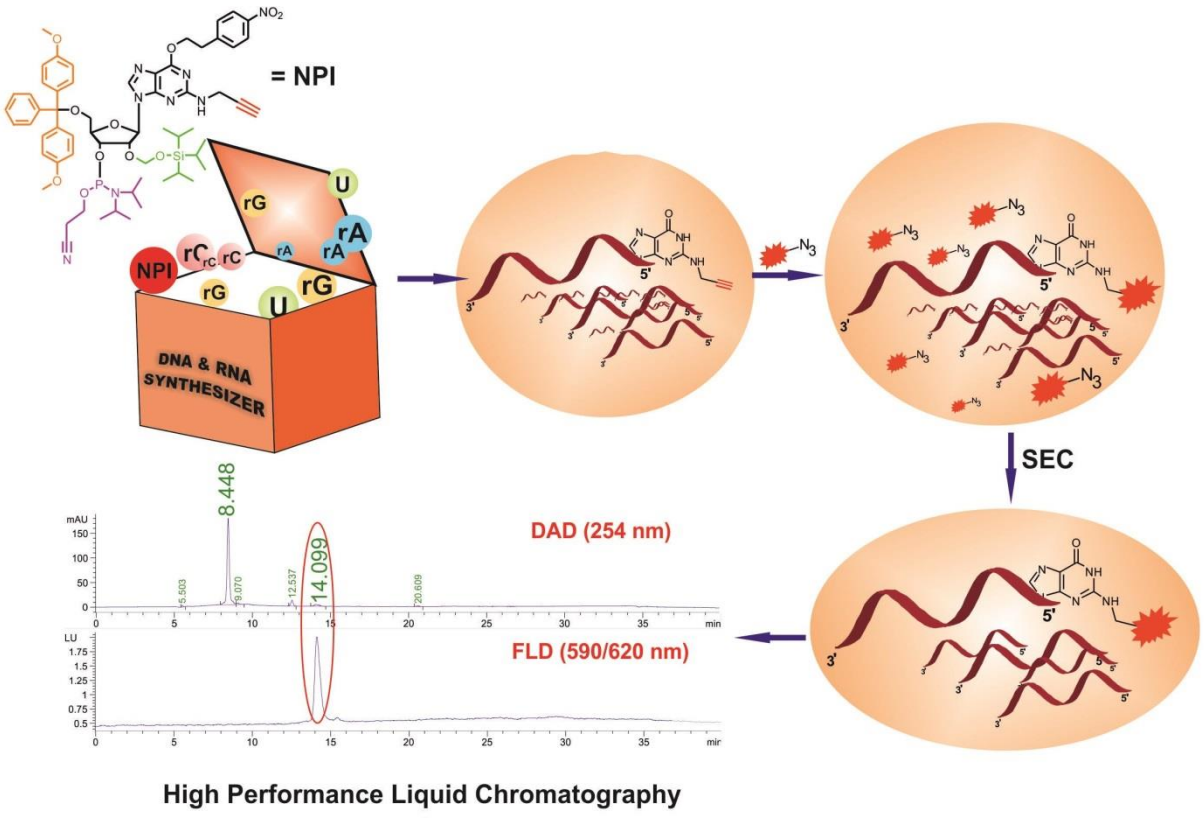

Fig. 3.4 Synthesis and purification of the modified siRNA strand: *(i)* Oligonucleotide synthesis and deprotection, *(ii)* CuAAC with Atto 590 azide, *(iii)* Size exclusion chromatography (SEC) for removal of unreacted dye and other small molecules and *(iv)* HPLC for separation of full-length, labeled oligonucleotide (14 min) from abortion products (8 min).

Despite the various advantages associated with such FRET applications and dye labeling of short RNA strands in general, the question arises whether fluorescent labeling may have a

negative impact on the capacity of synthetic RNA as biological agents. Seeing that siRNA is known to interact with cellular components, this is particularly applicable to them. It is also of concern whether base pairing between the two duplex strands may be compromised due to the attachment of a fluorescent label, irrespective of the labeling position.

In order to explore the labeling of RNA at the guanosine sugar edge in an siRNA model system, the propargyl containing guanosine phosphoramidite was incorporated onto the 5'-end of an antisense siRNA. This enabled click-ligation of the synthesized strand with an azido functionalized fluorophore onto the nucleobase sugar edge (figure 3.4).

Oligonucleotide synthesis was performed in the 'DMT-off' mode. The purification of the full-length antisense strand (containing the modification on the 5'-end) was simplified by performing a click reaction with the crude, which was obtained after standard deprotection procedures for the removal of the base and 2'OH protecting groups. This resulted in labeling of only the full-length oligonucleotide product with the desired fluorophore (Atto 590 azide), which could easily be separated and identified by reversed phase HPLC, mainly due to higher lipophilicity and fluorescence properties attributed to the attached dye. The HPLC purification was preceded by manual size exclusion chromatography (Nap 10), to remove unreacted dye and other small molecules (such as cleaved blocking groups) from the reaction mixture. After precipitation from ethanol, the mass of the labeled antisense strand was confirmed by MALDI-TOF analysis. The MALDI-TOF analyses were performed at the Institute of Pharmacy and Molecular Biotechnology, Department of Pharmaceutical Chemistry, Heidelberg University, by Heiko Rudy.

As can be gathered from the HPLC profile in figure 3.4, the labeled oligonucleotide comprises a mere 10% of the total RNA content and the abortion products of oligonucleotide synthesis makes up the majority of the UV/Vis absorption profile. This can either be explained by very low coupling sufficiency of the modified guanosine phosphoramidite during SPOS, possibly due to prior phosphoramidite decomposition, or insufficient click ligation between the modified oligonucleotide and the azido dye. The reaction conditions for the click ligation have been optimized, thus suggesting phosphoramidite decomposition as the cause of low alkyne containing oligonucleotide yields. This, in turn, of course resulted in lower yields of the labeled oligonucleotide.

3.4.3 Structural and functional analyses of labeled siRNA duplexes

Considering the possible effects of siRNA labeling, a range of structural and functional data were acquired for the synthesized strand. After hybridization to both the Atto 488 labeled and

the unlabeled complementary sense strands, respectively, temperature dependent differential UV-absorption spectra were measured to determine the thermal stability of the obtained siRNA duplexes.

Functional studies included the analysis of the knockdown efficiency of the modified siRNA against the eGFP reporter gene. In the past, several statements, some of which are contradicting one another, have been made with regard to the effect of labeling of siRNA oligonucleotides on their gene silencing efficacy. Here, positional labeling, *i.e.* 3'-sense *vs.* 5'-antisense labeling, was of particular interest. Chen *et al.* reported that a block of the 5'OH completely abolishes RNA interference (RNAi) activity of the given siRNA strand[166]. This is in accordance with former studies that stated that 5'OH methylation results in a complete loss of RNAi activity, possibly due to the resultant hindrance of 5'OH phosphorylation *in vivo*[166,167]. In contrast to 5'-*O*-methylation, 3'-block seems to have no effect on RNAi, as claimed by Schwarz *et al.* in 2002[167]. Surprisingly, results obtained by Harborth *et al.* suggested the exact opposite, *i.e.* the complete loss of silencing activity due to a fluorescent dye attached to the siRNA 3'-end[168].

In order to investigate these statements and provide a better explanation for these contradictory hypotheses, a comparison was made between the newly synthesized antisense strand, which carries the label on the guanosine sugar edge, thus leaving the 5'OH free and the commercially available antisense oligonucleotide that is labeled *via* its 5'-phosphate (see figure 3.5). Additional knockdown studies were performed to evaluate the influence of the physical properties of the dye on RNAi and how these results compare to results obtained for unmodified siRNA duplexes.

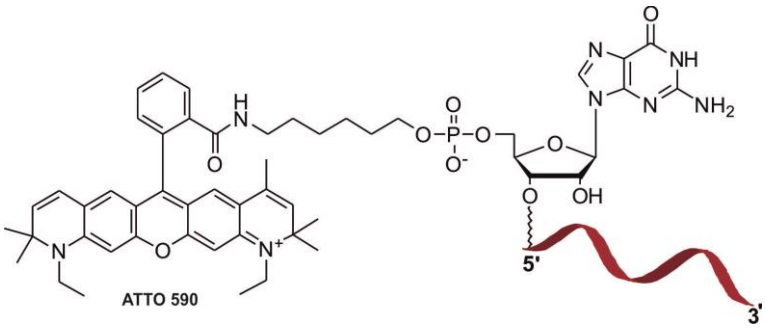

Fig. 3.5 Commercial antisense strand, containing the Atto 590 dye as label on the 5'-phosphate.

Cell transfection studies were performed to evaluate the uptake and *in vivo* tracking of siRNA during live cell imaging.

3.4.3.1 Electrophoretic mobility shift analysis

The synthesized antisense strand was hybridized to its complementary sense strand – unlabeled and 3'-Atto 488 labeled, respectively. The state of hybridization was confirmed by native polyacrylamide gel electrophoresis (PAGE). The unstained gels showed a shift in the bands of the hybridized strands. The fluorescence transfer from the donor to the acceptor dye could be observed when exciting the gel at 488 nm and detecting acceptor dye emission at 670 nm (figure 3.6).

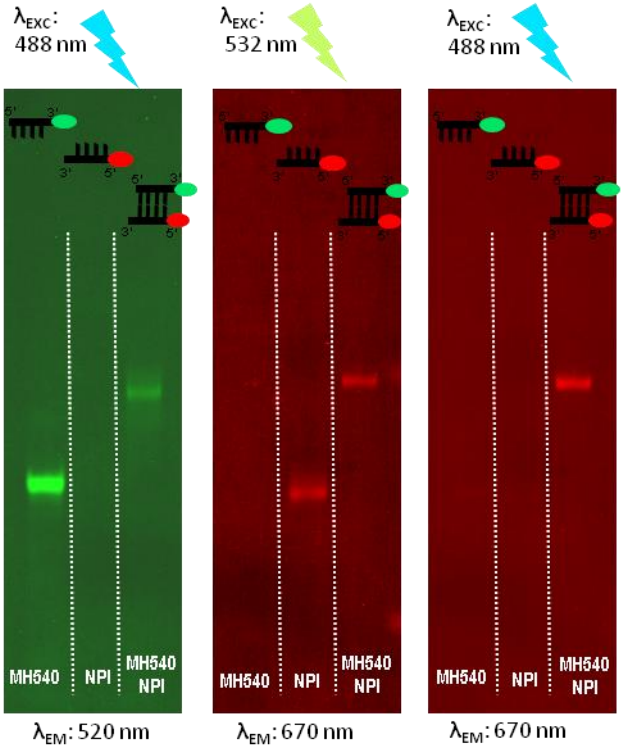

Fig. 3.6 Native PAGE analysis of the single stranded siRNAs, commercial sense strand (MH540) and the synthesized antisense strand (*NPI*), respectively and the double labeled construct (MH540/*NPI*). The gels were excited at 488 nm and emission was recorded at 520 nm and 670 nm for FRET, respectively (left and right). The middle gel shows excitation at 532 nm and emission at 670 nm.

3.4.3.2 Temperature-dependent differential UV-absorption measurements of siRNA duplexes

The thermodynamic stability of the siRNA duplex plays a significant role in RNAi. After strand separation, only one of the two strands is incorporated into the RNA induced silencing complexes (RISC) and the stability at the 5'-end determines which strand is selected as guide strand[150]. If modification of the siRNA leads to changes in duplex stability, the *in vivo* activity of such a strand would thus also be influenced.

For analyzing both the effect of oligonucleotide labeling and the effect of the method of labeling on base pairing and stability of the siRNA duplexes, temperature dependent differential UV-absorption melting measurements were performed. Both single and double labeled constructs were measured and compared to the thermal stability of unlabeled duplexes. Labeled constructs carried the Atto 590 dye on the 5'-end and/or Atto 488 on the 3'-end. As reference, the 5'-phosphate labeled antisense strand (figure 3.5) was used for comparison with our sugar edge labeled strand (*NPI*).

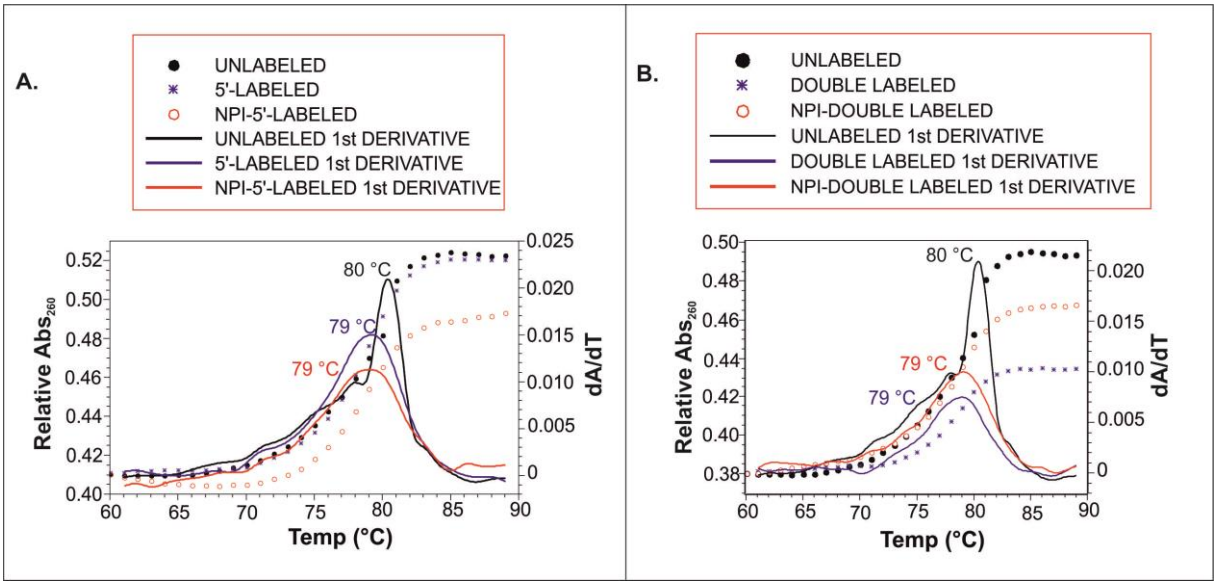

Fig. 3.7 Comparison of the UV melting curves of the unlabeled siRNA (black) with those of the **A.** single labeled and **B.** double labeled constructs.

Compared to unlabeled strands, the melting analyses of the siRNA double strands show only a very slight difference in the melting temperatures of labeled strands in general, as (figure 3.7). No significant difference could be observed for the 5'-phosphate labeled strand, as compared to labeling on the guanosine sugar edge and the slight destabilizing effect is rather associated with 5'-fluorescent labeling of siRNA duplexes as such. It can thus be concluded that, irrespective of the nature of 5'-labeling, the structural impact of labeling on this position is almost negligible. In correspondence with previous findings[169], 3'-labeling on the opposing strand had no significant effect on duplex stability.

3.4.3.3 Concentration dependent knockdown efficiency of the eGFP reporter gene

As mentioned earlier, siRNA labeling may have an influence on RNAi and controversy exists for particularly 5'-*O*-labeling of the antisense strand. Harborth *et al.* claimed that a 5'-

phosphate linkage on siRNA is tolerated in RNAi[168]. In total contrast, other groups have attributed a complete loss of siRNA activity to 5'-*O*-labeling, likely due to a loss of 5'-phosphorylation in the presence of the methylated 5'OH[166,167]. A clearly picture thus needs to be painted with regard to these controversies.

Thus, the effect on the activity of the siRNA by our new labeling method *vs.* 5'-*O*-labeling could be assessed by analyzing eGFP expression in cells that were transfected with these differently labeled siRNA strands directed against the same reporter gene, *i.e.* eGFP. The eGFP signal was analyzed in the presence of varying concentrations of the respective double strands by means of fluorescence activated cell-sorting (FACS). This quantitative analysis, performed by Bettina Krieg, made it possible to determine IC_{50}-values for the differently labeled and unlabeled siRNAs. Seeing that it is unlikely that any type of labeling would either completely abolish or even have absolutely no effect on RNAi, the comparison of IC_{50}-values between 5'-*O*-labeled and 5'-*O*-unlabeled duplexes could provide a better defined effect of masking the antisense 5'-OH on RNAi.

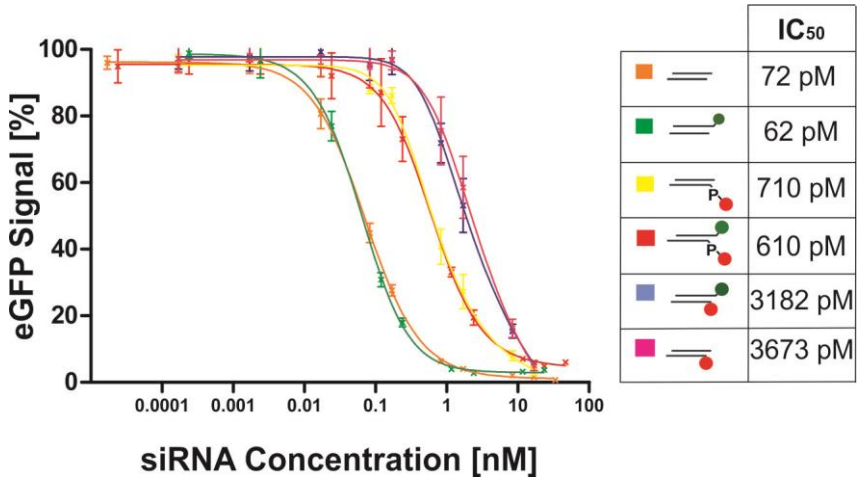

Fig. 3.8 Concentration dependent knockdown efficiencies of various constructs on the eGFP signal: (—) Unlabeled; (—) Only 3'-labeled; (—) Only 5'-labeled *via* phosphate; (—) Double labeled with 5'-label on phosphate; (—) Double labeled with 5'-label on guanosine sugar edge; (—) Only 5'-labeled *via* guanosine sugar edge (All Atto 488 labels were contained on the 3'-phosphate of the sense strand).

The results shown in figure 3.8 suggest that 3'-labeling, in general, has no effect on the knockdown efficiency. However, 5'-labeling seemed to have a more significant impact. In contrast to the previous findings that 5'-labeling completely abolishes RNAi activity[169–171], all our 5'-labeled constructs delivered good knockdown of the eGFP gene. Compared to the unlabeled construct, the 5'-phosphate labeled siRNA showed a mere ten fold increase in the IC_{50}-value and labeling *via* the sugar edge caused an IC_{50} increase by a factor of only 50.

These results show that avoiding the 5'OH of the ribose for labeling is not necessarily a requirement for RNAi.

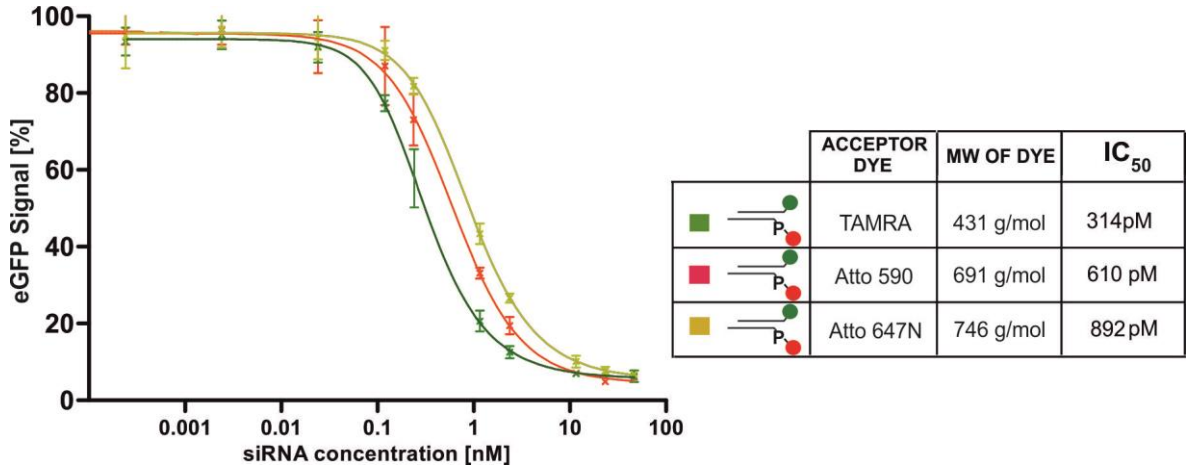

Fig. 3.9 Graph showing the dependence of the size of the 5'-dye on the knockdown efficiencies of the eGFP signal by different double labeled constructs (3'-label = Atto 488).

However, these results do not reflect to what extent the increased IC_{50}-values are influenced by the physical properties of the dye itself. For this reason, a new set of data was collected for siRNA strands carrying different dyes, *i.e.* tetramethylrhodamine (TAMRA), Atto 590 and Atto 647N on a linker attached to their 5'-phosphate. A rough correlation could be made between the increase in IC_{50}-value and molecular weight of the dye, where higher molecular weight dyes led to higher IC_{50}-values (figure 3.9). The dependence of RNAi activity on the size of the dye suggests that a steric clash may occur between the dye and protein factors in the RNAi pathway, which likely occurs during strand separation and incorporation of the antisense strand into RISC.

3.4.3.4 Cell transfection studies

The *in vivo* imaging of labeled siRNA is necessary to investigate the post-transfectional fate of the RNA and may thus contribute to a better understanding of the RNAi pathway. Especially the intracellular degradation of siRNA still raises a lot of questions. For this reason, a variety of molecular imaging techniques have been explored in literature for the *in vivo* imaging of RNAi[172–174].

After confirming the retained knockdown activity of the siRNA after labeling *via* the guanosine sugar edge, the cellular distribution of the duplexes could be investigated. A standard procedure for the transfection of synthetic siRNA in our laboratory was followed for

the uptake of our Atto 590 labeled siRNA into rat brain endothelial (RBE4) cells[175]. Oligofectamine was used as transfection agent, before fixing and optical imaging of the cells. These experiments were performed by Markus Hirsch. Images obtained with a confocal scanning microscope (figure 3.10) shows that neither transfection, cellular uptake, nor intracellular distribution of the labeled strand was influenced by labeling *via* the guanosine sugar edge. This post-synthetic labeling of the alkyne modified siRNA has the advantage that a variety of azide dyes can be used for functionalizing the antisense siRNA strand, thus making it possible to be used in combination with a variety of labeled sense strands during FRET imaging.

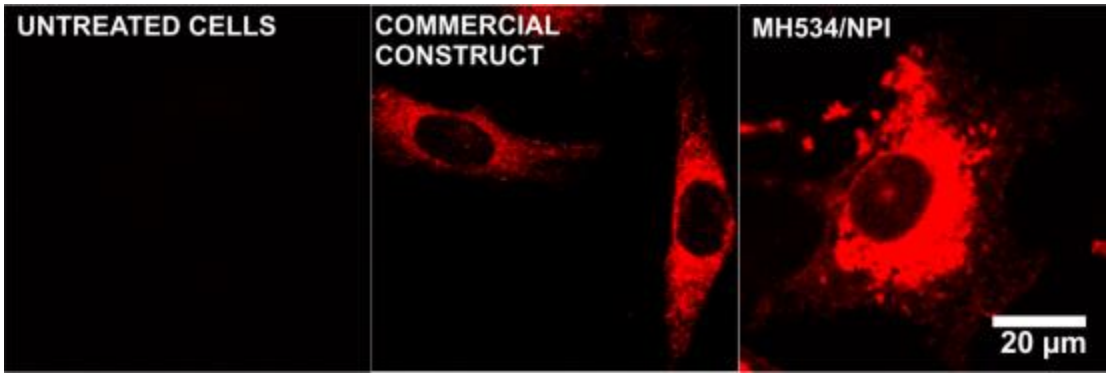

Fig. 3.10 Cell imaging after excitation at 561 nm of RBE4 cells, transfected with single labeled commercial (middle) and our *NPI* construct (right), respectively.

3.5 Conversion of thymidine to a 'clickable' 5-methylcytidine (m^5C) derivative for incorporation into oligonucleotides

3.5.1 Nucleoside modification and phosphoramidite synthesis

5-Methylcytosine (m^5C) is an epigenetic modification, formed by the methylation reaction of DNA methyltransferases (DNMTs)[3]. The deamination of m^5C by the activation induced cytidine deaminase (AID) enzymes leads to the formation of thymidine. On the other hand and from a synthetic point of view, the chemical synthesis of m^5C from thymidine was first reported in 1959 by Fox *et al.*[176]. The authors made use of a thiation (also known as thionation) reaction of thymidine at position four, followed by treatment with alcoholic ammonia, to chemically convert U-type nucleosides to their cytosine counterparts.

A different approach towards the aminolysis of position four of thymidine was *via* the intermediate, 4-(1,2,4-triazolyl)thymidine, which was formed after protecting the ribose alcohol functions with either trimethylsilyl or acetyl groups. Treatment of the triazolyl

intermediate with ammonia led to the formation of the desired 5-methylcytosine[177]. A more recent reaction route involves the activation of position four as aryl sulfonate ester, followed by a displacement reaction with ammonia[178] (see scheme 3.4).

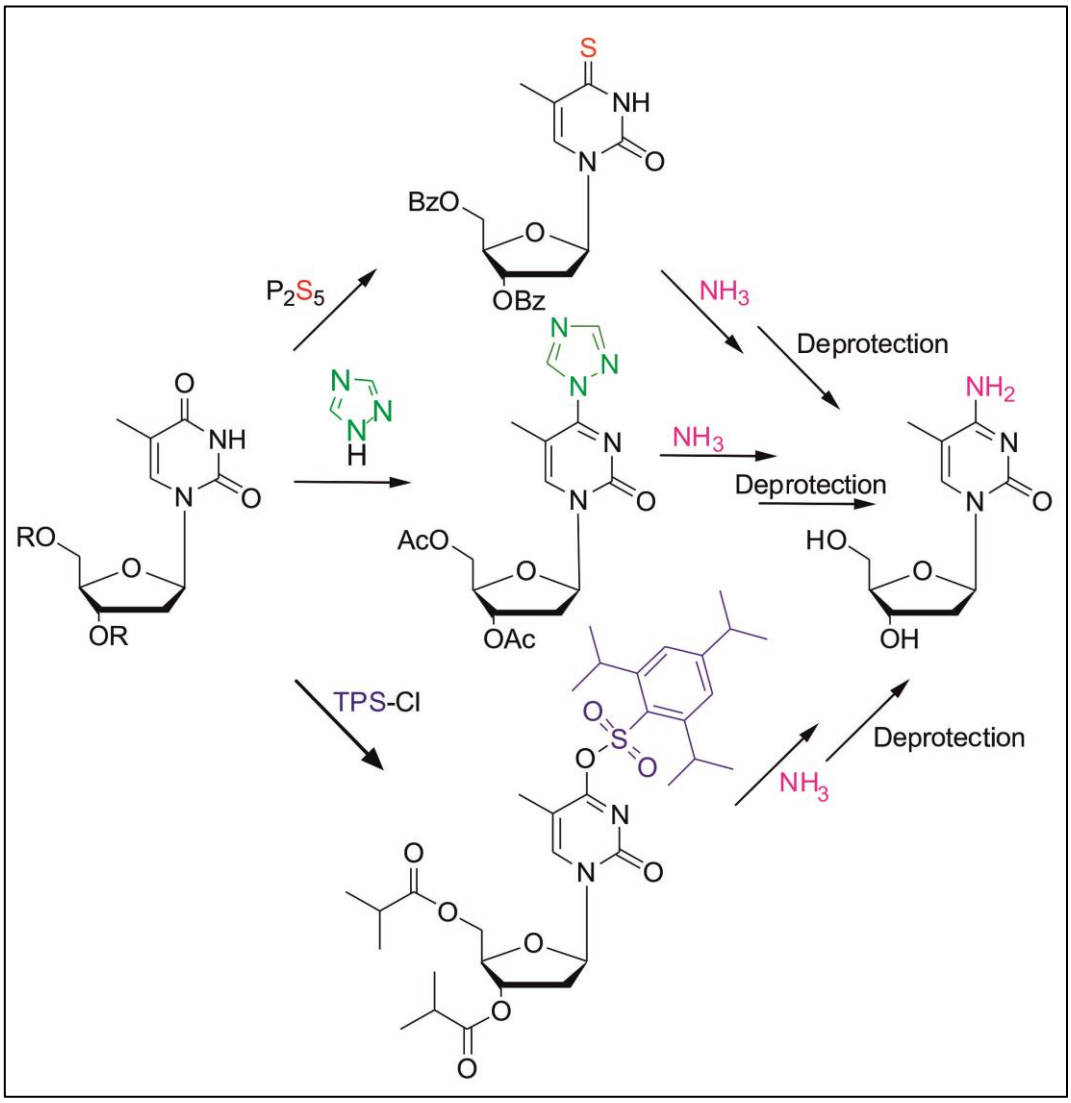

Scheme 3.4 General synthetic routes for the conversion of thymidines to cytosines. Thiation reaction (red) adapted from Fox *et al.*[176], triazolyl formation (green) adapted from Sung[177] and route *via* the aryl sulfonate ester (blue) adapted from Gaffney *et al.*[178].

This type of reactions not only makes the interconversion of uridines or thymidines to cytidines possible, but also provides the possibility to functionalize cytidine-type nucleosides at the N^4-position. The use of amines other than ammonia in the substitution reaction of the aryl sulfonate ester or triazolyl group would introduce the desired functionality at N^4 of cytidine. However, the use of temporary protecting groups for the 3'- and 5'-OH's is still required in these substitution reactions, making it necessary to employ additional protection and deprotection steps. In an attempt to produce the phosphoramidite of 5-hydroxymethyl-2'-

deoxycytidine from 2'-deoxyuridine, Hansen *et al.*[44] changed the reaction sequence for phosphoramidite synthesis. Instead of introducing the dimethoxytrityl (DMT) group for phosphoramidite synthesis after base modification, as is usually the case, the introduction of the 5'-DMT was implemented before the sulfonylation step. This step not only avoided the use of temporary protecting groups for the aminolysis, but also facilitated the purification of otherwise polar intermediates.

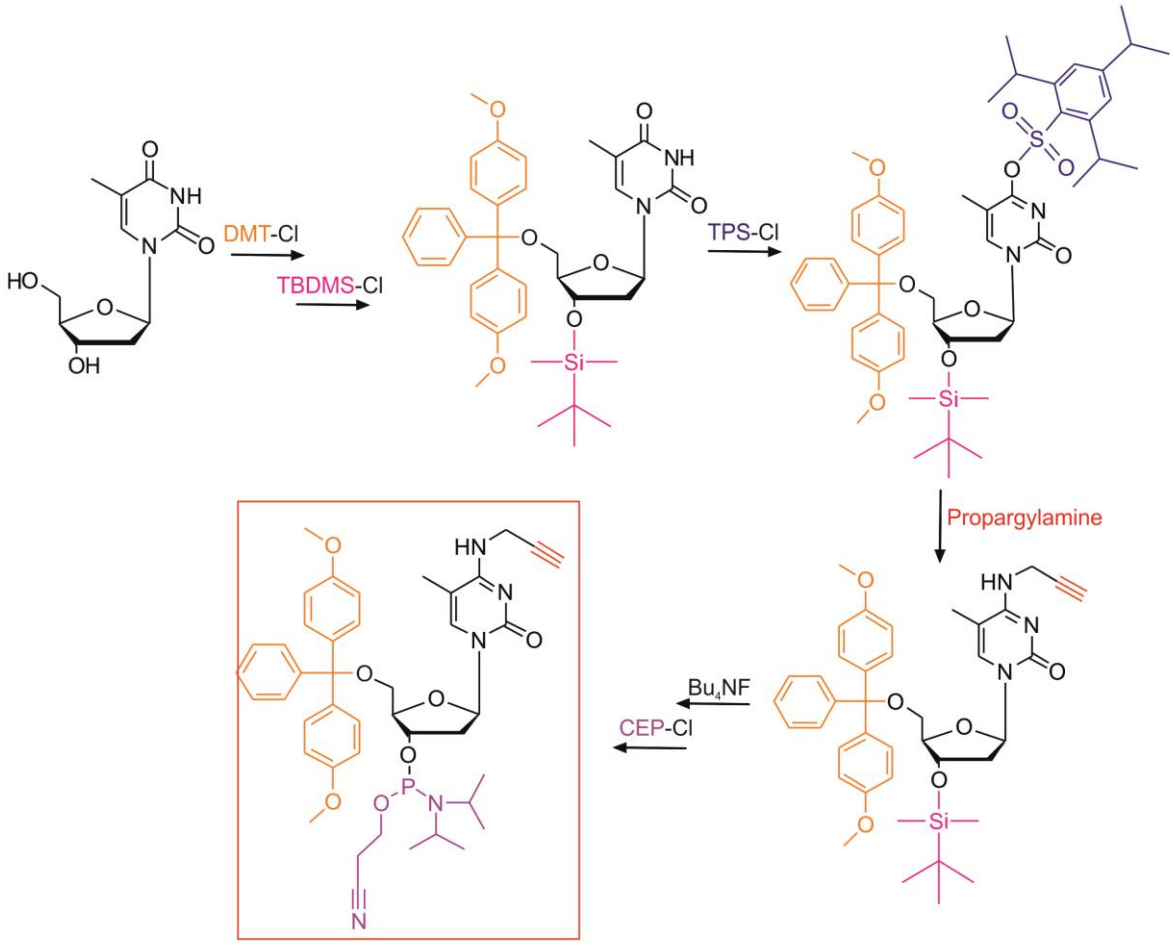

Scheme 3.5 Synthesis procedure towards 3'-*O*-CEP-5'-*O*-DMT-5-methyl-N^4-propargylaminyl-2'-deoxycytidine.

A similar approach was followed in this thesis for the functionalization of deoxycytidine. As was described by Hansen *et al.*[44], the conversion of thymidine to its sulfonyl ester derivative was preceded by the tritylation of the thymidine 5'OH. However, the current experiments included an additional protective group for the 3'OH, *i.e. tert*butyldimethylsilyl (TBDMS), was attached, followed by the sulfonylation reaction with triisopropylbenzenesulfonyl chloride and triethylamine, together with a catalytic amount of 4-dimethylaminopyridine (DMAP). The resulting 3'*O*-,5*O*'-protected O^4-triisopropylphenylsulfonyl thymidine was

isolated and reacted with propargylamine to introduce the functionalized amine on position 4 of cytidine.

The presence of the propargyl functionality on position N^4 eliminated the necessity of protecting the cytidinic amine, which is generally a requirement for oligonucleotide synthesis. Following the removal of the 3'*O*-TBDMS, the conversion of the modified cytidine derivative (already containing the trityl protection group on its 5'-position) to its phosphoramidite could thus easily be obtained *via* a simple phosphitylation step with 2-cyanoethyl-*N*,*N*-diisopropylchlorophosphoramidite (scheme 3.5).

3.5.2 Incorporation of the propargyl containing m^5C phosphoramidite into DNA

DNA and RNA form different double helix conformations. In general, the A-form geometry of RNA-only duplexes and RNA/DNA hybrids show higher thermodynamic stability than the common B-form of DNA/DNA duplexes. These differences may cause that base modifications within the respective secondary nucleic acid structures may be tolerated to distinctive extents.

With the aim of investigating the influence of the propargyl modification on duplex stability in both types of nucleic acid strands, a series of oligodeoxynucleotides have been synthesized that contain the propargyl 5-methylcytosine at varying positions. A random sequence was chosen and the strand complementary to the antisense siRNA directed against eGFP was decided upon. The differently modified DNA strands were later to be hybridized to their DNA and RNA complementary strands, respectively, in order to determine whether a major difference in stability could be detected between the effect of this type of modification on DNA-only *vs.* mixed (*i.e.* DNA/RNA) duplexes.

3.5.2.1 Oligonucleotide synthesis and mass spectrometric analysis

By singly substituting the C-residues in the DNA sense strand with 5-methyl-N^4-propargylaminyldeoxycytidine *via* SPOS, a total of seven DNA strands, each carrying the propargyl functionality at varying positions, was obtained (figure 3.11). The only exception was the incorporation of the modification instead of the adenosine base on the 3'-end. Here, the effect of terminal labeling (*i.e.* both 3'- and 5'-modification, respectively), as compared to the influence of internal modifications was of particular interest. Keeping in mind that standard siRNA contain two nucleotide overhangs on their 3'-end, it was envisaged that labeling at this position would have the lowest impact on the hybridization properties of the

resulting duplexes. As reference, the same DNA sequence was synthesized, with all unmodified cytidines in position.

Different from the procedure followed for the guanosine modified oligonucleotides, these 'DMT-off' synthesized strands were PAGE purified prior to their click labeling. Taking into account that the bulkiness and other characteristics of the dye itself may cause additional contributions to changes in melting behavior of the duplexes, the mere substitution of one of the hydrogens on N^4 with a propargyl group was to be investigated.

MALDI-TOF (by Heiko Rudy) and LC/MS (by Dr. Stefanie Kellner) measurements served as methods to confirm both the total mass of the synthesized strands, as well as the incorporation of the modified bases within the oligodeoxynucleotides. As internal standard for MALDI-TOF measurements, a commercial DNA strand of shorter length and lower molecular mass was used. With the exception of the modification carried on the 3'-overhang, where A was replaced instead of C, the calculated mass for the oligonucleotides carrying the modification was 6771 g/mol. The substitution of A instead of C resulted in a calculated mass of 6748 g/mol. The unmodified DNA sense strand weighs 6719 g/mol. Figure 3.12 shows MALDI-TOF spectra for four of the eight oligonucleotides, serving as example for the confirmation of the correct masses for all the synthesized oligonucleotides.

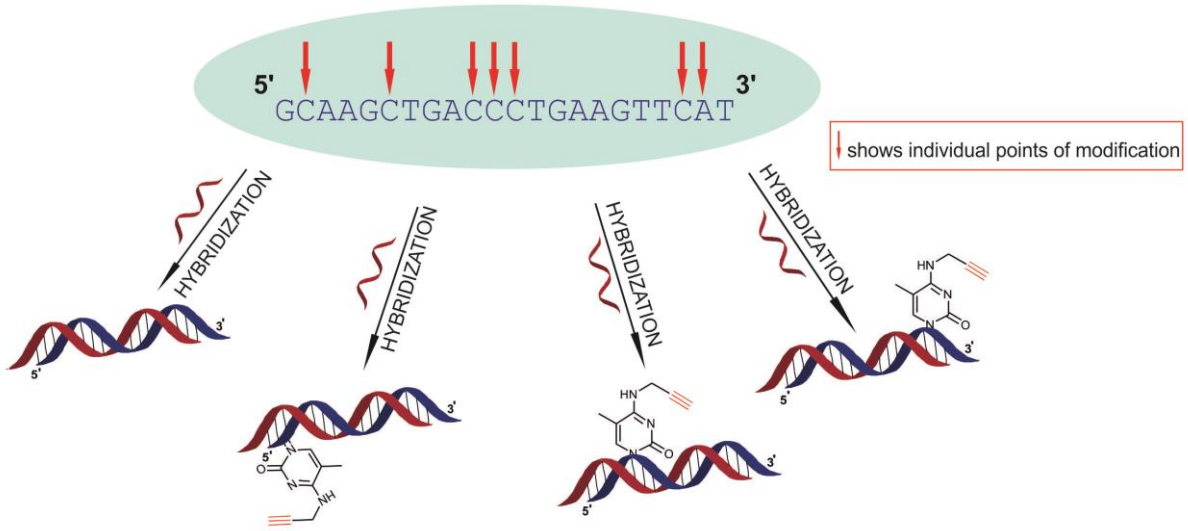

Fig. 3.11 Sequence of the synthesized DNA strand, showing positions of single incorporation of the propargyl containing cytidine derivative. The modified strands were hybridized to the complementary strand – both RNA and DNA, respectively.

For LC/MS analysis of the modified oligonucleotides, a standard was required of the modified base in order to predict its expected retention time after glycosidic bond cleavage. For this purpose the pre-phosphoramidite, 5'-*O*-DMT-5-methyl-N^4-propargylaminyldeoxycytidine,

was detritylated under acidic conditions (scheme 3.6) and purified *via* silica gel chromatography. Interesting to observe, was the presence of a second absorption peak with a similar mass fragmentation pattern, however, with an earlier retention time (t_R) during the reversed phase liquid chromatography run. This occurred both for the single nucleoside that was used as standard, as well as for the enzymatically digested oligonucleotides that contain the modification. Based on the absorption intensities of both chromatograms, the amount of the less polar component was estimated to be in the order of 1% of that of the main product.

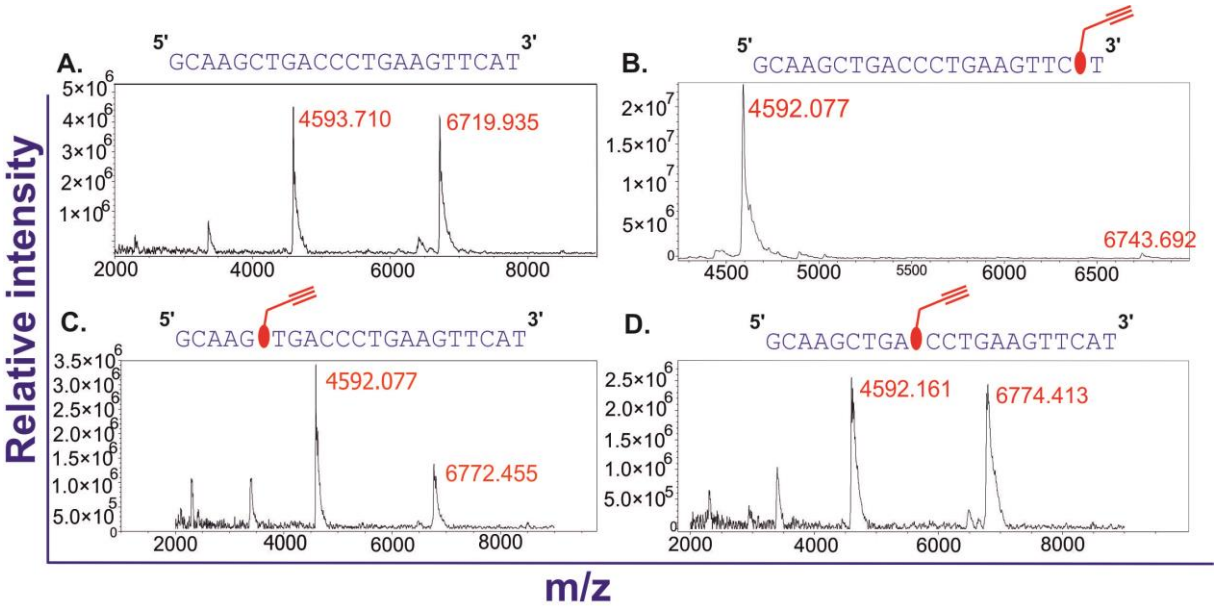

Fig. 3.12 MALDI-TOF results for four of the synthesized oligodeoxynucleotides. A shorter DNA strand *(MW: 4592 g/mol)* was used as internal standard in all cases: **A.** Unmodified *(calculated MW: 6719 g/mol)*; **B.** 3'-modified *(calculated MW: 6748 g/mol)*; **C** and **D.** internally modified oligodeoxynucleotides *(calculated MW: 6771 g/mol)*.

The similar mass fragmentation patterns of the two compounds suggest that an isomer of the desired propargylated cytidine derivative was formed during its chemical synthesis. The difference in retention times could be contributed to differences in electron density between the two isomers, caused by the varying charge distributions throughout the respective molecules. A structural analogue of 2'-deoxy-5-methyl*iso*cytidine, which carries the propargyl functionality on position 2, is a supposed structure for the isomer. Its suggested synthesis is depicted in scheme 3.7. The much higher abundance of the N^4-substituted compound can be explained by the influence of the methyl group on position five, which likely causes a stabilization of the intermediate products that form during substitution on position four of thymidine. An inductive effect is probably the result of an increased electron density in the aromatic ring, due to the presence of the methyl group. This mechanism is,

however, only a hypothesis and may be confirmed by subjecting 2'-deoxyuridine to similar reaction conditions.

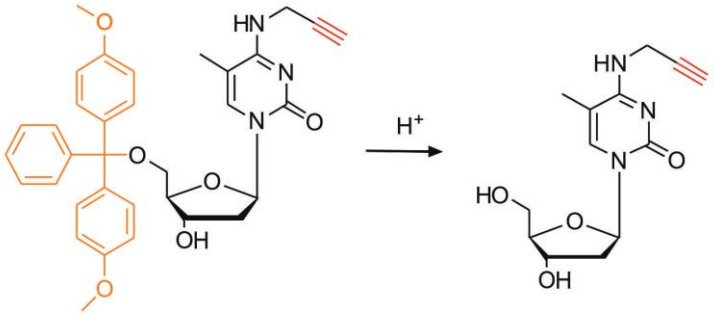

Scheme 3.6 Detritylation of 5'-*O*-DMT-5-methyl-N^4-propargylaminyldeoxycytidine.

The spatial proximity between the proton of the alkyne functionality and the 5-CH_3 protons were confirmed *via* 2D NOESY NMR and serves as support of the theory that the N^4-substituted derivative is indeed the main product formed during this experiment. The 2-dimensional NMR experiments were performed by Dr. Christoph Kreutz at the Institute of Organic Chemistry, Innsbruck University, Austria.

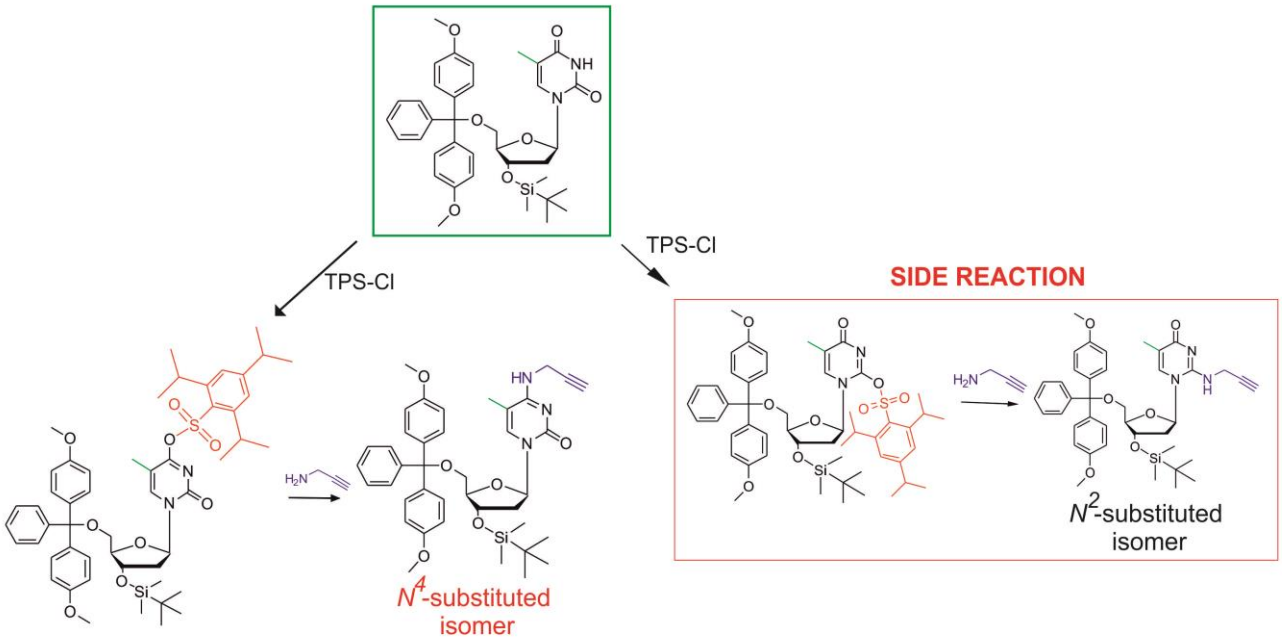

Scheme 3.7 Suggested reaction progress during the formation of the 4-substituted cytidine derivative, together with its less abundant 2-substituted isomer.

The side product, 2'-deoxy-5-methyl-N^2-propargyl*iso*cytidine shares structural similarities with the synthetic nucleoside, *iso*cytidine (*iso*C). *Iso*C forms part of a so-called artificially expanded genetic information system (AEGIS), created to extend the Watson-Crick rules.

Based on the simplicity of Watson-Crick base pairing, the creators reckoned that, by shuffling the hydrogen-bond donating and accepting groups on two pairing nucleobases (*e.g.* A-T or G-C), hydrogen bonding should still be a possibility. As a result, a total of eight additional nucleosides were generated, forming four base pairs additional to the natural Watson-Crick pairing[179].

These synthetic nucleosides have the ability to base pair with each other, without pairing with natural DNA. However, because of their structural similarities to the natural bases, they can still be recognized by enzymes normally used in molecular biology techniques. As a result, the synthetic genetic system has huge potential in both research and diagnostic applications. This warrants further isolation and analyses of our 'clickable' derivative of *iso*C.

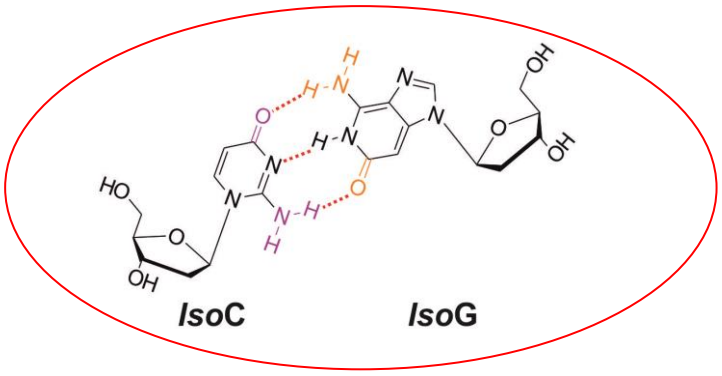

Fig. 3.13 Base pairing between the artificial nucleosides, *iso*C and *iso*G[179].

3.5.2.2 Click functionalization of the synthesized oligonucleotides

As proof of principle, one of the propargyl-containing oligodeoxynucleotides was reacted with the Atto 590 azide dye in a CuAAC reaction. The obtained product was PAGE-purified and analyzed *via* gel electrophoresis to show the presence of the fluorescent label on the DNA strand (see figure 3.14). In all cases GelRed staining was used to both render fluorescence to unlabeled oligonucleotides, as well as to act as loading control. The purpose of the latter was to obtain comparable fluorescent signals from already labeled oligonucleodites in a common excitation/emission channel.

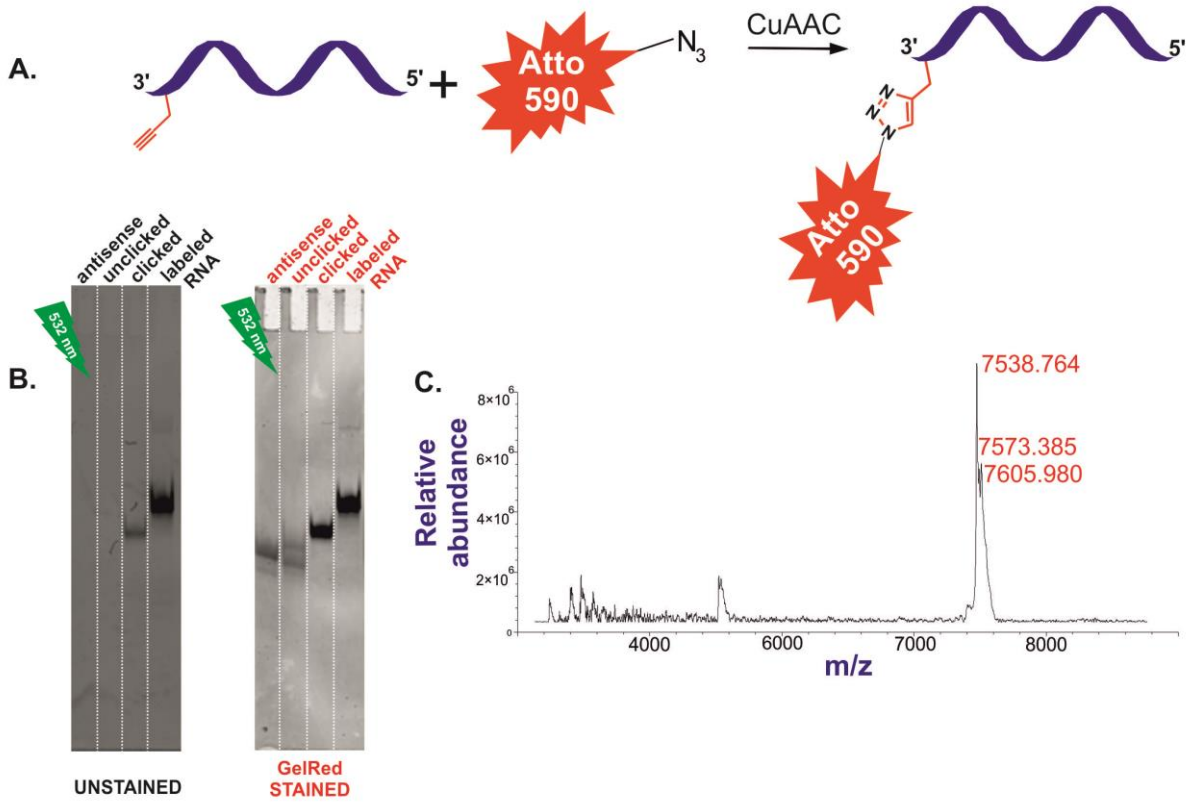

Fig. 3.14 Click functionalization of the modified oligonucleotide with Atto 590 azide. **A.** Reaction scheme for the CuAAC reaction between the propargyl containing oligodeoxynucleotide and the Atto 590 azide dye; **B.** Denaturing polyacrylamide gel electrophoresis of clicked and unclicked oligonucleotides, showing a fluorescent signal and band shift after the click reaction. The gel was excited at 532 nm, both before and after staining with GelRed. Emission signals were recorded at 670 nm and **C.** MALDI-TOF analysis of the clicked oligonucleotide, showing molecular mass of the DNA strand carrying the Atto 590 dye on its 3'-end (calculated mass: *7562 g/mol*).

3.5.2.3 Strand hybridization and electrophoretic mobility shift assays

Both the modified and unmodified sense oligodeoxynucleotides were hybridized to their DNA and RNA complementary strands, respectively. The state of hybridization was monitored on 20% native polyacrylamide gels, run at 20 W (figure 3.15). Surprisingly, only the unmodified duplexes showed proper hybridization under these conditions. A second gel (also 20% native) was run at 8 W and in contrast to the first, clear bands for duplexes for all the samples containing the modification at different positions, were visible (figure 3.15). These results – both for DNA-only duplexes, as well as DNA/RNA hybrids - suggested that the duplexes that contain the propargyl functionality are denatured at considerably lower temperatures than the unmodified duplexes. Temperature dependent absorption measurements would later confirm this. Even under the new electrophoresis conditions, the presence of a dye label on the sense strand still resulted in unstable DNA/RNA duplexes.

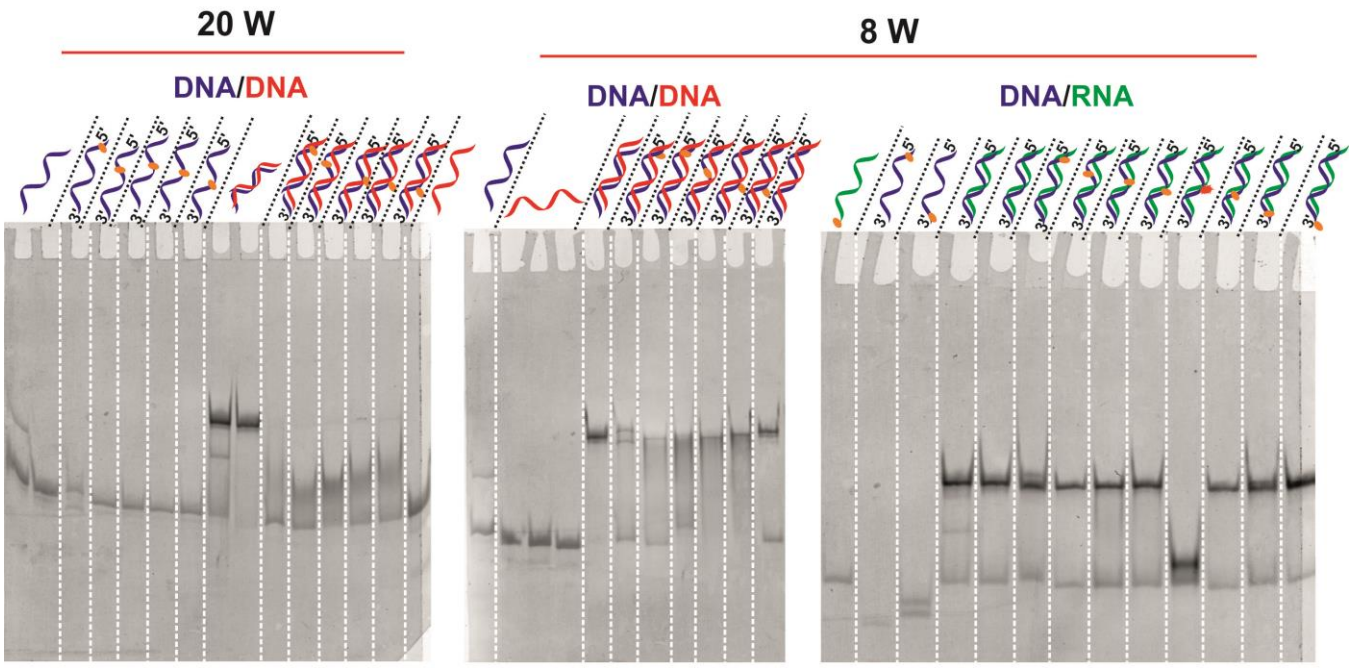

Fig. 3.15 Gel shift mobility assays of the duplexes run at 20 W and 8 W, respectively. ( ) DNA sense strand; ( ) DNA antisense strand; ( ) RNA antisense strand. ( ) represents the position of the alkyne functionality in the DNA strand. ( ) shows the position of the Atto 590 dye clicked onto the oligodeoxynucleotide.

3.5.2.4 Thermal denaturing studies

Temperature dependent differential UV-absorption measurements were carried out with duplexes that were formed between the positionally different modified DNA sense strands and their complementary antisense counterparts. Here, the effect that two simple modifications on the Watson-Crick and "C-H"-edges, respectively, of 2'-deoxy-5-methylcytidine may have on base pairing with both DNA and RNA was investigated. It is to be expected that RNA strands form more stable duplexes with DNA, than DNA with DNA. This effect is mainly caused by the differences in geometry of the two duplexes (A- *vs.* B-form), leading to DNA/RNA hybrid strands to be more thermodynamically stable.

Duplex geometry and therefore also thermodynamic stability is also dependent on the presence of ions surrounding the duplexes. Due to increasing electrostatic repulsion between the negative phosphate ions of the two strands in a duplex, a lower salt concentration automatically leads to strand separation at lower temperatures. Cations, such as sodium (Na^+) can act as shield between the phosphate charges and, as a result, decrease the repulsive potential energy between the oligonucleotide backbones. In the absence of this mutual repulsion, higher NaCl concentrations lead to an increase in the energy necessary to break the hydrogen bonds and other interaction forces among the bases, thus leading to higher T_m's[180].

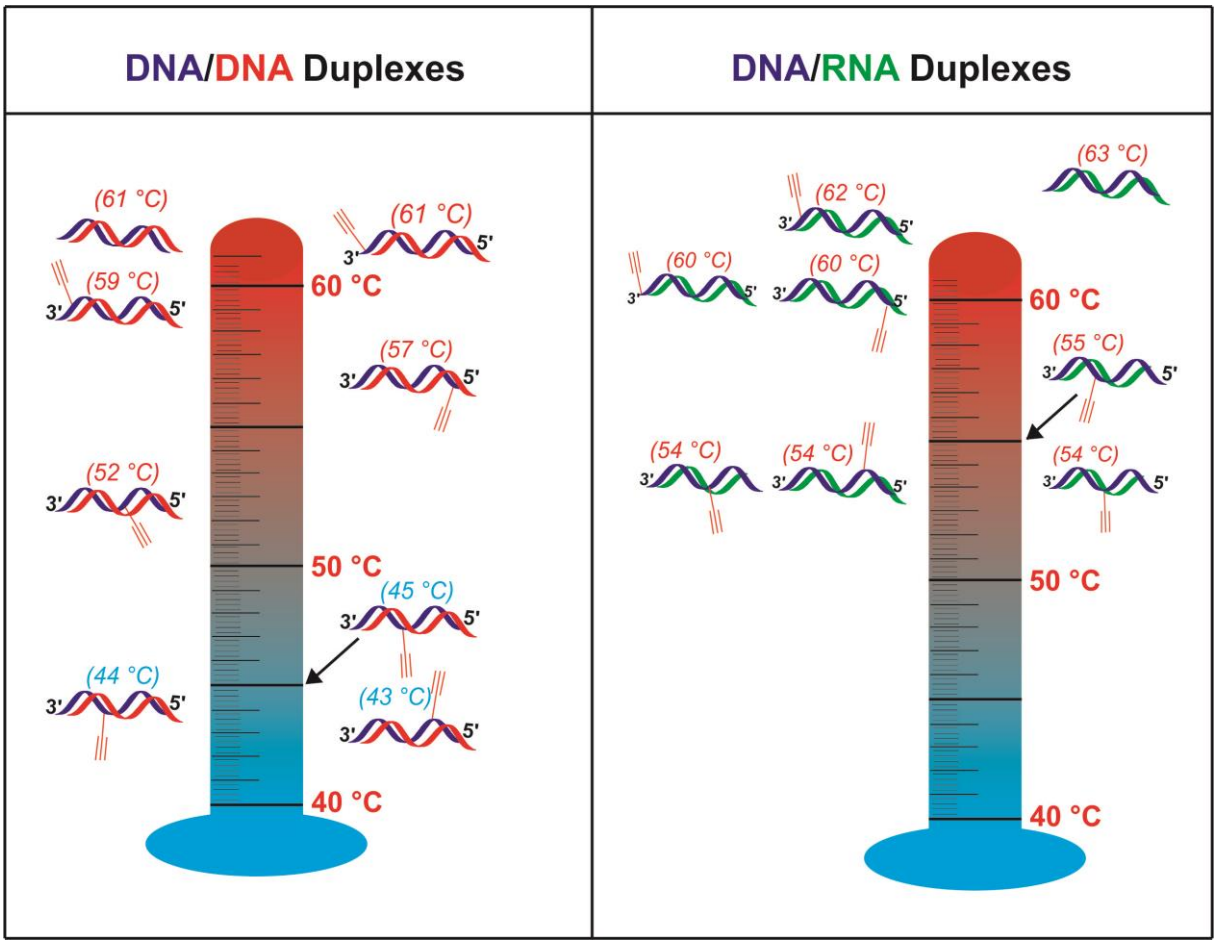

Fig. 3.16 Average melting temperatures observed for DNA/DNA and DNA/RNA duplexes, respectively. The red alkyne functionality indicates the position of the modification on the oligonucleotide strand.

As was expected, the duplexes containing the propargyl functionality on either one of the end terminals had very similar melting points to the unmodified strands. This was particularly significant for the 3'-modified oligonucleotides, where bases on the duplex overhang do not take part in base pairing with the opposing strand. Modifications contained on the 3'-end showed the least deviation from the T_m of unmodified strands, which can easily be rationalized by their unlikelihood of partaking in base pairing.

With the exception of the modification placed on position 10 from the 5'-end (*CpDC10*), the presence of the propargyl functionality caused a significant decrease (16 – 18 °C) in T_m for DNA-only duplexes for all internally modified oligonucleotides. This difference between internally modified strands and strands carrying the modification on the 5'- and 3'-ends raised the question whether the propargyl functionality causes a steric clash during base pairing.

It was previously reported in literature that a simple mono-methylation of the 4-amino group of cytidine already leads to a nucleoside with modified base pairing properties[130]. Although

the complete disruption of Watson-Crick base pairing is first observed after dimethylation on this position, the spatial orientation of a single N^4-substituent plays a trivial role in hydrogen bonding with the opposing base. We hypothesize that the presence of the methyl group on position five of cytidine causes the propargyl moiety to adapt a *cis* conformation, thus pointing the hydrogen atom on the Watson-Crick edge of cytidine away from the opposing guanosine base and, as a result, base pairing between the modified base and guanosine is abolished (figure 3.17).

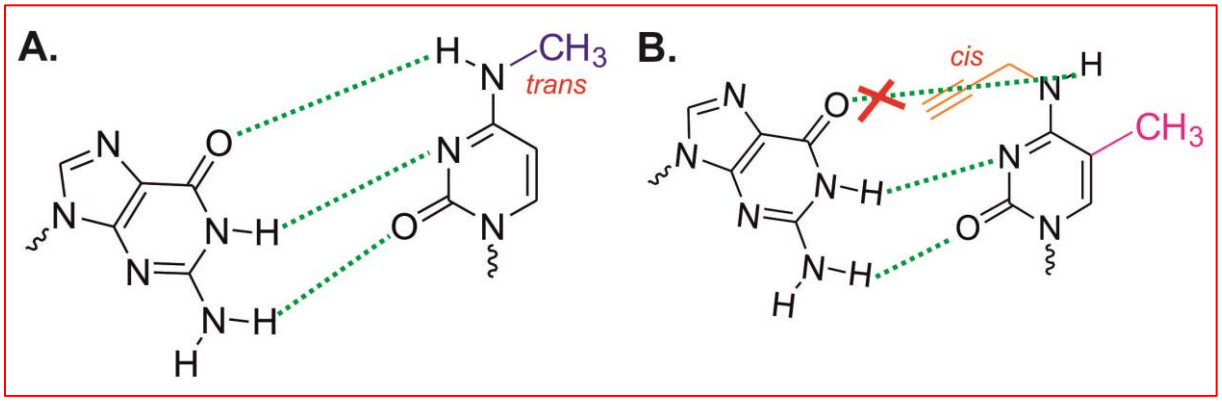

Fig. 3.17 Base pairing between **A.** N^4-methylcytidine; **B.** 5-methyl-N^4-propargylcytidine and guanosine. Due to the CH_3-group on position 5 in **B**, one of the hydrogen bonds is lost during base pairing.

This hypothesis was confirmed by rotating frame Overhauser effect spectroscopy (ROESY NMR) of the single nucleoside. As can be seen in figure 3.18, there is a strong nuclear Overhauser effect discernible between the remaining hydrogen atom on N^4 and the protons of the CH_3-group, indicating their close proximity with respect to one another. The ROESY NMR results thus dismiss the possibility of a *trans* conformation of the propargyl group.

In this way, the CH_3-group has a negative effect on base pairing. On the other hand methyl groups are known to contribute to hydrophobic attractive interactions with neighboring bases and can therefore form more thermodynamically stable duplexes than unmethylated cytidine[181]. The so-called 'methyl effect' on oligonucleotide stability, as was described by Sowers *et al.*[5] in 1987, attributes this duplex stabilization to an increased polarizability in pyrimidine nucleosides that contain a methyl group on position 5. However, in our case, the result of a lack of hydrogen bonding on the Watson-Crick edge due to the propargyl group caused an overall decrease in duplex stability.

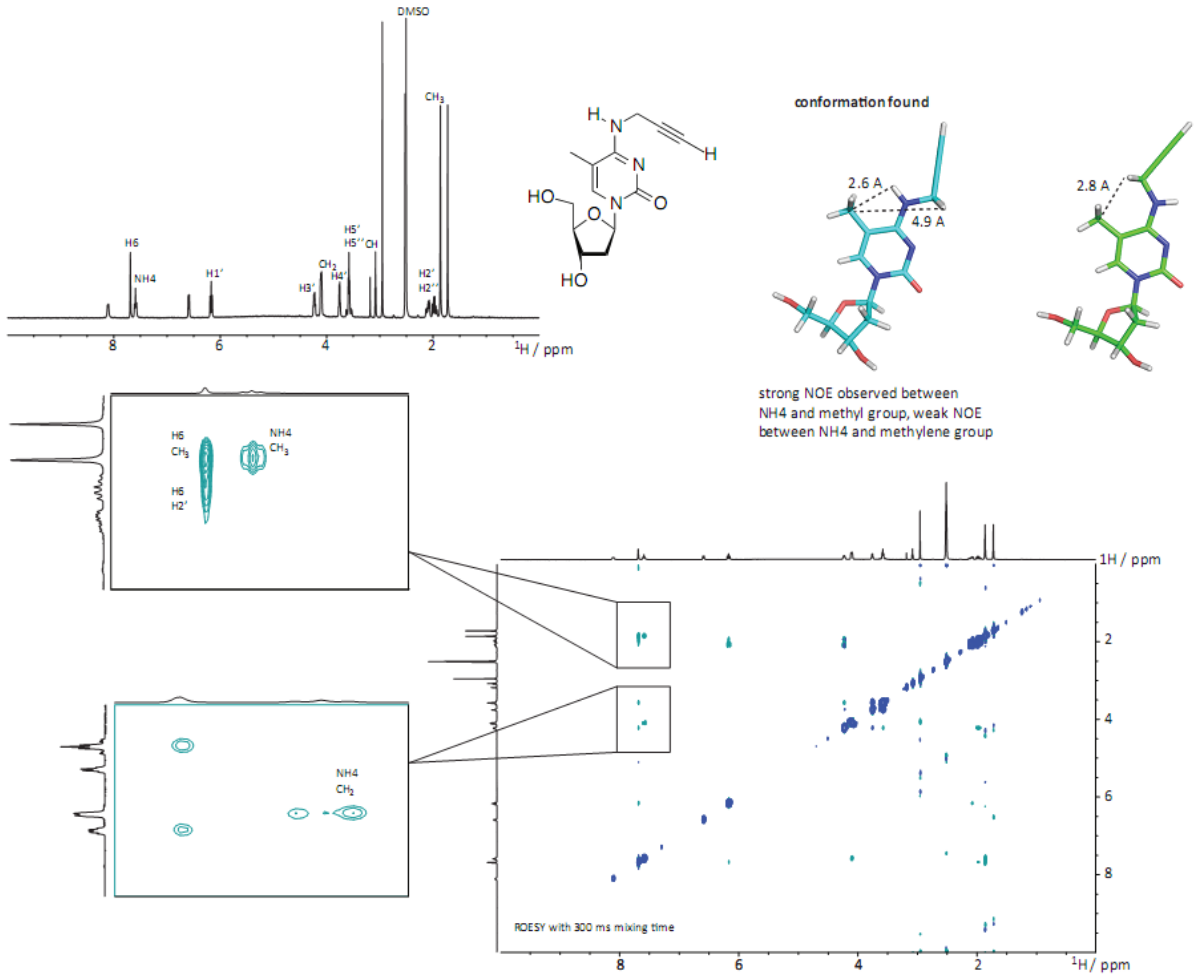

Fig. 3.18 ROESY NMR, indicating a strong NOE between the CH_3-group and the hydrogen on N^4 of the cytidine derivative.

To further address the matter of a spatial hindrance caused by the propargyl functionality, some of the modified oligonucleotides were hybridized to DNA strands that contain an abasic site opposite the modification. When comparing the obtained results to those of the unmodified oligonucleotide hybridized to DNA strands that contain the abasic site on the same position, it was evident that the propargyl functionality is indeed in the way of hydrogen bonding between the opposing bases. The increase in T_m for these duplexes suggests that the steric clash between the propargyl group and the opposing guanosine is rescued in the absence of the opposing base, *i.e.* with an abasic site instead of guanosine. A slightly higher T_m of the modified duplexes is possibly due to a contribution of the methyl group to form more stable duplexes (table 3.1).

An interesting observation with the above data is the substantial increase in T_m of the duplex containing the modification on position 11 from the 5'-end (*CpDC11*), when the opposing base is completely removed. Once again, the modification on position 10 (*CpDC10*) is an

exception to the rule, seeing that the absence of the opposing base has no effect on duplex stability at all.

Table 3.1 Melting temperatures of DNA duplexes formed between the unmodified sense strand, or selected modified sense strands and antisense strands carrying an abasic site. The black dot represents the abasic site on the antisense oligonucleotide.

Duplexes with DNA antisense strand	T_m	Duplexes with antisense strand carrying one abasic site	T_m
 *Unmodified*	61 °C	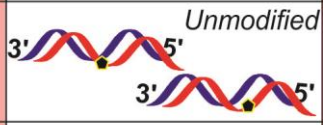 *Unmodified*	52 °C 50-51 °C
 *CpDC10/DNA*	52 °C	 *CpDC10/Abasic DNA*	52 °C
 *CpDC11/DNA*	45 °C	 *CpDC11/Abasic DNA*	54 °C

It was no surprise that the DNA/RNA hybrids, in general, required higher temperatures for strand separation as compared to the DNA-only duplexes. However, the pattern followed by the internally modified oligonucleotides, *i.e.* the significant decrease in T_m as compared to end labeled strands, was not followed for the DNA/RNA duplexes. This effect, in turn, caused a substantial difference in T_m of duplexes formed between these internally modified DNA strands with DNA, as compared to their duplexes with RNA.

As can be gathered from figure 3.19, the modified oligodeoxynucleotide that shows the most significant difference in T_m between DNA/DNA and DNA/RNA duplexes, is the one where the propargyl modification was introduced on the 12th position, as seen from the 5'-end (*CpDC12*). The same difference in T_m was obtained for the modification on position six, *i.e.* ΔT_m = 13 °C (not shown in figure 3.19). In the case of the terminally labeled oligodeoxynucleotides, no significant difference was obtained for ΔT_m between hybrids with the modified oligodeoxynucleotide and duplexes with DNA.

Still puzzling was the effects observed for *CpDC10* duplexes. The most reasonable explanation for this unexpected behavior may be the conformation and geometry of the DNA duplex. It is known that the local topology of nucleic acids in solution is highly dependent on the sequence of the strand[182]. The specific sequence in our oligonucleotide may allow the

propargyl group at position ten to somehow cause less of a steric hindrance than it does in strands that contain the internal label elsewhere. As a result, our carefully constructed hypothesis is holding up only partially to experimental verification and *CpDC10* is thus an exception to our explanation of the behavior of internally modified oligonucleotides in thermal stability tests.

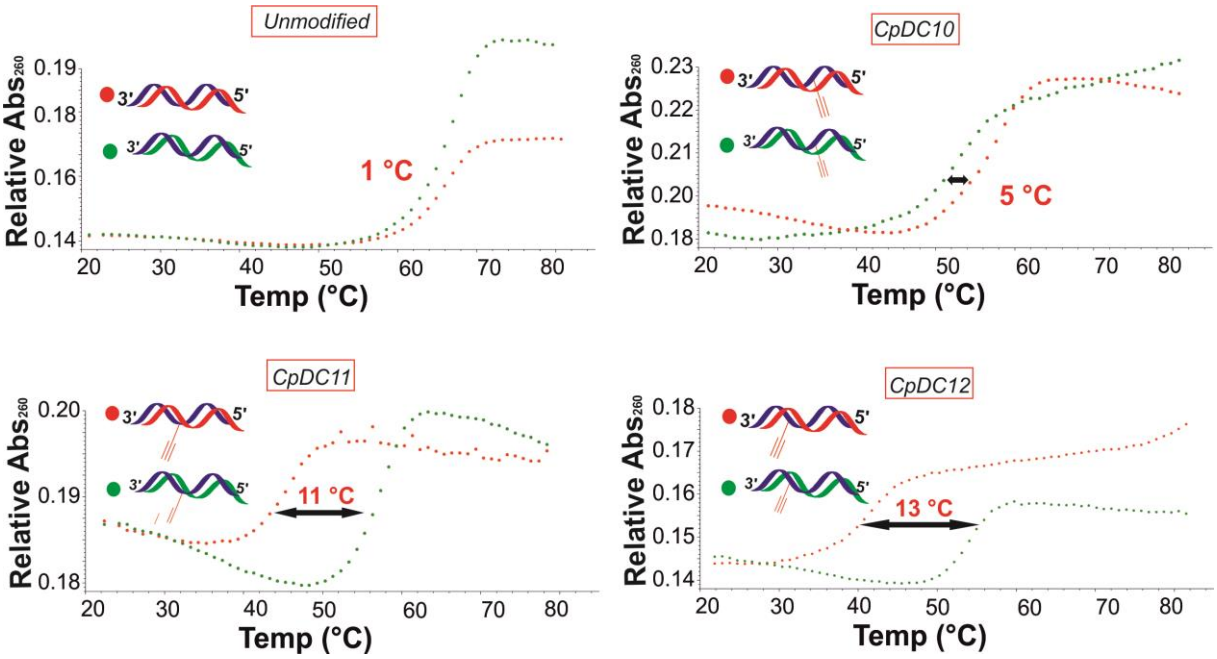

Fig. 3.19 Absorption melting curves showing the difference in thermal stability between DNA/DNA duplexes (red) *vs.* DNA/RNA duplexes (green).

This suspicion is supported by the identical melting points of this oligonucleotide in double stranded DNA, compared to the double strand with the abasic site directly opposite the modification. With *CpDC11*, the absence of the opposing base may have compromised for the lack of space for the modification, thus causing such a significant increase in T_m.

3.5.2.5 Competition assays between DNA and RNA strands for pairing with the complementary, modified oligonucleotides

RNA generally forms more stable duplexes than DNA. This is mainly due to differences in conformation between the duplexes formed. DNA/DNA duplexes usually adapt a B form helix that contains about 10 base pairs per turn. The A form geometry of RNA duplexes, with 11 base pairs per turn, is what contributes to its higher stability. The same is valid for DNA/RNA hybrids. As can be seen for the melting temperatures of DNA-only duplexes and the hybrids of the unmodified strands (62 °C *vs.* 63 °C), this difference in stability is, however, not very significant in usual aqueous solutions. For this reason, solvent systems

have formerly been developed to enhance the formation of hybrid duplexes, but at the same time lead to unstable DNA-only duplexes[183]. This technique has proven successful in experiments where the formation of DNA/RNA duplexes is favored to DNA-only duplexes in mixtures containing all three single strands.

Reversely, it has also been proven that the conformation of DNA-only duplexes is very dependent on the ionic strength of the solution. In a paper published on the effect of salt concentration on the conformation of a DNA duplex, Borah *et al.*[184] made use of two-dimensional nuclear Overhauser effect (2D NOE) NMR to show that high salt concentrations lead to duplex structures that are clearly distinct from both the B and Z forms of DNA. The interproton distances obtained during NMR measurements were consistent with an A form, or at least a closely related structure thereof.

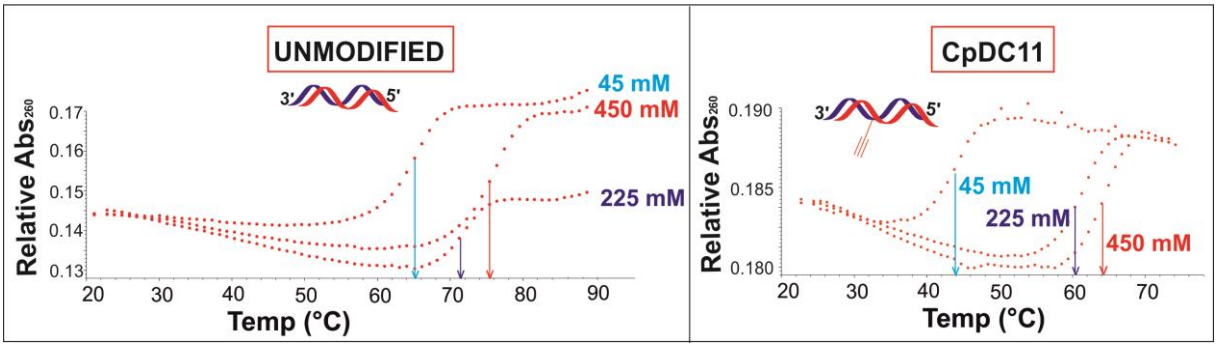

Fig. 3.20 Temperature dependent absorption curves showing the change in T_m for two DNA duplexes as a function of the NaCl concentration.

With this in mind, a series of absorption melting curves were measured of DNA duplexes in the presence of increasing NaCl concentrations (figure 3.20). Results were obtained for the unmodified duplex to compare with the DNA duplex that contains the propargyl functionality in the center of the sense strand (position 11). As was expected, an increase in NaCl concentration (45 mM - 450 mM) led to a significant increase in melting temperature. The same experiments were repeated for the duplexes containing antisense strands with an abasic site opposite the modification. These results are summarized in table 3.2.

Clearly, the affinity between complementary oligonucleotides is highly dependent on the nature of the opposing strand, *i.e.* whether DNA or RNA, positional labeling in one of the strands, as well as the composition of the buffer mixture. With this in mind, it is thus possible to fine tune reaction conditions to favor the hybridization of two selected partners out of a mixture of three single strands and use this to our advantage during fishing experiments.

Table 3.2 Summary of the effect of an increased NaCl concentration on the melting behavior of oligonucleotide duplexes.

			NaCl CONCENTRATION		
DUPLEX	**SENSE**	**ANTISENSE**	**45 mM**	**225 mM**	**450 mM**
	MH661 *(unmodified)*	MH 663 *(unmodified)*	*62 °C*	*69 °C*	*73 °C*
	MH661 *(unmodified)*	MH677 *(abasic site)*	*52 °C*	*61 °C*	*64 °C*
	MH661 *(unmodified)*	MH678 *(abasic site)*	*51 °C*	*59 °C*	*63 °C*
	CpDC11 *(modified pos.11)*	MH 663 *(unmodified)*	*46 °C*	*62 °C*	*65 °C*
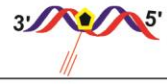	CpDC11 *(modified pos.11)*	MH677 *(abasic site)*	*54 °C*	*59 °C*	*63 °C*
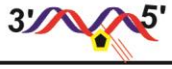	CpDC10 *(modified pos.10)*	MH678 *(abasic site)*	*52 °C*	*61 °C*	*62 °C*

In the presence of low salt concentrations - to ensure the less stable B form helix for possible DNA-only duplexes – a mixture between *CpDC11* or *CpDC12*, the antisense DNA strand and the antisense RNA strand, the formation of the hybrid between the modified oligonucleotide and the RNA strand is likely to be favored. With the major difference in T_m between *CpDC11*/DNA or *CpDC12*/DNA and *CpDC11*/RNA or *CpDC12*/RNA (Δ of 11 and 13 °C, respectively), hybrid formation would be further favored at temperatures closer to the T_m of the DNA-only duplexes. Observing the melting profiles of the duplexes formed with *CpDC11* and *CpDC12* in figure 3.19 it is to be expected that, at a temperature around 45 °C, more than 50% of the DNA-only duplexes should be resolved, whereas the hybrid duplexes should still be largely intact.

After full denaturation *via* incubation of the three strands at 90 °C for 3 minutes, similar amounts of the respective constructs (*i.e. CpDC11* and two antisense strands; *CpDC12* and two antisense strands, respectively) were incubated at 45 °C for 1 hour in a low salt concentration buffer. Native polyacrylamide gel electrophoresis was intended to indicate which duplex formation was rather favored under these conditions. However, it had to be kept in mind that the conditions for the PAGE mobility shift assay were to mimic the conditions for absorption melting temperature measurements of the constructs in the cuvette. The

running buffer was replaced with high concentration NaH_2PO_4 (pH 8), containing 45 mM NaCl and the electrophoresis chambers were placed in a 45 °C environment. The gels were run at low Wattage, so as to prevent an additional rise in temperature that could lead to undesired strand separation (see figure 3.21).

However, our hypothesis was not fully confirmed, as the expected results were not represented after fluorescent scanning of the GelRed stained gels. No distinction could be made with regard to the intensity of the DNA/RNA duplexes *vs.* the DNA/DNA duplexes and similar results were obtained for competition assays of the modified oligonucleotides as was for the unmodified ones.

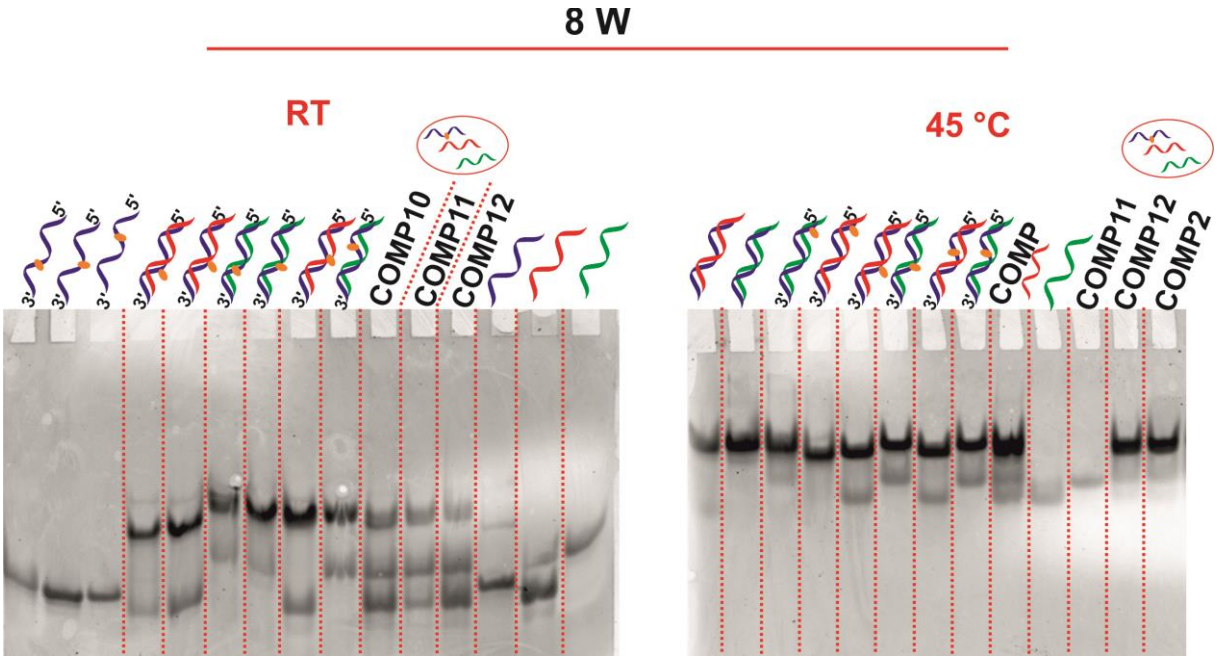

Fig. 3.21 Gel shift mobility assays of the duplexes run at room temperature and at 45 °C, respectively. ( ) DNA sense strand; ( ) DNA antisense strand; ( ) RNA antisense strand. ( ) represents the position of the alkyne functionality in the DNA strand. The abbreviation COMP indicates the lanes where the competition samples, *i.e.* a mixture of the unmodified strand, *CpDC2*, *CpDC10*, *CpDC11* and *CpDC12*, respectively, with the RNA and DNA antisense strands were loaded.

Due to differences in base composition, sense and antisense strands usually show different shifts during gel electrophoresis. However, because the strands used are of the same length, this slight difference in shift was not sufficient to prevent them from migrating together throughout the gel, despite the denaturing conditions brought about by the high outward temperatures. As a result, no clear proof could be presented to confirm a higher abundance of DNA/RNA hybrid duplexes after a competition assay. For this reason, a new and longer antisense strand was designed for confirming a higher binding affinity of the modified oligonucleotides for RNA instead of for DNA.

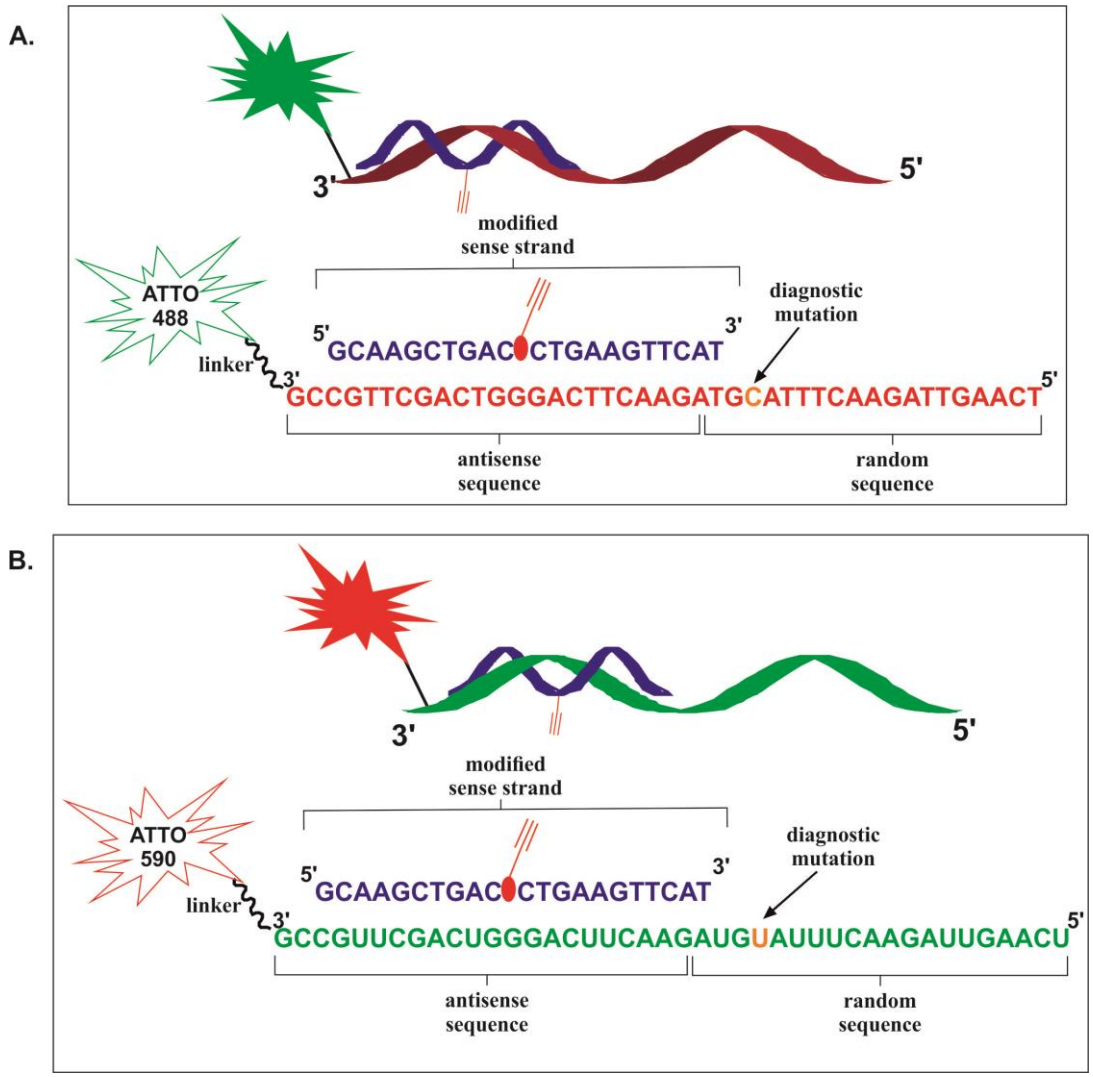

Fig. 3.22 Differently labeled 42mer **(A)** DNA and **(B)** RNA strands used in competition assay with the modified oligodeoxynucleotides. The oligodeoxynucleotide carrying the propargyl group in the middle of the strand is used as example for the modified, complementary strand here.

Figure 3.22 shows a graphical representation of the newly designed oligonucleotides – both DNA and RNA. Apart from a diagnostic mutation (indicated in orange), the sequences of the two strands are identical. The diagnostic mutation was incorporated for future work that may involve reverse transcription experiments in combination with nucleic acid sequencing. More detail about this work will follow later.

Following competition assays, upon implementing polymerization with the respective DNA or RNA templates, the resulting strands should deliver different base signals at the particular position of mutation. Together with the differences in fluorescent labeling, this method should make a quantification of the respective DNA and RNA strands possible, in order to eventually identify the thermodynamically more stable duplex.

Table 3.3 Summary of the differences in melting temperature of duplexes formed between the antisense oligonucleotides of different lengths (21mer *vs.* 42mer) and the differently modified sense strands. The unmodified sense strand, MH661, was used as reference.

DNA/DNA

	MH663 *(21mer)*	MH693 *(42mer)*
MH661	61 °C	62 °C
5' CpDC2 3'	57 °C	56 °C
5' CpDC6 3'	43 °C	54 °C
5' CpDC11 3'	45 °C	54-55 °C
5' CpDC12 3'	44 °C	55 °C
5' CpDC20 3'	59 °C	49 °C
5' CpDC21 3'	61 °C	62 °C

DNA/RNA

	MH533 *(21mer)*	MH692 *(42mer)*
MH661	63 °C	60 °C
5' CpDC2 3'	60 °C	58 °C
5' CpDC6 3'	54 °C	54 °C
5' CpDC11 3'	54 °C	53 °C
5' CpDC12 3'	55 °C	53 °C
5' CpDC20 3'	62 °C	56 °C
5' CpDC21 3'	62 °C	60 °C

For increasing the oligonucleotide length, a random sequence of 20 bases was added to the 5'-end of the antisense sequence that was used during the previous melting studies. For the choice of this sequence, the following factors had to be considered: *(i)* the obtained oligonucleotide should not form secondary structures due to self-complementarity, *(ii)* only one possible hybridization product should form with the opposing sense strand and *(iii)* for possible further sequencing studies, a diagnostic mutation, where one corresponding base between the DNA and RNA strands should differ, should be included. To further simplify identification of possible hybridization products, the two strands were 3'-labeled with different fluorescent tags – Atto 488 for DNA and Atto 590 for RNA.

The same procedures as before were followed for the longer oligonucleotides, *i.e.* hybridization with both modified and unmodified sense strands and temperature dependent absorption measurements to determine the differences in melting points for DNA-only duplexes *vs.* DNA/RNA hybrids. This was followed by competition assays between the two labeled oligonucleotides for the applicable modified sense strands, based on the results obtained during the melting point determinations and, finally, polyacrylamide gel electrophoresis of the obtained duplexes.

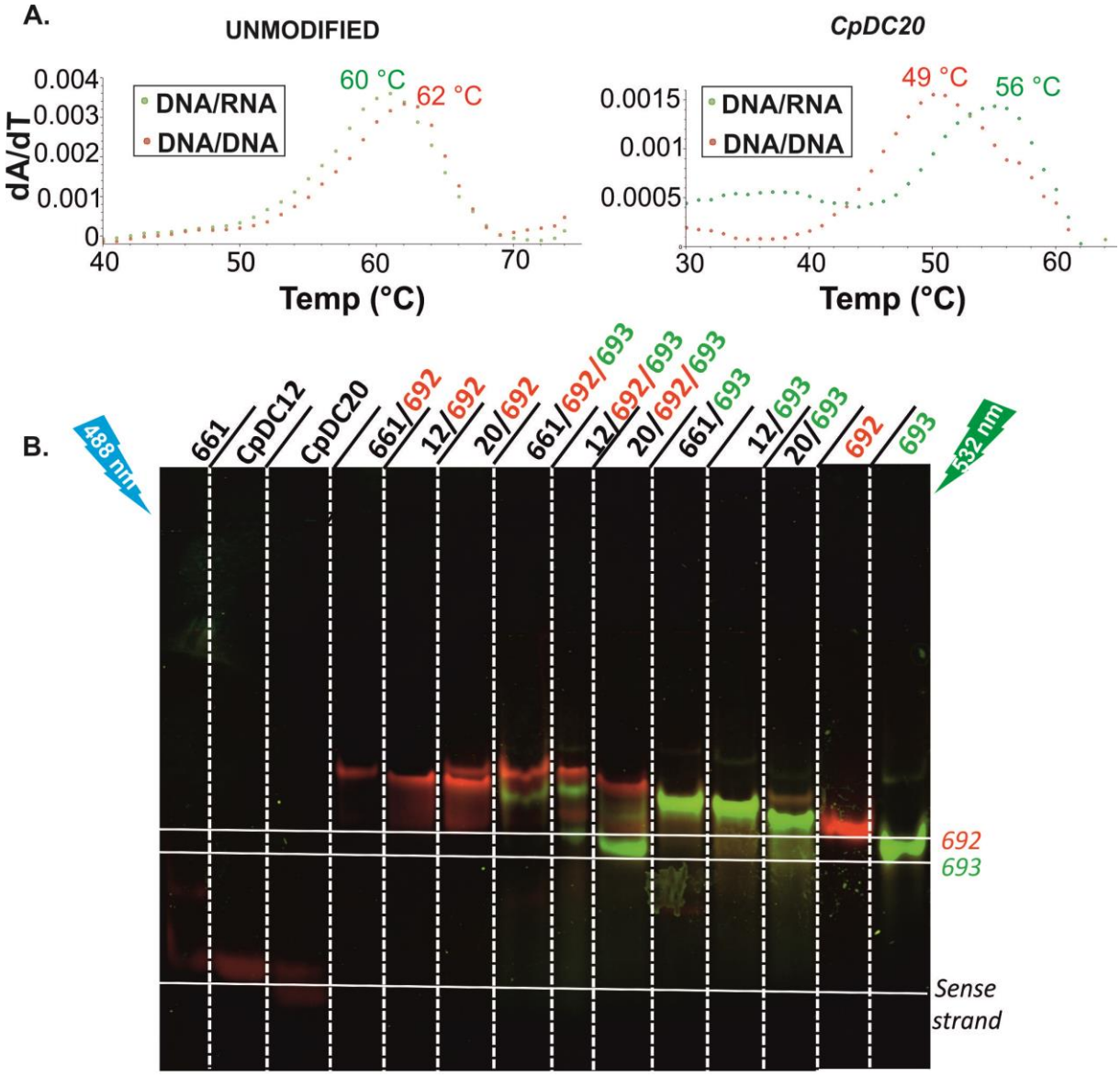

Fig. 3.23 A. Differential UV absorption melting curves of the oligonucleotides used in the competition assay. **B.** Overlay of the two scans of the native polyacrylamide gel electrophoresis showing the higher binding affinity of the oligonucleotide *CpDC20* for the RNA antisense strand.

Theoretically, a simple random elongation of the previously applied antisense strands should have no significant impact on the melting properties of the duplexes formed with the same complementary strand. Due to the 3'-overhang in these duplexes, even an additional fluorescent label on this end should also not affect duplex stability to any large extent. However, in contrast to what was expected, a different melting profile was followed for the duplexes formed with the modified oligonucleotides. These results, together with the initial results obtained for the 21mers, are summarized in table 3.3.

As was previously determined for the 21mer oligonucleotides, a significantly lower T_m could be observed for the DNA-only duplexes formed with *CpDC6*, *CpDC11* and *CpDC12*,

respectively, than with RNA. This resulted in a high difference in thermodynamic stability between these duplexes and their hybrid counterparts. Surprisingly, this was not the case for the longer oligonucleotides. As for the shorter oligonucleotides, modifications at either terminal end had no significant influence on melting behavior of the duplexes. However, only a small destabilizing effect could be seen for all internally modified oligonucleotides. An exception was the melting behavior for *CpDC20*, where a ΔT_m of 7 °C was measured, due to a much less stable DNA/DNA duplex.

As a result, the competition assay was carried out with *CpDC20*. Once again, a similar procedure was followed as for the shorter oligonucleotides. Gel electrophoresis was performed at 50 °C at low Wattage for 6 hours.

The temperature dependent gel electrophoresis experiment shows a clear preference of *CpDC20* for the RNA complementary strand. Bands of similar intensity were, however, obtained for both the unmodified sense strand and *CpDC12*, as could be predicted from their temperature dependent UV absorption measurements.

3.5.2.6 Summary

The newly synthesized propargyl functionalized cytidine derivative was incorporated at varying positions of a DNA oligonucleotide strand. After hybridization with complementary DNA and RNA strands, respectively, the obtained duplexes were subjected to temperature dependent absorption measurements, which is based on the principle of the hyperchromic effect associated with strand separation.

The combination of the methyl group on position five of cytidine, together with the propargyl functionality on N^4 has a noteworthy influence on the thermodynamic stability of duplexes formed with oligonucleotides containing the modification. Steric hindrances caused by the CH_3 likely forces the propargyl group to face the other direction, thus pointing towards the Watson-Crick face of the molecule.

When compared to DNA duplexes formed with sense strands not carrying the modification, there is a clear loss in duplex stability, depending on the position of the modification within the strand. Where modifications were placed on positions six, eleven and twelve from the 5'-end, this significant loss in stability led to major differences in melting temperature between DNA/DNA duplexes and their DNA/RNA counterparts. This might make possible the isolation of RNA strands from a mixture of DNA and RNA complementary to the modified oligonucleotides. The similar migration patterns between the sense and antisense strands made it difficult to prove the absence or less abundance of the DNA-only duplexes.

Therefore, to further solidify these results, the same experiments were repeated with duplexes of which the antisense DNA and RNA strands were differently labeled and also longer than the initial oligonucleotides. Contrary to what was expected for these duplexes, they did not mimic the melting behavior of the 21mers. The experiments that were carried out thus far are not sufficient to fully explain these differences in melting behavior and a continued investigation is warranted for further elucidation of the matter.

It should, however, still be kept in mind that the presence of a terminal alkyne functionality on the modified oligonucleotides still makes their click functionalization a possibility. This type of labeling could open a new avenue of approaches toward both physicochemical and biological evaluation of the modified oligonucleotides.

Firstly, a CuAAC based ligation between the modified oligonucleotides and an azido functionalized affinity tag, such as biotin or magnetic beads, could be a step in the right direction for proving the capability of these new modifications to fish out RNA strands from a mixture of oligonucleotides. Also, due to the higher sensitivity of a fluorescence signal, Förster resonance energy transfer (FRET) measurements between a triazole linked dye and a dye label on the complementary strand, as a function of temperature, would allow thermodynamic measurements of lower duplex concentrations[185].

With regard to biological applications of the newly synthesized oligonucleotides, future work may involve analysis of the knockdown efficiency of the duplexes containing the propargyl functionality. As was done for the RNA labeled antisense construct (see section 3.4.3), 3'-labeling of this DNA sense strand could be used in cell tracking experiments. The use of the less stable duplexes may contribute to less off-target effects during gene knockdown experiments[186].

3.5.3 Incorporation of the propargyl-containing cytidine phosphoramidite into a 2'*O*Me RNA/DNA chimera

It is possible to enzymatically cleave RNA in a site-specific manner by using 2'-*O*-methyl RNA/DNA chimeras[187]. The position of hydrolysis, which is brought about by the enzyme, RNase H, is determined by four deoxyribonucleotides in the chimeric splint that base pairs with the target RNA. The cleavage site is positioned 3' to the ribonucleotide that base pairs the 5'-most deoxyribonucleotide, as is illustrated in figure 3.24.

In literature, this method has been applied as diagnostic tool to detect sites of 2'*O*-methylation in RNA molecules as post-transcriptional modification in ribosomal RNA (rRNA)[188]. A different approach is the site-specific hydrolysis of RNA to obtain particularly defined RNA

fragments[187]. Based on this method it should be possible to obtain a unique cleavage by RNase H, by designing DNA/2'*O*Me RNA chimeric oligonucleotides to act as hybridization splint. The position of fragmentation can be controlled by simply altering the sequence and position of the tetradeoxynucleotide cluster in the chimeric oligonucleotide. It should be possible to apply this method to monitor biological processes of RNA, such as transfer RNA (tRNA) editing, which refers to a process during which a particular nucleotide sequence within the mature tRNA is altered from those encoded in the gene. An example of such editing, known as C-to-U editing, is the conversion of cytidine to uridine during an enzymatically catalyzed deamination reaction. Of particular interest in our laboratory is the conversion of the cytidine on position 8 of $tRNA^{Phe}$ to uridine. This modification has a significant impact on the tertiary structure of the tRNA and thus also on tRNA function[189,190]. The detection of U on position eight should give an indication of the rate of turnover of the C8-tRNA substrate. By making use of a 2'*O*Me RNA/DNA chimera, containing a tetradeoxynucleotide cluster that would only base pair in the presence of a uridine nucleoside on position 8, strand scission 5' to the modified base should take place.

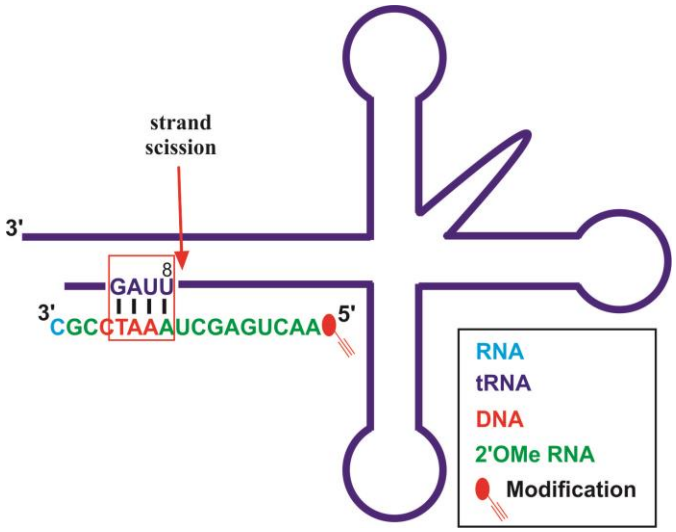

Fig. 3.24 Synthesized 2'*O*-methyl RNA/DNA chimera hybridized to tRNA. The arrow indicates the theoretical position of tRNA strand cleavage by RNase H.

For this reason, an 18mer oligonucleotide was designed, consisting mainly of 2'*O*-methyl RNA nucleosides, with the tetradeoxynucleotide cluster complementary to positions 5 to 8 of the tRNA. To enable fluorescent tracking of this chimeric strand, the propargylated cytidine moiety was incorporated as 'clickable' functionality onto the 5'-end. Labeling on this position would simplify post-synthetic purification of the oligonucleotide to a large extent and should not affect enzyme action.

3.5.3.1 Oligonucleotide synthesis and click functionalization

As reference, the unmodified oligonucleotide was synthesized in the 'DMT-ON' mode. After work-up, it was subjected to HPLC purification, leading to the pure DMT-ON product. Detritylation with 80% acetic acid, followed by manual size exclusion chromatography on Nap columns resulted in the unmodified DNA/2'*O*Me RNA chimera.

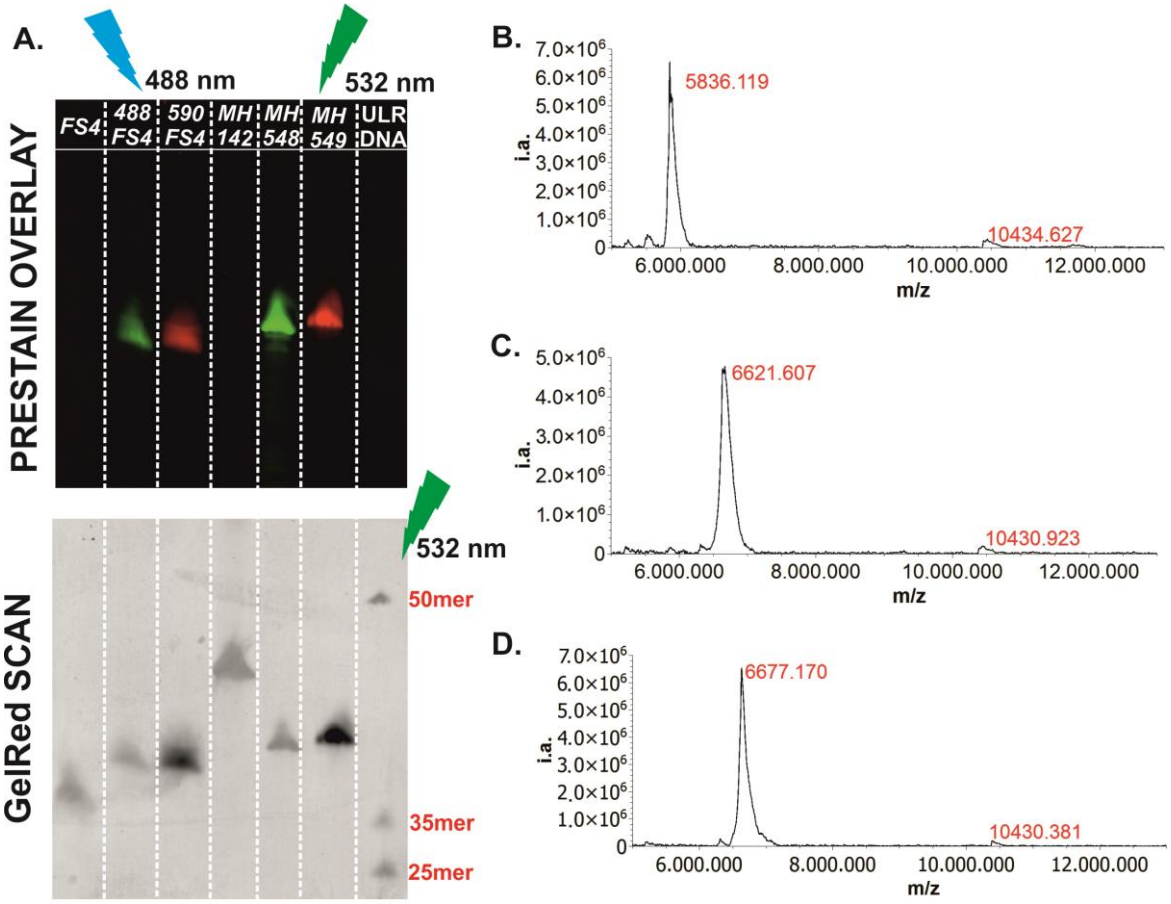

Fig. 3.25 A. Polyacrylamide gel electrophoresis and MALDI-TOF results of the unmodified and differently click labeled 2'-OMe RNA/DNA chimeras. Calculated masses: **B.** unclicked: *5832 g/mol*; **C.** Atto 488 clicked: *6622 g/mol* and **D.** Atto 590 clicked: *6623 g/mol*. Internal standard: *10430 g/mol.*

A different purification route was followed for the oligonucleotide carrying the modification. Because the alkyne functionality was incorporated directly onto the 5'-end, the synthesis was performed in the 'DMT-off' mode. After post-synthesis work-up, the oligonucleotide was subjected to click conditions with one of two azido functionalized dyes – Atto 488 and Atto 590. Manual size exclusion chromatography (Nap 10 columns) served for the removal of unreacted dye molecules. The labeled oligonucleotides were PAGE purified and precipitated, before their mass confirmation *via* MALDI-TOF analysis.

Mobility shift analyses were performed of oligonucleotides *via* 20% denaturing polyacrylamide gel electrophoresis. The gel electrophoresis would also confirm the presence

of the two different labels on the synthesized oligonucleotides after click functionalization. As reference, the same amount of three commercial 2'*O*Me RNA containing oligonucleotides – two labeled and one unlabeled – were also loaded onto the same gel: *MH142*: 34mer, unlabeled 2'*O*Me RNA/DNA chimera; *MH548*: 22mer RNA, containing four Atto 488 labeled 2'*O*Me bases; *MH549*: 22mer RNA, containing four Atto 590 labeled 2'*O*Me bases (see figure 3.25).

The *in vitro* experiments of these oligonucleotides with $tRNA^{Phe}$ are still in progress and no results with regard to the efficiency of this method are available as yet.

3.6 An alkyne functionalized derivative of uridine

3.6.1 Synthesis of 5-ethynyluridine

The incorporation of 5-ethynyluridine (EU) into cellular RNA marked the very first application of click chemistry in RNA modification[128]. This study proved that a modified derivative of uridine could be incorporated into transcribed RNA by the polymerase enzymes I, II and III. After incorporation of the 5-ethynyluridine - with an average of once every 35 uridine residues in total RNA - the EU-labeled cells could be reacted in a CuAAC reaction with an azide containing dye, resulting in the rapid detection of transcribed RNA, with high levels of sensitivity. Concurrently, a new method for measuring rates of total transcription in cells was identified.

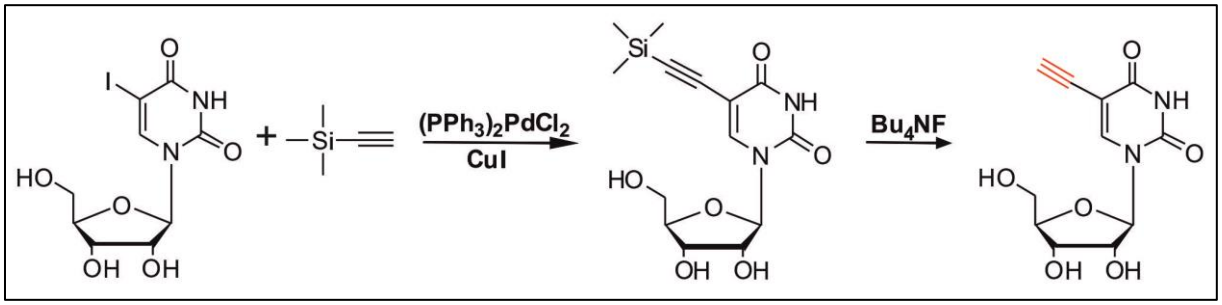

Scheme 3.8 Synthesis of 5-ethynyluridine.

To further investigate the enzymatic tolerance of 5-ethynyluridine in live cells, this compound was synthesized *via* the Sonogashira cross-coupling reaction between 5-iodouridine and trimethylsilyl (TMS) acetylene[128]. The TMS group was removed with a tetrabutylammonium fluoride solution (Bu_4NF), resulting in a terminal alkyne (Scheme 3.8) that would allow the click reaction of the modified base with azides. The yields of the two respective steps were 66% and 44%.

3.6.2 Incorporation of 5-ethynyluridine into RBE4 cells

In 2008 Salic and Mitchison[191] published the successful incorporation of 5-ethynyl-2'-deoxyuridine (EdU) into proliferating cells for the detection of DNA synthesis *via* CuAAC. This method proved to show many advantages to the standard procedures for detecting DNA synthesis and was soon followed by studies on the use of the RNA variant, 5-ethynyluridine (EU), for imaging transcription in live cells[128].

In the present studies RBE4 cell cultures were used to test the incorporation of the synthesized EU into cellular RNA. 1 mM EU was incubated with the cell cultures for different time lengths (0 hours; 8 hours; 16 hours; 24 hours), after which the EU containing medium was replaced with normal culturing medium. The cells were fixed onto coverslips and each of the coverslips were treated with the Alexa 594 azide dye, together with $CuSO_4 \bullet 5H_2O$ and ascorbic acid in HEPES buffer (pH 8.5). After rinsing off all excess dye, the coverslips were placed onto mounting slides with mounting medium and stored at 2-8 °C until imaging. 4',6-diamidino-2-phenylindole dihydrochloride (DAPI) was used for counterstaining the cell nuclei.

The confocal microscope images were recorded by exciting the cells at 480 nm for the DAPI stains and 516 nm for the Alexa 594 dye, respectively. As can be seen from the confocal images in figure 3.24, there is a clear increase in fluorescence intensity of the Alexa dye with an increase in incubation time of the cells with the EU. Particular staining of the cell nuclei with the Alexa dye, which is especially visible in the 8 hours incubation sample, suggests strong incorporation of the 5-ethynyluridine at ribosomal RNA transcription sites. These results support the idea that 5-ethynyluridine is a specific transcriptional label and is probably not incorporated into cellular DNA to a significant extent. Cytoplasmic staining became more visible with an increase in incubation times. The presence of only very low background fluorescence in the control samples proves that the EU incorporation is indeed that which is responsible for the fluorescent cells. In these experiments the small size of the alkyne functionality as modification enabled the prevailing recognition of the nucleoside by the polymerase enzymes, which led to its incorporation into the cells.

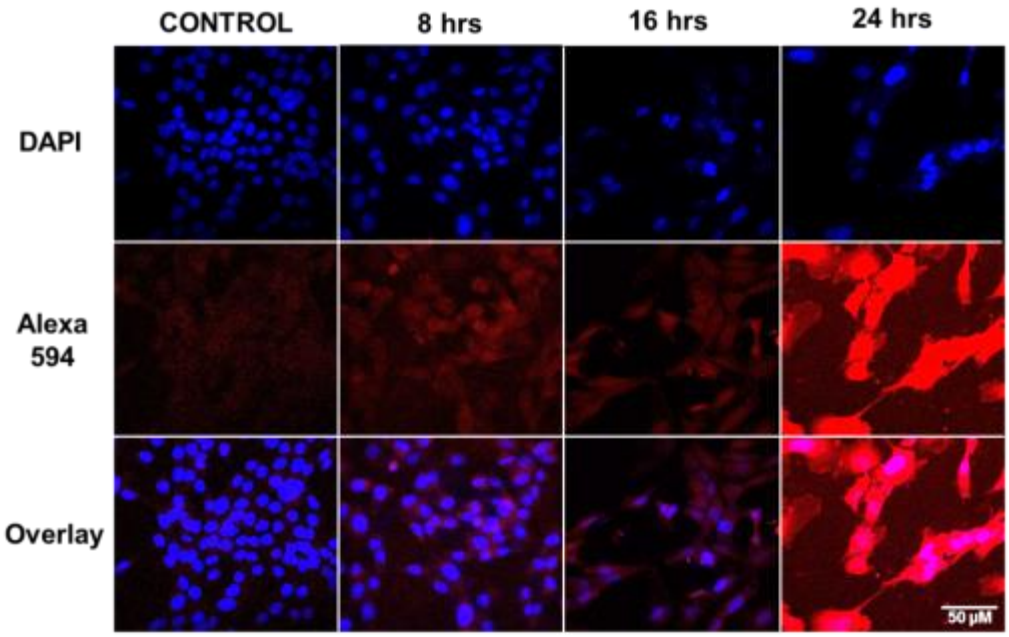

Fig. 3.26 Confocal microscopy images of RBE4 cells after incubation with 5-EU for different periods of time, followed by the CuAAC reaction of each with the Alexa 594 azide dye. DAPI counterstaining was used to visualize the cell nuclei.

3.6.3 Incorporation of 5-ethynyluridine into *E. coli* cells

To further extend the application of the 5-EU transcriptional labeling to prokaryotic cells, the above procedure was applied to *Escherichia coli* cultures. 5-EU was added to *E. coli* at the beginning of their log phase and the cells were incubated until the stationary growth phase was reached (see figure 3.25 A). The presence of the modified nucleoside had no significant effect on the growth of the bacteria. Total tRNA was isolated and reacted with an Alexa 594 azide dye in a click reaction, to stain possibly incorporated ethynyluridine. An oligodeoxynucleotide (28mer) containing a 5'hexynyl modification was used as control for the click reactions. Polyacrylamide gel electrophoresis was utilized to detect fluorescence of the isolated tRNA and thus evaluate the extent of EU incorporation into the bacterial cells.

As can be seen from the GelRed stained polyacrylamide gel (figure 3.25 B, right), the isolation of total tRNA proved to be successful. However, the lack of a fluorescence band for the EU treated cells on the unstained gels (figure 3.25 B, left) suggests that the ethynyluridine was probably not incorporated into the isolated tRNA. It is possible that the EU did not penetrate the bacterial cell membrane or if incorporation of the modified nucleoside did indeed take place, it was somewhere other than the total RNA of the bacteria.

A similar experiment was done by Ferullo *et al.*[192] to determine DNA content in individual *E. coli* cells by the *in vivo* incorporation of 5-ethynyldeoxyuridine (EdU). In their case, whole

cells were fixed and reacted with azido dyes, after which fluorescence was detected directly in the labeled cells. This method does, however, not confirm the incorporation of the modified nucleoside into specifically DNA neither does it prove the toleration of DNA polymerases for the EdU.

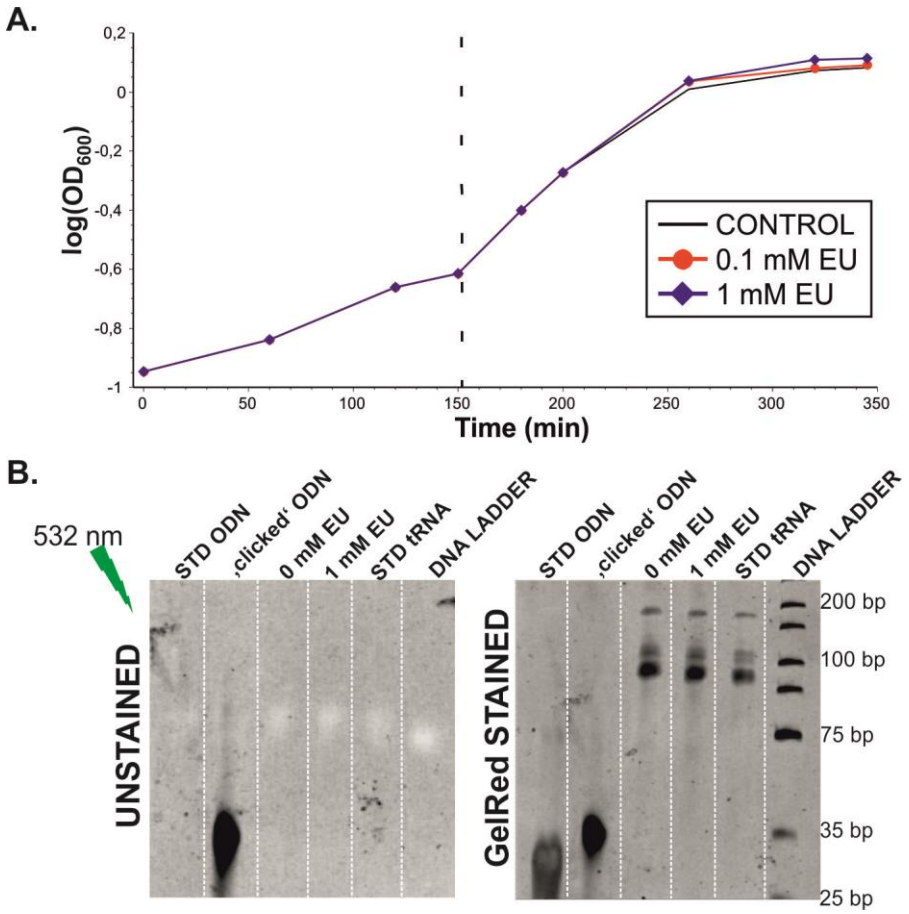

Fig. 3.27 A. Bacterial growth curves, showing the point of EU-addition, as indicated by broken line. **B.** Unstained and GelRed stained 10% PAGE of bacterial RNA and oligodeoxynucleotide used as standard. Both gels were excited at 532 nm and fluorescence was detected at 670 nm.

Future studies may include analysis of the DNA, which was contained in the interphase, which formed during the isolation of RNA from the *E. coli* cells, in order to obtain a better understanding of the tolerance of other enzymes for the modified ribonucleoside.

3.7 Base modifications for click functionalization on the Hoogsteen edge of guanosine

For the investigation of the influence of Hoogsteen labeling on structure and function of guanosine, the synthesis of 8-ethynylguanosine was planned. As precursor for this compound,

8-bromoguanosine, which was formed *via* the bromination of guanosine, was first synthesized.

3.7.1 Halogenation of guanosine and further modification for click functionalization

3.7.1.1 Synthesis of 8-Bromoguanosine

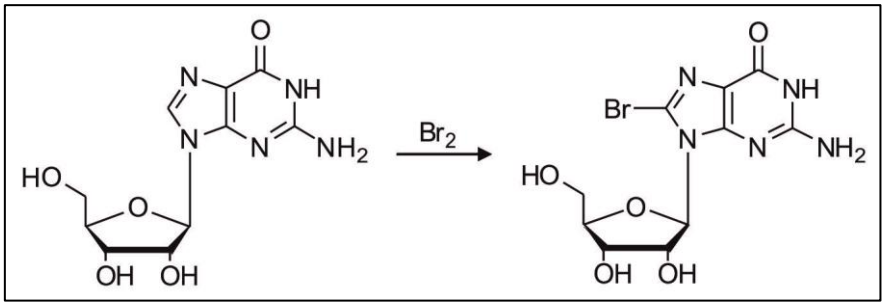

Scheme 3.9 Bromination of guanosine.

Unprotected guanosine was converted to its 8-bromo derivative *via* a radical substitution reaction. Saturated bromine water was slowly added to a suspension of the guanosine in water and a recrystallization from water resulted in pure 8-bromoguanosine in 51% yield[193]. The product was confirmed by NMR, IR and mass spectrometric analyses.

3.7.1.2 Synthesis of 8-ethynylguanosine

Motivated by the success of the 5-ethynyluridine synthesis by means of the Sonogashira cross-coupling reaction with 5-iodouridine, a similar approach for the attachment of a terminal alkyne to guanosine on its Hoogsteen edge was attempted. Starting from the brominated guanosine, various reaction conditions were tested for Sonogashira cross-coupling with trimethylsilyl acetylene (Scheme 3.10). However, none of these reaction conditions led to the successful conversion to produce significant amounts of pure product.

In the palladium catalyzed sp^2-sp coupling reactions between aryl halides and terminal alkynes, the iodide bonds are generally more reactive than the bromide bonds and may thus partially explain the lower reactivity of bromoguanosine, as compared to iodouridine. In addition to this, guanosine is known to coordinate with palladium under basic conditions (figure 3.26), thus decreasing its reactivity in this particular reaction even further. Studies have shown that palladium catalyzed cross-coupling reactions with guanosine take place much less readily as compared to the corresponding adenosine derivatives and the presence of

non-halogenated guanosine in the same reaction mixtures even inhibits the palladium catalyzed conversion of 8-bromoadenosines[194].

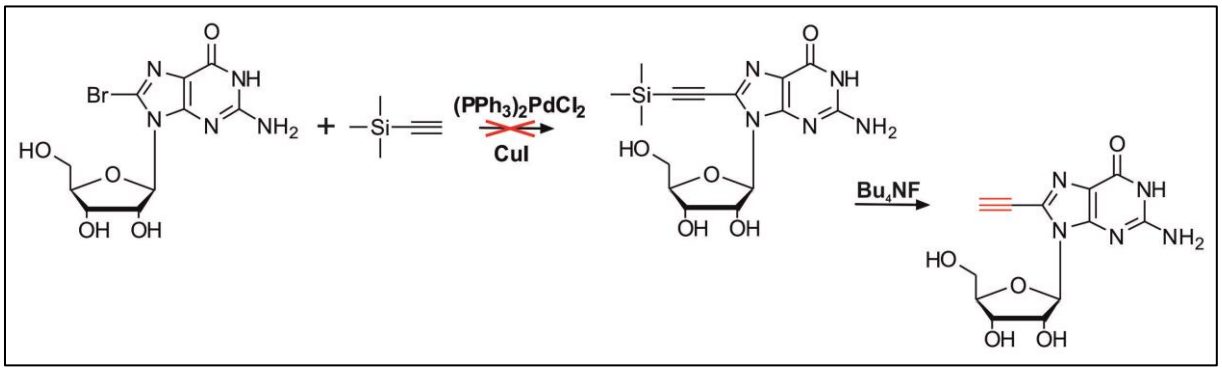

Scheme 3.10 The conversion of 8-bromoguanosine to 8-trimethylsilylethynyl guanosine *via* the Sonogashira cross-coupling reaction was unsuccessful.

In an attempt to develop a new approach towards the Sonogashira alkylynation of brominated purines, Firth *et al.*[195] found the key to the success in these reactions to be low palladium loadings in combination with an optimal ratio between Pd(II) and Cu(I). Although they achieved the successful alkylynation of unprotected bromoguanosine in under 2 hours, the reaction conditions still required temperatures above 100 °C. This poses a problem for the reaction with our trimethylsilylacetylene for the introduction of a terminal alkyne due to the low boiling point of this reagent.

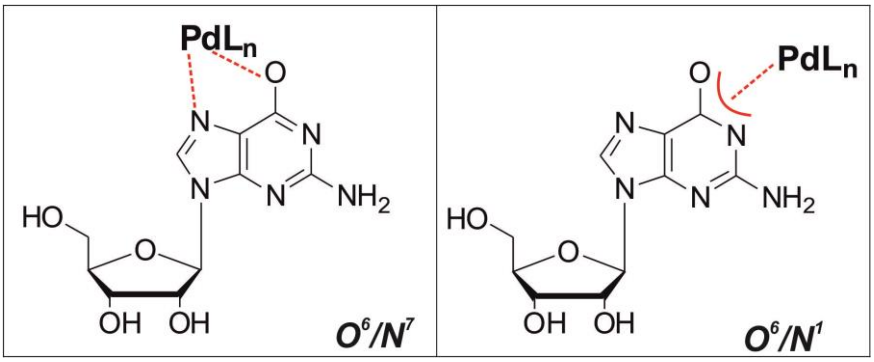

Fig. 3.28 Possible coordinations of palladium with guanosine under basic conditions. Figure adapted from Western and Shaugnessy[194].

The temporary protection of the oxygen at position six of 8-bromoguanosine may prevent the deprotonation of guanosine under basic conditions and thus hinder complexation of the negatively charged base with the palladium-ligand complex.

4. Conclusion and Outlook

The effect of 5'-labeling of an antisense siRNA strand on its knockdown efficiency showed that this position is indeed significant when choosing a conjugation site for siRNA duplexes. 5'-Labeling is particularly applicable in techniques that make use of Förster resonance energy transfer (FRET) to monitor the level of degradation of siRNA duplexes in cells[165], where the 3'-end of one strand and the 5'-end of the opposing strand are usually chosen as positions for dye conjugation. Because the strand with the weakest paired 5'-end is incorporated into the RNA interference-induced silencing complex (RISC)[151], careful consideration should be taken when labeling this particular terminal of the respective single strands in the duplex. Due to the complementarity of the antisense strand to the target messenger RNA (mRNA), it is preferable that its 5'-end is less stable. However, our studies suggested that not only terminal end stability is what determines the efficiency of gene suppression. Even though the effect of 5'-labeling on the thermodynamic stability of the duplex was negligible, such labeling still resulted in higher IC_{50}-values and thus a less sufficient knockdown of the eGFP gene. This may indicate a possible steric clash of the dye with protein factors within the RNA interference pathway during strand recognition. This hypothesis was supported by a further decrease in knockdown efficiency with increasing molecular weight of the dye on the 5'-end. 3'-End labeling had no significant effect on knockdown efficiency.

As mentioned earlier, 5'-labeling *via* the sugar edge of guanosine had no significant impact on duplex stability. This was in accordance with previous studies conducted with N^2-methylated guanosine, where a complete loss in base pairing was first observed upon dimethylation on this position[138]. An *s-trans* conformation of the alkylamine on position 2 of guanosine would still enable base pairing with the opposing cytosine[137]. In principle, a similar pattern should be expected for the N^4-labeling of cytosine. However, base pairing was abolished for our N^4-propargylated cytosine derivative. The presence of the methyl group on position 5 of our modified base probably causes a steric interaction with the propargyl functionality, thus forcing it to point in the direction of the Watson-Crick edge and, as a result, disable base pairing with the opposing guanosine.

Possibly due to the local geometry of DNA-only duplexes, hybridized products between DNA and strands containing the modification at internal positions showed a significant loss in T_m. The modification was, however, much better tolerated in DNA/RNA hybrids, which ultimately led to significant differences in melting temperatures between these and the same DNA-only duplexes. By fine-tuning hybridization conditions, a selective hybridization of

RNA complementary strands from a pool of same-sequenced DNA and RNA oligonucleotides may be achieved.

Due to similar mobility patterns of the two opposing strands during gel electrophoresis, a better affinity of the internally modified DNA strands for RNA could not be proven where the sense and antisense strands were of the same length. An increase in the length of the opposing strand, *i.e.* the antisense strand, resulted in a loss of the significant difference in T_m between DNA-only duplexes and DNA/RNA hybrids for all but one construct. For the oligonucleotide containing the modification on the second position from the 3'-end, it was possible to obtain a difference in T_m of 7 °C. This higher affinity of this particular strand for the 42mer RNA than for the 42mer DNA could additionally be proven by means of a gel shift mobility assay. These results were, however, not in accordance with results obtained for the shorter strands and, even though a change in the local geometry of the duplex formed with the longer DNA strand is suspected, the outcome of the latter experiments still remain puzzling and warrant further analyses. Thus, even with the successful synthesis of a modified oligonucleotide that can discriminate between DNA and RNA strands, the complete logic behind the behavior of the different strands that contain the 5-methyl-N^4-propargylcytidine derivative is not yet fully understood.

Future fishing experiments with the shorter oligonucleotides may include the use of a 'clickable' biotin azide, to enable isolation with streptavidin as affinity tag. Since the effect of labeling of the free alkyne group on hybridization properties is still unknown, hybridization patterns prior to labeling should be compared to hybridization in the presence of a triazole linked functional group on the modified DNA strand.

Not only did the cytidine 5-CH_3 diminish base pairing properties of the nucleoside by causing a *cis*-conformation of the propargyl group, but it may even have had an effect on the mechanism involved in the formation of the modified cytidine derivative. It would be interesting to see whether the absence of the methyl group might lead to a preferred formation of the N^2-substituted side-product, which was discovered during LC/MS analysis of the modified oligonucleotides and single nucleoside. Even if the formation of the N^2-substituted product would not be preferred, the future use of 2'-deoxyuridine instead of thymidine as starting material during the reaction with triisopropylbenzenesulfonyl chloride may also be an interesting approach to determine the effect of the N^4-propargyl functionality on the base pairing properties of cytidine in the absence of the sterically hindering methyl group. In the absence of a methyl group that is likely to force the propargyl in the direction of the Watson-

Crick face, it is to be expected that base pairing would be fundamentally different from what was determined during the present experiments.

In addition to investigations into the effect of base modification on duplex stability, the incorporation of 5-ethynyluridine into both eukaryotic and prokaryotic cells was attempted. Its successful incorporation into RBE4 cells was confirmed by a click reaction of the treated cells with an azido functionalized dye and concomitant microscopic cell imaging. The incorporation into *E. coli* RNA could, however not be confirmed. After isolation of the cellular RNA from EU-incubated *E. coli* cells, a click reaction with a fluorescent dye was performed. No fluorescent click product could be detected *via* gel electrophoresis, suggesting that the modification was not successfully incorporated into the bacterial RNA.

The Sonogashira reaction between 8-bromoguanosine and TMS-acetylene also proved to be unsuccessful. A possible complex formation between the palladium and the guanosine nucleoside may result in a deactivation of the catalyst during the reaction. A similar experiment with 8-bromoadenosine may be attempted in the future.

5. Experimental section

Instruments and Materials

8-well chamber, *mu* slides	Ibidi (Martinsried, Germany)
AlexaFluor 594 azide	Invitrogen (Karlsruhe, Germany)
Ampicillin	Roth (Karlsruhe, Germany)
Analytical Balances:	
- Sartorius	Sartorius (Goettingen, Germany)
- Mettler Toledo PM460	Mettler (Gießen, Germany)
Atto 488 azide	Atto-Tec (Siegen, Germany)
Atto 590 azide	Atto-Tec (Siegen, Germany)
bFGF, human recombinant	Invitrogen (Karlsruhe, Germany)
Buffers and Staining Solutions:	
- Ammonium acetate (puris)	Sigma Aldrich (Steinheim, Germany)
- Ammonium peroxydisulfate	Roth (Germany)
- GelRed	Biotium (Hayward, CA, USA)
- $LiClO_4$ for precipitation	2% (m/v) in acetone (Sigma Aldrich, Steinheim)
- PAGE loading buffer without dye markers	1x TBE (diluted from Rotiphorese 10x TBE) 90% (v/v) formamide
- PAGE loading buffer	1x TBE (diluted from Rotiphorese 10x TBE), 90% (v/v) formamide, 0.1% bromophenol blue, 0.1% xylene cyanol
- Rotiphorese sequencing gel buffer concentrate	Roth (Germany)
- Rotiphorese sequencing gel concentrate	Roth (Germany)
- Rotiphorese sequencing gel diluents	Roth (Germany)
- Rotiphorese 10x TBE buffer	Roth (Germany)
- Sodium acetate (pH adjusted to 5.2)	Sigma Aldrich (Munich, Germany)
- Triethylammonium acetate buffer	2 mol Et_3N (Acros, Niderrau, Germany) +

(2 M, pH adjusted to 7)	2 mol acetic acid (AppliChem, Darmstadt, Germany) in 1 L H_2O
- TBE buffer	100 mM Tris (pH 8.3) 90 mM boric acid 1 mM EDTA
- TEMED	Roth (Germany)
Centrifuges:	
- 1-15 PK Sigma	Osterode am Harz, Germany
- Eppendorf Centrifuge 5810R	Hamburg, Germany
Chloramphenicol (35 µg/mL in 90% ethanol)	BioChemica (Dresden, Germany)
Collagen, Type I, from rat tail	Sigma Aldrich (St. Louis, USA)
DAPI	Sigma Aldrich (Munich, Germany)
DMEM	Gibco (Invitrogen, Germany)
DNA/RNA Synthesizer, Applied Biosystems Expedite TM 8909	Genecust (Dudelange, Luxembourg)
DyeEx 2.0 Spin Kit 250	Qiagen (Hilden, Germany)
Electrophoresis Chamber	CBS Scientific, VWR (Darmstadt, Germany)
Enzymes:	
- FastAP thermosensitive Alkaline phosphatase	Fermentas (St. Leon-Rot, Germany)
- Nuclease P1	Sigma Aldrich (Steinheim, Germany)
- Snake venom phosphodiesterase	Worthington (Lakewood, USA)
Eppendorf tubes (Silanized)	Roth (Germany)
Flow cytometer	LSR-FortessaSORP, BD (Heidelberg, Germany)
Fluorescent mounting medium	DAKO Cytomation (Hamburg, Germany)
Formamide, > 99.5%	Roth, Karlsruhe (Germany)
FCS	Invitrogen (Darmstadt, Germany)
Freeze dryer	Alpha 2-4 LD plus, Christ (Osterode am Harz,Germany)
Greiner tubes	CellStar (Frickenhausen, Germany)
HAM's F-10 culture medium	Invitrogen (Darmstadt, Germany)
HEPES	Sigma Aldrich (Munich, Germany)

HPLC	Agilent 1100 Series, Merck-Hitachi Agilent 1260, Merck-Hitachi

HPLC Columns:

- C18 Reversed-phase column, LiChroCART 250-10, Merck (Darmstadt, Germany)
- Synergy fusion RP, 4 µm particle size, 80 Å pore size, 250 mm length, 2 mm inner diameter, Phenomenex (Aschaffenburg, Germany)

Inverted confocal microscope	TCS SP5, Leica (Wetzlar, Germany)
IR Spectrometer	AVATAR 330FT-IR (Thermo nicolet)
JASCO FP-6500 fluorimeter	Jasco (Groß-Umstadt, Germany)
JASCO V-6500 spectrophotometer	Jasco (Groß-Umstadt, Germany)
Lipofectamine 2000	Invitrogen (Darmstadt, Germany)
Lithium perchlorate, battery grade, dry	Sigma Aldrich (Steinheim, Germany)

Mass Spectrometry:

- MALDI-TOF	Bruker BIFLEX III *(Situated at the IPMB at the Heidelberg University)*
- FAB and EI	JEOL JMS-700 *(Situated in the Department of Organic Chemistry, Mainz University)*
- ESI	Finnigan MAT TSQ 700 *(Situated in the Department of Organic Chemistry, Mainz University)*
- FD	Finnigan MAT 95 *(Situated in the Department of Organic Chemistry, Mainz University)*

- Triple Quadropole mass spectrometer, Agilent 6460 with ESI Jetstream ion source

Microscopy:

- Nikon C1Si confocal microscope	Nikon (Düsseldorf, Germany) (*Situated in the Nikon Imaging Center at the University of Heidelberg)*
- Leica TC S SP5 confocal microscope	Leica (Wetzlar, Germany) (*Situated at the Institute of Molecular Biology in Mainz)*
MicroSpin G-25 columns	GE Healthcare (Munich, Germany)
NanoDrop ND-2000	Peqlab (Erlangen, Germany)
NAP columns, Sephadex G-25	GE Healthcare (Munich, Germany)

NMR spectrometers:

- Avance III HD 400
- Bruker AC-300 and AM-400
- Varian 300

Oligofectamine	Invitrogen (Darmstadt, Germany)
OptiMem	Invitrogen (Darmstadt, Germany)
pEGFP-N1	Invitrogen (Darmstadt, Germany)
pH-Meter	Mettler Toledo FE20/EL20 (Gießen, Germany)
Pipettes P2, P20, P100, P200, P1000	Abimed (Langenfeld, Germany)
Rotary evaporator	RV 06-ML
Silica gel 60 (0.063-0.200 nm)	Merck (Darmstadt, Germany)
Silica gel plates,Polygram® Sil G/UV_{254}	Macherey-Nagel (Düren, Germany)
SpeedVac Concentrator plus	Eppendorf (Hamburg, Germany)
Spin filters Nanosep® MF Centrifugal devices, 0.2 μm	Roth (Karlsruhe, Germany)
SPOS Reagents:	Sigma Aldrich, Proligo (Hamburg, Germany)
- Activator 42	5-[3,5-Bis(trifluoromethyl)phenyl]-1*H*-tetrazole (0,1 M in CH_3CN)
- Caps A	Acetic anhydride in THF (11% v/v)
- Caps B	*N*-Methylimidazole in THF (16% v/v)
- DCA Deblock	Dichloroacetic acid in DCM (3% v/v)
- TCA Deblock	Trichloroacetic acid in DCM (3% v/v)
- Wash	Acetonitrile (extra dry)
Thermomixer comfort	Eppendorf (Hamburg, Germany)
Trifast FL kit	PeqLab (Erlangen, Germany)
Triton X-100	Sigma (Munich, Germany)
Typhoon 9400 variable mode imager	GE Healthcare (München, Germany)
Ultrapure Water Purification System	Milli-Q, Millipore (Schwalbach, Germany)
UV cuvettes, SUPRASIL quartz glass cuvettes, 10 mm pathlength	Hellma (Müllheim, Germany)
UV-Lamp 254 nm	Herolab Molekulare Trenntechnik (Wiesloch, Germany)

UV/Vis Spectrophotometry:

- NanoDrop ND-2000 PeqLab (Erlangen, Germany)
- V-6500 spectrophotometer Jasco (Groß-Umstadt, Germany)

ZipTip Millipore (Schwalbach, Germany)

All other solvents, salts and reagents not included in the list were either obtained from the Heidelberg University, 'Zentralbereich', Neuenheimer Feld, or from the Mainz University, Institute of Pharmacy's in-house chemical store.

A. General organic synthesis procedures

Chemical reagents and solvents were obtained from various commercial suppliers. For the purpose of manual liquid chromatography purifications, some organic solvents were distilled prior to use. Deuterated solvents were purchased from Deutero (Kastellaun, Germany).

Thin layer chromatography (TLC): Pre-coated silica gel plates, Polygram® Sil G/UV_{254} (40 x 80 mm) from Macherey-Nagel (Düren, Germany) were used for monitoring chemical reactions. Compounds were visualized under UV-light at λ = 254 nm and/or Seebach's reagent, consisting of 2,5 g phosphomolybdic acid, 1 g $Ce(SO_4)_2$ and 6 mL concentrated H_2SO_4 in 94 mL water.

Column chromatography (CC): Silica gel 60 (230-400 mesh) from Fluka, Silica gel 60 (230-400 mesh), Merck KGaA, Darmstadt (Germany).

NMR-spectroscopy: Varian 300 MHz (^{1}H: 300 MHz, ^{13}C: 75 MHz) and Bruker 500 MHz (^{1}H: 500 MHz, ^{13}C: 125 MHz), IPMB, Heidelberg University Bruker AC 300 MHz, Institute of Pharmacy and Biochemistry, Mainz University. Bruker 400 MHz (^{1}H: 400 MHz, ^{13}C: 100 MHz), Institute of Inorganic and Analytical Chemistry, Mainz.University Avance III HD 400 MHz (^{31}P: 200 MHz), Institute of Organic Chemistry, Mainz University.

^{1}H and ^{13}C NMR spectra were calibrated to Me_4Si on the basis of the relative chemical shift of the solvent as an internal standard. Chemical shifts (δ) are in ppm and abbreviations used are as follows: br s = broad singlet, s = singlet, d = doublet, pd = pseudo doublet, t = triplet, m= multiplet.

Mass spectrometry: FAB and EI mass spectra were recorded on a JEOL JMS-700 sector field mass spectrometer. MALDI-TOF (positive mode) mass spectra were recorded on a Bruker BIFLEX III spectrometer with matrix 3-hydroxypicolinic acid, ammonium citrate. HR-ESI mass spectra were recorded on a Bruker MicroTOF-Q II spectrometer. FD-MS spectra were recorded on a Finnigan MAT 95 and ESI-MS spectra on a Micromass LCT at the Institute of Organic Chemistry, Mainz University.

IR spectroscopy: Nicolet Avatar 330 FT-IR, Thermo electron corporation, Institute of Pharmacy and Biochemistry, Mainz University.

Melting points: Electrothermal IA 9200, Institute of Pharmacy and Biochemistry, Mainz University.

Microscopy: For cell imaging, the **Nikon C1Si** spectral imaging confocal laser scanning system in a Nikon Ti fully automated inverted microscope (Nikon, Düsseldorf, Germany) was

used. A 63x or 40x oil immersion objective (CFI Plan Apo) was applied. The microscope was equipped with three excitation laser lines and the following were used for imaging: 488 nm and 561 nm. For maintaining focus in live-cell imaging the C1Si contains a perfect focus system (PFS). The EZC1FreeViewer (Nikon) and ImageJ[196] were used for data processing.

5.1 Synthesis of *tris*-(3-hydroxypropyltriazolylmethyl)amine (TPTA)

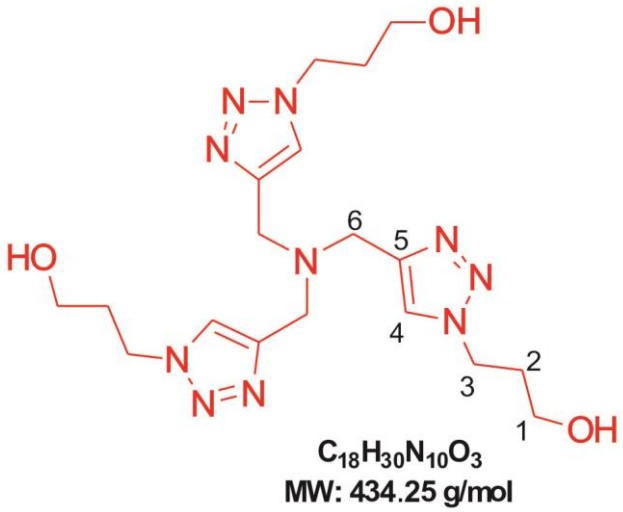

5.1.1 Azidation of 3-bromo-1-propanol

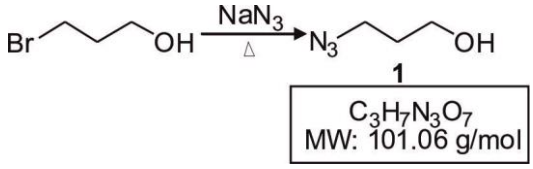

7,5 mL (83 mmol) 3-bromo-1-propanol was dissolved in 100 mL H_2O, to which was added 3 eq. (250 mmol; 16 g) of NaN_3. The reaction mixture was stirred at 90 °C for 48 hours. The aqueous phase was extracted with DCM (3 x 50 mL), the organic phase was then washed with H_2O (50 mL) and dried over Na_2SO_4. The product was concentrated *in vacuo* at RT to afford **1** as a pale yellow oil in 63% yield[197].

TLC (silica gel, Et_2O:*c*Hex, 1:1): R_f = 0.28.

^{1}H NMR (300 MHz, $CDCl_3$, 25 °C): δ = 1.83 (m, ^3J = 6.6 Hz, 2H, H2); 3.45 (t, ^3J = 6.6 Hz, 2H, H3); 3.75 (t, ^3J = 6.0 Hz, 2H, H1) ppm.

^{13}C NMR (100 MHz, DMSO-d_6, 25 °C): δ = 31.52 (C2); 47.81 (C3); 57.82 (C1) ppm.

FD-MS *m/z* 101.4 (M^+, 100%).

5.1.2 Synthesis of *tris*-(3-hydroxypropyltriazolylmethyl)amine (TPTA)

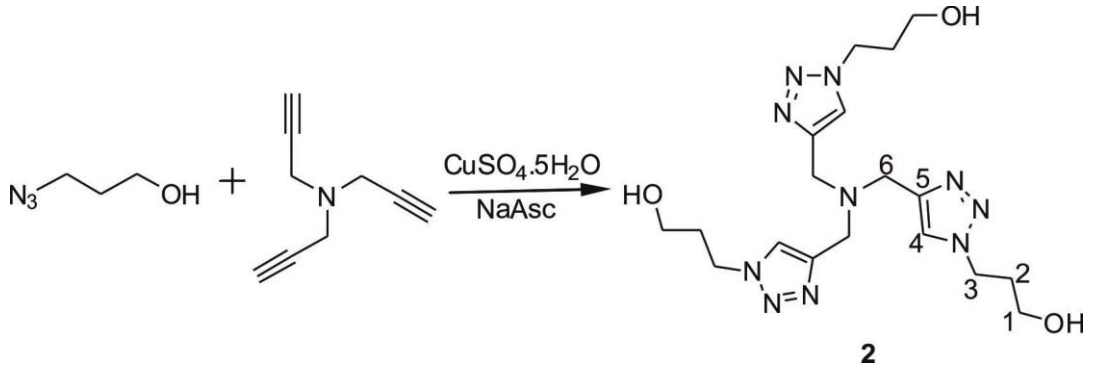

2

1.6 mL tripropargylamine (11.3 mmol) was dissolved in 20 mL of a 9:1 mixture of CH_3CN:H_2O. The reagents were added in the following order: 5.15 g of 3-azido-1-propanol **(1)** (51 mmol; 4.5 eq.); 855 mg $CuSO_4$•$5H_2O$ (3.4 mmol; 0.3 eq.); 1 g sodium ascorbate (5.1 mmol; 4.5 eq.) and 7.9 mL Et_3N (56.5 mmol; 5 eq.). The reaction mixture was allowed to stir overnight at RT and the reaction progress was monitored by TLC, with DCM:MeOH:30% NH_3 (89:10:1) as mobile phase. After complete conversion of all starting material, the reaction mixture was evaporated to dryness. Silica gel chromatography of the crude in DCM:MeOH:30% NH_3 (89:10:1) delivered the product as a beige solid (1.8 g; 36%).

Mp: 101 – 103 °C.

TLC (silica gel, DCM:MeOH:30% NH_3; 89:10:1): R_f = 0.05.

^{1}H NMR (300 MHz, DMSO-d_6, 25 °C): δ = 1.96 (m, ^3J = 6.0 Hz, 6H, H2); 3.40 (dt, ^3J = 6.0 Hz, 6H, H1); 3.62 (s, ^3J = 6.0 Hz, 6H, H6); 4.41 (t, ^3J = 6.0 Hz, 6H, H3); 4.68 (br s, 3H, OH); 8.03 (s, 3H, H4) ppm.

^{13}C NMR (100 MHz, DMSO-d_6, 25 °C): δ = 33.02 (C2); 46.61 (C3); 47.11 (C4); 57.40 (C1); 124.05 (C6); 143.41 (C5) ppm.

HR-ESI-TOF-MS: 457.2406 [M + Na].

FT-IR $\tilde{\nu}$ *(cm^{-1})*: 3354 ν (OH); 2945 ν (CH_2, aliph.); 1462 ν (CH_2, aliph.); 1266 ν (C-O).

5.2 Synthesis of 3'-*O*-CEP-2'-*O*-TOM-5'-*O*-DMT-5-methyluridine

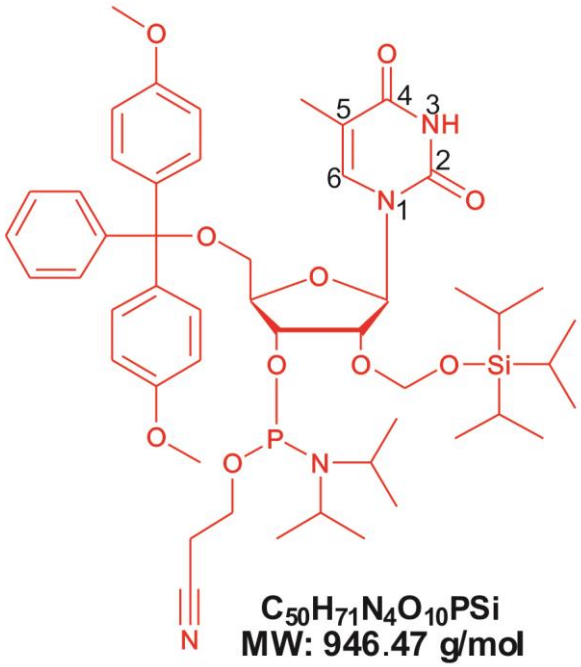

5.2.1 Tritylation of 5-methyluridine (m^5U)

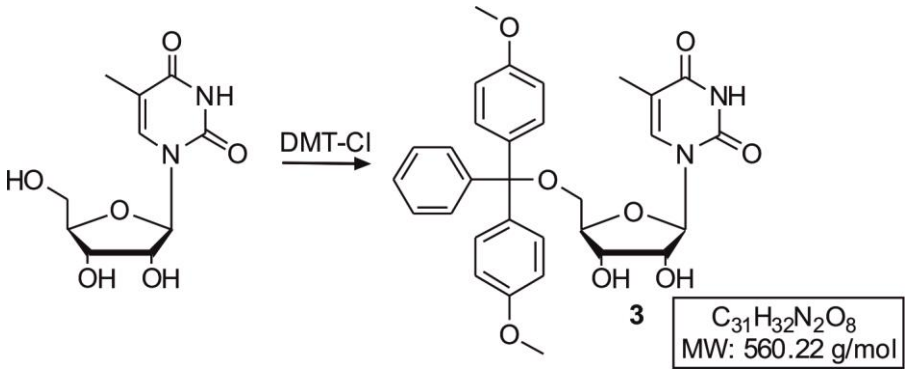

5 g (19.4 mmol) m^5U was placed in a round bottomed flask and placed under an argon atmosphere. To this was added 0.78 eq. Et_3N (2.2 mL). The mixture was dissolved in 120 mL anhydrous pyridine. 1.5 eq. (7.9 g) DMT-Cl was slowly added as solution in 5 mL pyridine and the reaction mixture was allowed to stir overnight. The mixture was co-concentrated with toluene, resulting in an orange solid foam, which was purified by means of column chromatography (silica gel). The following gradient system was used as eluent system: DCM:MeOH (0% MeOH → 5% MeOH → 10% MeOH) + 1% Et_3N. The yield for this reaction was 62%.

Mp: Decomposes at 190 °C.

TLC (silica gel, DCM:MeOH; 15:1): R_f = 0.49.

^{1}H NMR (400 MHz, DMSO-*d6*, 25 °C): δ = 1.41 (s, 3H, CH_3); 3.17 (dd, ^3J = 4,4 Hz & 4.0 Hz, 1H, H5'); 3.23 (dd, ^3J = 2,8 Hz & 2,4 Hz, 1H, H5'); 3.74 (s, 6H, OCH_3 x 2); 3.96 (q,

^3J = 4.0 Hz & 2.8 Hz, 1H, H4‘); 4.10 (dd, ^3J = 4.8 Hz & 5.2 Hz, 1H, H2’); 4.18 (dd, ^3J = 5.2 Hz & 5.6 Hz, 1H, H3‘); 5.17 (d, ^3J = 5.2 Hz, 1H, 3’OH); 5.47 (d, ^3J = 5.6 Hz, 1H, 2’OH); 5.80 (d, ^3J = 5.2 Hz, 1H, H1’); 6.90 (d, 4H, ^3J = 8.8 Hz, trityl Hs); 7.24 –7.40 (m, 9H, trityl Hs); 7.50 (s, 1H, H6); 11.37 (br s, 1H, NH) ppm.

^{13}C NMR (100 MHz, DMSO-d_6, 25 °C) δ = 11.74 (CH_3); 55.15 (OCH_3 x 2); 63.60 (C5’); 70.21 (C2’); 73.29 (C3’); 82.91 (C4’); 85.98 (1 trityl C); 88.06 (C1’); 109.60 (C5); 113.37 (4 trityl C); 126.91 (1 trityl C); 127.73 (1 trityl C); 128.04 (1 trityl C); 129.82 (6 trityl C); 135.26 (1 trityl C); 135.47 (1 trityl C); 135.95 (C4); 144.81 (1 trityl C); 150.74 (C2); 158.26 (2 trityl C); 163.76 (C6) ppm.

FD-MS *m/z* 560.24 (M^+, 100%).

FT-IR $\tilde{V}$ *(cm^{-1})*: 3195 ν (OH); 3064 ν (C-H, alkene); 2933 ν (C-H, alkane); 1691 ν (C=O); 1605 ν (N-H); 1680 ν (C=C); 1380 ν (CH_3); 1245 ν (C-O); 1029 ν (C-N).

5.2.2 2’OH-protection of 5’-*O*-DMT-m^{5}U

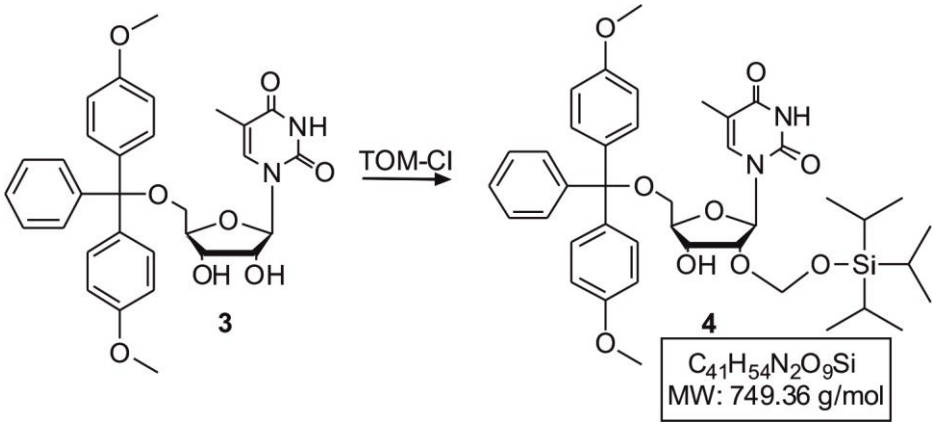

5’-O-DMT-m^{5}U **(3)** (0.7 mg; 1.2 mmol) was dissolved in 8 mL anhydrous 1,2-dichloroethane. 3,5 eq. (0.73 mL; 4.2 mmol) *N*,*N*-diisopropylethylamine was added under stirring. 0.4 g of Bu_2SnCl_2 (1.1 eq.; 1.3 mmol) was dissolved in 5 mL anhydrous 1,2-dichloroethane and added to the above solution. The mixture was stirred for 1 hour at RT, after which 1.2 eq. (0.4 mL) of TOM-Cl was added. The reaction mixture was heated to 80 °C and refluxed for 1 hour, during which the reaction progress was monitored by TLC. After complete conversion of all starting material to either 2’- or 3’-*O*-TOM protected forms, 15 mL DCM and 25 mL saturated aqueous $NaHCO_3$ were added and the mixture was stirred for another 10 – 15 minutes. The two phases were separated and the aqueous phase was washed one last time with 15 mL DCM. The organic phase was dried over anhydrous $MgSO_4$ and concentrated *in vacuo*. Silica gel column chromatography with *c*Hex:EtOAc (3:2) + 2% Et_3N resulted in 480 mg of the 2’-*O*-TOM protected product. YIELD: 52%.

Mp: 105 – 108 °C.

TLC (silica gel, *c*Hex:EtOAc (1:1): R_f = 0.61.

^{1}H NMR (400 MHz, DMSO-*d6*, 25 °C): δ = 0.96 (s, 6H, *i*Pr_3Si); 0.98 (s, 12 H, [*i*Pr_3Si] x 2); 0.99 – 1.07 (m, 3H, C**H**[CH_3]$_2$ x 3); 1.43 (s, 3H, CH_3); 3.18 – 3.25 (m, 2H, H5‘); 3.73 (s, 6H, OCH_3 x 2); 3.99 (q, ^3J = 3.6 Hz & 2.8 Hz, 1H, H4‘); 4.20 (m, 1H, H2’); 4.38 (t, ^3J = 6.4 Hz & 5.6 Hz, 1H, H3‘); 4.92 (d, ^3J = 5.6 Hz, 1H, OCH_2O); 4.97 (d, ^3J = 5.6 Hz, 1H, OCH_2O); 5.22 (d, ^3J = 5.6 Hz, 1H, 3’OH); 5.97 (d, ^3J = 6.8 Hz, 1H, H1’); 6.89 (d, ^3J = 8.8 Hz, 4H, trityl Hs); 7.24 – 7.40 (m, 9H, trityl Hs); 7.48 (s, 1H, H4); 11.39 (br s, 1H, NH) ppm.

^{13}C NMR (100 MHz, DMSO-d_6, 25 °C) δ = 11.70 (CH_3); 17.59 (*i*Pr – CH_3 x 6); 26.36 (*i*Pr – CH x 3); 55.06 (OCH_3 x 2); 63.71 (C5’); 68.89 (C3’); 77.02 (C3’); 83.91 (C4’); 86.08 (1 trityl C); 88.36 (C1’); 110.09 (C5); 113.27 (4 trityl C); 126.87 (1 trityl C); 127.67 (1 trityl C); 127.94 (1 trityl C); 129.74 (6 trityl C); 135.21 (1 trityl C); 135.38 (1 trityl C); 135.62 (C4); 144.63 (1 trityl C); 150.57 (C2); 158.18 (2 trityl C); 163.57 (C6) ppm.

MALDI-TOF-MS *m/z* 789.54 (M^+, 2%); 785.35 (100).

FT-IR $\tilde{\nu}$ *(cm^{-1})***:** 3186 ν (OH); 3064 ν (C-H, alkene); 2941 ν (C-H, alkane); 1691 ν (C=O); 1680 ν (C=C); 1617 ν (N-H); 1380 ν (CH_3); 1245 ν (C-O); 1090 ν (C-N).

5.2.3 Phosphitylation of 2’-*O*-TOM-5’-*O*-DMT-m^{5}U

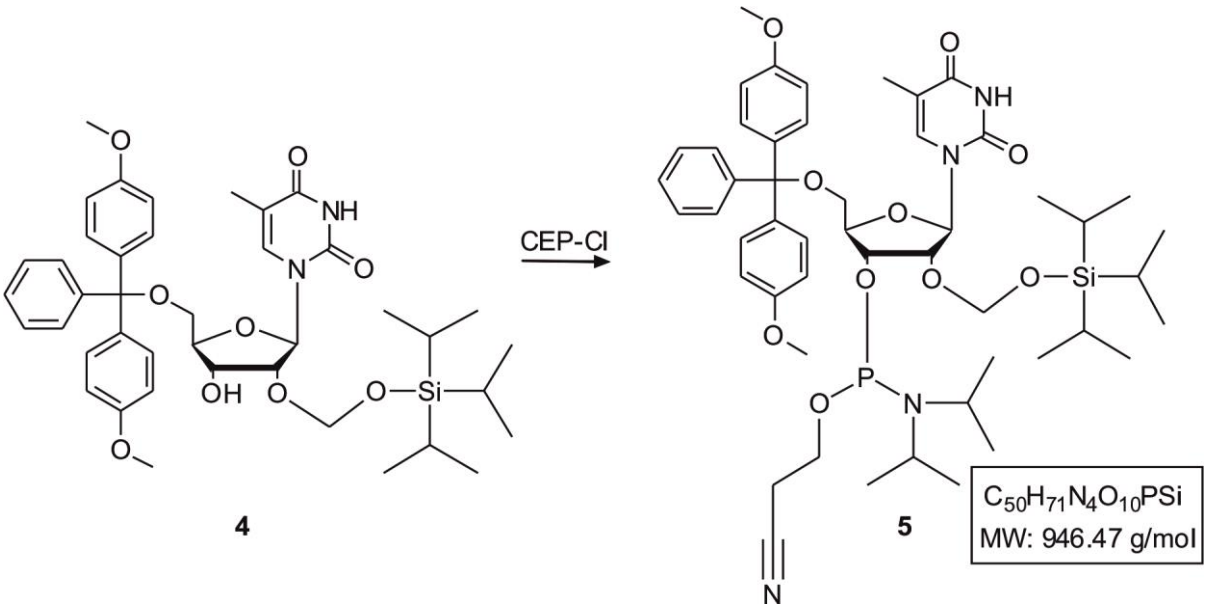

4 (150 mg; 0.20 mmol) was dissolved in 5 mL anhydrous DCM and placed under an argon atmosphere. To this solution was added 5 eq. *N,N*-diisopropylethylamine (0.18 mL; 1.0 mmol). While stirring the mixture, CEP-Cl (1.3 eq.; 60 µL) was added, ensuring to exclude oxygen from the reaction. The reaction mixture was stirred for 2 hours at RT. TLC analysis clearly showed the formation of the two phosphoramidite diastereomers. The crude mixture

was evaporated to dryness and purified *via* silica column chromatography. The mobile phase *c*Hex:EtOAc (2:1) + 3% Et_3N was used to obtain the pure product **(5)** in a yield of 24%.

Mp: 80 °C.

TLC (silica gel, *c*Hex:EtOAc (1:1): R_f = 0.65.

^{1}H NMR (400 MHz, DMSO-*d6*, 25 °C): δ = 0.94 (s, 12H, *i*Pr_3Si); 0.96 (s, 24 H, [*i*Pr_3Si] x 4); 1.00 – 1.08 (m, 6H, C**H**[CH_3]$_2$ x 6); 1.09 – 1.20 (m, 24H, [$(CH_3)_2CH]_2N$); 1.46 (s, 6H, CH_3); 2.58 (t, 2H, ^3J = 5.6 Hz, CH_2CN); 2.75 – 2.83 (m, 2H, CH_2CN); 3.20 – 3.38 (m, 4H, 5‘H); 3.44 – 3.68 (m, 8H, [$POCH_2]_2$; (CHN]$_2$ x 2); 3.73 (s, 12H, OCH_3 x 4); 4.09 (q, ^3J = 3.6 Hz & 3.2 Hz, 1H, 4‘H); 4.15 (q, ^3J = 2.8 Hz & 3.2 Hz, 1H, 4‘H); 4.30–4.34 (m, 1H, 2’H); 4.37–4.42 (m, 1H, 2’H); 4.49–4.55 (m, 2H, 3‘H); 4.88 - 4.99 (m, 4H, OCH_2O x 2); 5.95 (d, ^3J = 6.4 Hz, 2H, 1’H); 6.86 – 6.90 (m, 8H, trityl Hs); 7.22 – 7.41 (m, 18H, trityl Hs); 7.49 (s, 1H, H4); 7.51 (s, 1H, H4); 11.43 (br s, 2H, NH) ppm.

^{13}C NMR (100 MHz, DMSO-d_6, 25 °C) δ = 11.34 (CH_3); 11.73 (CH_3); 17.52 (*i*Pr - CH_3 x 12); 19.68 (CH_2CN); 19.76 (CH_2CN); 24.12 (CH_3 – *i*Pr_3 x 2); 24.20 (CH_3 – *i*Pr_3 x 2); 24.29 (CH_3 – *i*Pr_3 x 2); 24.37 (CH_3 – *i*Pr_3 x 2); 26.34 (*i*Pr_3Si – CH x 6); 42.42 (*i*Pr_3N – CH x 2); 42.61 (*i*Pr_3N – CH x 2); 55.03 (OCH_3 x 4); 58.67 ($POCH_2$); 58.90 ($POCH_2$); 63.13 (C5’); 63.28 (C5’); 70.28 (C3’); 70.52 (C3’); 75.73 (C2’); 75.79 (C2’); 82.74 (C4’); 82.77 (C4’); 85.87 (OCH_2O x 2); 86.19 (trityl C); 86.31 (trityl C); 88.68 (C1’); 88.73 (C1’); 110.18 (C5); 110.20 (C5); 113.23 (8 trityl Cs); 118.69 (CN); 118.80 (CN); 126.87 (trityl C x 2); 127.67 (2 trityl Cs x 2); 127.90 (2 trityl Cs x 2); 129.77 (4 trityl Cs x 2); 135.00 (C4); 135.17 (C4); 135.21 (2 trityl Cs x 2); 135.42 (2 trityl Cs); 135.61 (2 trityl Cs); 144.44 (trityl C); 144.55 (trityl C); 150.50 (C2 x 2); 158.23 (2 trityl Cs); 163.50 (C6 x 2) ppm.

^{31}P NMR (200 MHz, DMSO-*d6*, 25 °C) δ = 149.78; 148.05 ppm.

HR-ESI-TOF-MS: 969.4543 [M + Na].

FT-IR $\tilde{\nu}$ *(cm^{-1})*: 3187 ν (OH); 3064 ν (C-H, alkene); 2864 ν (C-H, alkane); 1691 ν (C=O); 1617 ν (N-H); 1462 ν (C-H, alkane); 1364 ν (CH_3); 1245 ν (C-N).

5.3 Synthesis of 3'-*O*-CEP-2'-*O*-TOM-5'-*O*-DMT-O^6-nitrophenyl-2-propargylaminylinosine

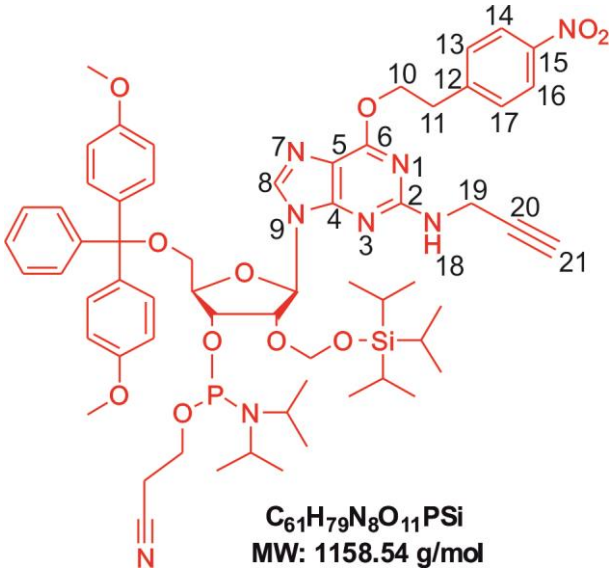

5.3.1 Synthesis of 2',3',5'-*O*-triacetylguanosine (6)

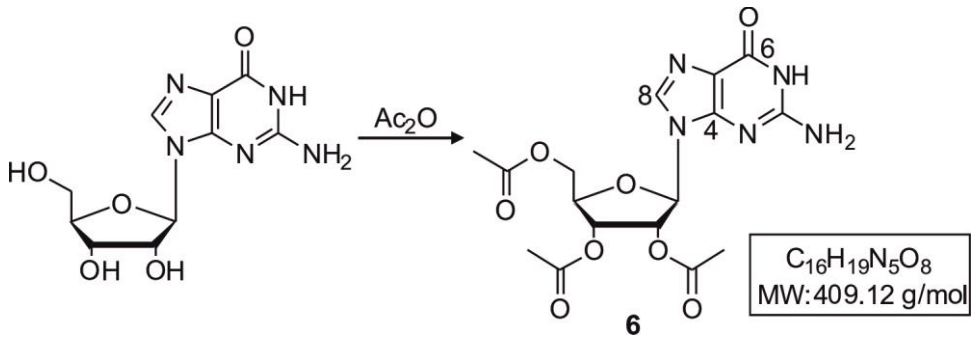

To a suspension of 9.5 g of guanosine (33.5 mmol) in 15 mL dry pyridine was added 30 mL acetic anhydride in 40 mL DMF. The suspension was stirred for 4 hours at 75 °C, after which the temperature was cooled to RT. Stirring was continued overnight. The mixture was concentrated *in vacuo* and the product was obtained *via* recrystallization from MeOH in 93% yield[198].

Mp: 230 – 232 °C.

TLC (silica gel, MeOH:$CHCl_3$; 1:20): R_f = 0.13.

^{1}H NMR (400 MHz, DMSO-d_6, 25 °C): δ = 2.03 (s, 3H, 2'*O*Ac); 2.04 (s, 3H, 3'*O*Ac); 2.11 (s, 3H, 5'*O*Ac); 4.23 – 4.39 (m, 3H, H4' & H5'); 5.49 (t, ^3J = 5.9 Hz, 1H, H3'); 5.79 (t, ^3J = 6.0 Hz, 1H, H2'); 5.98 (d, ^3J = 6.0 Hz, 1H, H1'); 6.54 (br s, 2H, NH_2); 7.93 (s, 1H, H8); 10.75 (br s, 1H, NH) ppm.

^{13}C NMR (100 MHz, DMSO-d_6, 25 °C): δ = 20.21 (C7'); 20.40 (C9'); 20.55 (C11'); 63.09 (C5'); 70.31 (C3'); 72.04 (C2'); 79.54 (C4'); 84.38 (C1'); 116.81 (C5); 135.64 (C8); 151.11 (C4); 153.88 (C2); 156.63 (C6); 158.44 (C6'); 169.46 (C8'); 170.10 (C10') ppm.

MALDI-TOF-MS: 410.1315 [M + H].

FT-IR $\tilde{\nu}$ *(cm^{-1})*: 3309 ν (N-H); 1744 ν (C=O); 1625 ν (N-H); 1601 ν (aromatic); 1380 ν (CH_3); 1364 ν (C-H, alkane); 1200 ν (C-O); 1070 ν (C-N).

5.3.2 Mitsunobu reaction of 2',3',5'-*O*-triacetylguanosine

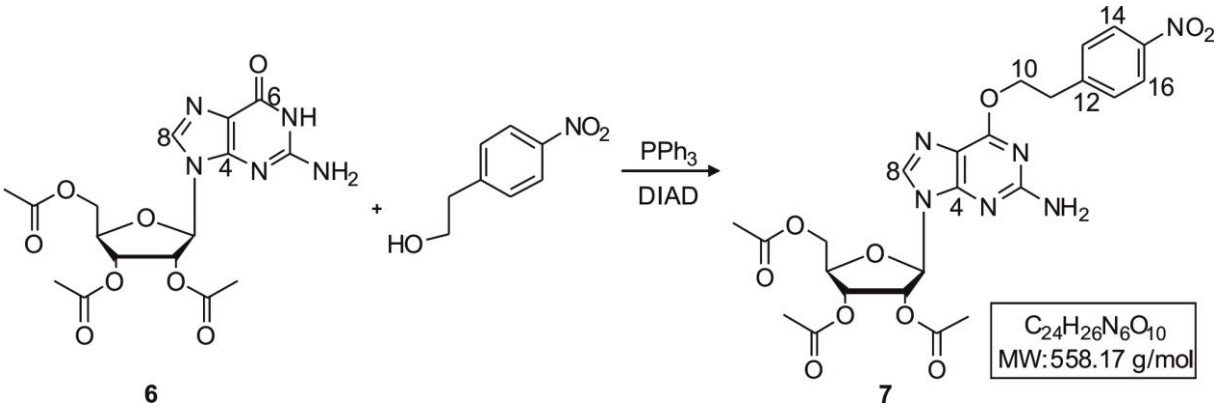

6 7

2 g of **6** (4.9 mmol) was suspended in 120 mL dry dioxane, to which was added 1.5 eq. triphenylphosphine (1.93 g; 7.4 mmol) and 2 eq. 2-(*p*-nitrophenyl) ethanol (1.64 g; 9.8 mmol). The reaction mixture was heated to 80 °C and stirred for 45 minutes at this temperature, or until a clear solution was obtained. 1.5 mL diisopropyl azadicarboxylate (1.5 eq.; 1.5 mmol) was added and the temperature was reduced to 60 °C. After 1 hour, the reaction mixture was concentrated under reduced pressure[198] and the product was isolated by column chromatography using the following gradient system as eluent: Et_2O:DCM (9:1) → (4:1) → (1:1) → 100% DCM → DCM:MeOH (49:1) → (19:1). The product was obtained with a yield of 60%.

Mp: 75 - 79 °C.

TLC (silica gel, Et_2O:DCM; 1:1): R_f = 0.25.

^{1}H NMR (400 MHz, $CDCl_3$, 25 °C): δ = 2.02 (s, 3H, 2'*O*Ac); 2.03 (s, 3H, 3'*O*Ac); 2.08 (s, 3H, 5'*O*Ac); 3.20 (t, ^3J = 6.8 Hz, 2H, H11); 4.29 – 4.42 (m, 3H, H4' & H5'); 4.66 (t, ^3J = 6.8 Hz, 2H, H10); 5.74 (t, ^3J = 4.8 Hz, 1H, H3'); 5.92 (t, ^3J = 4.8 Hz, 1H, H2'); 5.98 (d, ^3J = 4.8 Hz, 1H, H1'); 7.41 (pd, 2H, ^3J = 8.4 Hz, H13 & H17); 7.71 (s, 1H, H8); 8.07 (pd, ^3J = 8.4 Hz, 2H, H14 & H16) ppm.

^{13}C NMR (100 MHz, $CDCl_3$, 25 °C): δ = 20.35 (2'*O*Ac); 20.46 (3'*O*Ac); 20.63 (5'*O*Ac); 35.02 (C11); 62.97 (C5'); 66.19 (C10); 70.46 (C4'); 72.76 (C3'); 79.72 (C2'); 86.37 (C1'); 115.69 (C5); 128.37 (C14); 128.49 (C16); 129.89 (C12); 131.88 (C13); 131.92 (C17); 137.96 (C8); 145.93 (C15); 153.40 (C4); 159.23 (C2); 160.83 (C6); 169.33 (2'*O*-CO); 169.55 (3'*O*-CO); 170.43 (5'*O*-CO) ppm.

FD-MS *m/z* 558.4 (M^+, 100%).

FT-IR $\tilde{\nu}$ *(cm^{-1})*: 1744 ν (C=O); 1610 ν (NO_2); 1581 ν (N-H); 1409 ν (C-H, alkane); 1344 ν (C-N); 1227 ν (C-O); 695 ν (C-H, alkene).

5.3.3 Synthesis of *O*^{6}-nitrophenyl-2-propargylaminylinosine (8)

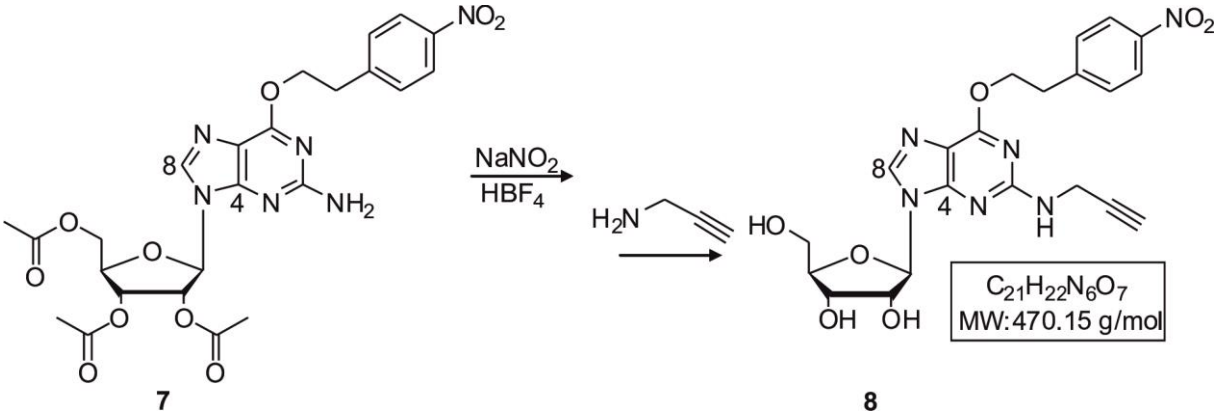

7 8

0.7 g (1,2 mmol) of *O*^{6}-nitrophenyl-2',3',5'-*O*-triacetylguanosine **(7)** was dissolved in 20 mL acetone. 14 mL HBF_4 (50% in H_2O) was added and the reaction was stirred at -40 °C for 1 hour. 3 eq. $NaNO_2$ (3.7 mmol; 0.26 g) was added in a dropwise fashion (as solution in a small amount of H_2O) and the mixture was allowed to stir overnight. NaOH (8 M) was used to neutralize the reaction mixture and the product was extracted into DCM, which was dried over anhydrous Na_2SO_4, filtered and concentrated *in vacuo*[161,199]. This crude mixture was further used for the nucleophilic substitution reaction with propargylamine. Propargylamine (5 eq.; 6.0 mmol) was added (8 M in MeOH; 0.75 mL) to the dried crude mixture and the reaction mixture was allowed to stir for 3 days at RT. **8** was obtained after silica gel column chromatography, using the gradient system, starting from pure DCM and slowly increasing the polarity with MeOH to a final ratio of DCM:MeOH 15:1. The final yield after the three steps was 54%.

Mp: 82 - 83 °C.

TLC (silica gel, MeOH: $CHCl_3$; 1:20): R_f = 0.63.

^{1}H NMR (400 MHz, DMSO-*d*$_6$, 25 °C) δ = 3.00 (t, 1H, H21); 3.29 (t, 2H, ^3J = 6.9 Hz, H10); 3.50 – 3.67 (m, 2H, H5'); 3.89 (m, 1H, H4'); 4.07 (dd, 2H, ^3J = 1.2 Hz, H19); 4.13 (m, 1H, H3'); 4.56 (m, 1H, H2'); 4.73 (t, 2H, ^3J = 6.9 Hz, H11); 4.97 (t, 1H, 5'OH); 5.18 (d, 1H, ^3J =4.8 Hz, 3'OH); 5.41 (d, 1H, ^3J = 4.8 Hz, 2'OH); 5.80 (d, 1H, ^3J = 5.4 Hz, H1'); 7.36 (t, 1H, ^3J = 1.3 Hz, H18); 7.64 (pd, 2H, ^3J = 8.7 Hz, H13 & H17); 8.13 (s, 1H, H8); 8.19 (pd, 2H, ^3J = 8.7 Hz, H14 & H16) ppm.

^{13}C NMR (100 MHz, DMSO-*d*$_6$, 25 °C) δ = 31.38 (C19); 35.02 (C11); 62.24 (C5'); 66.30 (C10); 71.06 (C3'); 72.77 (C21); 73.88 (C2'); 86.00 (C4'); 87.62 (C1'); 115.01 (C5); 124.12

(C14 & C16); 130.96 (C13, C17 & C12); 139.52 (C8); 147.30 (C15), 158.68 (C2); 160.65 (C6) ppm.

FD-MS *m/z* 470.3 (M^+, 100%).

FT-IR $\tilde{V}$ *(cm^{-1})***:** 3285 ν (C-H, alkyne); 2920 ν (C-H, alkane); 1740 ν (C=O); 1664 ν (C=C, alkene); 1590 ν (N-H); 1515 ν (NO_2); 1453 ν (C-H, alkane); 1342 ν (NO_2); 1237 ν (C-O); 1074 ν (C-N).

5.3.4 Synthesis of 5'-*O*-DMT-*O*^{6}-nitrophenyl-2-propargylaminylinosine (9)

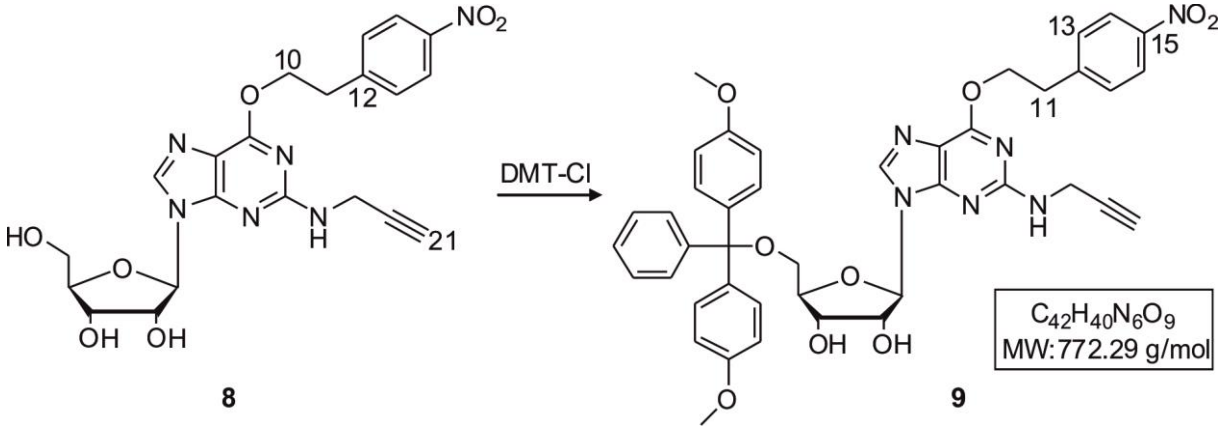

8 9

110 mg of **8** (0.24 mmol) was dissolved in 3 mL dry pyridine. 100 mg DMT-Cl (1.2 eq., 0.28 mmol) was added as solution in a small amount of pyridine. DMAP (10 mg; 0.3 eq.; 0.08 mmol) was added and the reaction mixture was stirred at RT for 12 hours. The reaction was quenched with water and evaporated to dryness at 25 °C. Silica gel column chromatography with Et_2O:EtOAc (2:3) + 3% Et_3N, followed by DCM + 3% Et_3N and DCM:MeOH (10:1) + 3% Et_3N resulted in a pure product. YIELD: 95%.

Mp.: 180 - 185 °C.

TLC (silica gel, *c*Hex:EtOAc; 1:1): R_f = 0.06.

^{1}H NMR (400 MHz, DMSO-*d*$_6$, 25 °C) δ = 2.96 (t, 1H, H21); 3.18 (m, 2H, H5'); 3.28 (t, 2 H, ^3J = 6,8 Hz, H11); 3.71 (s, 6H, OCH_3 x 2); 3.98 (m, 1H, H4'); 4.02 (dd, 2H, ^3J = 4.4 Hz, H19); 4.27 (m, 1H, H3'); 4.64 (m, 1H, ^3J = 4.8 Hz H2'); 4.72 (t, 2H, ^3J = 6.8 Hz, H10); 5.21 (d, 1H, ^3J = 5.6 Hz, 3'OH); 5.56 (d, 1H, ^3J =5.6 Hz, 2'OH); 5.85 (d, 1H, ^3J = 4.8 Hz, H1'); 6.81 (m, 4H, trityl-Hs); 7.18 – 7.24 (m, 9H, trityl-Hs); 7.34 (t, 1H, ^3J =1.3 Hz, H18); 7.63 (pd, 2H, ^3J = 8.4 Hz, H13 & H17); 8.03 (s, 1H, H8); 8.17 (pd, 2H, ^3J =8.4 Hz, H14 & H16) ppm.

^{13}C NMR (100 MHz, DMSO-*d*$_6$, 25 °C) δ = 31.18 (C19); 34.81 (C11); 55.47 (OCH_3 x 2); 64.55 (C5'); 66,13 (C10); 70.97 (C3'); 72.56 (C21); 73.39 (C2'); 83.46 (C20); 85.93 (C4'); 89.68 (C1'); 113.59 (C8); 123.92 (C14 & C16); 130.11 (C13); 130.17 (C17); 130.77 (C12); 136.01 (C8); 145.33 (C15), 158.50 (C2); 160.47 (C6) ppm.

FD-MS *m/z* 773.68 (M^+, 13.9%); 303.15 (100).

FT-IR $\tilde{V}$ *(cm^{-1})***:** 1744 ν (C=O); 1581 ν (N-H); 1409 ν (C-H, alkane); 1344 ν (C-N); 1227 ν (C-O); 695 ν (C-H, alkene); 610 ν (NO_2).

5.3.5 Synthesis of 2'-*O*-TOM-5'-*O*-DMT-O^6-nitrophenyl-2-propargyl-aminylinosine

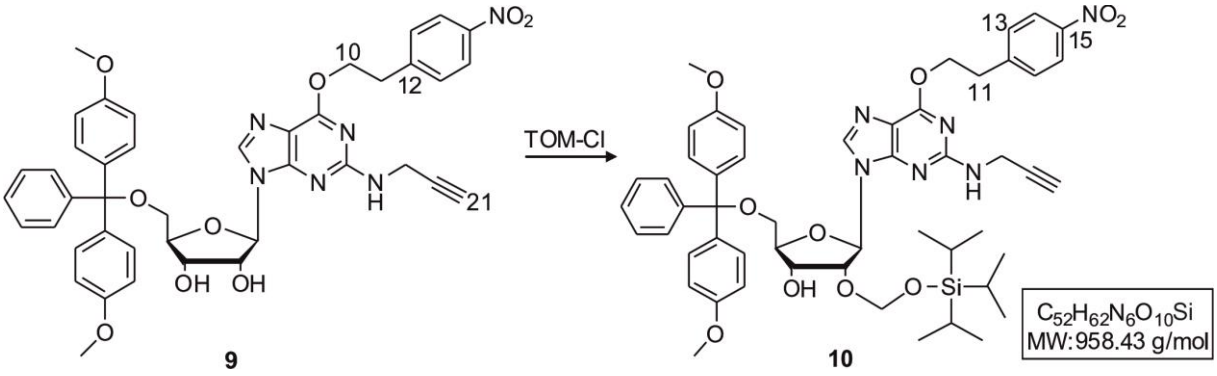

5'-*O*-DMT-O^6-nitrophenyl-2-propargylaminylinosine **(9)** (110 mg; 0.14 mmol) was dissolved in 6 mL DCE. 1.1 eq. tBu$_2$SnCl$_2$ (66 mg; 0.15 mmol) was added and the reaction mixture was heated to 65 °C. 1.2 eq. TOM-Cl (36 µL; 0.17 mmol) and 0.4 mL Et_3N were subsequently added. The reaction mixture was allowed to cool to RT and stirring was continued at RT. After 5 hours, the reaction was quenched by the addition of MeOH and following concentration of the crude mixture under reduced pressure, the product was isolated *via* flash column chromatography. The following gradient solvent system was used: DCM + 3% Et_3N → DCM:MeOH (70:1) + 1% Et_3N. The regioselectivity of 2'-O-alkylated over 3'-O-alkylated product was approximately 7:2.

Mp: 70 - 75 °C.

TLC (silica gel, *n*Hex:EtOAc; 1:1): R_f = 0.41.

^{1}H NMR (400 MHz, $CDCl_3$, 25 °C) δ = 1.04 (s, 6H, iPr$_3$Si); 1.05 (s, 12 H, [iPr$_3$Si] x 2); 1.07 – 1.12 (m, 3H, C**H**[CH_3]$_2$ x 3); 1.03-1.07 (m, 18H, iPr$_3$Si); 3.05 (br s, 1H, H21); 3.28 (t, ^3J = 6.8 Hz, 2H, H11); 3.35 – 3.39 (dd, 1H, H5'); 3.44 – 3.48 (dd, 1H, H5') 3.48 (d, 1H, H2'); 3.77 (s, 6H, OCH_3 x 2); 4.05 – 4.08 (m, 2H, ^3J = 2.4 Hz, H19); 4.25 (q, 1H, H4'); 4.58 (t, 1H, H3'); 4.74 (t, 2H, ^3J = 6,8 Hz, H10); 4.98 (t, 2H, ^3J = 4,8 Hz, OCH_2O); 6.03 (d, 1H, ^3J = 5.6 Hz, H1'); 6.79 (m, 4H, trityl-Hs); 7.18 – 7.33 (m, 9H, trityl-Hs); 7.44 (t, 1H, H18); 7.48 (d, 2H, ^3J = 8.4 Hz, H13 & H17); 7.76 (s, 1H, H8); 8.16 (pd, 2H, ^3J =8.4 Hz, H14 & H16) ppm.

^{13}C NMR (100 MHz, $CDCl_3$, 25 °C) δ = 11.85 [$(CH_3)_2$**C**H]; 17.72 [$(CH_3)_2$**C**H]; 29.70 (C19); 35.21 (C11); 55.19 (OCH_3 x 2); 63.58 (C5'); 66,06 (C10); 70.54 (C3'); 71.03 (C21); 81.02 (C20); 81.42 (C2'); 83.83 (C4'); 86.71 (C1'); 90.89 (OCH_2O); 113.14 (4 trityl C); 115.99

(C5); 123.73 (C14); 126.87 (C16); 127.85 (C15); 128.20 (4 trityl C); 129.93 (2 trityl C); 130.09 (C12); 135.71 (trityl C); 135.77 (trityl C); 138.59 (C8); 144.59 (trityl C); 146.02 (C17); 146.82 (C13); 153.80 (C2), 157.93 (C4); 158.50 (2 trityl C); 160.60 (C6) ppm.

FD-MS *m/z* 958.51 (M^+, 69%); 530.45 (100).

FT-IR $\tilde{V}$ *(cm^{-1})***:** 3411 ν (O-H); 3288 ν (C-H, alkyne); 3068 ν (C-H, alkene); 2929 ν (C-H, alkane); 1605 ν (NO_2); 1585 ν (N-H); 1462 ν (C-H, alkane); 1245 ν (C-O); 1176 ν (C-N).

5.3.6 Phosphitylation of 2'-*O*-TOM-5'-*O*-DMT-O^6-nitrophenyl-2-propargyl-aminylinosine

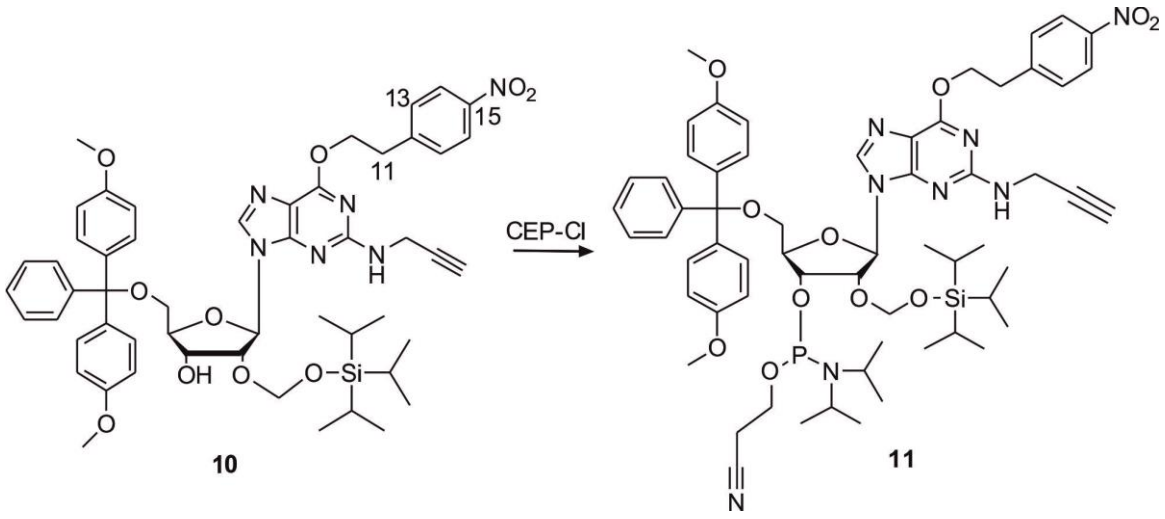

120 mg (0.13 mmol) of vacuum dried 2'-*O*-TOM-5'-*O*-DMT-O^6-nitrophenyl-2-propargylaminylinosine **(10)** was dissolved in 4 mL dry DCM. To this solution was added 300 µL dimethylethylamine and 1.5 eq. CEP-Cl (100 mg; 0.18 mmol). The reaction was stirred at RT for 2 hours. After drying the crude, silica gel chromatography with *c*Hex:EtOAc (2:1) + 2% Et_3N → (1:1) + 2% Et_3N was used to obtain a mixture of the two diastereomers in the ratio of 3:2 (as determined by NMR).

TLC (silica gel, *c*Hex:EtOAc; 1:1): R_f = 0.55.

^{1}H NMR (400 MHz, $CDCl_3$, 25 °C) δ = 0.95 - 1.36 (m, 42H, *i*Pr_3Si); 2.34 (t, 2H, H21); 2.14 - 2.16 (m, 2H, CH_2CN); 2.62 – 2.68 (m, 2H, CH_2CN); 3.09 (br s, 1H, H21); 3.29 (t, ^3J = 6.8 Hz, 4H, H11); 3.35 (dd, ^3J = 4.8 Hz, 2H, 5'H); 3.47 – 3.71 (m, 9H, 5'H & $[NCH]_2$, $POCH_2$); 3.77 (s, 6H, OCH_3 x 2); 3.78 (s, 6H, OCH_3 x 2); 3.84 – 3.97 (m, 2H, $POCH_2$); 4.01 – 4.14 (m, 4H, H19); 4.30 (q, ^3J = 4.0 Hz, 1H, 4'H); 4.36 (q, ^3J = 4.0 Hz, 1H, 4'H); 4.61-4.69 (m, 2H, NH); 4.74 (t, 4H, ^3J = 6.8 Hz, H10); 4.79 (t, 2H, 3'H); 4.89 – 4.97 (m, 4H, OCH_2O); 5.09 – 5.13 (m, 2H, 2'H); 5.99 (d, ^3J = 6.0 Hz, 1H, 1'H); 6.03 (d, ^3J = 6.4 Hz, 1H, 1'H); 6.77 – 6.81 (m, 8H, trityl-Hs); 7.17 – 7.34 (m, 18H, trityl-Hs); 7.40 – 7.44 (m, 2H, H18); 7.48 (pd, 4H, H13 & H17); 7.74 (s, 2H, H8); 8.15 (pd, 4H, H14 & H16) ppm.

^{31}P NMR (200 MHz, $CDCl_3$, 25 °C) δ = 151.16; 151.58 ppm.

FD-MS *m/z* 1159.57 (M^+, 14%); 1160.58 (10); 1181.56 (8); 1198.55 (5); 303.15 (100).

FT-IR $\tilde{V}$ ***(cm^{-1})*****:** 3288 ν (C-H, alkyne); 3068 ν (C-H, alkene); 2929 ν (C-H, alkane); 1605 ν (NO_2); 1585 ν (N-H); 1462 ν (C-H, alkane); 1245 ν (C-O); 1240 ν (C-N); 1180 ν (C-N).

5.4 Synthesis of 3'-*O*-CEP-5'-*O*-DMT-5-methyl-N^4-propargyl-aminyldeoxycytidine

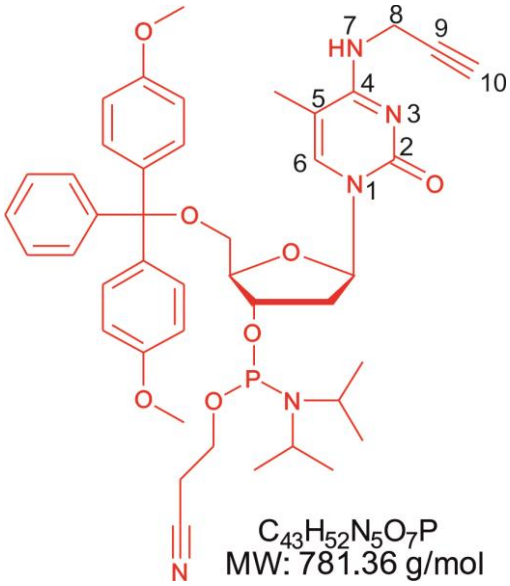

5.4.1 Tritylation of thymidine

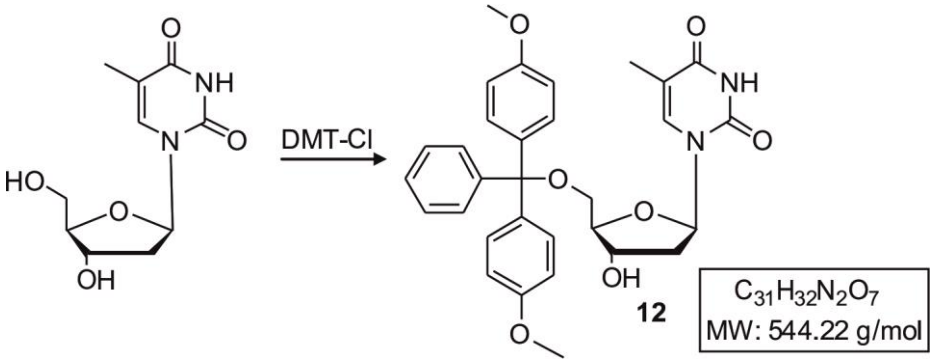

610 mg thymidine (2.5 mmol) was dissolved in 10 mL dry pyridine and the solution was placed under argon. DMAP (0.5 eq., 153 mg, 1.25 mmol) was added as solution in 2 mL dry pyridine, followed by the slow addition of DMT-Cl (1.2 eq., 1.3 g, 3.8 mmol). The reaction mixture was stirred at RT and under an argon atmosphere for 12 hours. After conversion of all starting material to product, the reaction was quenched with 2 mL MeOH and concentrated *in vacuo*. Flash column chromatography with DCM:MeOH (15:1) + 1% Et_3N, followed by the more polar DCM:MeOH (10:1) + 1% Et_3N was used for the purification of the tritylated product. 1.28 g of **12** was obtained, *i.e.* in 94% yield.

Mp: 225 - 228 °C.

TLC (silica gel, DCM:MeOH; 15:1): R_f = 0.43.

^{1}H NMR (400 MHz, DMSO-d_6, 25 °C) δ = 1.44 (s, 3H, CH_3); 2.12 – 2.17 (m, 1H, H2'); 2.21 – 2.28 (m, 1H, H2'); 3.14 – 3.17 (m, 1H, H5'); 3.19 – 3.23 (m, 1H, H5'); 3.73 (s, 6H, OCH_3 x 2); 3.88 (m, 1H, H4'); 4.29 – 4.34 (m, 1H, H3'); 5.36 (d, ^3J = 4.4 Hz, 1H, 3'OH); 6.20 (t,

1H, ^{3}J = 6.8 Hz, H1'); 6.89 (d, ^{3}J = 9.2 Hz, 4H, trityl Hs); 7.23 – 7.40 (m, 9H, trityl Hs); 7.51 (s, 1H, H6); 11.35 (br s, 1H, NH) ppm.

^{13}C NMR (100 MHz, DMSO-d_6, 25 °C) δ = 11.45 (CH_3); 45.42 (C2'); 54.78 (OCH_3 x 2); 63.51 (C5'); 70.72 (C3'); 83.47 (C1'); 85.22 (trityl C); 85.56 (C4'); 109.31 (C5); 112.98 (4 trityl Cs); 126.52 (trityl C); 127.14 (2 trityl Cs); 127.39 (2 trityl Cs); 127.64 (2 trityl Cs); 129.46 (4 trityl Cs); 135.00 (trityl C); 135.17 (trityl C); 135.44 (trityl C); 144.47 (C6); 150.11 (C2); 157.88 (2 trityl Cs); 163.40 (C4) ppm.

FD-MS *m/z* 544.7 (M^+, 100%).

FT-IR $\tilde{\nu}$ *(cm^{-1})***:** 2876 ν (C-H, alkane); 1683 ν (C=O); 1609 ν (N-H); 1380 ν (CH_3)**;** 1356 ν (C-H, alkane); 1249 ν (C-O); 1033 ν (C-N).

5.4.2 3'OH protection of 5'-*O*-DMT-thymidine

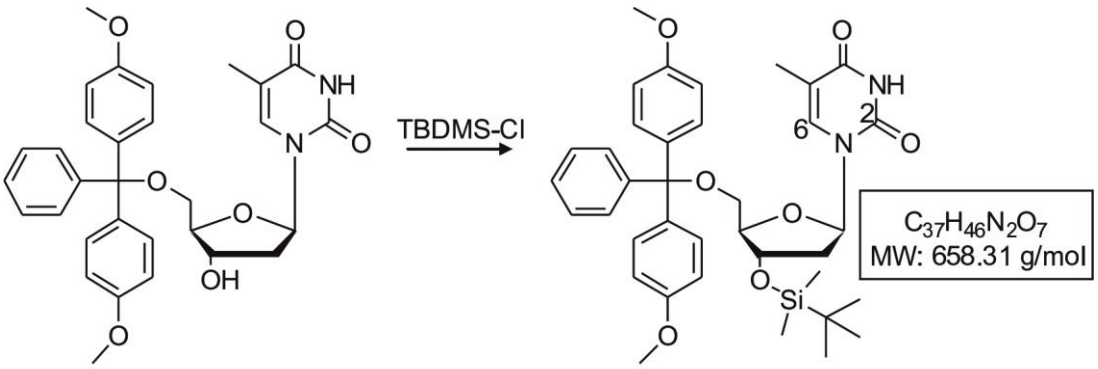

12 **13**

12 (3.5 g, 6.4 mmol) was dissolved in 10 mL dry DCM and placed under argon. To this solution was added 4.4 eq. imidazole (1.9 g, 28.2 mmol), followed by 4 eq. TBDMS-Cl (3.9 g, 27.7 mmol). The reaction was stirred at RT until all starting material was converted to product (12 hours). 2 mL MeOH was added and the solution was poured into EtOAc (70 mL). The organic phase was extracted [5% aqueous $NaHCO_3$ (2 x 50 mL) and brine (1 x 50 mL)], dried over anhydrous $MgSO_4$ and evaporated to dryness. This resulted in the pure product as a fluffy, white solid (3.64 g; 87% yield).

Mp: 108 – 112 °C.

TLC (silica gel, DCM:MeOH; 15:1): R_f = 0.75.

^{1}H NMR (300 MHz, DMSO-d_6, 25 °C) δ = -0.05 (s, 3H, $SiCH_3$); 0.00 (s, 3H, $SiCH_3$); 0.78 (s, 9H, $SiC(CH_3)_3$); 1.51 (s, 3H, CH_3); 2.10 – 2.17 (m, 1H, H2'); 2.28 – 2.35 (m, 1H, H2'); 3.13 – 3.17 (m, 1H, H5'); 3.22 – 3.26 (m, 1H, H5'); 3.73 (s, 6H, OCH_3 x 2); 3.81 (m, 1H, H4'); 4.45 (q, 1H, ^{3}J = 5,1 Hz, H3'); 6.15 (t, 1H, ^{3}J = 6,3 Hz, H1'); 6.89 (d, ^{3}J = 8.4 Hz, 4H, trityl Hs); 7.40 – 7.44 (m, 9H, trityl Hs); 7.54 (s, 1H, H6); 11.36 (br s, 1H, NH) ppm.

^{13}C NMR (100 MHz, DMSO-d_6, 25 °C) δ = -5.09 ($SiCH_3$); -4.77 ($SiCH_3$); 11.88 (CH_3); 17.63 (SiC); 25.62 (SiC[CH_3]$_3$); 39.66 (C2'); 55.08 (OCH_3 x 2); 62.99 (C5'); 71.53 (C3'); 83.77 (C1'); 85.17 (trityl C); 85.94 (C4'); 109.57 (C5); 113.25 (4 trityl Cs); 126.85 (trityl C); 127.67 (2 trityl C); 127.91 (2 trityl C); 129.73 (4 trityl C); 135.25 (trityl C); 135.35 (trityl C); 135.81 (trityl C); 144.63 (C6); 150.34 (C2); 158.21 (2 trityl C); 163.71 (C4) ppm.

FD-MS *m/z* 658.6 (M^+, 100%).

FT-IR $\tilde{\nu}$ *(cm^{-1})***:** 2945 ν (C-H, alkane); 1687 ν (C=O); 1605 ν (N-H); 1397 ν (C-H, alkane); 1380 ν (CH_3); 1364 ν (C-H, alkane); 1249 ν (C-O); 1094 ν (C-N); 829 ν (C-H, aromatic).

5.4.3 Synthesis of 3'-*O*-TBDMS-5'-*O*-DMT-*O*^{4}-triisopropylphenylsulfonyl thymidine

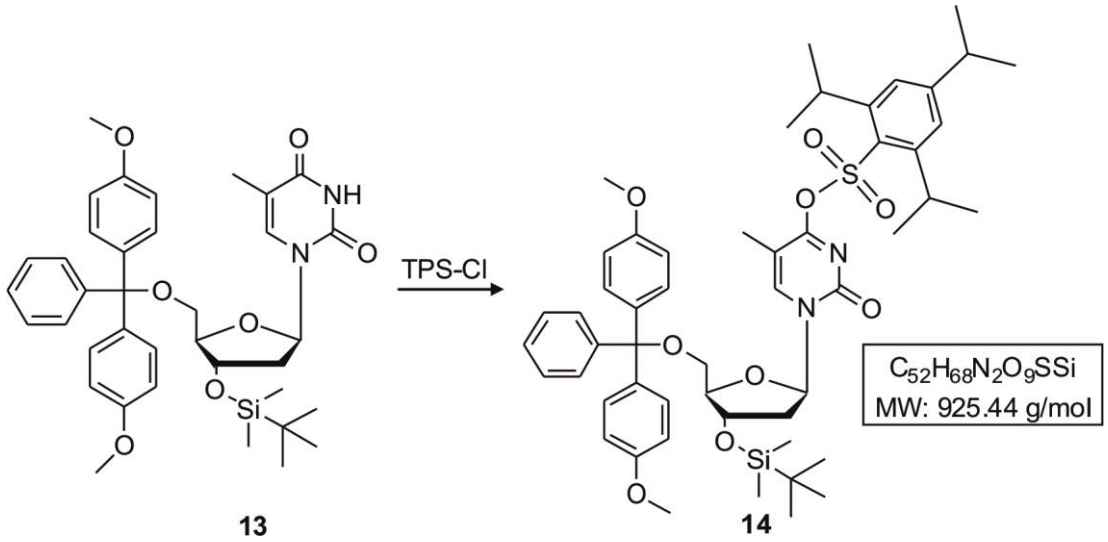

13 14

1.3 g of **13** (1.9 mmol) was dissolved in 10 mL dry DCM, to which was added DMAP (0.09 eq., 21 mg, 0.17 mmol) and Et_3N (5 eq., 1.3 mL, 9.5 mmol).1.2 eq. TPS-Cl (0.7 g, 2.3 mmol) was added as solution in a minimal amount of DCM. The reaction was stirred at RT overnight under an argon atmosphere. TLC analysis showed about 60% conversion of starting material to product. The reaction mixture was concentrated *in vacuo* and purified *via* aluminium oxide column chromatography, using *c*Hex:EtOAc as eluent system in the ratio of 3:1. The yield after column chromatography was 50%.

Mp: 108 - 111 °C.

TLC (silica gel, *c*Hex:EtOAc; 3:1): R_f = 0.7.

^{1}H NMR (300 MHz, DMSO-d_6, 25 °C) δ = -0.01 (s, 3H, Si[CH_3]$_2$); 0.03 (s, 3H, Si[CH_3]$_2$); 0.74 (s, 9H, SiCH[C**H$_3$**]$_3$); 1.13 (d, 6H, ^3J = 6.8 Hz, CH(CH_3)$_2$; 1.21 (d, 12 H, ^3J = 6.8 Hz, [CH(CH_3)$_2$]$_2$; 1.61 (s, 3H, CH_3); 2.26 (m, 2H, H2'); 2.96 (h, 1H, ^3J = 6.8 Hz & 7.2 Hz, CH(CH_3)$_2$); 3.14 – 3.21 (m, 1H, H5'); 3.73 (s, 6H, OCH_3 x 2); 3.87 (m, 1H, H4'); 4.18 (h, 2H,

^3J = 6.8 Hz, [CH(CH_3)$_2$]$_2$); 5.98 (t, 1H, ^3J = 6.0 Hz & 7.6 Hz, H1'); 6.87 (d, 4H, 8.8 Hz, trityl Hs); 7.20 – 7.35 (m, 9H, trityl Hs); 8.19 (s, 1H, H6) ppm.

^{13}C NMR (100 MHz, DMSO-d_6, 25 °C) δ = -3.18 (Si[CH_3]$_2$); 12.28 (CH_3); 17.82 (SiC); 23.86 (TPS – [CH_3]$_2$); 24.83(TPS – [CH_3]$_4$); 25.81 (TBDMS – [CH_3]$_3$); 26.36 (TPS – CH); 28.04 (TPS – [CH]$_2$); 33.28 (C2'); 55.01 (OCH_3 x 2); 61.34 (C5'); 70.44 (C3'); 79.92 (C1'); 83.73 (4'C); 87.25 (trityl C); 109.36 (C5); 112.77 (4 trityl Cs); 121.38 (TPS – [CH_2]$_2$); 126.45 (trityl C); 127.43 (2 trityl Cs); 127.65 (2 trityl Cs); 128.92 (6 trityl Cs); 136.12 (2 trityl Cs); 140.24 (SO_2CH); 141.79 (C6); 146.80 (trityl C); 147.26 (TPS – CH); 148.36 (TPS – CH); 150.47 (TPS – CH); 157.82 (C2); 163.75 (C4) ppm.

FD-MS *m/z* 923.49 (M^+, 100%).

FT-IR $\tilde{\nu}$ *(cm^{-1})***:** 3010 ν (C-H, alkane); 2953 ν (C-H, alkane); 2929 ν (CH_3, alkane); 2868 ν (CH_2, alkane); 1683 ν (C=O); 1503 ν (C=C); 1462 ν (C-H, alkane); 988 ν (alkene); 874 ν (C-H, aromatic).

5.4.4 Synthesis of 3'-*O*-TBDMS-5'-*O*-DMT-5-methyl-*N*^{4}-propargylaminyl-deoxycytidine (15)

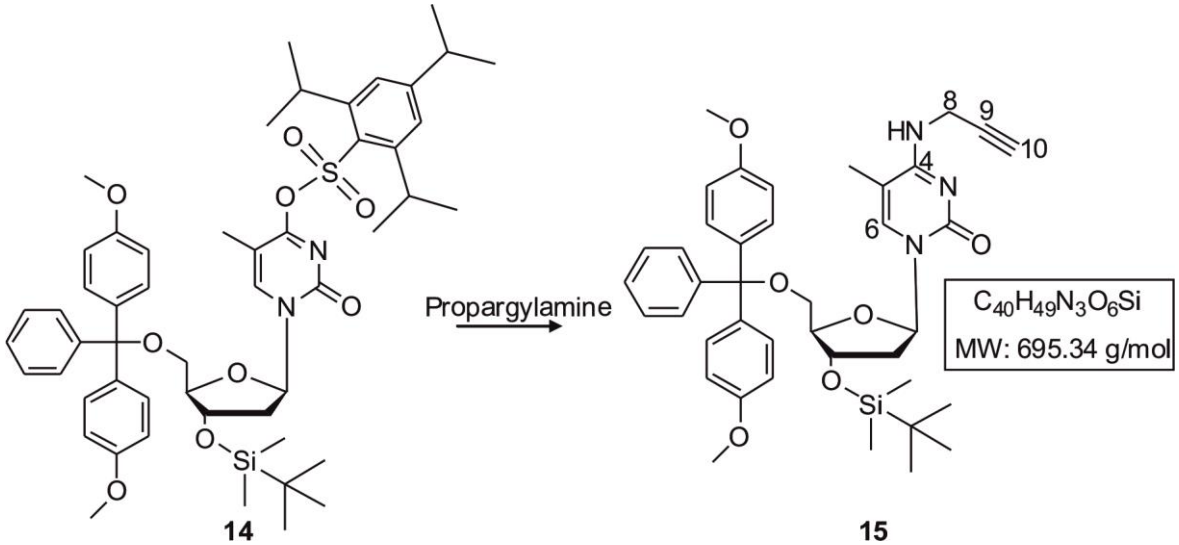

3'-*O*-TBDMS-5'-*O*-DMT-*O*^{4}-triisopropylphenylsulfonyl thymidine was dissolved in dry dioxane (0.9 g in 15 mL). Propargylamine (1.5 mL; 20 eq.) was added and the reaction mixture was stirred at RT overnight. The product was purified by silica gel column chromatography, using the mobile phase *c*Hex:EtOAc (2:1) + 3% Et_3N. This produced **15** in 10% yield. In the ^{1}H NMR small traces of the *N*^{2}-substituted isomer can be detected (see appendix).

Mp: 75 – 78 °C.

TLC (silica gel, DCM:MeOH; 30:1): R_f = 0.45.

^{1}H NMR (300 MHz, DMSO-d_6, 25 °C) δ = -0.06 (s, 3H, $SiCH_3$); -0.01 (s, 3H, $SiCH_3$); 0.78 (s, 9H, $SiCH(CH_3)_3$); 1.54 (s, 3H, CH_3); 2.27 – 2.37 (m, 2H, H2'); 3.11 (t, 1H, ^4J = 2.4 Hz, H10); 3.12 – 3.17 (dd, 1H, H5'); 3.27 – 3.31 (m, 1H, H5'); 3.73 (s, 6H, OCH_3); 3.81 (q, 1H, ^3J = 3.9 Hz, H4'); 4.06 – 4.09 (m, 2H, H8); 4.43 (m, 1H, ^3J = 5.1 Hz, H3'); 6.16 (t, 1H, ^3J = 6.3 Hz, H1'); 6.89 (d, 4H, ^3J = 8.4 Hz, trityl Hs); 7.24 – 7.40 (m, 9H, trityl Hs); 7.58 (s, 1H, H6); 7.59 (t, 1H, ^3J = 5.4 Hz, NH) ppm.

^{13}C NMR (100 MHz, DMSO-d_6, 25 °C) δ = -5.09 ($SiCH_3$); -4.77 ($SiCH_3$); 12.69 (CH_3); 20.77 (C8); 25.63 ([$SiC\mathbf{C}H_3$]$_3$); 29.44 (SiC); 40.71 (2'C); 55.08 (OCH_3 x 2); 62.78 (5'C); 71.45 (C3'); 72.66 (C9 & C10); 81.39 (C1'); 84.54 (C4'); 85.17 (trityl C); 101.75 (C5); 113.25 (4 trityl Cs); 126.85 (trityl C); 127.69 (2 trityl Cs); 127.91 (2 trityl Cs); 129.71 (4 trityl Cs); 135.35 (2 trityl Cs); 137.39 (C6); 144.54 (trityl C); 154.61 (C2); 158.21 (2 trityl Cs); 162.35 (C4) ppm.

FD-MS *m/z* 695.6 (M^+, 100%).

FT-IR $\tilde{\nu}$ *(cm^{-1})***:** 3288 ν (C-H, alkyne); 3080 ν (C-H, alkene); 2949 ν (C-H, alkane); 1699 ν (C=O); 1658 ν (C=C, alkene); 1625 ν (N-H); 1458 ν (C-H, alkane); 1245 ν (C-O); 1102 ν (C-N); 824 ν (C-H, aromatic); 669 ν (C-H, alkyne).

5.4.5 Desilylation of 3'-*O*-TBDMS-5'-*O*-DMT-5-methyl-N^4-propargylaminyl-deoxycytidine (16)

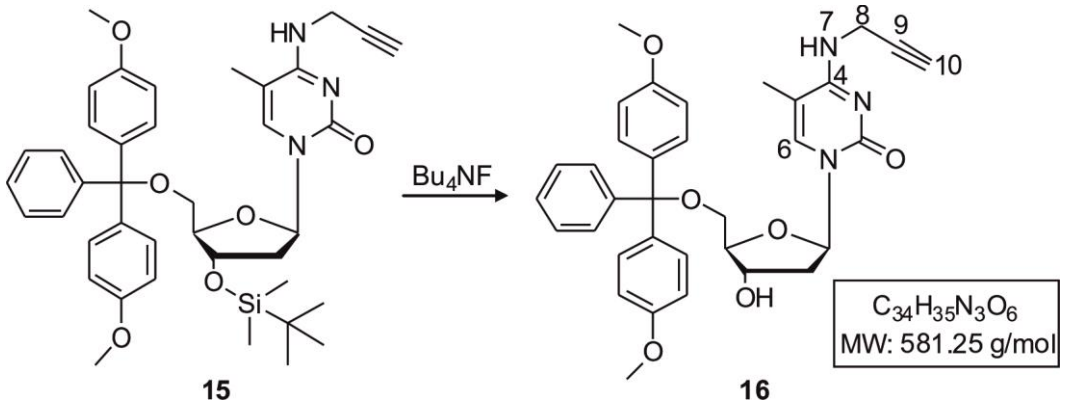

15 16

400 mg of **15** (0.6 mmol) was dissolved in anhydrous THF and the solution was placed under argon. 1.6 eq. of Bu_4NF (0.9 mL of a 1 M solution in THF) was added and the reaction was stirred for 1 hour at RT, after which TLC analysis showed complete conversion of starting material to product. 50 mL EtOAc was added and the product solution was washed with saturated aqueous $NaHCO_3$ (3 x 30 mL). The organic layer was dried over anhydrous Na_2SO_4, filtered and concentrated *in vacuo*. Basic aluminium oxide was used for the purification of the product *via* column chromatography with the following gradient system: *c*Hex:EtOAc (1:2) → (1:3) → EtOAc:MeOH (5:1) → 4:1. The product was isolated in 42% yield.

Mp: 125 °C.

TLC (silica gel, DCM:MeOH; 15:1): R_f = 0,25.

^{1}H NMR (400 MHz, DMSO-d_6, 25 °C) δ = 1.45 (s, 3H, CH_3); 2.08 - 2.14 (m, 1H, H2'); 2.17 - 2.22 (m, 1H, H2'); 3.00 (t, ^4J = 2.4 Hz, 1H, H10); 3.12-3.18 (m, 2H, H5'); 3.70 (s, 6H, OCH_3); 3.82 (m, 1H, H4'); 4.06-4.09 (m, 2H, H8); 4.31 (m, 1H, H3'); 5.49 (d, ^3J = 4.4 Hz, 1H, 3'OH); 6.18 (t, ^3J = 6.4 Hz, 1H, H1'); 6.87 (d, ^3J = 8.8 Hz, 4H, trityl Hs); 7.20 – 7.36 (m, 9H, trityl Hs); 7.52 (s, 1H, H6); 7.62 (t, 1H, ^3J = 5.6 Hz, NH) ppm.

^{13}C NMR (100 MHz, DMSO-d_6, 25 °C) δ = 12.89 (CH_3); 29.86 (C8); 40.97 (C2'); 55.52 (OCH_3 x 2); 63.94 (C5'); 70.95 (C3'); 72.96 (C9 & C10); 81.77 (C1'); 85.15 (C4'); 85.78 (trityl C); 102.59 (C5); 113.70 (4 trityl Cs); 127.37 (trityl C); 128.11 (2 trityl C); 128.42 (2 trityl C); 130.18 (4 trityl C); 135.74 (trityl C); 135.89 (trityl C); 137.83 (C6); 145.00 (trityl C); 155.47 (C2); 158.58 (2 trityl C); 162.82 (C4) ppm.

FD-MS *m/z* 582.15 (M^+, 2%), 242.21 (100).

HR-ESI-TOF-MS: 604.2419 [M + Na].

FT-IR $\tilde{\nu}$ *(cm^{-1})***:** 3280 ν (OH); 3305 ν (C-H, alkyne); 3080 ν (C-H, alkene); 2953 ν (C-H, alkane); 2249 ν (C≡C, alkyne); 1658 ν (C=C, alkene); 1605 ν (C=C, aromatic); 1417 ν (C-H, alkane); 1376 ν (CH_3); 1249 ν (C-O); 1339 ν (C-N); 824 ν (C-H, aromatic); 681 ν (C-H, alkyne).

5.4.6 Synthesis of 3'-*O*-CEP-5'-*O*-DMT-5-methyl-*N*^{4}-propargylaminyl-deoxycytidine (17)

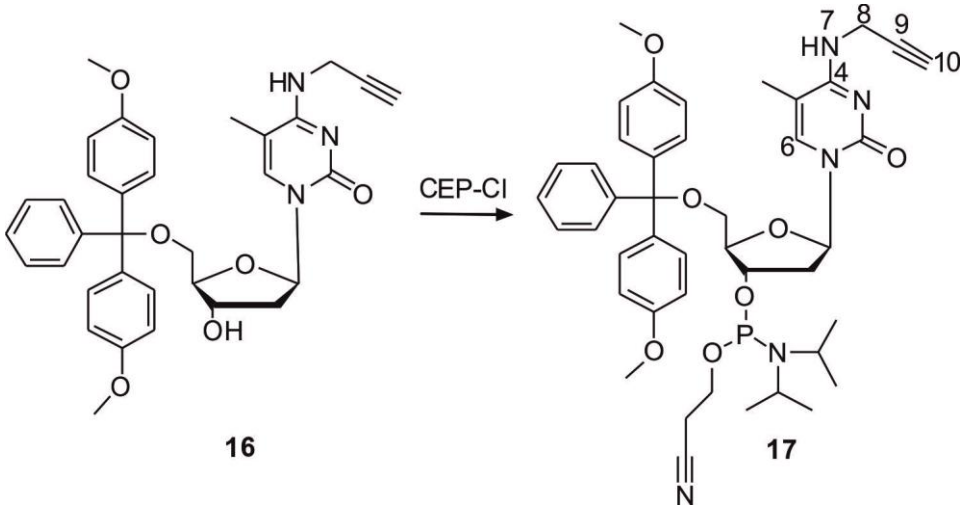

16 17

16 (235 mg; 0.4 mmol) was dissolved in 10 mL anhydrous DCM and placed under an argon atmosphere. To this solution was added 5 eq. *N,N*-diisopropylethylamine (0.35 mL; 2 mmol). While stirring the mixture, CEP-Cl (1.3 eq.; 0.12 mL) was added, all the while ensuring to exclude oxygen. The reaction mixture was stirred for 2 hours at RT. TLC analysis clearly

showed the formation of the two diastereomers of **17** 40 mL of a 5% aqueous $NaHCO_3$ solution was added and the product was extracted with DCM (3 x 20 mL). The organic phase was dried over anhydrous $MgSO_4$ and the crude mixture was concentrated *in vacuo*, to produce a light yellow foam. The product was purified by column chromatography (aluminium oxide, basic), with DCM:MeOH (70:1) and obtained in 52% yield.

Mp: 81 – 85 °C

TLC (silica gel, DCM:MeOH; 15:1): R_f = 0.47 & 0.53.

^{1}H NMR (400 MHz, DMSO-d_6, 25 °C) δ = 1.08 - 1.20 (m, 24H, [(**CH_3**)$_2$CH]$_2$N); 1.51 (s, 3H, CH_3);1.54 (s, 3H, CH_3); 2.21 – 2.39 (m, 4H, H2'); 2.64 (t, 2H, ^3J = 5.6 Hz, CH_2CN); 2.76 (t, 2H, ^3J = 5.6 Hz, CH_2CN); 3.10 (t, ^4J = 2.4 Hz, 2H, H10); 3.19 – 3.31 (m, 4H, H5'); 3.39 – 3.70 (m, 8H, [$POCH_2$]$_2$; [CHN]$_2$ x 2); 3.73 (s, 12H, OCH_3); 3.98 – 4.10 (m, 6H, H4' & H8); 4.48 – 4.55 (m, 2H, H3'); 6.22 (t, 1H, H1'); 6.23 (t, 1H, H1'); 6.87 – 6.91 (m, 8H, trityl Hs); 7.23 – 7.40 (m, 18H, trityl Hs); 7.52 (s, 1H, H6); 7.55 (s, 1H, H6); 7.60 (t, 1H, NH); 7.61 (t, 1H, NH) ppm.

^{13}C NMR (100 MHz, DMSO-d_6, 25 °C) δ = 12.64 (CH_3); 19.77 (CH_2CN); 19.90 (CH_2CN); 24.21 (CH_3 – *i*Pr_3 x 2); 24.28 (CH_3 – *i*Pr_3 x 2); 24.38 (CH_3 – *i*Pr_3 x 2); 24.45 (CH_3 – *i*Pr_3 x 2); 29.49 (C8); 38.94 (C2'); 42.54 (CH – *i*Pr_3); 42.67 (CH – *i*Pr_3); 55.12 (OCH_3 x 2); 58.24 ($POCH_2$); 58.43 ($POCH_2$); 63.26 (C5'); 72.77 (C9); 81.39 (C3'); 84.61 (C4'); 84.67 (C4'); 85.96 (trityl C); 86.03 (trityl C); 96.80 (1'C); 101.97 (C5); 102.05 (C5); 113.29 (trityl C x 4); 118.84 (CN); 119.03 (CN); 126.90 (trityl C); 127.70 (trityl C x 2); 127.75 (trityl C x 2); 129.75 (trityl C); 129.79 (trityl C); 135.21 (trityl C); 135.24 (trityl C); 135.37 (trityl C); 137.55 (C6); 144.62 (trityl C); 154.61 (C2); 158.23 (trityl C x 2); 158.85 (C4) ppm.

^{31}P NMR (200 MHz, DMSO-d_6, 25 °C) δ = 147.61; 147.97 ppm.

HR-ESI-TOF-MS: 804.3495 [M + Na].

FT-IR $\tilde{\nu}$ *(cm^{-1})***:** 3288 ν (C-H, alkyne)**;** 2929 ν (C-H, alkane); 2157 ν (C≡C, alkyne); 1662 ν (C=C, alkene); 1629 ν (aromatic); 1605 ν (C=C, aromatic); 1462 ν (C-H, alkane); 1249 ν (C-O); 1332 ν (C-N); 824 ν (C-H, aromatic); 694 ν (C-H, alkyne).

5.4.7 Detritylation of 5'-*O*-DMT-5-methyl-N^4-propargylaminyldeoxycytidine

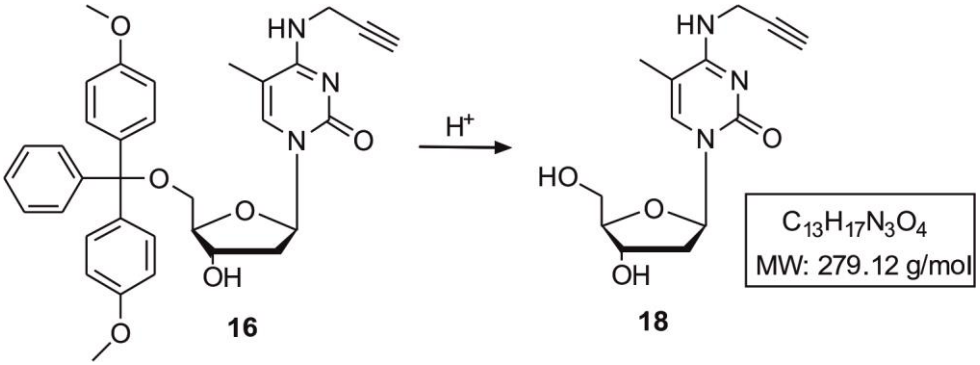

240 mg (0.3 mmol) of **16** was dissolved in 5 mL DCM. To this solution was added 50 µL (2 eq., 0.6 mmol) TFA and the mixture was stirred at RT until TLC showed complete detritylation of the starting material. **18** was purified *via* silica gel chromatography with the mobile phase DCM:MeOH (15:1). YIELD: 70%.

Mp: Decomposes at 181 °C.

TLC (silica gel, DCM:MeOH; 10:1): R_f = 0.05.

^{1}H NMR (400 MHz, DMSO-d_6, 25 °C) δ = 1.84 (s, 3H, CH_3); 1.91 – 2.00 (m, 1H, H2'); 2.04-2.11 (m, 1H, H2'); 3.09 (t, 1H, ^4J = 2.4 Hz, H10); 3.74 (m, 1H, H4'); 4.07-4.09 (m, 2H, H8); 4.21 (m, 1H, H3'); 5.04 (t, 1H, 5'OH); 5.22 (d, 1H, ^3J = 4.4 Hz, 3'OH); 6.16 (t, 1H, ^3J = 6.4 Hz, H1'); 7.60 (t, 1H, ^3J = 5.6 Hz, NH); 7.66 (s, 1H, H6) ppm.

^{13}C NMR (100 MHz, DMSO-d_6, 25 °C) δ = 13.08 (CH_3); 29.43 (C8); 38.69 (C2'); 61.23 (C5'); 70.19 (C3'); 72.67 (C9 & C10); 81.53 (C1'); 84.63 (C4'); 101.55 (C5); 149.38 (C6); 154.81 (C2); 162.33 (C4) ppm.

HR-ESI-TOF-MS: 302.1127 [M + Na].

FT-IR $\tilde{\nu}$ (cm^{-1}): 3500-3300 ν (N-H, amine); 3333-3267 ν (C-H, alkyne); 3280 ν (OH); 3080-3020 ν (C-H, alkene); 2929 ν (C-H, alkane); 2100 ν (C≡C, alkyne); 1711 ν (C=O, aldehyde); 1679 ν (C=C, alkane); 1609 ν (N-H, amine); 1335 ν (C-N); 1000 ν (C-O).

5.5 Synthesis of 5-ethynyluridine (20)

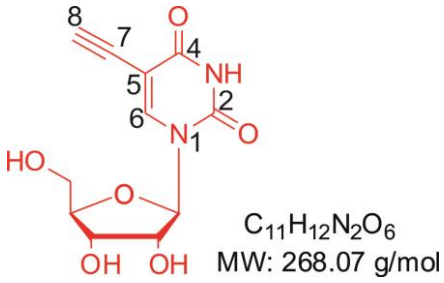

5.5.1 Sonogashira cross-coupling with 5-iodouridine

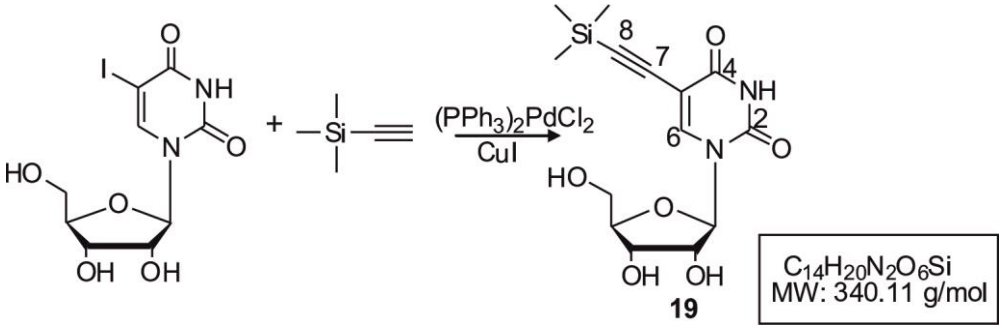

1 g of 5-iodouridine (2.7 mmol) was dissolved in 66 mL of a 1:1 mixture of CH_3CN:Et_3N. The solution was placed under argon, followed by the addition of 4 eq. trimethylsilylacetylene (1.54 mL; 10.8 mmol), 21 mol% bistriphenylphosphinepalladium(II) chloride (0.4 g; 0.57 mmol) and 20 mol% copper(I) iodide (0.1 g; 0.53 mmol). The reaction mixture was stirred at 50 °C for 3.5 hours. The solvent was removed *in vacuo*, resulting in a black residue. The product was obtained after silica gel flash column chromatography, using MeOH:$CHCl_3$ (1:4) as eluent[200]. YIELD: 66%.

Mp: Decomposes at 110 °C

TLC (silica gel, MeOH:$CHCl_3$; 1:4): R_f = 0.50.

^{1}H NMR (300 MHz, CD_3OD, 25 °C): δ = 0.20 (s, 9H, TMS); 3.52 – 3.57 (dd, ^3J = 2.7 Hz, 1H, H5'); 3.66 – 3.71 (dd, ^3J = 2.7 Hz, 1H, H5'); 4.01-4.18 (m, ^3J = 2.7 Hz, 1H, H4'); 4.16 – 4.18 (d, ^3J = 3.9 Hz, 2H, H2' & H3'); 5.88 (d, ^3J = 3.6 Hz, 1H, H1'); 8.39 (s, 1H, H6) ppm.

^{13}C NMR (100 MHz, CD_3OD, 25 °C): δ = -0.54 (TMS); 61.38 (C5'); 70.48 (C3'); 75.58 (C2'); 85.91 (C7); 90.60 (C4'); 96.80 (C8); 98.65 (C1'); 100.19 (C5); 145.63 (C6); 150.98 (C2); 163.74 (C4) ppm.

ESI-MS *m/z* 363.10 (M^+, 100%).

FT-IR $\tilde{\nu}$ (cm^{-1}): 3350 ν (OH); 2949 ν (CH, aliph.); 1680 ν (C=C); 1617 ν (NH); 1270 ν (C-N); 1102 ν (C-O); 1691 ν (C=O).

5.5.2 Desilylation of 19 to produce 5-ethynyluridine (20)

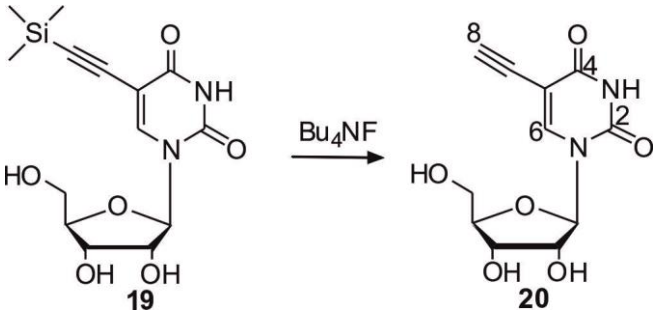

3.31 g (9.72 mmol) of **19** was dissolved in 150 mL dry MeOH. 5 equivalents of Bu_4NF (49 mL; 1 M in THF) was added and the reaction was refluxed at 80 °C. After 1 hour, the reaction mixture was concentrated *in vacuo* and the crude was purified *via* silica gel chromatography, using MeOH:$CHCl_3$ (1:5) as eluent. 5-Ethynyluridine was obtained as an off-white solid in 95% yield (2.47 g).

Mp: Decomposes at 180 °C.

TLC (silica gel, MeOH:$CHCl_3$; 1:4): R_f = 0.33.

^{1}H NMR (300 MHz, DMSO-d_6, 25 °C): δ = 2.72 - 2.88 (m, 2H, H5‘); 3.03 (m, 1H, H4‘); 3.15 (dd, ^3J = 4.5 Hz, 1H, H2’); 3.21 (dd, ^3J = 4.5 Hz, 1H, H3‘); 3.27 (s, 1H, acetylene H); 4.23 (d, ^3J = 5.10 Hz, 1H, 3’OH); 4.40 (t, ^3J = 4.5 Hz, 1H, 5’OH); 4.59 (d, ^3J = 5.4 Hz, 1H, 2’OH); 4.91 (d, ^3J = 4.4 Hz, 1H, H1’); 7.55 (s, 1H, H6) ppm; 10.81 (br s, 1H, NH) ppm.

^{13}C NMR (100 MHz, DMSO-d_6, 25 °C): δ = 60.20 (C5’); 69.32 (C3’); 73.98 (C2’); 76.34 (C7); 83.64 (C8); 84.74 (C4’); 88.41 (C1’); 97.62 (C5); 144.62 (C6); 149.66 (C2); 161.60 (C4) ppm.

HR-ESI-TOF-MS: 291.0603 [M + Na].

FT-IR $\tilde{\nu}$ ***(cm^{-1})*****:** 3350 ν (OH); 3239 ν (C-H, alkyne); 3047 ν (C-H, alkene); 2831 ν (C-H, alkane); 2161 ν (C≡C, alkyne); 1691 ν (C=O); 1680 ν (C=C); 1617 ν (NH); 1335 ν (C-N); 1045 ν (C-O).

5.6 Synthesis of 8-bromoguanosine (21)

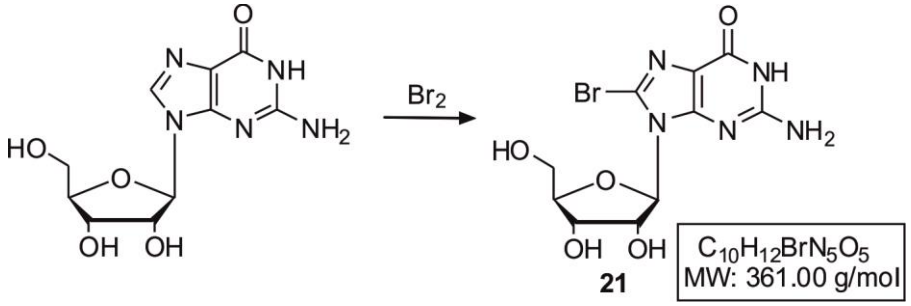

A suspension of 5 g guanosine (17.7 mmol) in 20 mL water was prepared. 100 mL of a saturated solution of bromine water was slowly added in a dropwise fashion and the reaction mixture was allowed to continue stirring at RT for 24 hours. The resulting white precipitate was filtered and washed with cold water and then cold acetone. The pure product was obtained by recrystallization from water. YIELD: 57% (3.65 g).

Mp: 111-113 °C.

TLC (silica gel, MeOH:$CHCl_3$; 2:1): R_f = 0.77.

^{1}H NMR (400 MHz, DMSO-*d*$_6$, 25 °C) δ = 3.48 - 3.54 (m, 1H, H5'); 3.62 - 3.67 (m, 1H, H5'); 3.83 – 3.87 (m, 1H, H4'); 4.11 – 4.15 (m, 1H, H3'); 4.93 (t, 1H, ^3J =5.2 Hz, 5'OH); 5.01 (m, 1H, H2'); 5.11 (d, 1H, ^3J =5.2 Hz, 3'OH); 5.47 (d, 1H, ^3J =6.4 Hz, 2'OH); 5.68 (d, 1H, ^3J =6.4 Hz, H1'); 6.51 (br s, 2H, NH_2); 10.83 (br s, 1H, NH) ppm.

^{13}C NMR (100 MHz, DMSO-*d*$_6$, 25 °C) δ = 62.04 (C5'); 70.36 (C3'); 73.07 (C2'); 85.88 (C4'); 89.68 (C1'); 117.56 (C8); 121.27 (C5); 152.15 (C4); 153.47 (C2); 155.48 (C6) ppm.

HR-ESI-TOF-MS: 383.9925 [M + Na].

FT-IR $\tilde{V}$ *(cm^{-1})*: 3300 ν (OH); 3109 ν (N-H), 2921 ν (C-H, alkane); 1674 ν (C=C, alkene); 1462 ν (C-H, alkane); 1294 ν (C-O); 1200 ν (C-N); 1082 ν (C-O); 524 ν (alkyl halides).

B. Molecular biology procedures

Table 5.1 List of in-house synthesized (1-13) and commercially obtained (14-28) oligomers used in this study. DNA bases are written in capital letters, RNA in small letters and 2'*O*Me RNA in blue.

NAME	SEQUENCE (5'→3')	SYSTEM	MODIFICATION (*)
NPI	*aacuucagggucagcuugccg	Antisense RNA	N^2-propargylaminylinosine
590NPI	*gaacuucagggucagcuugccg	Antisense RNA	NPI clicked with Atto 590
CpDC2	G*AAGCTGACCCTGAAGTTCAT	Sense DNA	5-methyl-N^4-propargyldeoxycytidine
CpDC6	GCAAG*TGACCCTGAAGTCAT	Sense DNA	5-methyl-N^4-propargyldeoxycytidine
CpDC10	GCAAGCTGA*CCTGAAGTCAT	Sense DNA	5-methyl-N^4-propargyldeoxycytidine
CpDC11	GCAAGCTGAC*CTGAAGTTCAT	Sense DNA	5-methyl-N^4-propargyldeoxycytidine
CpDC12	GCAAGCTGACC*TGAAGTTCAT	Sense DNA	5-methyl-N^4-propargyldeoxycytidine
CpDC20	GCAAGCTGACCCTGAAGT*AT	Sense DNA	5-methyl-N^4-propargyldeoxycytidine
CpDC21	GCAAGCTGACCCTGAAGTTC*T	Sense DNA	5-methyl-N^4-propargyldeoxycytidine
590CpDC21	GCAAGCUGACCCUGAAGUUC*U	Sense DNA	*CpDC21* clicked to Atto 590
FS4	cgcCTAAaucgagucaa*	2'*O*Me RNA/DNA chimera	5-methyl-N^4-propargyldeoxycytidine
488FS4	cgcCTAAaucgagucaa*	2'*O*Me RNA/DNA chimera	*FS4* clicked to Atto 488
590FS4	cgcCTAAaucgagucaa*	2'*O*Me RNA/DNA chimera	*FS4* clicked to Atto 590
MH142	uggggccuaagaccaATGGauagcuguuaucuu	2'*O*Me RNA/DNA chimera	None
MH330	*gaacuucagggucagcuugccg	Antisense RNA	TAMRA
MH533	gaacuucagggucagcuugccg	Antisense RNA	None
MH534	gcaagcugacccugaaguucau	Sense RNA	None

MH540	gcaagcugacccugaaguucau*	Sense RNA	Atto 488
MH542	*gaacuucagggucagcuugccg	Antisense RNA	Atto 590
MH543	*gaacuucagggucagcuugccg	Antisense RNA	Atto 647*N*
MH548	ga*a*cuuca*ggguca*gcuugccg	RNA strand with four 2'*O*Me bases	Atto 488
MH549	ga*a*cuuca*ggguca*gcuugccg	RNA strand with four 2'*O*Me bases	Atto 590
MH661	GCAAGCTGACCCTGAAGTCAT	Sense DNA	None
MH663	GAACTTCAGGGTCAGCTTGCCG	Antisense RNA	None
MH677	GAACTTCAG*GTCAGCTTGCCG	Antisense DNA	Abasic site
MH678	GAACUUCAGG*UCAGCUUGCCG	Antisense DNA	Abasic site
MH692	ucaaguuagaacuuuaugua gaacuucaggg ucagcuugccg*	Antisense RNA	Random sequence Atto 590
MH693	TCAAGTTAGAACTTTACGTA GAACT TCAGGGTCAGCTTGCCG*	Antisense DNA	Random sequence Atto 488

5.7 Solid phase oligonucleotide synthesis (SPOS) and purification

All oligonucleotides were custom-synthesized on a 1 µmol scale on an Expedite 8909 DNA/RNA synthesizer (ABI/PerSeptiveBiosystems), starting from preloaded controlled pore glass (CPG). In all cases, due to the insoluble nature of the guanosine phosphoramidites, a slight modification was made to the synthesis protocol. Instead of 0.1 M, as was the concentration of all other phosphoramidites, the guanosine phosphoramidites were all diluted to a final concentration of 50 mM in acetonitrile. To compensate for this, both the coupling times and injection volumes of this monomer were increased by a factor of two. Also, the amount of pulses, as well as the time allowed for the reagents to react, was higher for RNA, as it was for DNA (see table 5.2).

Post synthesis and purification, the molecular masses of all synthesized oligonucleotides were confirmed by means of MALDI-TOF mass spectrometry.

Table 5.2 Protocols followed for the syntheses of DNA and RNA oligonucleotides.

Dblk: Deblocking reagent; Wsh: Acetonitrile; Act: Activator; Cap: Capping reagents; Ox: Oxidizer

STEP	FUNCTION	MODE	AMOUNT		TIME (sec)		DESCRIPTION
			DNA	RNA	DNA	RNA	
DEBLOCKING	*144 /* *Index Fract. Coll.	N/A	1	1	0	0	Event out ON
	0 / *Default	WAIT	0	0	1.5	1.5	Wait
	141 / *Trityl Mon. On/Off	N/A	1	1	1	1	START data collection
	16 / *Dblk	PULSE	10	10	0	0	Dblk to column
	16 / *Dblk	PULSE	50	50	49	60	Deblock
	38 / *Diverted Wsh A	PULSE	40	40	0	0	Flush system with
	141 / *Trityl Mon. On/Off	N/A	0	0	1	1	Wsh A
	38 / *Diverted Wsh A	PULSE	40	40	0	0	STOP data collection
	144 / *Index Fract. Coll.	N/A	2	2	0	0	Flush system with Wsh A Event out OFF
COUPLING	1 / *Wsh	PULSE	5	5	0	0	Flush system with
	2 / *Act	PULSE	5	5	0	0	Wsh
	# / *Base + Act	PULSE	5	6	0	0	Flush system with Act
	# / *Base + Act	PULSE	2	9	16	402	Monomer + Act to
	2 / *Act	PULSE	3	0	24	0	column
	1 / *Wsh	PULSE	7	8	56	357	Couple monomer
	1 / *Wsh	PULSE	8	7	0	0	Couple monomer
	(Repeat for guanosine)						Couple monomer Flush system with Wsh
CAPPING	12 / *Wsh A	PULSE	20	20	0	0	Flush system with
	13 / *Caps	PULSE	8	7	0	0	Wsh A
	13 / *Caps	PULSE	0	6	0	15	Caps to column
	12 / *Wsh A	PULSE	6	6	15	15	Cap
	12 / *Wsh A	PULSE	14	14	0	0	Cap Flush system with Wsh A

OXIDIZING	15 / *Ox 12 / *Wsh A	PULSE PULSE	15 15	20 15	0 0	0 0	Ox to column Flush system with Wsh A
CAPPING	13 / *Caps 12 / *Wsh A	PULSE PULSE	7 30	7 30	0 0	0 0	Caps to column End of cycle wash

5.7.1 Antisense oligoribonucleotide, carrying 2-propargylaminylinosine on the 5'-end

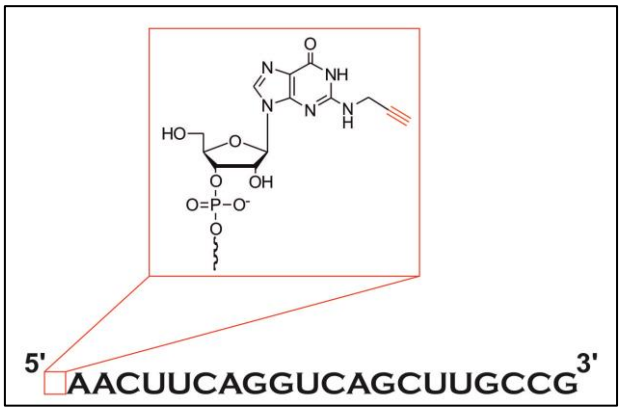

Fig. 5.1 Antisense oligoribonucleotide, carrying the modified guanosine base on its 5'-end.

The oligoribonucleotide containing the modified guanosine was synthesized and purified *via* polyacrylamide gel electrophoresis at Purimex, Grebenstein, Germany. However, only a fraction of this sample contained the full-length oligonucleotide. The dimethoxytrityl group of the modification on the 5'-end was removed before release of the synthesized oligonucleotide from the solid support. Cleavage of the oligonucleotide from the solid support, as well as the deprotection of the fast deprotection groups on the exocyclic amines of the bases were achieved by incubating the CPG in a 3:1 mixture of concentrated aqueous ammonia (28 - 33%) and ethanol for 3 hours at RT. The supernatant was collected and the residue was washed with a mixture of MilliQ water, ethanol and acetonitrile (1:3:1). Excess ammonia and other solvents were removed from the combined aqueous solutions with the aid of a SpeedVac. The TBDMS protection groups of the commercial phosphoramidites and the TOM group for protecting the 2'OH of our modified phosphoramidite were removed with Bu_4NF, applied as a 1 M solution in THF. An initial purification step was done *via* polyacrylamide gel electrophoresis. After desalting, using NAP-10 prepacked columns, the crude

oligoribonucleotide was lyophilized and treated with the Atto 590 azide dye under CuAAC conditions (see below).

The crude mixture was, once again, treated on a NAP-10 column, this time not only to desalt, but also to remove the smaller, unreacted dye molecules before further HPLC purification. Semi-preparative HPLC, with pure CH_3CN as buffer A and triethylammonium acetate (pH 7) as buffer B, was used to separate the labeled oligonucleotide form the unlabeled fractions. A flow rate of 3 mL/min was applied to the C18 reversed phase HPLC column, using the gradient system for CH_3CN as indicated in figure 5.2. The fluorescent product was collected at 14 minutes, whereas abortion and unclicked products eluted at approximately 8 minutes.

TIME (min)	% CH_3CN
0	5
20	85
30	85
35	5
40	5

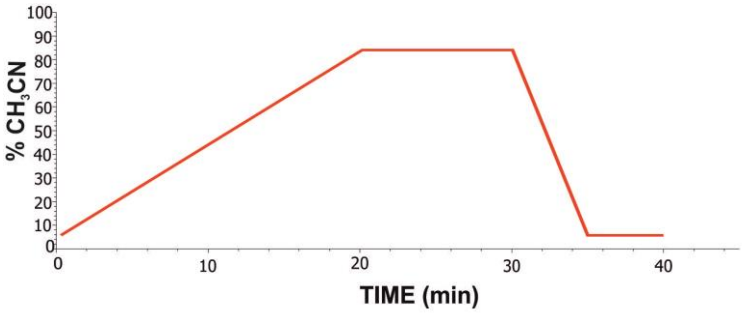

Fig. 5.2 Gradient eluent system for reversed phase HPLC purification of the clicked oligonucleotide, *590NPI*.

After precipitation from ethanol, the pure oligonucleotide, containing the Atto 590 dye on the 5'-end was obtained. MALDI-TOF analysis of the ZipTip treated oligonucleotide confirmed the calculated mass of the clicked product. The commercial, unlabeled antisense RNA strand (*MH533*) was used as internal standard.

5.7.2 DNA sense oligonucleotide, carrying the alkyne containing cytidine derivative at varying positions within the strand

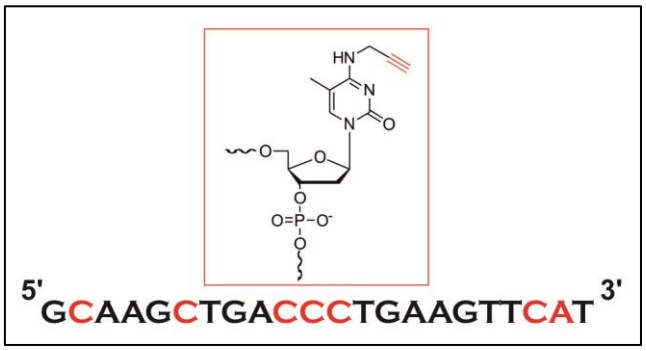

Fig. 5.3 Sequence of the sense oligonucleotide strand. The bases in red were singularly substituted with the modified nucleoside.

All oligonucleotides – both modified and unmodified - were synthesized in the DMT-off mode, using the protocol as described in table 5.2 for DNA. Deprotection of the synthesized oligonucleotides and their cleavage from the solid support was achieved by incubating the CPG with a 3:1 mixture of concentrated ammonia (28 - 33%) and ethanol at 55 °C for 16 hours. After rinsing the solid support with CH_3CN:H_2O:EtOH (1:1:3) and combining the solvent fractions, the crude oligonucleotides were dried overnight in a SpeedVac, redissolved in MilliQ water and desalted on a NAP-10 column. All oligonucleotides were PAGE purified prior to their click functionalization.

The crude oligonucleotides were loaded onto a 20% denaturing polyacrylamide gel. The relevant bands were identified by means of UV shadowing and following their excision, were eluted overnight in 0.5 M NH_4OAc (pH 5.3).

After filtering off the gel pieces, a $LiClO_4$ precipitation was carried out by adding 10x the volume 2% $LiClO_4$ in acetone. The samples were centrifuged at RT for 1 hour at 10 000 x g. After removal of the supernatant, the pellet was rinsed with a small volume of acetone. The pellet was allowed to air dry and the obtained DNA strand was redissolved in MilliQ water. The final oligonucleotide concentration was determined by means of A_{260} measurements on a NanoDrop apparatus.

5.7.3 2'*O*Me RNA/DNA chimera, carrying the alkyne containing cytidine derivative on the 5'-end

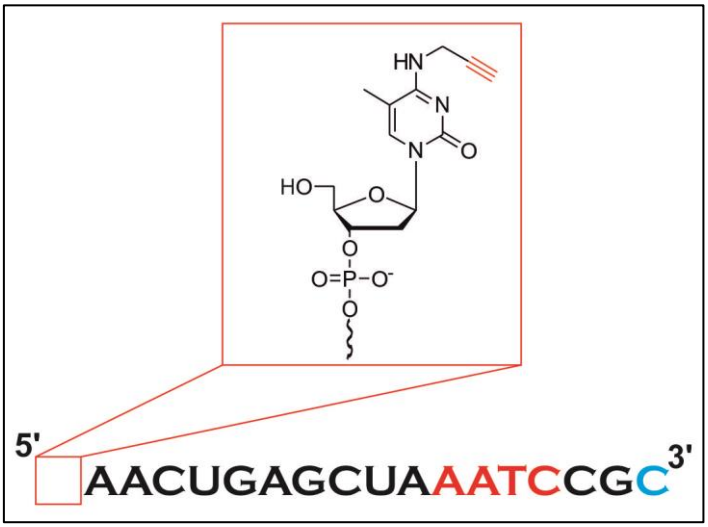

Fig. 5.4 2'*O*Me RNA/DNA chimera, showing the modification on the 5'-end. Blue: RNA; Red: DNA; Black: 2'*O*Me RNA bases.

Starting from an RNA base on the 3'-end (CPG), the 2'*O*Me RNA/DNA chimera was synthesized in the DMT-off mode, using the protocol as described in table 5.2 for DNA and RNA, depending on the relevancy. Deprotection of the synthesized oligonucleotide and its cleavage from the solid support was achieved by incubating the CPG with a 3:1 mixture of concentrated ammonia (28 - 33%) and ethanol at 55 °C for 16 hours. After rinsing the solid support with CH_3CN:H_2O:EtOH (1:1:3) and combining the solvent fractions, the crude oligonucleotides were dried overnight in a SpeedVac, redissolved in MilliQ water and desalted on a NAP-10 column. All oligonucleotides were PAGE purified prior to their click functionalization with either the Atto 488 or Atto 590 azido dye. The same procedures for PAGE purification and precipitation were followed as for the sense DNA strand (see 5.7.2).

5.7.4 MALDI-TOF analysis of synthesized oligonucleotides

A Bruker BIFLEX III, operated by Heiko Rudy at the Institute of Pharmacy and Molecular Biotechnology, Heidelberg University, was used for the mass determination of the synthesized oligonucleotides. ZipTip pipette tips were used to desalt the samples prior to measurement, eluting with CH_3CN/H_2O (1:1). The minimum concentration of the oligonucleotides after elution was 1 µM, as determined by NanoDrop measurement.
The measurements were performed in the positive modus and 3-hydroxypicolinic acid was used as matrix. The samples were applied using the sandwich method, together with ammonium citrate to mask possible remaining salts.

5.8 General procedure for click reactions with alkyne functionalized oligonucleotides

All click reactions of the synthesized oligonucleotides with the azido functionalized dyes were run in DMSO/water solutions. NaH_2PO_4 (pH 8) was used as buffer. The $CuSO_4$•$5H_2O$ (0.1 eq.), *tris*-[4-(3-hydroxypropyl)-(1,2,3)triazolyl-1-methyl)amine (TPTA) (0.5 eq.) and sodium ascorbate (1 eq.), were added and the reaction mixtures were agitated under light protection at 25 °C for 24 h. Excess dye was removed *via* manual size exclusion chromatography on NAP-10 columns.

5.9 Purification and concentration of the synthesized oligonucleotides by precipitation

5.9.1 Ethanol precipitation

0.1x volumes 3 M NaOAc (pH 5.2) and 2.2x volumes – 80 °C ethanol were added, the mixture was vortexed and incubated for at least 1 hour at – 20 °C. The samples were centrifuged at 12 000 x g for 30 minutes, after which the supernatant was removed. The pellet was carefully rinsed with 70% ice cold ethanol and centrifuged again at 12 000 x g for 10 minutes. The supernatant was removed and the pellet was allowed to air dry, before redissolving in MilliQ water.

5.9.2 Lithium perchlorate precipitation

A 2% m/v solution of $LiClO_4$ in acetone was used for precipitation of oligonucleotides. A volume ten times that of the oligonucleotide solution was added and centrifuged at 10 000 x g for 1 hour at RT. The supernatant was removed and the pellet was rinsed with 100 µL acetone. After another 30 minutes of centrifugation at 10 000 x g, the acetone was removed and the pellet was allowed to air dry.

5.10 Hybridization of the synthesized sense and antisense oligonucleotides to their respective complementary strands

5.10.1 General procedure for hybridization assays

All hybridization experiments were carried out in 1 x PBS (pH 5.3). The two complementary strands were added in a ratio of 1:1, resulting in a final duplex concentration of 5 µM. In order to ensure complete denaturation, the strands were first incubated at 90 °C for 1 minute. Duplex formation was allowed at 37 °C over 1 hour. For the less stable duplexes, the incubation temperature was lowered to 30 °C. Native polyacrylamide gel electrophoresis served as method to analyze differences in mobility shifts between single and double stranded oligonucleotides, as well as to quantify the ratios of unhybridized single strands.

5.10.2 Competition assays

Similar to the hybridization experiments, the competition assays were carried out in 1x PBS (pH 5.3). The two antisense strands, *i.e.* DNA and RNA, as well as the modified sense strand

were added to each, to give a final concentration of 5 µM in solution. The mixture was agitated and incubated at 90 °C for 3 minutes. Incubation was continued at 50 °C for 1 hour, after which the mixture was slowly cooled to room temperature.

5.11 Electrophoresis mobility shift analyses by means of polyacrylamide gel electrophoresis (PAGE)

Denaturing polyacrylamide gel electrophoresis was used for purification and identification of the synthesized single stranded oligonucleotides (both labeled and unlabeled). The state of hybridization between complementary oligonucleotide strands was confirmed and quantified on native polyacrylamide gels. Both denaturing and native gels were prepared at a concentration of 20% polyacrylamide. Samples were loaded as a 1:1 mixture with 60% glycerol in H_2O and bromophenol blue/xylene cyanol were used to monitor and visualize migration progress during electrophoresis. With the exception of the competition assays, all gels were run in 1x TBE buffer.

Following electrophoresis and staining with GelRed where necessary, gels were scanned on a Typhoon laser scanner. For FRET measurements between Atto 488 and Atto 590, the two channels were merged.

Table 5.3 Typhoon settings for scanning polyacrylamide gels.

DYE	LASER	EMISSION FILTER
Atto 488	488 nm	520 BP 40
Atto 590	532 nm	670 BP 30
Atto 647N	633 nm	670 BP 30
GelRed	532 nm	670 BP 30
TAMRA	532 nm	580 BP 30
FRET (Atto 488/590)	488 nm	670 BP 30

5.11.1 Denaturing polyacrylamide gel electrophoresis

For the purification of the 5-methyl-N^4-propargyldeoxycytidine containing oligonucleotides, (*i.e.* oligonucleotides numbers 3-10 in table 5.1) 20 x 30 cm gels were prepared with 1.5 mm spacers. Samples were loaded as a 1:1 mixture with 60% glycerol. Bromophenol blue and xylene cyanol were used to monitor the progress of migration. After electrophoresis at 20 W for 6 hours, the bands were visualized by means of UV shadowing, using 20 x 20 cm

fluorescent TLC plates. For recovery of the pure products from the gel matrix, the bands of interest were excised, crushed and incubated with 0.5 M NH_4OAc (pH 5.3), while shaking at RT for 30 minutes. The product was concentrated by means of a $LiClO_4$ precipitation.

The composition of the 10% and 20% denaturing polyacrylamide gels was as follows:

	10% PAGE	20% PAGE
Sequencing gel concentrate	40 mL	80 mL
Sequencing gel diluter	50 mL	10 mL
Sequencing gel buffer concentrate	10 mL	10 mL
TEMED	40 µL	40 µL
APS	400 µL	400 µL

A second incubation of the crushed gel pieces overnight under the above conditions, followed by a similar $LiClO_4$ precipitation ensured maximum elution of the product from the gel.

5.11.2 Native polyacrylamide gel electrophoresis

The composition of the 20% native polyacrylamide gels was as follows:

- 25 mL 40% acrylamide
- 5 mL 10x TBE
- 20 mL distilled H_2O
- 40 µL TEMED
- 400 µL APS

The native gels were prepared between 20 x 20 cm glass plates with 1 mm thick spacers. Gels were run at 20 W for 2 hours, during which metal plates aided the distribution of heat generated during the electrophoresis procedure. In the case of less stable duplexes, the gels were run at 8 W for 6 hours. The visualization of non-fluorescent bands was made possible with GelRed staining, followed by scanning of the gel on a Typhoon laser scanner.

For the competition assays between the antisense DNA and RNA strands for the modified DNA sense strands, the buffer and gel compositions were adjusted to match conditions of the temperature dependent melting curves.

The running buffer consisted of 100 mM NaH_2PO_4 (pH 8) and 45 mM NaCl. The electrophoresis chamber was placed in an environment of 50 °C and the samples were loaded after equilibration of the system at this temperature. The bands were visualized by GelRed staining and scanning on a Typhoon laser scanner.

Table 5.4 Composition of native polyacrylamide gels for competition assays.

	[STOCK]	[FINAL]	Volume
Acrylamide	40%	20%	25 mL
NaH_2PO_4 (pH 8)	500 mM	100 mM	1 mL
NaCl	5 M	45 mM	450 µL
H_2O	---	---	*ad* 50 mL

5.12 Temperature-dependent differential UV-absorption measurements of duplexes

All UV melting profiles were acquired on a Jasco V-650 spectrophotometer, equipped with a Jasco ETC-505T Peltier temperature programmer, using a 10 mm path-length quartz cell (either 200 µL or 1 mL cuvettes). Melting curves were recorded at 260 nm, with a heating rate of 0.4 °C/min, a slit of 2 nm and a response of 0.2 s. All measurements were carried out at least three times in the temperature ranges between 20 and 90 °C.

5.12.1 UV melting profiles for siRNA duplexes

The siRNA duplexes were resuspended in degassed, RNase-free buffer (10 mM NaH_2PO_4, pH 8; 45 mM NaCl), to yield duplexes in a final concentration of 1 µM. The measurements were carried out in a volume of 150 µL in 200 µL cuvettes.

5.12.2 UV melting profiles for duplexes formed with the modified DNA sense strand

The duplexes were diluted to a final concentration of 0.5 µM in degassed, RNase-free buffer, containing 10 mM NaH_2PO_4 (pH 8) and 45 mM NaCl to a final volume of 800 µL. Buffer solutions with a final NaCl concentration of 45 mM, 225 mM and 450 mM, respectively, were prepared for investigating the influence of salt concentration on duplex stability.

5.13 Determination of gene silencing activity of siRNA duplexes

HEK 293T cells were cultivated under standard conditions in DMEM, containing 10% fetal calf serum and 1% penicillin/streptomycin. One day prior to transfection, 8 x 10^5 cells were seeded in 1 mL medium without antibiotics in 24-well tissue culture treated plates. At the time of transfection, cells had a confluency of 70-80%. Medium was aspirated off and 500 µL fresh

medium was added. 400 ng of pEGFP-N1 (GenBank Accession #U55762) and the respective amount of siRNA were diluted in a final volume of 50 µL OptiMem (Invitrogen). After addition of 1 µL Lipofectamine 2000 in a final volume of 50 µL OptiMem, the 100 µL transfection mix was incubated for 20 min at room temperature. The mix was added dropwise onto each well.

After 24 h incubation, cells were washed once with PBS, trypsinated and dissolved in 600 µL PBS. eGFP expression was analyzed by flow cytometry on an LSR-FortessaSORP, with excitation at 488 nm and detection at 530/30nm. The eGFP signal was calculated as the product of mean fluorescence intensity and number of transfected cells compared to the value of a positive control. IC_{50} curves resulted of three biological triplicates, each done in technical triplicate. Curves were calculated with GraphPad Prism (asymmetric 5 parameter dose-response model). These experiments were carried out by Bettina Krieg, at the Institute of Molecular Biology in Mainz.

5.14 Cell imaging of labeled oligonucleotides

RBE4 cells[175] were cultivated under standard conditions in a medium consisting of 45% v/v DMEM, 45% v/v HAM's F-10, 10% v/v serum (*e.g.* fetal calf or bovine serum), 100 µg/mL penicillin/streptomycin mix and 1 ng/mL basic fibroblast growth factor. For the confocal imaging, the cells were grown on 8-well µ-slides. One day before transfection, 20 000 cells per well were seeded in 250 µL growth medium without antibiotics, resulting in 50% confluency at the day of transfection. An optimized standard protocol for Oligofectamine was used to transfect RBE4 cells with labeled siRNA duplexes.

0.8 µL of a 5 µM siRNA solution were diluted with 14.5 µL of OptiMem medium and combined with a mixture of 0.85 µL Oligofectamine and 3.5 µL OptiMem and incubated for 20 min. Before adding the formed lipoplexes dropwise to the cells, the medium was replaced with transfection medium (medium without serum and antibiotics) resulting in a final culture volume of 150 µL. Cells were incubated at 37 °C until fixation. For fixation, cells were washed once with PBS and fixated for 10 min in 4% formaldehyde, diluted in PBS. After two further washing steps with PBS and one with water, cells were mounted by adding three droplets of IBIDI Mounting medium to the well. Samples were stored at 4 °C until imaging. Fixed cell samples were imaged on a Leica inverted confocal microscope TCS SP5, equipped with an oil-immersion objective (63x magnification; NA 1.4) and a 561 nm laser. Images were recorded at 512x512 8-bit-pixel resolution with a pinhole of 130 µm and confocal plane

depth of 1.0 µm, resulting in a total image size width and height of 246x246µm. Atto 590 was excited at 561 nm and the emission was recorded between 605-635 nm.
These experiments were carried out by Markus Hirsch at the Institute of Molecular Biology in Mainz.

5.15 LC/MS analysis of the 5-methyl-N^4-propargylaminyldeoxycytidine containing oligodeoxynucleotides

All experiments involving the LC/MS analysis of the modified base, as well as the oligonucleotides into which it was incorporated, were performed by Dr. Stefanie Kellner at the Institute of Pharmacy and Biochemistry, Department of Pharmaceutical Chemistry at the Mainz University.

5.15.1 Enzymatic digestion of oligonucleotides

The modified oligonucleotides were enzymatically digested by the consecutive addition of nuclease P1, snake venom phosphodiesterase and alkaline phosphatase. The following protocol was followed:

A)
(Nuclease P1 buffer: 90 µL ammonium acetate – 250 mM; pH 5.0 + 10 µL $ZnCl_2$ – 2 mM)

	[STOCK]	[FINAL]	Volume
Oligodeoxynucleotide	4 µM	3 µM	10 µL
Nuclease P1	0.3 u/µL	20 mu/µL	1 µL
Nuclease P1 buffer	10x	~ 1x	1 µL
Snake venom phosphodiesterase	0.1 u/µL	8 mu/µL	1 µL

Incubate at 37 °C for 5 hours

B)

	[STOCK]	[FINAL]	Volume
Mixture A	3 µM	2.3 µM	13 µL
Alkaline phosphatase	1 u/µL	0.12 u/µL	2 µL
Buffer alkaline phosphatase	10x	~ 1x	2 µL

Incubate at 37 °C for 1 hour

5.15.2 LC/MS analysis

Chromatographic parameters:

As reference sample for analysis of liquid chromatographic behavior, as well as mass fragmentation patterns, the single nucleoside, 5-methyl-N^4-propargylaminyldeoxycytidine **(18)**, was injected as solution in water (5 µL; 1 M). A 5 mM solution of ammonium acetate (pH 5.3) was used as buffer A. The flow rate was 0.5 mL/min and column temperature was adjusted to 35 °C.

The following gradient system for CH_3CN (solvent B) was used on a Synergy Fusion RP column (4 µM particle size, 80 Å pore size, 250 mm length, 2 mm inner diameter):

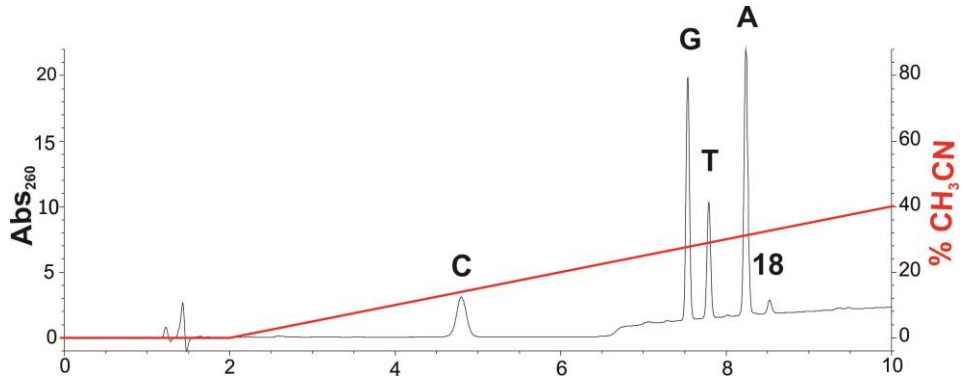

Fig. 5.5 Gradient system of percentage CH_3CN during column chromatography in red and the absorption intensities of the differently eluting nucleobases in black. Ammonium acetate (5 mM, pH 5.3) was used as buffer A, with a flow rate of 0.5 mL/min.

Mass spectrometric parameters:

Triple quadrupole mass spectrometer Agilent 6460 with ESI Jetstream ion source

Delta EMV standard analytics	0 V
Delta EMV high sensitivity	+ 400 V
Fragmentor voltage	80 V
Cell Accelerator	2 V
Ionization	Electrospray ionization, positive

Source parameters:

Gas temperature	300 °C
Gas flow	8 L/min
Nebulizer	35 psi
Sheath gas temperature	350 °C
Sheath gas flow	12 L/min
Capillary	3500 V
Nozzle	500 V

For both the single nucleoside and the digested oligonucleotides, the MS parameters above, together with + 400 V EMV for high sensitivity was used.

5.16 Incorporation of 5-ethynyluridine (EU) into RBE4 cells and consequent click labeling

5.16.1 Cell culture

RBE4 cells[175] were cultivated on collagen treated glass coverslips in DMEM, supplemented with 10% fetal calf serum, basic fibroblast growth factor (1 ng/mL) and penicillin/streptomycin (100 µg/mL). Cells were incubated in a standard cell culture incubator at 37 °C, under high humidity and a 5% CO_2 atmosphere until 50% confluency was reached. The cell medium was replaced with pre-warmed culture medium, containing 1 mM EU in DMSO, resulting in a final amount of 5 µmol EU per well. The final DMSO concentration did not exceed 1%. The control wells were incubated with culture medium containing 1% DMSO. The cells containing the EU were incubated for 8, 16 and 24 hours, respectively, after which the cells were rinsed with 1x PBS and the medium was replaced with standard growth medium. All cells were incubated under normal growth conditions until fixation and staining.

5.16.2 Click functionalization with Alexa 594

Cells were washed with 1x PBS and fixed onto coverslips by incubating them with 4% formaldehyde in PBS for 10 minutes. The coverslips were stored at 2-8 °C until staining. The following solution was prepared for click functionalization of the EU containing cells:

Table 5.5. Pipetting scheme for the CuAAC reaction of EU-labeled cells.

	[STOCK]	[FINAL]	Volume
HEPES buffer (pH 8.5)	500 mM	100 mM	1.2 mL
$CuSO_4 \bullet 5H_2O$	50 mM	500 µM	60 µL
Alexa 594 azide	300 µM	1 µM	20 µL
Ascorbic acid	75 mM	50 mM	4 mL
			6 mL

The staining mix was prepared fresh before use and each well was incubated with 1 mL of the staining solution. The ascorbic acid was added to the wells last and directly before incubation of the cells at RT for 30 minutes. After staining, the cells were washed several times with

0.5% Triton X-100 in PBS. The non-EU incubated, control cells were treated in a similar fashion.

Prior to imaging on a Nikon C1Si confocal laser scanning system, cells were counterstained with a 500 nM solution of DAPI in PBS for 5 minutes at RT, followed by a rinsing step with PBS and mounting of the cells onto mounting plates in the absence of mounting medium.

5.16.3 Fluorescent cell imaging

The cell imaging experiments were carried out at the Nikon Imaging Centre in Heidelberg. A Nikon C1Si confocal laser scanning system on a Nikon Ti fully automated inverted microscope was used for imaging the fixed cells after staining. The microscope was equipped with a 60x or 40x oil immersion objective, together with three laser lines for excitation (408 nm, 488 nm and 561 nm) and a three color beamsplitter/filter cube system for detection (408/488/561).

The following microscopic settings were used:

Objective magnification	60.0
Objective NA	1.400
Pixel size	512 x 512 pixel

Table 5.6 Microscopic settings for the two respective channels used for imaging DAPI and Alexa 594 emission of the RBE4 cells.

	CHANNEL 1	CHANNEL 3
NAME	DAPI	Alexa 594
LASER	408 nm	561 nm
LASER INTENSIY	89.9%	89.9%
ACQUISITION MODULES	BA 450/35	BA 650 LP
GAIN	100	131
PINHOLE	30 µm small	60 µm medium

After imaging, the data were processed with the aid of the EZC1 FreeViewer (Nikon) or ImageJ software[196].

5.17 Incorporation of 5-ethynyluridine into *Eschericia.coli* cells, RNA isolation and click labeling

5.17.1 Bacterial cell culture

Eschericia coli (E. coli) cells from a Rosetta cell line was used for the incorporation of the alkyne modified uridine derivative (*i.e.* EU). After thawing, the bacteria were incubated for 1 hour at 37 °C in S.O.C. medium. The cells were then cultured in chloramphenicol supplemented LB-medium overnight at 37 °C.

The optical density (OD_{600}) was measured at regular intervals, in order to monitor bacterial growth. Upon reaching an OD_{600} of 0.5, different concentrations of EU in water was added to give the following final concentrations of EU: 0 µM; 10 µM; 100 µM; 1 mM. The addition of EU had no significant impact on cell growth.

After reaching the stationary phase (OD_{600} ~ 1.4), the cells were centrifuged at 5000 rpm for 15 minutes at 4 °C. The supernatant was carefully removed and the pellet washed twice with PBS. After freezing in liquid nitrogen, the samples were stored at -80 °C until RNA extraction.

5.17.2 Extraction of total RNA from *E. coli* cultures

The pellet was thawed and redissolved in MilliQ water. The TriFast FL kit was used for the isolation of the RNA. Chloroform was added and the mixture was vortexed for 15 seconds at RT. After centrifugation (5000 RPM for 15 minutes), the colorless aqueous phase was transferred to an Eppendorf tube. Isopropanol was added and incubated at RT for 15 minutes. The sample was, once again, centrifuged at 12 000 x g for 10 minutes (4 °C).The supernatant was carefully removed, the pellet was washed with 75% ethanol and allowed to air dry.

5.17.3 Click functionalization of EU treated bacterial cells

The RNA pellets were redissolved in NaH_2PO_4 buffer (pH 8), to which was added TPTA (50 mM), sodium ascorbate (5 mM), $CuSO_4 \cdot 5H_2O$ (1 mM) and the Alexa 594 azide dye (50 µM). Enough water was added to yield the final concentration of substances as indicated in brackets. The reaction mixture was incubated at 25 °C for 3 hours, after which excess dye was removed by means of gel filtration.

The samples were loaded onto a 10% denaturing polyacrylamide gel and run at 18 W for 2 hours. Fluorescent scanning on the Typhoon was done, by exciting the unstained gel at 532 nm. The same settings were used for scanning the GelRed stained gel.

Abbreviations

5-EU	5-Ethynyluridine
5-EdU	5-Ethynyl-2'-deoxyuridine
A_{260}	Absorption at 260 nm
Ac_2O	Acetic anhydride
ACE	*Bis*(acetoxyethoxy)methyl
APS	Ammonium peroxydisulfate
BA	Barrier filter
bFGF	Basic fibroblast growth factor
br s	Broad singlet
BTT	5-Benzylthio-(*1H*)-tetrazole
Bu_4NF	Tetrabutylammonium fluoride
CEP-Cl	2-Cyanoethyl-*N*,*N*-diisopropylchlorophosphoramidite
$CHCl_3$	Chloroform
CH_3CN	Acetonitrile
*c*Hex	Cyclohexane
$CDCl_3$	Deuterated chloroform
CPG	Controlled pore glass
CuAAC	Copper catalyzed azide-alkyne cycloaddition
DAD	Diode array detector
DAPI	4',6-diamidino-2-phenylindole dihydrochloride
DCA	Dichloroacetic acid
DCE	Dichloroethane
DCM	Dichloromethane
dd	Doublet of doublets
DIAD	Diisopropyl azodicarboxylate
DMAP	4-*N*,*N*-Dimethylaminopyridine
DMEM	Dulbecco's modified Eagle medium
DMF	*N*,*N*-Dimethylformamide
DMSO	Dimethylsulfoxide
DMSO-d_6	Deuterated DMSO
DNA	Deoxyribonucleic acid
EDTA	Ethylenediaminetetraacetic acid

eGFP	Enhanced green fluorescent protein
EI-MS	Electron ionization mass spectrometry
EMV	Electron multiplier voltage
Eq.	Equivalents
ESI-MS	Electronspray ionization mass spectrometry
Et_2O	Diethylether
EtOAc	Ethylacetate
EtOH	Ethanol
Et_3N	Triethylamine
FAB-MS	Fast atom bombardment mass spectrometry
FCS	Fetal calf serum
FD-MS	Field Desorption Mass Spectrometry
FT-IR	Fourier Transform Infrared Spectrometry
FRET	Förster Resonance Energy Transfer
HBF_4	Tetrafluoroboronic acid
HEK 293T	Human embryonic kidney 293 cells
HEPES	4-(2-Hydroxyethyl)-1-piperazineethanesulfonic acid
HOMO	Highest occupied molecular orbital
HPLC	High-performance liquid chromatography
IC_{50}	Half maximal inhibitory concentration
iEDDA	Inverse electron demand Diels-Alder cycloaddition
J	Coupling constant
$LiClO_4$	Lithium perchlorate
LP	Long pass filter
LUMO	Lowest unoccupied molecular orbital
m	Multiplet
MALDI-TOF	Matrix assisted laser desorption/ionization time-of-flight
MeOH	Methanol
$MgSO_4$	Magnesium sulfate
Mp	Melting point
NA	Numerical aperture
$NaHCO_3$	Sodium bicarbonate
NaH_2PO_4	Sodiumdihydrogen phosphate
$NaNO_2$	Sodium nitrite

Na_2SO_4	Sodium sulfate
NaOAc	Sodium acetate
NH_4OAc	Ammonium acetate
NMR	Nuclear magnetic resonance
NO	Nitric oxide
NOE	Nuclear Overhauser effect
PAGE	Polyacrylamide gel electrophoresis
PBS	Phosphate buffered saline
pd	Pseudo doublet
PPh_3	Triphenylphosphine
ppm	Parts per million
RBE4	Rat brain endothelial 4 cells
RNA	Ribonucleic acid
RNAi	RNA interference
ROESY	Rotating frame Overhauser effect spectroscopy
RT	Room temperature
s	Singlet
siRNA	Small interfering RNA
S.O.C. medium	Super optimal broth, supplemented with glucose
SPAAC	Strain Promoted azide-alkyne cycloaddition
SPOS	Solid phase oligonucleotide synthesis
t	Triplet
TAMRA	Tetramethylrhodamine
TBE	Tris/Borate/EDTA buffer
TCA	Trichloroacetic acid
TBDMS-Cl	*Tert*butyldimethylsilyl chloride
TEMED	*N*,*N*,*N'*,*N'*-tetramethylethylene diamine
tBu_2SnCl_2	Di-*tert*butyltin dichloride
TFA	Trifluoroacetic acid
THF	Tetrahydrofuran
TLC	Thin layer chromatography
T_m	Melting temperature
TMS	Trimethylsilyl
TOM-Cl	Triisopropylsilyloxymethyl chloride

TPS-Cl	2,4,6-Triisopropylbenzenesulfonyl chloride
t_R	Retention time
UV	Ultraviolet

References

1. Limbach, P. A., Crain, P. F. & McCloskey, J. A. Summary: the modified nucleosides of RNA. *Nucleic Acids Research* **22,** 2183–2196 (1994).

2. Helm, M. Post-transcriptional nucleotide modification and alternative folding of RNA. *Nucleic acids research* **34,** 721–733 (2006).

3. Goll, M. G. & Bestor, T. H. Eukaryotic cytosine methyltransferases. *Annual Review of Biochemistry* **74,** 481–514 (2005).

4. Davis, D. R. in *Modification and editing of RNA* (Grosjean, Henri and Benne, R.) 85–102 (ASM Press, 1998).

5. Sowers, L., Shaw, B. & Sedwick, W. Base stacking and molecular polarizability: effect of a methyl group in the 5-position of pyrimidines. *Biochemical and biophysical Journal* **148,** 790–794 (1987).

6. Goodchild, J. Review of Their Synthesis and Properties. *Bioconjugate chemistry* **1,** 165–187 (1990).

7. Beaucage, S. L. & Caruthers, M. H. Deoxynucleoside phosphoramidites-a new class of key intermediates for deoxypolynucleotide synthesis. *Tetrahedron Letters* **22,** 1859–1862 (1981).

8. Khorana. Total synthesis of a gene. *Science* **203,** 614–625 (1979).

9. Chaix, C., Molko, D. & Téoule, R. The use of labile base protecting groups in oligoribonucleotide synthesis. *Tetrahedron Letters* **30,** 71–74 (1989).

10. Sinha, N.D., Davis, P., Usman, N. Perez, J., Hodge, R., K. & & Casale, R. Labile exocyclic amine protection of nucleosides in DNA, RNA and oligonucleotide analog synthesis facilitating N-deacylation, minimizing depurination and chain degradation. *Biochimie* **75,** 13–23 (1993).

11. Welz, R. and Müller, S. 5- (Benzylmercapto) -1 H -tetrazole as activator for 2 ’ - O - TBDMS phosphoramidite building blocks in RNA synthesis. *Tetrahedron* **43,** 795–797 (2002).

12. Sinha, N.D. Biernat, J., Köster, H. Polymer support oligonucleotides synthesis. *Nucleic Acids Res* **12,** 4539–4557 (1984).

13. Tener, G. 2-Cyanoethyl Phosphate and its Use in the Synthesis of Phosphate Esters1. *Journal of the American Chemical Society* **2023,** 159–168 (1961).

14. Nöth, H. and Vetter, H. Darstellung und Reaktionen von Dimethylamino-halogen-phosphanen. *Chemische Berichte* **96,** 1109–1118 (1963).

15. Usman, N., Ogilvie, K. K. & Cedergrens, R. J. Automated Chemical Synthesis of Long Oligoribonucleotides a Controlled-Pore Glass Support : Synthesis of a 43-Nucleotide

Sequence Similar to the 3 ’ -Half Molecule of an Escherichia coli Formylmethionine tRNA ’. *Journal of the American Chemical Society* **5,** 7845–7854 (1987).

16. Wu, X. & Pitsch, S. Synthesis and pairing properties of oligoribonucleotide analogues containing a metal-binding site attached to beta-D-allofuranosyl cytosine. *Nucleic acids research* **26,** 4315–4323 (1998).

17. Scaringe, S. A., Wincott, F. E. & Caruthers, M. H. Novel RNA Synthesis Method Using 5 ′ - O -Silyl-2 ′ - O -orthoester Protecting Groups Uni V ersity of Colorado , Boulder , Colorado 80309 The ability to routinely synthesize RNA has become increasingly important as research reveals the multitude of RNA. *Journal of the American Chemical Society* **120,** 11820–11821 (1998).

18. Froehler, B.C. and Matteucci, M. D. substituted 5-phenyl tetrazoles: improved activators of deoxynucleoside phosphoramidites in deoxyoligonucleotide synthesis. *Tetrahedron Letters* **24,** 3171–3174 (1983).

19. Scaringe, S. a, Francklyn, C. & Usman, N. Chemical synthesis of biologically active oligoribonucleotides using beta-cyanoethyl protected ribonucleoside phosphoramidites. *Nucleic acids research* **18,** 5433–5441 (1990).

20. Wu, T., Ogilvie, K. and Pon, R. T. Nucleic Acids Research. *Nucleic Acids Research* **17,** 3501–3517 (1989).

21. Reddy, M.P., Farooqui, F. and Hanna, B. Methylamine Deprotection Increased Yield of Olgoribonucleotides. *Tetrahedron Letters* **36,** 8929–8932 (1995).

22. Vinayak, R., Anderson, P., McCollum, C. & Hampel, A. Chemical synthesis of RNA using fast oligonucleotide deprotection chemistry. *Nucleic acids research* **20,** 1265–1269 (1992).

23. Seidu-Larry, S., Krieg, B., Hirsch, M., Helm, M. & Domingo, O. A modified guanosine phosphoramidite for click functionalization of RNA on the sugar edge. *Chemical communications Cambridge England* **48,** 11014–11016 (2012).

24. Peacock, H., Maydanovych, O. & Beal, P. A. N2 -Modified 2-aminopurine ribonucleosides as minor-groove-modulating adenosine replacements in duplex RNA. *Journal of Organic Chemistry* **12,** 1044–1047 (2010).

25. Sproat, B. S. Chemistry and applications of oligonucleotide analogues. *Journal of biotechnology* **41,** 221–238 (1995).

26. Schoch, J., Staudt, M., Samanta, A., Wiessler, M. & Jäschke, A. Site-specific one-pot dual labeling of DNA by orthogonal cycloaddition chemistry. *Biojonjugate Chemistry* **23,** 1382–6 (2012).

27. McFarland, G. & Borer, P. Separation of oligo-RNA by reverse-phase HPLC. *Nucleic acids research* **7,** 1067–1080 (1979).

28. Fritz, H. J. *et al.* High-pressure liquid chromatography in polynucleotide synthesis. *Biochemistry* **17,** 1257–1267 (1978).

29. McInnes, J. L., Forster, A. C. & Symons, R. H. Photobiotin-labeled DNA and RNA hybridization probes. *Methods In Molecular Biology Clifton Nj* **4,** 401–414 (1988).

30. Pon, R. A long chain biotin phosphoramidite reagent for the automated synthesis of 5′-biotinylated oligonucleotides. *Tetrahedron letters* **32,** 1715–1718 (1991).

31. Pieles, U., Sproat, B. & Lamm, G. A protected biotin containing deoxycytidine building block for solid phase synthesis of biotinylated oligonucleotides. *Nucleic acids research* (1990). at <http://nar.oxfordjournals.org/content/18/15/4355.short>

32. Alves, A., Holland, D. & Edge, M. A chemical method of labelling oligodeoxyribonucleotides with biotin: A single step procedure using a solid phase methodology. *Tetrahedron letters* **30,** 3089–3092 (1989).

33. Langer, P. R., Waldrop, A. A. & Ward, D. C. Enzymatic synthesis of biotin-labeled polynucleotides: novel nucleic acid affinity probes. *Proceedings of the National Academy of Sciences* **78,** 6633–6637 (1981).

34. Igloi, G. L. & Schiefermayr, E. Enzymatic addition of fluorescein- or biotin-riboUTP to oligonucleotides results in primers suitable for DNA sequencing and PCR. *Biotechniques* **15,** 486–497 (1993).

35. Olejnik, J., Krzymańska-Olejnik, E. & Rothschild, K. J. Photocleavable biotin phosphoramidite for 5'-end-labeling, affinity purification and phosphorylation of synthetic oligonucleotides. *Nucleic acids research* **24,** 361–366 (1996).

36. Soukup, G., Cerny, R. & III, L. M. Preparation of oligonucleotide-biotin conjugates with cleavable linkers. *Bioconjugate chemistry* **6,** 135–138 (1995).

37. Oildea, B., Coull, J. & Köster, H. A versatile acid-labile linker for modification of synthetic biomolecules. *Tetrahedron letters* **31,** 7095–7098 (1990).

38. Leikauf, E., Barnekow, F. & Köster, H. Heterobifunctional trityl derivatives as linking reagents for the recovery of nucleic acids after labeling and immobilization. *Tetrahedron* **51,** 3793–3802 (1995).

39. Dirksen, A., Yegneswaran, S. & Dawson, P. E. Bisaryl hydrazones as exchangeable biocompatible linkers. *Angewandte Chemie (International ed. in English)* **49,** 2023–2037 (2010).

40. Zatsepin, T. S. & Oretskaya, T. S. Synthesis and applications of oligonucleotide-carbohydrate conjugates. *Chemistry & biodiversity* **1,** 1401–1417 (2004).

41. Horváth, I. & Rábai, J. Facile catalyst separation without water: fluorous biphase hydroformylation of olefins. *Science* **266,** 72–75 (1994).

42. Horváth, I. Fluorous biphase chemistry. *Accounts of chemical research* **31,** 641–650 (1998).

43. Pearson, W. H., Berry, D. A., Stoy, P., Jung, K. & Sercel, A. D. Fluorous Affinity Purification of Oligonucleotides synthesis is product purity , an issue that has become. *Journal of Organic Chemistry* **2005,** 7114–7122 (2005).

44. Hansen, A. S., Thalhammer, A., El-Sagheer, A. H., Brown, T. & Schofield, C. J. Improved synthesis of 5-hydroxymethyl-2'-deoxycytidine phosphoramidite using a 2'-deoxyuridine to 2'-deoxycytidine conversion without temporary protecting groups. *Bioorganic & medicinal chemistry letters* **21,** 1181–1184 (2011).

45. Höbartner, C. K., , C., Flecker, E., Ottenschläger, E., Pils, W., G. & , K. and Micura, R. The Synthesis of 2 0 -O-[(Triisopropylsilyl)oxy] methyl (TOM) Phosphoramidites of Methylated Ribonucleosides (m 1 G, m 2 G, m 2 2 G, m 1 I, m 3 U, m 4 C, m 6 A, m 6 2 A) for Use in Automated RNA Solid-Phase Synthesis. *Monatshefte für Chemie* **134,** 851–873 (2003).

46. Ferentz, A. & Verdine, G. Disulfide-crosslinked oligonucleotides. *Journal of the American Chemical Society* **113,** 4000–4002 (1991).

47. Wolfe, S. & Verdine, G. Ratcheting torsional stress in duplex DNA. *Journal of the American Chemical Society* 12585–12586 (1993). at <http://medcontent.metapress.com/index/A65RM03P4874243N.pdf>

48. Osborne, S. & Völker, J. Design, synthesis, and analysis of disulfide cross-linked DNA duplexes. *Journal of the …* **7863,** 1751–1758 (1996).

49. Ranasinghe, R. T. & Brown, T. Fluorescence based strategies for genetic analysis. *Chemical communications (Cambridge, England)* 5487–54502 (2005). doi:10.1039/b509522k

50. Tardy-Planechaud, S., Fujimoto, J., Lin, S. S. & Sowers, L. C. Solid phase synthesis and restriction endonuclease cleavage of oligodeoxynucleotides containing 5-(hydroxymethyl)-cytosine. *Nucleic acids research* **25,** 553–559 (1997).

51. Freier, S. & Altmann, K. The ups and downs of nucleic acid duplex stability: structure-stability studies on chemically-modified DNA: RNA duplexes. *Nucleic acids research* **25,** 4429–4443 (1997).

52. Parey, N., Baraguey, C., Vasseur, J.-J. & Debart, F. First evaluation of acyloxymethyl or acylthiomethyl groups as biolabile 2'-O-protections of RNA. *Organic letters* **8,** 3869–3872 (2006).

53. Karpeisky, A., Sweedler, D., Haeberli, P., Read, J., Jarvis, K. and Beigelman, L. scaleable and efficient synthesis of 2'-deoxy-2'-N-phtaloyl nucleoside phosphoramidites for oligonucleotide synthesis. *Bioorganic* **12,** 3345–3347 (2002).

54. Dai, Q., Deb, S. K., Hougland, J. L. & Piccirilli, J. a. Improved synthesis of 2'-amino-2'-deoxyguanosine and its phosphoramidite. *Bioorganic & medicinal chemistry* **14,** 705–713 (2006).

55. Behlke, M. Chemical modification of siRNAs for in vivo use. *Oligonucleotides* **18,** 305–320 (2008).

56. Micura, R. Preparation of 2’-deoxy-2'-methylselenomodified phosphoramidites and RNA. *Current Protocols in Nucleic Acid Chemistry* **1,** 1.15.1–1.15.34 (2007).

57. Obika, S., Nanbu, D., Hari, Y., Morio., K., In, Y., Ishida, T. and Imanishi, T. Synthesis of 2’-O,4'-C-Methyleneuridine and -cytidine. Novel bicyclic nucleosides having a fixed C3-endo sugar puckering. *Tetrahedron letters* **38,** 8735–8738 (1997).

58. Kaur, H., Babu, B. & Maiti, S. Perspectives on chemistry and therapeutic applications of locked nucleic acid (LNA). *Chemical reviews* **107,** 4672–4697 (2007).

59. Miller, P., Yano, J., Yano, E. & Carroll, C. Nonionic nucleic acid analogs. Synthesis and characterization of dideoxyribonucleoside methylphosphonates. *Biochemistry* **18,** 5134–5143 (1979).

60. Miller, P., Fang, K., Kondo, N. & Ts’o, P. Syntheses and properties of adenine and thymine nucleoside alkyl phosphotriesters, the neutral analogs of dinucleoside monophosphates. *Journal of the American Chemical Society* **93,** 6657–6665 (1971).

61. Letsinger, R., Groody, E., Lander, N. & Tanaka, T. Some developments in the phosphitetriester method for synthesis of oligonucleotides. *Tetrahedron* **40,** 137–143 (1984).

62. Eckstein, F. Nucleoside phosphorothioates. *Annual review of biochemistry* **54,** 367–402 (1985).

63. Eckstein, F. & Gish, G. Phosphorothioates in molecular biology. *Trends in biochemical sciences* **14,** 97–100 (1989).

64. Chen, J. & Schultz, R. Synthesis of oligodeoxyribonucleotide N3′→ P5′ phosphoramidates. *Nucleic Acids Research* **23,** 2661–2668 (1995).

65. Anderson, D. & Reischer, R. Preparation and Characterization of Oligonucleotides of D-and L-2’Deoxyuridine. *Nucleosides and Nucleotides* **3,** 37–41 (1984).

66. Jager, A., Levy, M. & Hecht, S. Oligonucleotide N-alkylphosphoramidates: synthesis and binding to polynucleotides. *Biochemistry* **27,** 7237–7246 (1988).

67. Froehler, B. Deoxynucleoside H-phosphonate diester intermediates in the synthesis of internucleotide phosphate analogues. *Tetrahedron letters* **27,** 5575–5578 (1986).

68. Summers, J. S. & Shaw, B. R. Boranophosphates as mimics of natural phosphodiesters in DNA. *Current Medicinal Chemistry* **8,** 1147–1155 (2001).

69. Iyer, R.P., Egan, W., Regan, J.B. and Beaucage, S. L. 3H-benzodithiole-3-one 1,1,-dioxide as an improved sulfurizing reagent in the solid-phase synthesis of oligodeoxyribonucleoside phosphorothioates. *Journal of the American Chemical Society* **112,** 1253–1254 (1989).

70. Wang, L. *et al.* Phosphorothioation of DNA in bacteria by dnd genes. *Nature chemical biology* **3,** 709–10 (2007).

71. Miller, P. S. *et al.* Solid-phase syntheses of oligodeoxyribonucleoside methylphosphonates. *Biochemistry* **25,** 5092–7 (1986).

72. Stirchak, E.P., Summerton, J.E. and Weller, D. D. Uncharged stereoregular nucleic acid analogs: 2. Morpholino nucleoside oligomers with carbamate iternucleoside linkages. *Nucleic Acids Research* **17,** 6129–6141 (1989).

73. Jørgensen, A. & Shaikh, K. The synthesis of double-headed nucleosides by the CuAAC reaction and their effect in secondary nucleic acid structures. *Organic & …* **9,** 1381–1388 (2011).

74. Shibutani, S. Translesional Synthesis on DNA Templates Containing a Single Abasic Site. A MECHANISTIC STUDY OF THE "A RULE."*Journal of Biological Chemistry* **272,** 13916–13922 (1997).

75. Seela and Kehne 1985 Biochemistry.pdf.

76. Seela, F. and Driller, H. Palindromic oligonucleotides containing 7-deaza-2'-deoxyguanosine: solid-phase synthesis of d[(p)GG*AATTCC] octamers and recognition by the endodeoxyribonuxlease EcoRI. **14,** 2319–2332 (1986).

77. Greco, N. & Tor, Y. Furan decorated nucleoside analogues as fluorescent probes: synthesis, photophysical evaluation, and site-specific incorporation. *Tetrahedron* **63,** 3515–3527 (2007).

78. Godde, F., Toulmé, J. J. & Moreau, S. Benzoquinazoline derivatives as substitutes for thymine in nucleic acid complexes. Use of fluorescence emission of benzo[g]quinazoline-2,4-(1H,3H)-dione in probing duplex and triplex formation. *Biochemistry* **37,** 13765–75 (1998).

79. Sandin, P. *et al.* Fluorescent properties of DNA base analogue tC upon incorporation into DNA--negligible influence of neighbouring bases on fluorescence quantum yield. *Nucleic acids research* **33,** 5019–25 (2005).

80. Netzel, T. L. *et al.* Photophysics of 2 ' -Deoxyuridine (dU) Nucleosides Covalently Substituted with Either 1 -Pyrenyl or 1 -Pyrenoyl : Observation of Pyrene-to-Nucleoside Charge-Transfer Emission in. *Journal of the American Chemical Society* **39,** 9119–9128 (1995).

81. Kawai, R. *et al.* Site-specific fluorescent labeling of RNA molecules by specific transcription using unnatural base pairs. *Journal of the American Chemical Society* **127,** 17286–17295 (2005).

82. Roget, A., Bazin, H. & Teoule, R. Synthesis and use of labelled nudeoside phosphoramidite building blocks bearing a reporter group: biotinyl, dinitrophenyl, pyrenyl and dansyl. *Nucleic acids research* **17,** 7643–7651 (1989).

83. Kim, S., Bang, E., Kwon, H., Shim, J. & Kim, B. Modified oligonucleotides containing lithocholic acid in their backbones: Their enhanced cellular uptake and their mimicking of hairpin structures. *ChemBioChem* **5,** 1517–1522 (2004).

84. Nakahara, M. *et al.* Synthesis and base-pairing properties of C-nucleotides having 1-substituted 1H-1,2,3-triazoles. *Bioorganic & medicinal chemistry letters* **19,** 3316–3319 (2009).

85. Agrawal, S., Christodoulou, C. & Gait, M. Efficient methods for attaching non-radioactive labels to the 5′ ends of synthetic oligodeoxyribonucleotides. *Nucleic acids research* **14,** 6227–6246 (1986).

86. Blanks, R. & McLaughlin, L. An oligodeoxynucleotide affinity column for the isolation of sequence specific DNA binding proteins. *Nucleic acids research* **16,** 10283–10299 (1988).

87. Mayer, E. *et al.* 1-Ethynylpyrene as a tunable and versatile molecular beacon for DNA. *Chembiochem : European journal of chemical biology* **5,** 865–868 (2004).

88. Wagner, C., Rist, M., Mayer-Enthart, E. & Wagenknecht, H.-A. 1-ethynylpyrene-modified guanine and cytosine as optical labels for DNA hybridization. *Organic & biomolecular chemistry* **3,** 2062–2063 (2005).

89. Okamoto, A., Ochi, Y. & Saito, I. Fluorometric sensing of the salt-induced B-Z DNA transition by combination of two pyrene-labeled nucleobases. *Chemical communications* **1,** 1128–1130 (2005).

90. Kolb, H. C., Finn, M. G. & Sharpless, K. B. Click Chemistry: Diverse Chemical Function from a Few Good Reactions. *Angewandte Chemie (International ed. in English)* **40,** 2004–2021 (2001).

91. Rostovtsev, V. V, Green, L. G., Fokin, V. V & Sharpless, K. B. A stepwise huisgen cycloaddition process: copper(I)-catalyzed regioselective "ligation" of azides and terminal alkynes. *Angewandte Chemie (International ed. in English)* **41,** 2596–2599 (2002).

92. Tornøe, C. W., Christensen, C. & Meldal, M. Peptidotriazoles on solid phase: [1,2,3]-triazoles by regiospecific copper(i)-catalyzed 1,3-dipolar cycloadditions of terminal alkynes to azides. *The Journal of organic chemistry* **67,** 3057–3064 (2002).

93. Gibson, K. & Benkovic, S. Synthesis and application of derivatizable oligonucleotides. *Nucleic acids research* **15,** 6455–6467 (1987).

94. Gramlich, P. M. E., Warncke, S., Gierlich, J. & Carell, T. Click-click-click: single to triple modification of DNA. *Angewandte Chemie (International ed. in English)* **47,** 3442–3444 (2008).

95. Seela, F. & Sirivolu, V. R. DNA containing side chains with terminal triple bonds: Base-pair stability and functionalization of alkynylated pyrimidines and 7-deazapurines. *Chemistry & biodiversity* **3,** 509–514 (2006).

96. Aigner, M. *et al.* Chemical synthesis of site-specifically 2'-azido-modified RNA and potential applications for bioconjugation and RNA interference. *Chembiochem : a European journal of chemical biology* **12,** 47–51 (2011).

97. Gierlich, J., Burley, G. A., Gramlich, P. M. E., Hammond, D. M. & Carell, T. Click chemistry as a reliable method for the high-density postsynthetic functionalization of alkyne-modified DNA. *Organic Letters* **8,** 3639–3642 (2006).

98. Staudinger, H. & Meyer, J. Über neue organische Phosphorverbindungen. *Helvetica Chimica Acta* **2,** 635–646 (1919).

99. Letsinger, R.L. and Ogilvie, K. K. Synthesis of oligothymidylates via phosphotriester intermediates. *Journal of the American Chemical Society* **91,** 3350–3355 (1969).

100. Reese, C. The chemical synthesis of oligo-and poly-nucleotides by the phosphotriester approach. *Tetrahedron* **34,** 3143–3179 (1978).

101. Polushin, N. N., Smirnov, I. P., Verentchikov, A. N. & Coull, J. M. Synthesis of Oligonucleotides Containing 2 ’ -Azido- and 2 ' -Amino-2 ' -deoxyuridine Using Phosphotriester Chemistry t. *Tetrahedron Letters* **37,** 3227–3230 (1996).

102. Kirschenheuter, G. P., Zhai, Y. & Pieken, W. An improved synthesis of 2′-azido-2′-deoxyuridine. *Tetrahedron Letters* **35,** 8517–8520 (1994).

103. Belsito, E., Liguori, A., Napoli, A., Siciliano, C. & Sindona, G. Straightforward Synthesis of Lipophilic Thymidine Glucopyranosyl Monophosphates as Models for a Drug Delivery System Across Cellular Membranes. *Nucleosides and Nucleotides* **18,** 2565–2580 (1999).

104. Gaetke, L. Copper toxicity, oxidative stress, and antioxidant nutrients. *Toxicology* **189,** 147–163 (2003).

105. Chambers, R. D. *Fluorine in Organic Chemistry*. 14–15; 224–225 (Blackwell, 2004).

106. Agard, N., Baskin, J. & Prescher, J. A comparative study of bioorthogonal reactions with azides. *ACS chemical biology* **1,** 644–648 (2006).

107. Baskin, J. M. *et al.* Copper-free click chemistry for dynamic in vivo imaging. *Proceedings of the National Academy of Sciences of the United States of America* **104,** 16793–16797 (2007).

108. Van Delft, P. *et al.* Synthesis of oligoribonucleic acid conjugates using a cyclooctyne phosphoramidite. *Organic letters* **12,** 5486–5489 (2010).

109. Jayaprakash, K.N., Peng, C.G., Butler, D., Varghese, J.P., Maier, M.A., Rajeev, K.G. and Manoharan, M. Non-nucleoside building blocks for copper-assisted and copper-free click chemistry for the efficient synthesis of RNA conjugates. *Organic Letters* **12,** 5410–5413 (2010).

110. Chen, W., Wang, D., Dai, C., Hamelberg, D. & Wang, B. Clicking 1,2,4,5-tetrazine and cyclooctynes with tunable reaction rates. *Chemical communications (Cambridge, England)* **48,** 1736–8 (2012).

111. Taylor, M. & Blackman, M. Design and synthesis of highly reactive dienophiles for the tetrazine–trans-cyclooctene ligation. *Journal of the American …* **133,** 9646–9649 (2011).

112. Foster, R. a a & Willis, M. C. Tandem inverse-electron-demand hetero-/retro-Diels-Alder reactions for aromatic nitrogen heterocycle synthesis. *Chemical Society reviews* **42,** 63–76 (2013).

113. Karver, M. R., Weissleder, R. & Hilderbrand, S. a. Bioorthogonal reaction pairs enable simultaneous, selective, multi-target imaging. *Angewandte Chemie (International ed. in English)* **51,** 920–2 (2012).

114. Patterson, D. M., Nazarova, L. a, Xie, B., Kamber, D. N. & Prescher, J. a. Functionalized cyclopropenes as bioorthogonal chemical reporters. *Journal of the American Chemical Society* **134,** 18638–43 (2012).

115. Saxon, E. and Bertozzi, C. R. Cell Surface Engineering by a Modified Staudinger Reaction. *Science* **287,** 2007–2010 (2000).

116. Wang, C., Seo, T. & Li, Z. Site-specific fluorescent labeling of DNA using Staudinger ligation. *Bioconjugate chemistry* **14,** 697–701 (2003).

117. MacMillan, A. M., Chen, L. & Verdine, G. L. Synthesis of an oligonucleotide suicide substrate for DNA methyltransferases. *The Journal of Organic Chemistry* **57,** 2989–2991 (1992).

118. MacMillan, A. M., Chen, L. & Verdine, G. L. Synthesis of an oligonucleotide suicide substrate for DNA methyltransferases. *The Journal of Organic Chemistry* **57,** 2989–2991 (1992).

119. Xu, Y., Zheng, Q. and Swann, P. F. Synthesis of DNA containing modified basis by postsynthetic substitution. *Journal of Organic Chemistry* **57,** 3839–3845 (1992).

120. Xu, Y., Zheng, Q. & Swann, P. Synthesis by post-synthetic substitution of oligomers containing guanine modified at the 6-position with S-, N-, O-derivatives. *Tetrahedron* **48,** 1729–1740 (1992).

121. Ali, M. M. *et al.* Sequence- and base-specific delivery of nitric oxide to cytidine and 5-methylcytidine leading to efficient deamination. *Journal of the American Chemical Society* **126,** 8864–5 (2004).

122. Onizuka, K., Taniguchi, Y. & Sasaki, S. Development of novel thioguanosine analogs with the ability to specifically modify cytidine. *Nucleic acids symposium series (2004)* 5–6 (2007). doi:10.1093/nass/nrm003

123. Onizuka, K. & Taniguchi, Y. Site-specific modification of RNA by functionality-transfer ODN probes. *Nucleic Acids …* **53,** 67–68 (2009).

124. Onizuka, K., Taniguchi, Y. & Sasaki, S. A new usage of functionalized oligodeoxynucleotide probe for site-specific modification of a guanine base within RNA. *Nucleic acids research* **38,** 1760–1766 (2010).

125. Leontis, N. B. & Westhof, E. Conserved geometrical base-pairing patterns in RNA. *Quarterly reviews of biophysics* **31,** 399–455 (1998).

126. Watson, J. D. & Crick, F. H. Molecular structure of nucleic acids; a structure for deoxyribose nucleic acid. *Nature* **171,** 737–738 (1953).

127. Cecil, B. R. & Ogston, A. G. The Sedimentation of. (1947).

128. Jao, C. Y. & Salic, A. Exploring RNA transcription and turnover in vivo by using click chemistry. *Proceedings of the National Academy of Sciences of the United States of America* **105,** 15779–15784 (2008).

129. Jablonski, E., Moomaw, E. W., Tullis, R. H. & Ruth, J. L. Preparation of oligodeoxynucleotide-alkaline phosphatase conjugates and their use hybridization probes. *Nucleic Acids Research* **14,** 6115–6128 (1986).

130. Guennewig, B., Stoltz, M., Menzi, M., Dogar, A. M. & Hall, J. *Properties of N(4)-Methylated Cytidines in miRNA Mimics. Nucleic acid therapeutics* (2012). doi:10.1089/nat.2011.0329

131. Horn, T. & Urdea, M. S. Forks and combs and DNA: the synthesis of branched oligodeoxyribonucleotides. *Nucleic Acids Research* **17,** 6959–6967 (1989).

132. Urdea, M. S. *et al.* A comparison of non-radioisotopic hybridization assay methods using fluorescent, chemiluminescent and enzyme labeled synthetic oligodeoxyribonucleotide probes. *Nucleic Acids Research* **16,** 4937–4956 (1988).

133. Maier, T. & Pfleiderer, W. Nucleotides: Part LXXV. New types of fluorescence labeling of 2′-deoxycytidine. *Helvetica Chimica Acta* **92,** 2722–2736 (2009).

134. Ono, A. and Ueda, T. Synthesis of decadeoxyribonucleotides containing N6-methyladenine, N4-methylcytosine, and 5-methylcytosine: recognition and cleavage by restriction endonucleases. *Nucleic Acids Research* **15,** 219–232 (1987).

135. Hayakawa, Y. & Kataoka, M. Facile Synthesis of Oligodeoxyribonucleotides via the Phosphoramidite Method without Nucleoside Base Protection. *Journal of the American Chemical Society* **120,** 12395–12401 (1998).

136. Crain, P. F. & McCloskey, J. A. The RNA modification database. *Nucleic Acids Research* **24,** 126–127 (1998).

137. Rife, J. P., Cheng, C. S., Moore, P. B. & Strobel, S. A. N 2-methylguanosine is iso-energetic with guanosine in RNA duplexes and GNRA tetraloops. *Nucleic Acids Research* **26,** 3640–3644 (1998).

138. Pallan, P. S., Kreutz, C., Bosio, S., Micura, R. & Egli, M. Effects of N2,N2-dimethylguanosine on RNA structure and stability: Crystal structure of an RNA duplex with tandem m2 2G:A pairs. *Rna New York Ny* **14,** 2125–2135 (2008).

139. Micura, R. *et al.* Methylation of the nucleobases in RNA oligonucleotides mediates duplex-hairpin conversion. *Nucleic Acids Research* **29,** 3997–4005 (2001).

140. Telser, J., Cruickshank, K. A., Schanze, K. S. & Netzel, T. L. DNA oligomers and duplexes containing a covalently attached derivative of tris(2,2'-bipyridine)ruthenium(II): synthesis and characterization by thermodynamic and optical spectroscopic measurements. *Journal of the American Chemical Society* **111,** 7221–7226 (1989).

141. Bannwarth, W. and Schmidt, D. Oligonucleotides containing spin-labeled 2'-deoxycytidine and 5-methyl-2'-deoxycytidine as probes for structural motifs of DNA. *Bioorganic and medicinal chemistry letters* **4,** 977–980 (1994).

142. Napoli, C., Lemieux, C. & Jorgensen, R. Introduction of a Chimeric Chalcone Synthase Gene into Petunia Results in Reversible Co-Suppression of Homologous Genes in trans. *The Plant cell* **2,** 279–289 (1990).

143. Fire, A., Xu, S., Montgomery, M. & Kostas, S. Potent and specific genetic interference by double-stranded RNA in Caenorhabditis elegans. *nature* **391,** 806–811 (1998).

144. Elbashir, S. M. RNA interference is mediated by 21- and 22-nucleotide RNAs. *Genes & Development* **15,** 188–200 (2001).

145. Kubo, T., Takei, Y., Mihara, K., Yanagihara, K. & Seyama, T. Amino-modified and lipid-conjugated dicer-substrate siRNA enhances RNAi efficacy. *Bioconjugate chemistry* **23,** 164–73 (2012).

146. Terrazas, M. & Eritja, R. Synthesis and properties of small interfering RNA duplexes carrying 5-ethyluridine residues. *Molecular diversity* **15,** 677–86 (2011).

147. Abe, T., Goda, K., Futami, K. & Furuichi, Y. Detection of siRNA administered to cells and animals by using a fluorescence intensity distribution analysis polarization system. *Nucleic acids research* **37,** e56 (2009).

148. Hong, H., Zhang, Y. & Cai, W. In vivo imaging of RNA interference. *Journal of nuclear medicine : official publication, Society of Nuclear Medicine* **51,** 169–72 (2010).

149. Wahba, A. S. *et al.* Phenylpyrrolocytosine as an unobtrusive base modification for monitoring activity and cellular trafficking of siRNA. *ACS chemical biology* **6,** 912–9 (2011).

150. Liu, Q. *et al.* R2D2, a bridge between the initiation and effector steps of the Drosophila RNAi pathway. *Science (New York, N.Y.)* **301,** 1921–5 (2003).

151. Schwarz, D. S. *et al.* Asymmetry in the assembly of the RNAi enzyme complex. *Cell* **115,** 199–208 (2003).

152. Bramsen, J. B. *et al.* A screen of chemical modifications identifies position-specific modification by UNA to most potently reduce siRNA off-target effects. *Nucleic acids research* **38,** 5761–5773 (2010).

153. Martinez, J. & Tuschl, T. RISC is a 5' phosphomonoester-producing RNA endonuclease. *Genes & development* **18,** 975–80 (2004).

154. Feulgren, R. & Rossenbeck, H. -chemischer Nachweis einer Nucleinsäure vom Typus der Thymonucleinsäure und die-darauf beruhende elektive Färbung von Zellkernen in mikroskopischen. *Hoppe-Seyler´ s Zeitschrift für …* **135,** 203–248 (1924).

155. El-Sagheer, A. H. & Brown, T. Click chemistry with DNA. *Chemical Society reviews* **39,** 1388–405 (2010).

156. Liu, X.-M., Thakur, A. & Wang, D. Efficient synthesis of linear multifunctional poly(ethylene glycol) by copper(I)-catalyzed Huisgen 1,3-dipolar cycloaddition. *Biomacromolecules* **8,** 2653–8 (2007).

157. Chan, T. R., Hilgraf, R., Sharpless, K. B. & Fokin, V. V. Polytriazoles as copper(I)-stabilizing ligands in catalysis. *Organic letters* **6,** 2853–5 (2004).

158. Smith, M., Ramller, D.H., Goldberg, I.H. and Khorana, H. G. Studies on Polynucleotides . XIV . Specific Synthesis of the C3'-C5' Interribonucleotide linkage. Syntheses of uridyl-(3'-> 5')-uridine and uridylyl-(3'->5')-Adenosine. *Journal of the American Chemical Society* **931,** 430–440 (1961).

159. Ogilvie, K., Sadana, K. & Thompson, E. The use of silyl groups in protecting the hydroxyl functions of ribonucleosides. *Tetrahedron …* **33,** 2861–2863 (1974).

160. Pitsch, S. An Efficient Synthesis of Enantiomeric Ribonucleic Acids from D-Glucose. *Helvetica chimica acta* **80,** 2286–2314 (1997).

161. Gerster, J. F. & Robins, R. K. Purine nucleosides. X. The synthesis of certain naturally occurring 2-substituted amino-9-ß-6(1H)-ones (N2-substituted guanosines). *Journal of the American Chemical Society* **6,** 3752–3759 (1965).

162. Järve, A., Müller, J. & Kim, I. Surveillance of siRNA integrity by FRET imaging. *Nucleic acids …* **35,** e124 (2007).

163. Vader, P., Aa, L. van der & Engbersen, J. A method for quantifying cellular uptake of fluorescently labeled siRNA. *Journal of Controlled …* **148,** 106–109 (2010).

164. Uhler, S. a, Cai, D., Man, Y., Figge, C. & Walter, N. G. RNA degradation in cell extracts: real-time monitoring by fluorescence resonance energy transfer. *Journal of the American Chemical Society* **125,** 14230–14231 (2003).

165. Hirsch, M., Strand, D. & Helm, M. Dye selection for live cell imaging of intact siRNA. *Biological chemistry* **393,** 23–35 (2012).

166. Chen, P. Y. *et al.* Strand-specific 5'-O-methylation of siRNA duplexes controls guide strand selection and targeting specificity. *RNA (New York, N.Y.)* **14,** 263–74 (2008).

167. Schwarz, D. S., Hutvágner, G., Haley, B. & Zamore, P. D. Evidence that siRNAs function as guides, not primers, in the Drosophila and human RNAi pathways. *Molecular cell* **10,** 537–48 (2002).

168. Harborth, J. *et al.* Sequence, chemical, and structural variation of small interfering RNAs and short hairpin RNAs and the effect on mammalian gene silencing. *Antisense nucleic acid drug development* **13,** 83–105 (2003).

169. Chiu, Y.-L. & Rana, T. M. RNAi in human cells: basic structural and functional features of small interfering RNA. *Molecular cell* **10,** 549–61 (2002).

170. Martinez, J., Patkaniowska, A., Urlaub, H., Lührmann, R. & Tuschl, T. Single-stranded antisense siRNAs guide target RNA cleavage in RNAi. *Cell* **110,** 563–574 (2002).

171. Nykänen, A., Haley, B. & Zamore, P. ATP requirements and small interfering RNA structure in the RNA interference pathway. *Cell* **107,** 309–321 (2001).

172. Chang, E., Zhu, M.-Q. & Drezek, R. Novel siRNA-based molecular beacons for dual imaging and therapy. *Biotechnology journal* **2,** 422–5 (2007).

173. Chen, C. *et al.* Real-time quantification of microRNAs by stem-loop RT-PCR. *Nucleic acids research* **33,** e179 (2005).

174. Derfus, A. M., Chen, A. a, Min, D.-H., Ruoslahti, E. & Bhatia, S. N. Targeted quantum dot conjugates for siRNA delivery. *Bioconjugate chemistry* **18,** 1391–6 (2007).

175. Roux, F. Regulation of Gamma-Clutamy l Transpeptidase and Alkaline Phosphatase Activities in Immortalized Rat Brain. *Journal of Cellular Physiology* **113,** 101–113 (1994).

176. Fox, J.J:, Van Praag, D., Wempen, I., Doerr, I.L., Cheong, L., Knoll, J.E., Eidinoff, M.L., Bendich, A. and Brown, G. B. Thiation of Nucleosides. II. Synthesis of 5-Methyl-2 ’-deoxycytidine and Related Pyrimidine Nucleosides. *Journal of the American Chemical Society* **81,** 178–187 (1959).

177. Sung, W. L. synthesis of 4-(1,2,4-triazolyl-1-yl)pyrimidin-2(1H)-one ribonucleotide and its application in synthesis of oligoribonucleotides. *Journal of Organic Chemistry* **47,** 3623–3628 (1982).

178. Gaffney, B.L., Marky, L.A. and Jones, R. A. The influence of the purine 2-amion group on DNA conformation and stability. *Tetrahedron* **40,** 3–13 (1984).

179. Geyer, C.R., Battersby, T.R and Benner, S. A. Nucleobse pairing in expanded Watson-Crick-like genetic information systems. *Structure* **11,** 1485–1498 (2003).

180. Schildkraut, C. & Lifson, S. Dependence of the melting temperature of DNA on salt concentration. *Biopolymers* **3,** 195–208 (1965).

181. Uesugi, S., Miyashiro, H., Tomita, K. and Ikehara, M. Synthesis and properties of d(ATACGCGTAT) and its derivatives containing one and two 5-methylcytosine residues. Effect of the methylation on deoxyribnocleic acid conformation. *ChemPharmBull* **34,** 51–60 (1986).

182. Chuprina, V.P., Lipanoc, A.A., Fedoroff, O.Y., Kim, S., Kintanar, A. and Reid, B. R. Seuqence effects on local DNA topology. *Proceedings of the National Academy of Sciences* **88,** 9087–9091 (1991).

183. Chein, Y. & Davidson, N. RNA: DNA hybrids are more stable than DNA: DNA duplexes in concentrated perchlorate and trichloroacetate solutions. *Nucleic acids research* **5,** 1627–1638 (1978).

184. Borah, B., Cohen, J.S., Howard, F.B. and Miles, H. T. Poly(d2NH2A-dT): Two-dimension NMR shows a B to A conversion in high salt. *Biochemistry* **24,** 7456–7462 (1985).

185. You, Y., Tataurov, A. V & Owczarzy, R. Measuring thermodynamic details of DNA hybridization using fluorescence. *Biopolymers* **95,** 472–86 (2011).

186. Hohjoh, H. RNA interference (RNAi) induction with various types of synthetic oligonucleotide duplexes in cultured human cells. *FEBS letters* **521,** 195–199 (2002).

187. Inoue, H., Hayase, Y., Iwai, S. & Ohtsuka, E. Sequence-dependent hydrolysis of RNA using modified oligonucleotide splints and RNase H. *FEBS letters* **215,** 327–30 (1987).

188. Yu, Y. T., Shu, M. D. & Steitz, J. a. A new method for detecting sites of 2'-O-methylation in RNA molecules. *RNA (New York, N.Y.)* **3,** 324–31 (1997).

189. Randau, L., Stanley, B., Kohlway, A. & Mechta, S. A cytidine deaminase edits C to U in transfer RNAs in Archaea. *Science* **324,** 657–659 (2009).

190. Su, A. & Randau, L. A-to-I and C-to-U editing within transfer RNAs. *Biochemistry (Moscow)* **76,** 932–937 (2011).

191. Salic, A. & Mitchison, T. J. A chemical method for fast and sensitive detection of DNA synthesis in vivo. *Proceedings of the National Academy of Sciences of the United States of America* **105,** 2415–20 (2008).

192. Ferullo, D. J., Cooper, D. L., Moore, H. R. & Lovett, S. T. Cell cycle synchronization of Escherichia coli using the stringent response, with fluorescence labeling assays for DNA content and replication. *Methods (San Diego, Calif.)* **48,** 8–13 (2009).

193. Sheu, C. & Foote, C. Reactivity toward singlet oxygen of a 7, 8-dihydro-8-oxoguanosine (" 8-hydroxyguanosine") formed by photooxidation of a guanosine derivative. *Journal of the American Chemical Society* **117,** 6439–6442 (1995).

194. Western, E. C. & Shaughnessy, K. H. Inhibitory effects of the guanine moiety on Suzuki couplings of unprotected halonucleosides in aqueous media. *The Journal of organic chemistry* **70,** 6378–88 (2005).

195. Firth, A. G., Fairlamb, I. J. S., Darley, K. & Baumann, C. G. Sonogashira alkynylation of unprotected 8-brominated adenosines and guanosines: fluorescence properties of compact conjugated acetylenes containing a purine ring. *Tetrahedron Letters* **47,** 3529–3533 (2006).

196. Schneider, C. A., Rasband, W. S. & Eliceiri, K. W. NIH Image to ImageJ: 25 years of image analysis. *Nature Methods* **9,** 671–675 (2012).

197. Hong, V., Kislukhin, A. a & Finn, M. G. Thiol-selective fluorogenic probes for labeling and release. *Journal of the American Chemical Society* **131,** 9986–9994 (2009).

198. Schirmeister, H., Himmelsbach, F. and Fleiderer, W. The2-(4-Nitrophenyl)ethoxycarbonyl (npeoc) and 2-(2,4-Dinitrophenyl)ethoxycarbonyl (dnpeoc) groups for protection of hydroxy functions in ribonucleosides and 2'-deoxyribonucleosides. *Helvetica chimica acta* **76,** 385–401 (1993).

199. Gerster, J.F. and Robins, K. The synthesis of 2-fluoro- and 2-chloroinosine and certain purine nucleosides. *Journal of Organic Chemistry* **31,** 3258–3262 (1966).

200. Cristofoli, W. a *et al.* 5-Alkynyl Analogs of Arabinouridine and 2'-Deoxyuridine: Cytostatic Activity Against Herpes Simplex Virus and Varicella-Zoster Thymidine Kinase Gene-Transfected Cells. *Journal of medicinal chemistry* **50,** 2851–2857 (2007).

Appendix

Contents

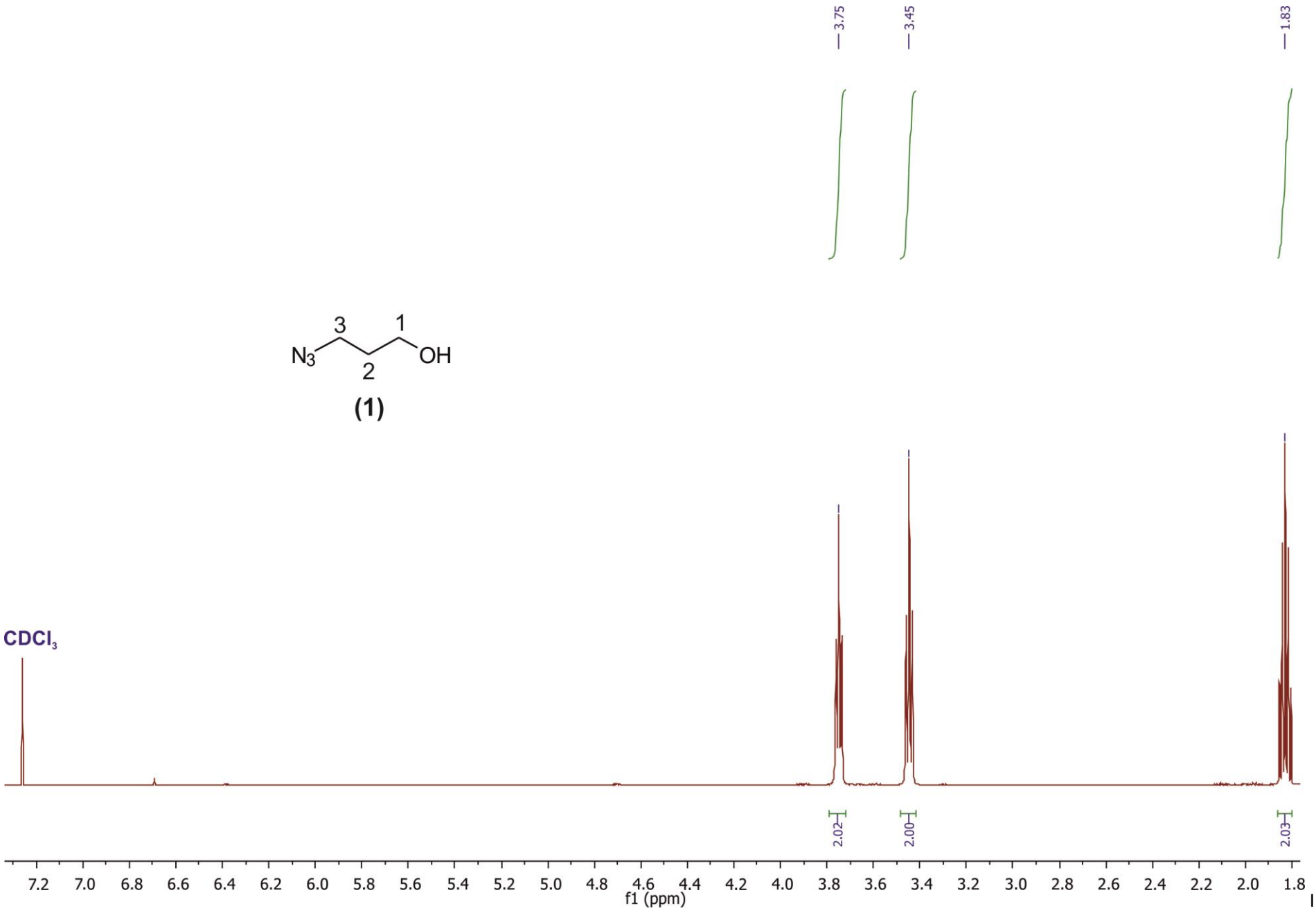
3.75
3.45
1.83
3
1
N3
OH
2
(1)
CDCl3
2.02
2.00
2.03
7.2 7.0 6.8 6.6 6.4 6.2 6.0 5.8 5.6 5.4 5.2 5.0 4.8 4.6 4.4 4.2 4.0 3.8 3.6 3.4 3.2 3.0 2.8 2.6 2.4 2.2 2.0 1.8
f1 (ppm)

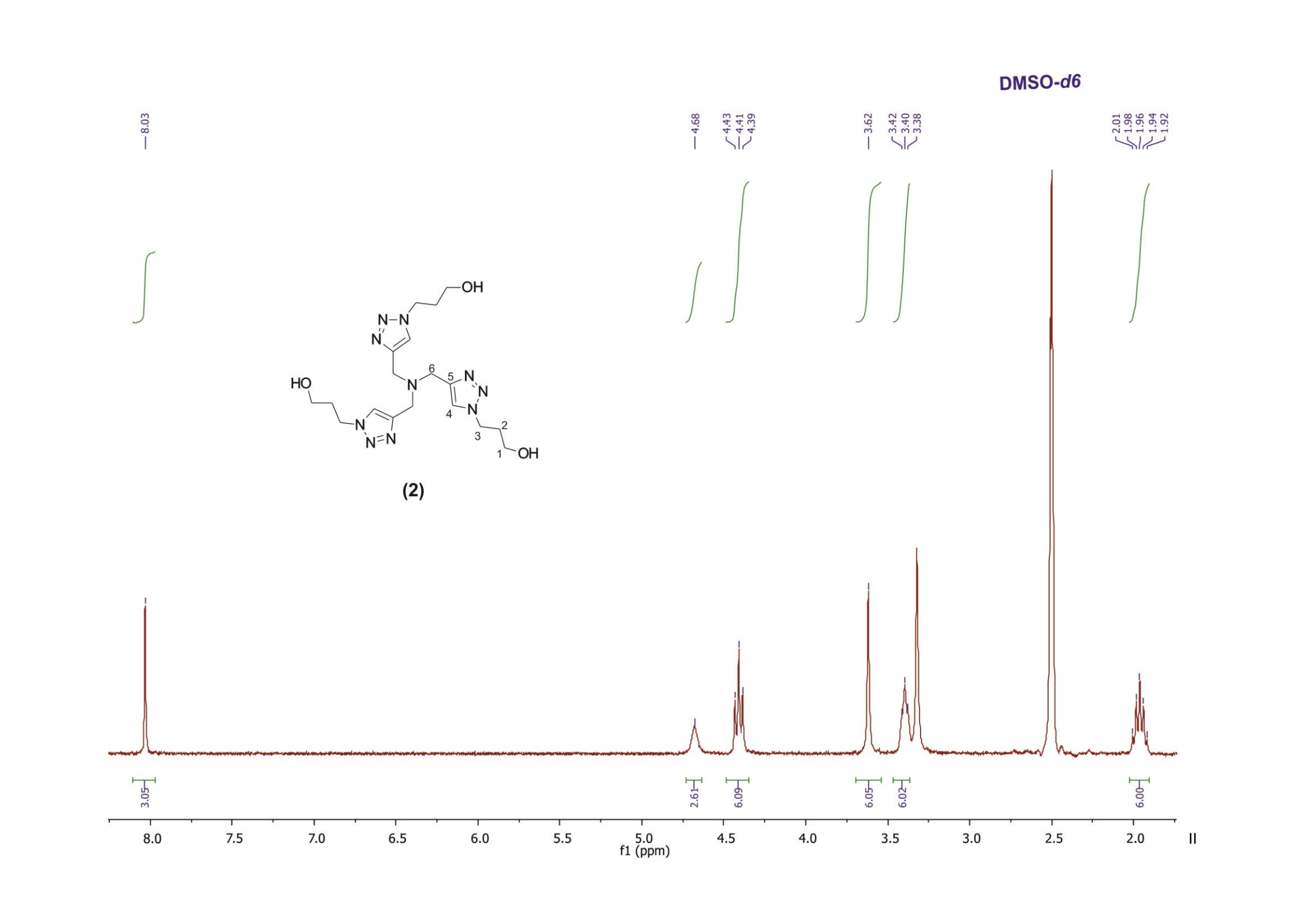
DMSO-d6
8.03
4.68
4.43
4.41
4.39
3.62
3.42
3.40
3.38
2.01
1.98
1.96
1.94
1.92
OH
HO
N
N
N
N
N
N
N
N
N
6
5
4
3
2
1
OH
(2)
3.05
2.61
6.09
6.05
6.02
6.00
8.0
7.5
7.0
6.5
6.0
5.5
5.0
4.5
4.0
3.5
3.0
2.5
2.0
f1 (ppm)

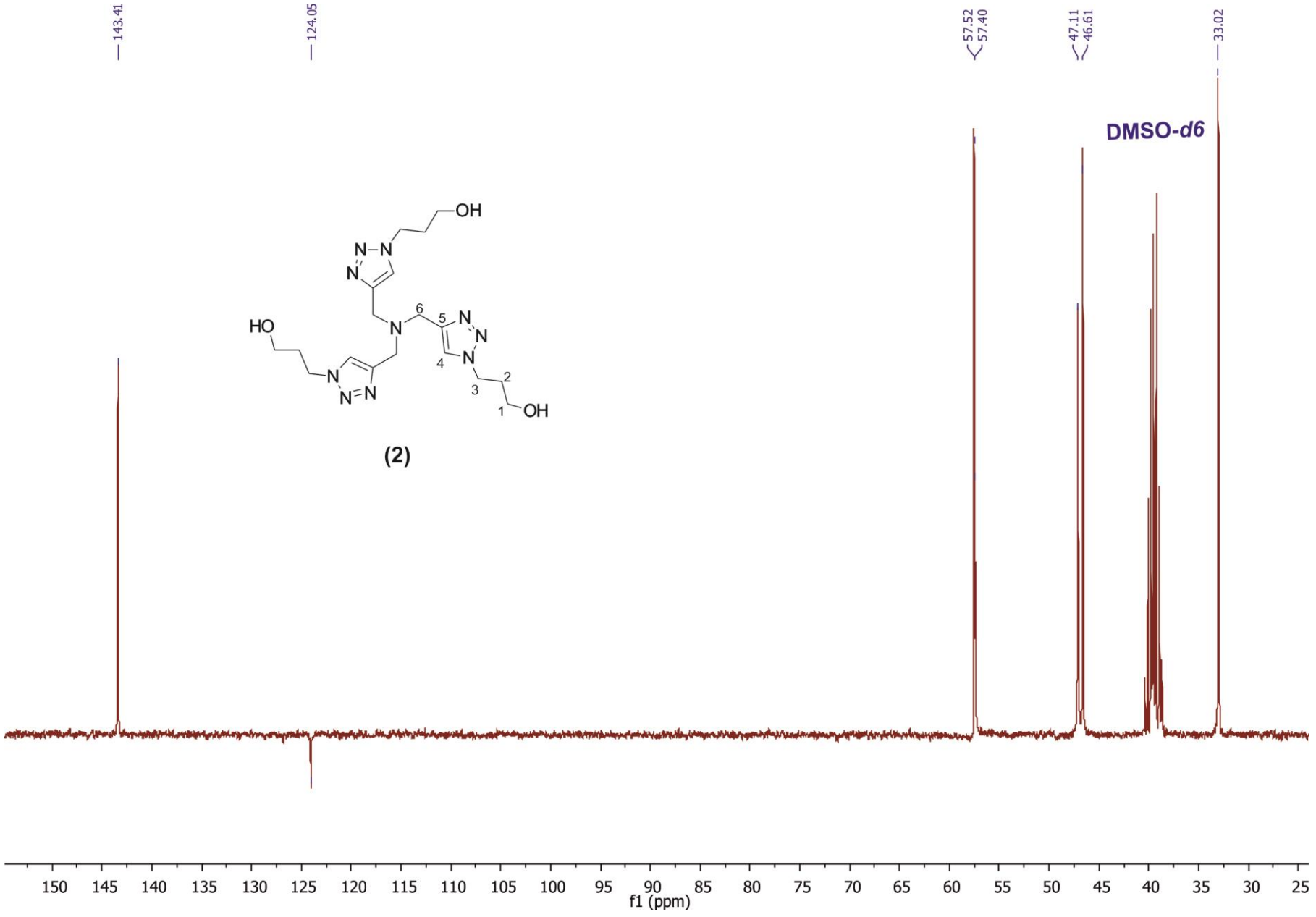
143.41
124.05
57.52
57.40
47.11
46.61
33.02
DMSO-d6
OH
HO
OH
(2)
150 145 140 135 130 125 120 115 110 105 100 95 90 85 80 75 70 65 60 55 50 45 40 35 30 25
f1 (ppm)

III

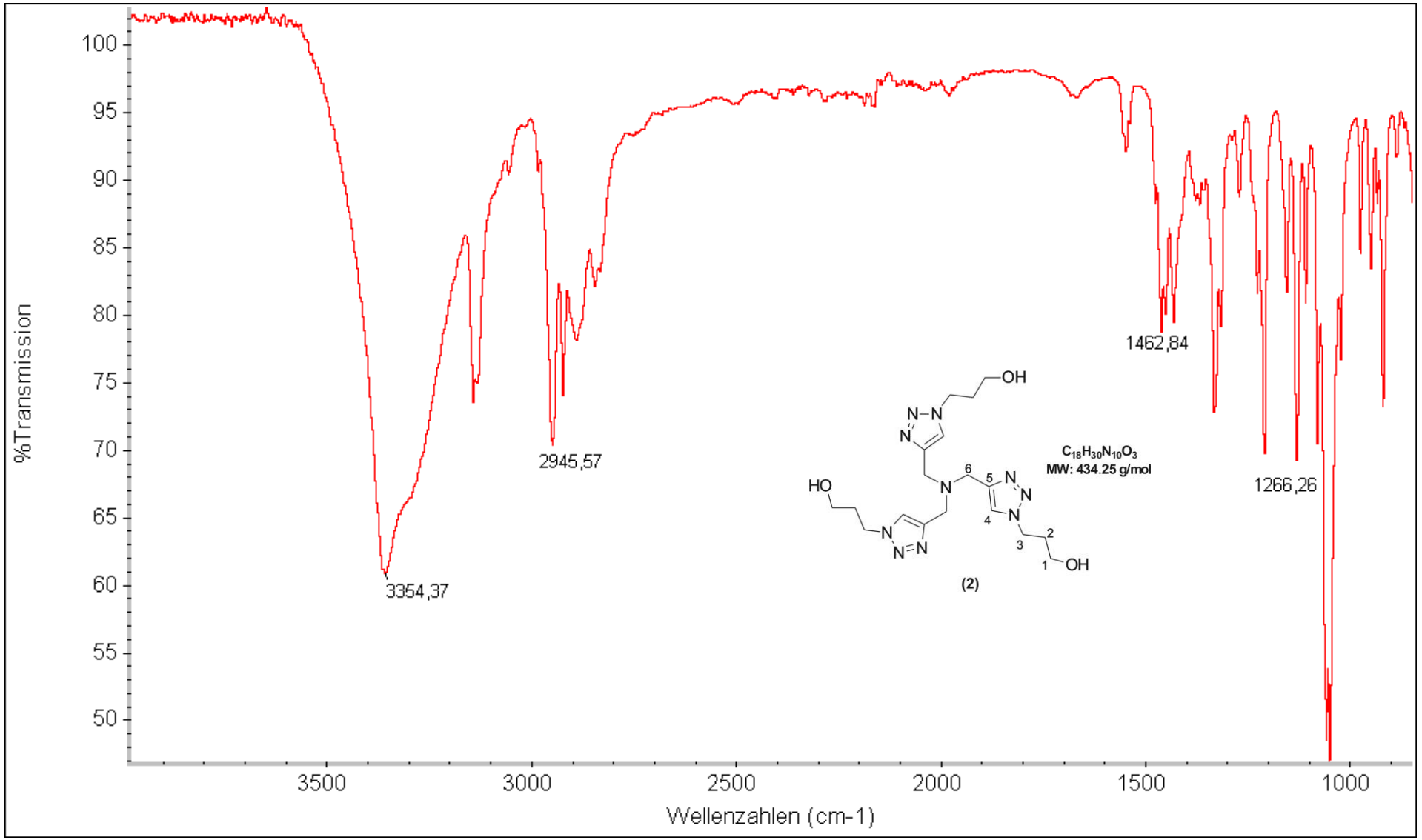
%Transmission
100
95
90
85
80
75
70
65
60
55
50
3500
3000
2500
2000
1500
1000
Wellenzahlen (cm-1)
3354,37
2945,57
1462,84
1266,26
OH
HO
N
N
N
N
N
N
N
N
OH
1
2
3
4
5
6
$C_{18}H_{30}N_{10}O_3$
MW: 434.25 g/mol
(2)

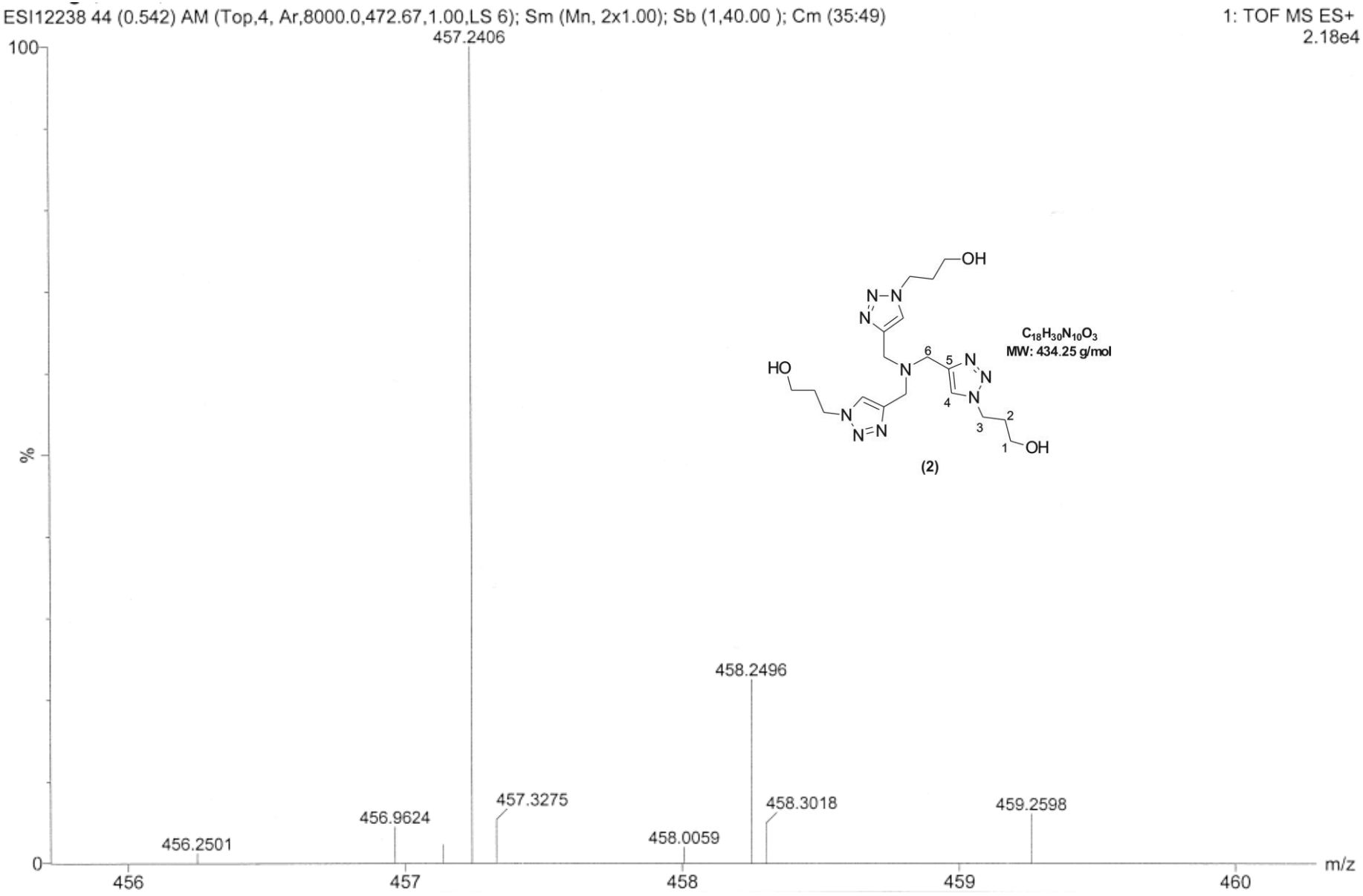
ESI12238 44 (0.542) AM (Top,4, Ar,8000.0,472.67,1.00,LS 6); Sm (Mn, 2x1.00); Sb (1,40.00); Cm (35:49)
1: TOF MS ES+
2.18e4
100
%
0
457.2406
458.2496
457.3275
456.9624
458.3018
459.2598
456.2501
458.0059
456
457
458
459
460
m/z
OH
HO
N
N
N
N
N
N
N
N
N
OH
6
5
4
3
2
1
$C_{18}H_{30}N_{10}O_3$
MW: 434.25 g/mol
(2)

V

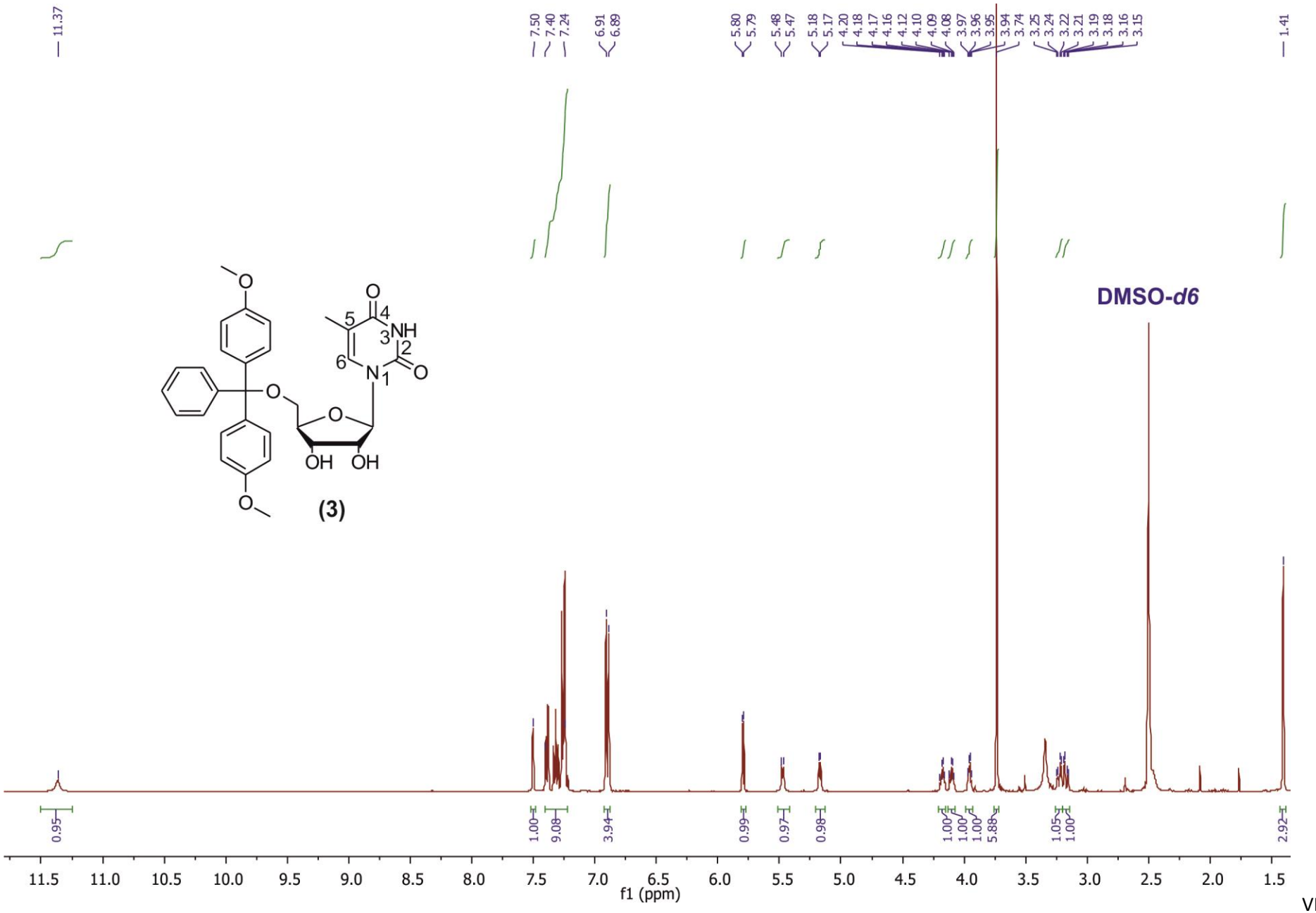
11.37
7.50
7.40
7.24
6.91
6.89
5.80
5.79
5.48
5.47
5.18
5.17
4.20
4.18
4.17
4.16
4.12
4.10
4.09
4.08
3.97
3.96
3.95
3.94
3.74
3.25
3.24
3.22
3.21
3.19
3.18
3.16
3.15
1.41
DMSO-d6
(3)
0.95
1.00
9.08
3.94
0.99
0.97
0.98
1.00
1.00
1.00
5.88
1.05
1.00
2.92
f1 (ppm)

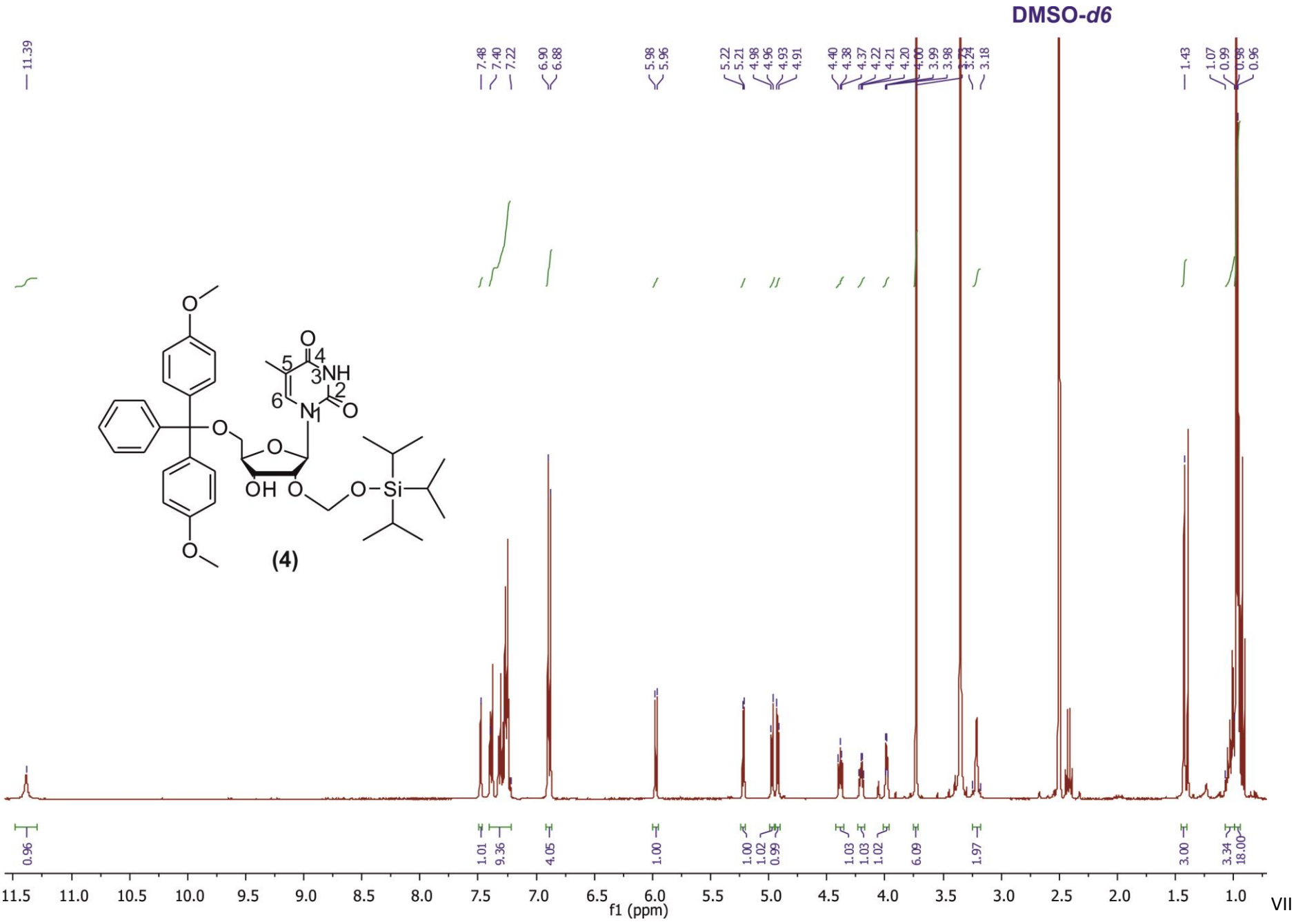
DMSO-d6
11.39
7.48
7.40
7.22
6.90
6.88
5.98
5.96
5.22
5.21
4.98
4.96
4.93
4.91
4.40
4.38
4.37
4.22
4.21
4.20
4.00
3.99
3.98
3.24
3.18
1.43
1.07
0.99
0.98
0.96
(4)
f1 (ppm)

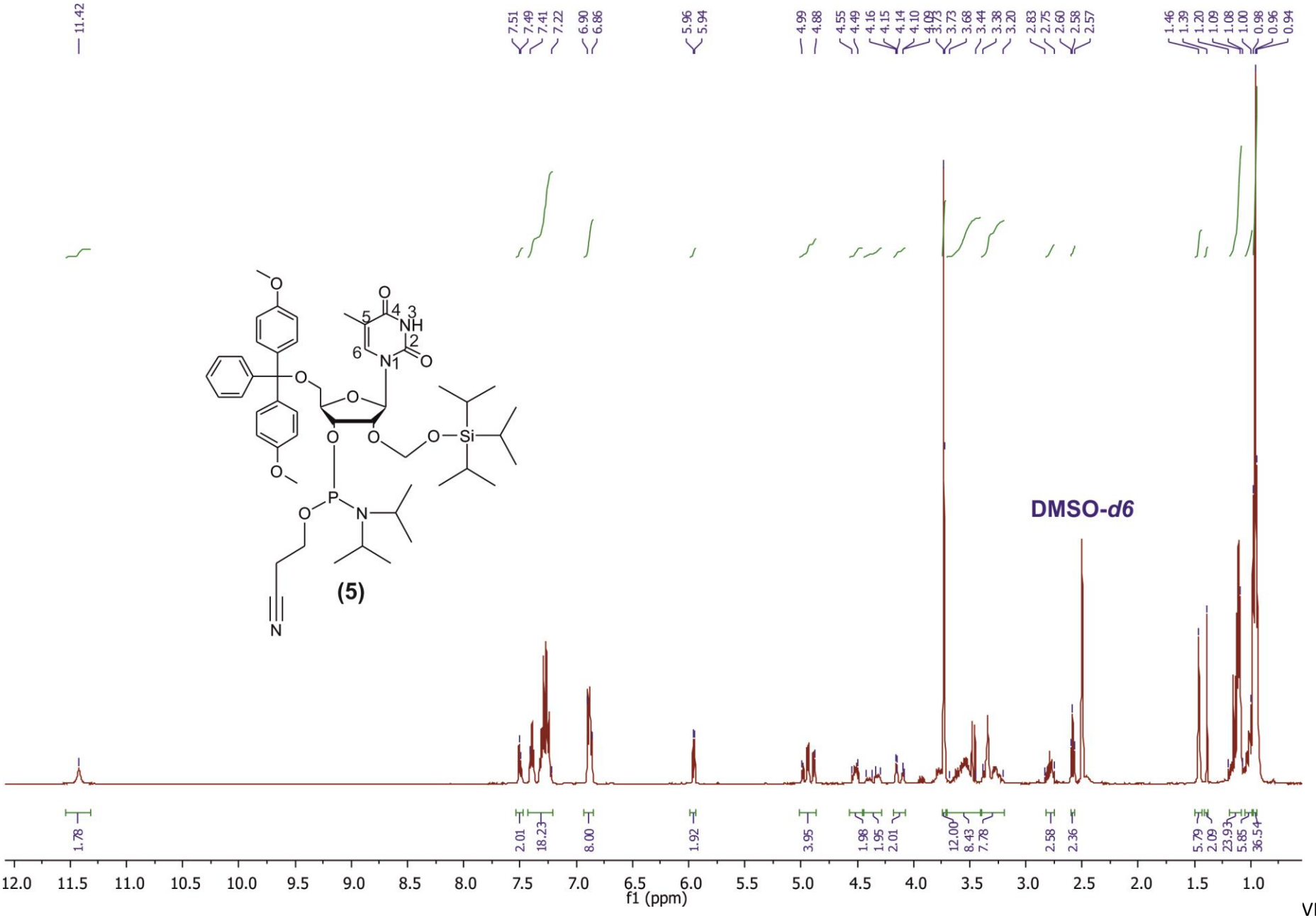
11.42
7.51
7.49
7.41
7.22
6.90
6.86
5.96
5.94
4.99
4.88
4.55
4.49
4.16
4.15
4.14
4.10
3.73
3.68
3.44
3.38
3.20
2.83
2.75
2.60
2.58
2.57
1.46
1.39
1.20
1.09
1.08
1.00
0.98
0.96
0.94
DMSO-d6
(5)
1.78
2.01
18.23
8.00
1.92
3.95
1.98
1.95
2.01
12.00
8.43
7.78
2.58
2.36
5.79
2.09
23.93
5.85
36.54
f1 (ppm)

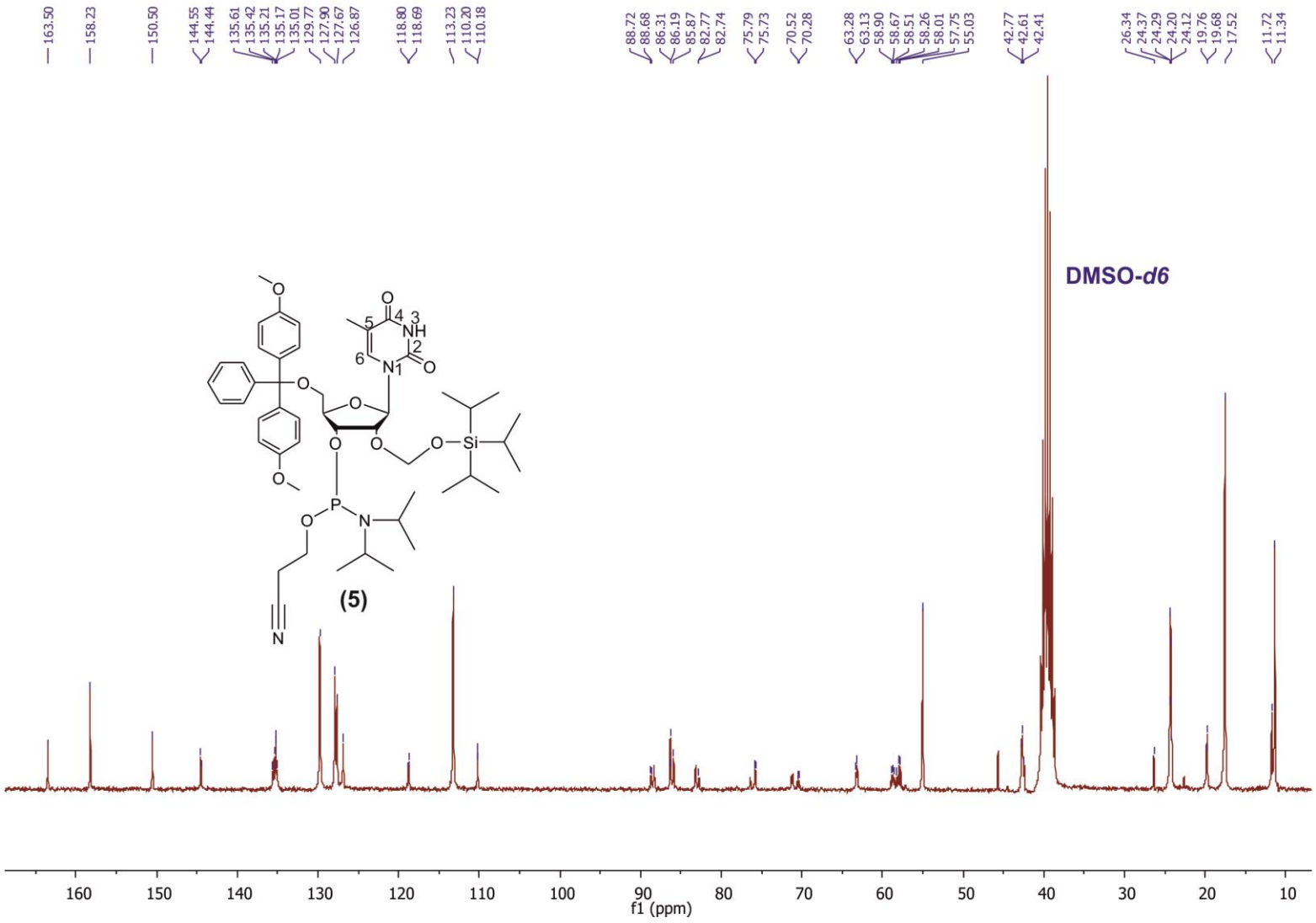
163.50
158.23
150.50
144.55
144.44
135.61
135.42
135.21
135.17
135.01
129.77
127.90
127.67
126.87
118.80
118.69
113.23
110.20
110.18
88.72
88.68
86.31
86.19
85.87
82.77
82.74
75.79
75.73
70.52
70.28
63.28
63.13
58.90
58.67
58.51
58.26
58.01
57.75
55.03
42.77
42.61
42.41
26.34
24.37
24.29
24.20
24.12
19.76
19.68
17.52
11.72
11.34
DMSO-d6
(5)
160
150
140
130
120
110
100
90
80
70
60
50
40
30
20
10
f1 (ppm)

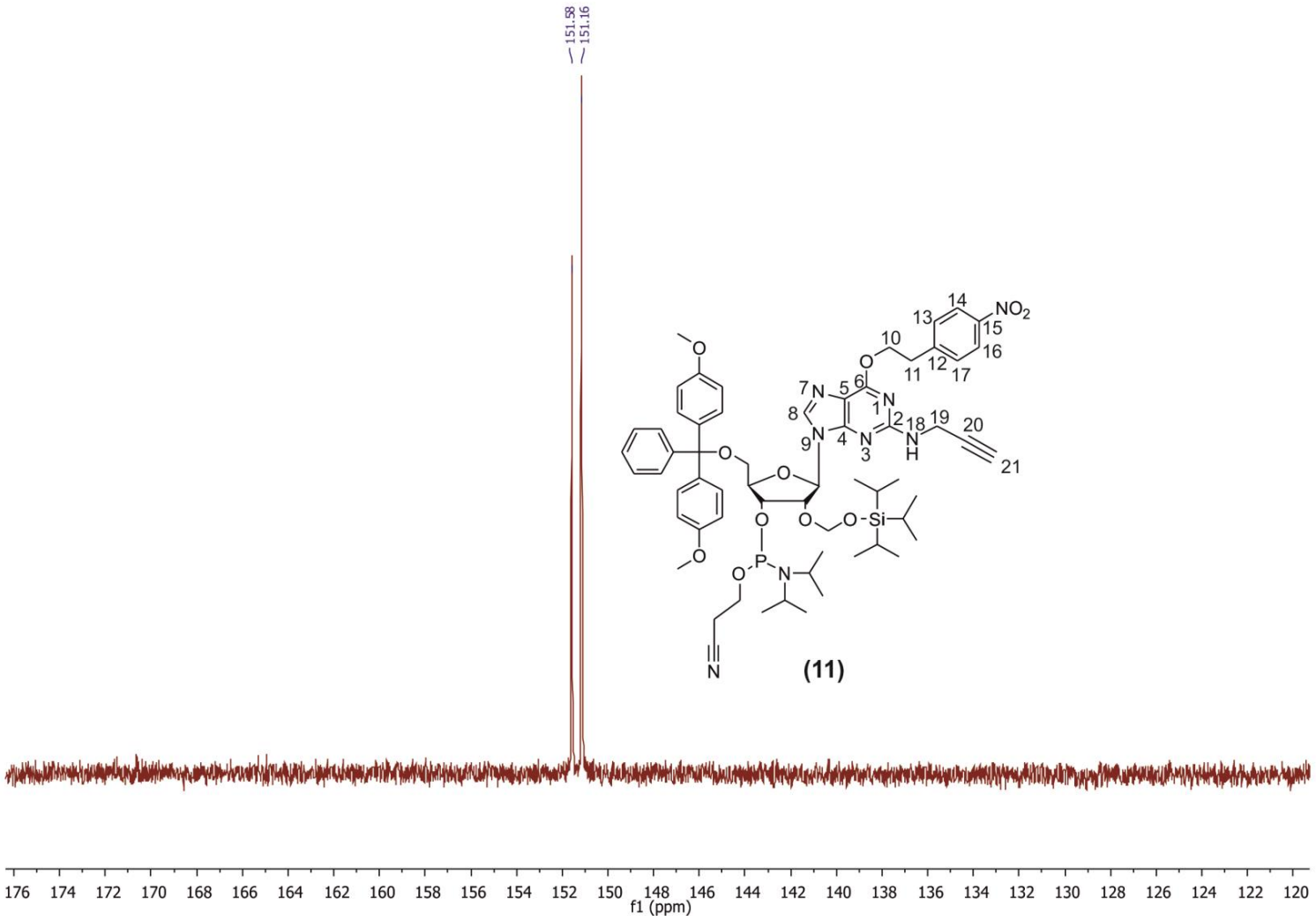
151.58
151.16
(11)
176 174 172 170 168 166 164 162 160 158 156 154 152 150 148 146 144 142 140 138 136 134 132 130 128 126 124 122 120
f1 (ppm)

X

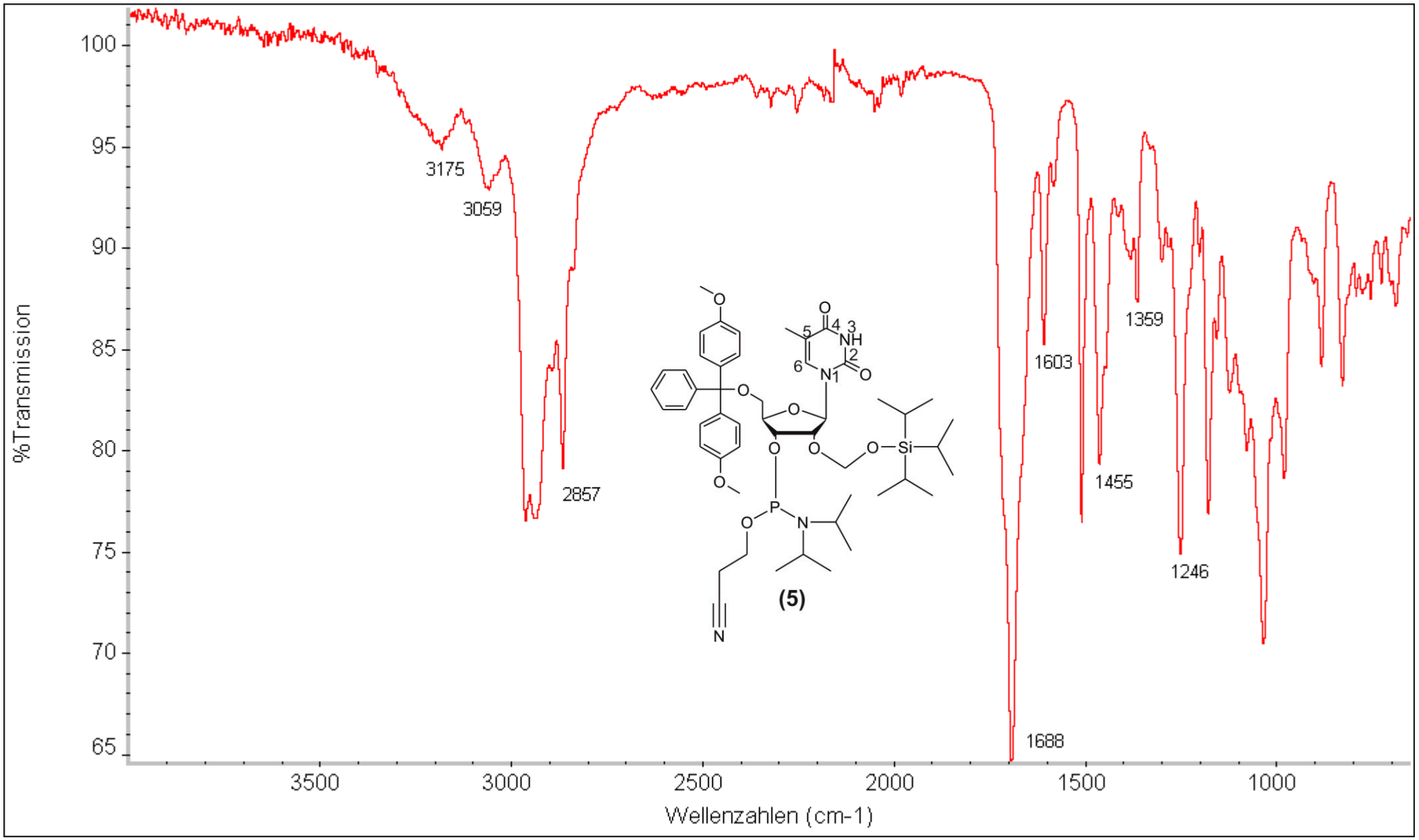
100
95
90
85
80
75
70
65
%Transmission
3500
3000
2500
2000
1500
1000
Wellenzahlen (cm-1)
3175
3059
2857
1688
1603
1455
1359
1246
(5)

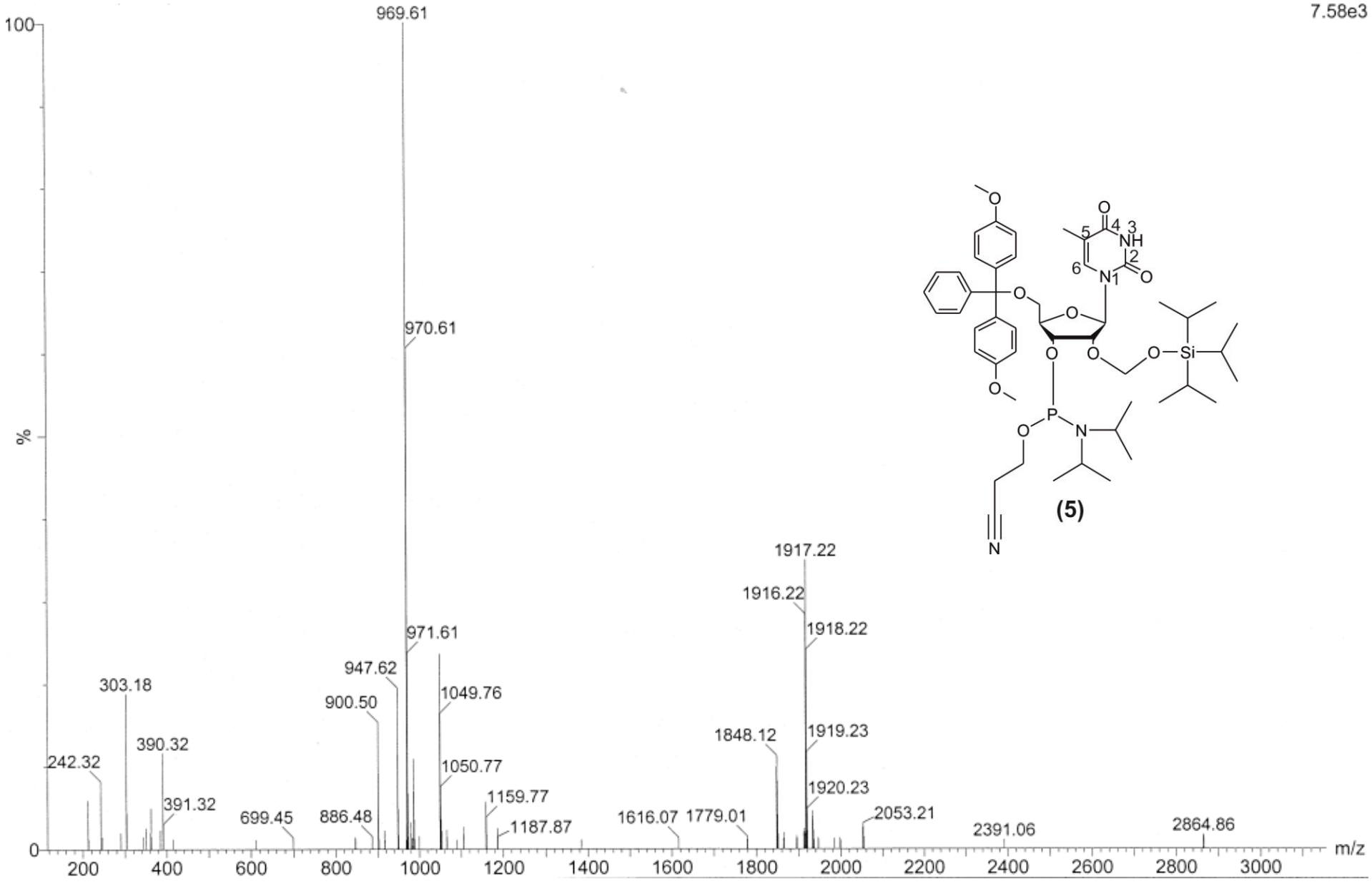
7.58e3
100
%
0
969.61
970.61
971.61
947.62
900.50
1049.76
1050.77
1159.77
1187.87
303.18
390.32
391.32
242.32
699.45
886.48
1616.07
1779.01
1848.12
1916.22
1917.22
1918.22
1919.23
1920.23
2053.21
2391.06
2864.86
m/z
200
400
600
800
1000
1200
1400
1600
1800
2000
2200
2400
2600
2800
3000
(5)

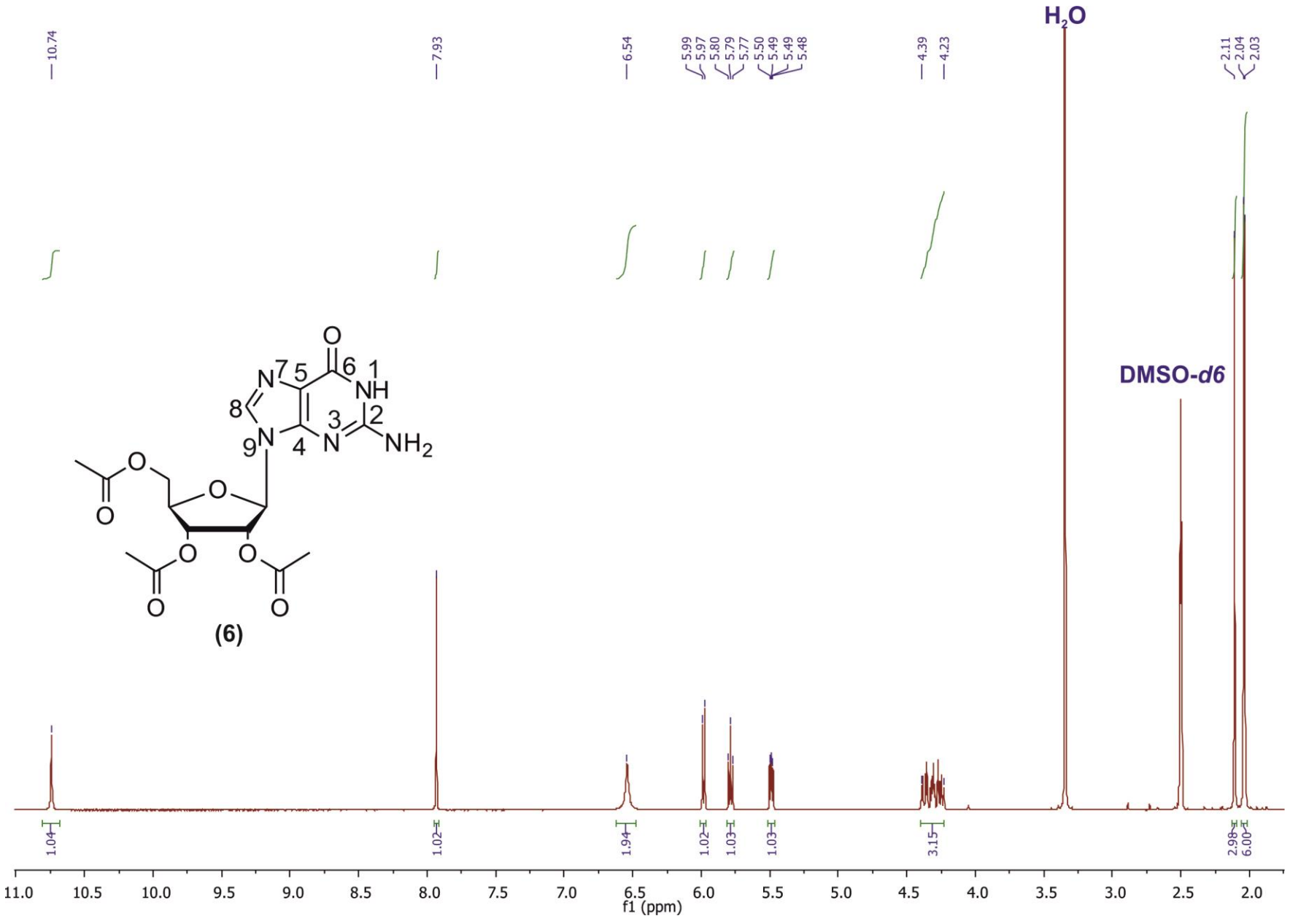
10.74
7.93
6.54
5.99
5.97
5.80
5.79
5.77
5.50
5.49
5.49
5.48
4.39
4.23
2.11
2.04
2.03
H2O
DMSO-d6
1.04
1.02
1.94
1.02
1.03
1.03
3.15
2.98
6.00
11.0
10.5
10.0
9.5
9.0
8.5
8.0
7.5
7.0
6.5
6.0
5.5
5.0
4.5
4.0
3.5
3.0
2.5
2.0
f1 (ppm)

(6)

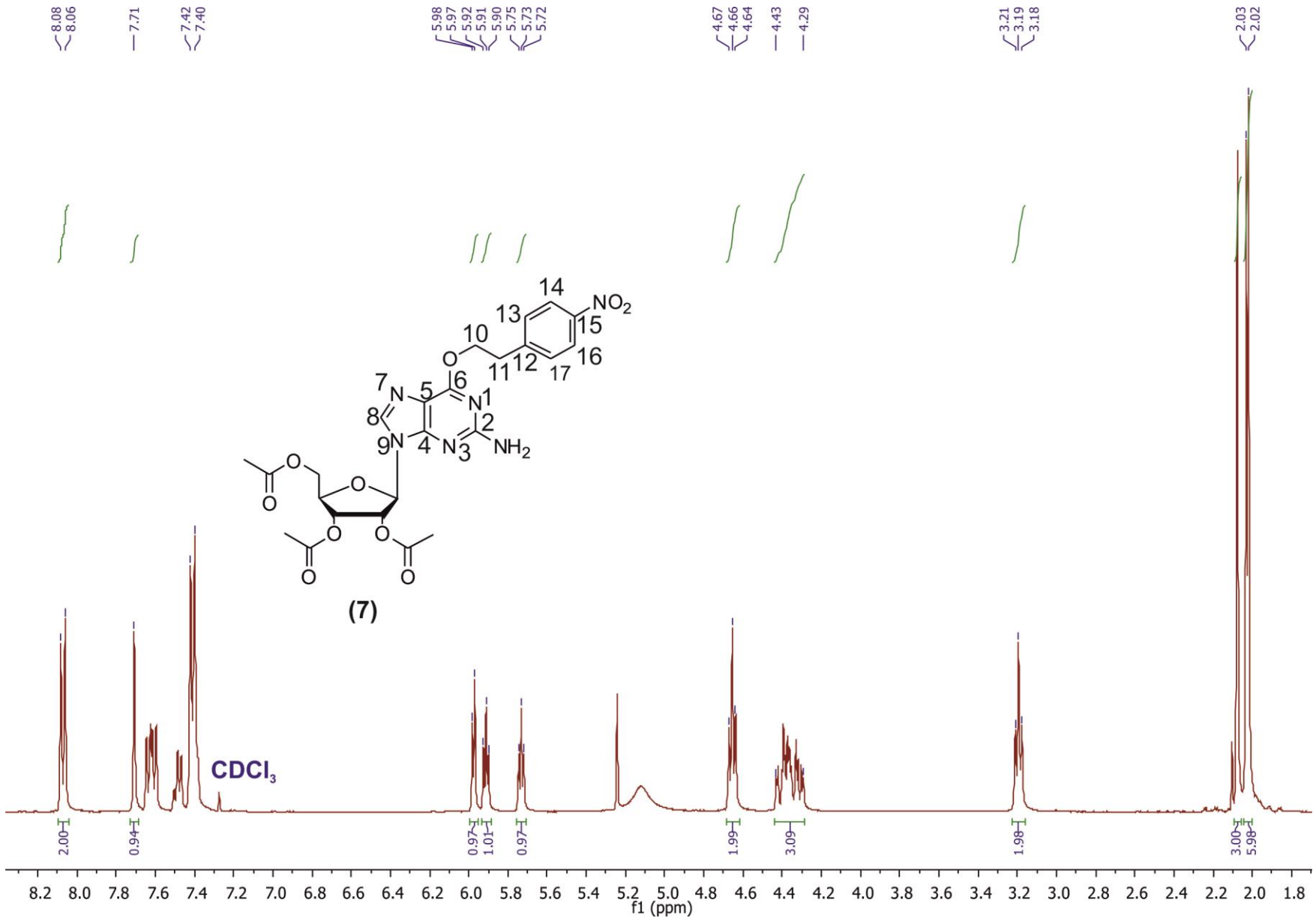
8.08
8.06
7.71
7.42
7.40
5.98
5.97
5.92
5.91
5.90
5.75
5.73
5.72
4.67
4.66
4.64
4.43
4.29
3.21
3.19
3.18
2.03
2.02
CDCl3
2.00
0.94
0.97
1.01
0.97
1.99
3.09
1.98
3.00
5.98
f1 (ppm)

(7)

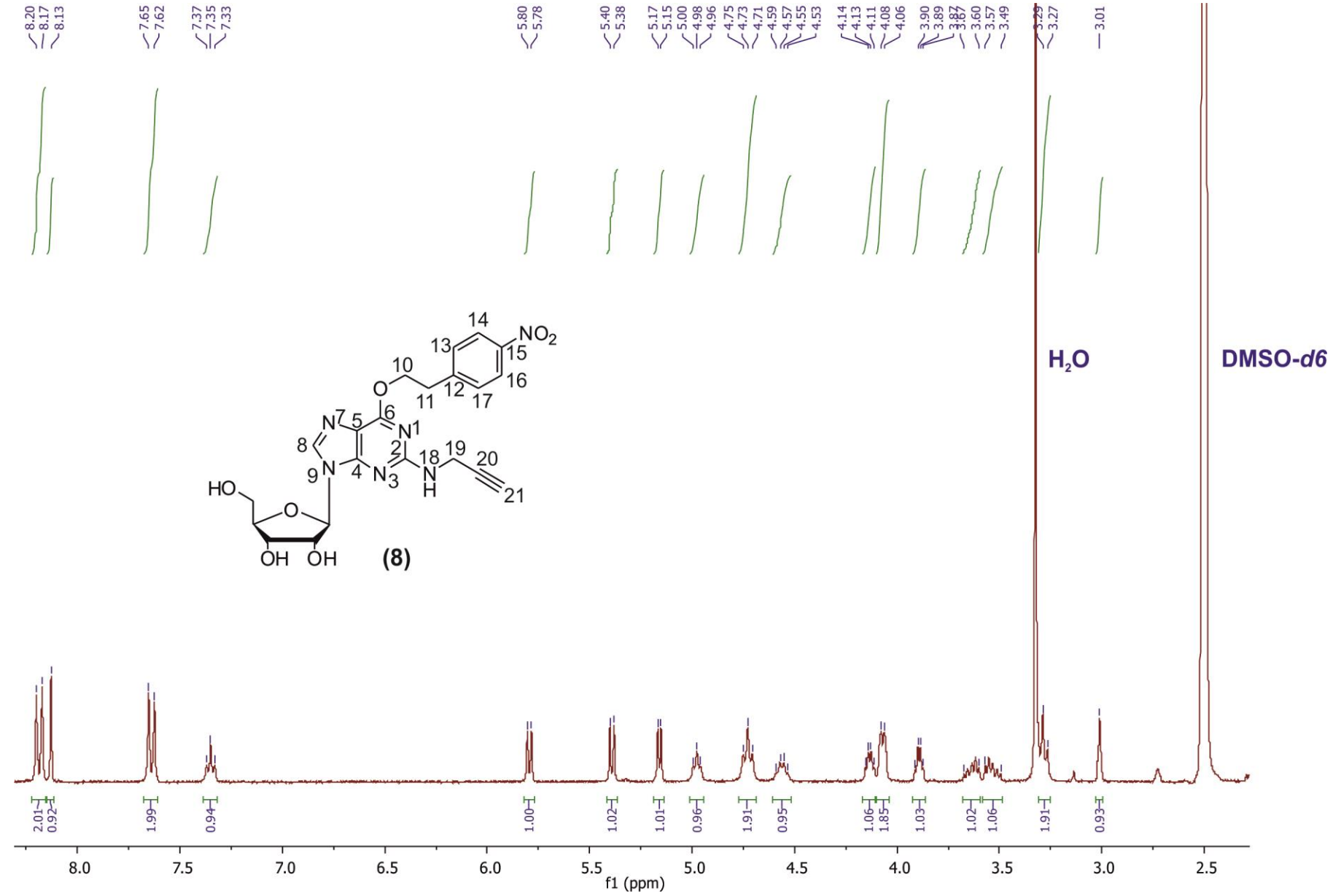
8.20
8.17
8.13
7.65
7.62
7.37
7.35
7.33
5.80
5.78
5.40
5.38
5.17
5.15
5.00
4.98
4.96
4.75
4.73
4.71
4.59
4.57
4.55
4.53
4.14
4.13
4.11
4.08
4.06
3.90
3.89
3.87
3.60
3.57
3.49
3.29
3.27
3.01
H2O
DMSO-d6
(8)
2.01
0.92
1.99
0.94
1.00
1.02
1.01
0.96
1.91
0.95
1.06
1.85
1.03
1.02
1.06
1.91
0.93
8.0
7.5
7.0
6.5
6.0
5.5
5.0
4.5
4.0
3.5
3.0
2.5
f1 (ppm)

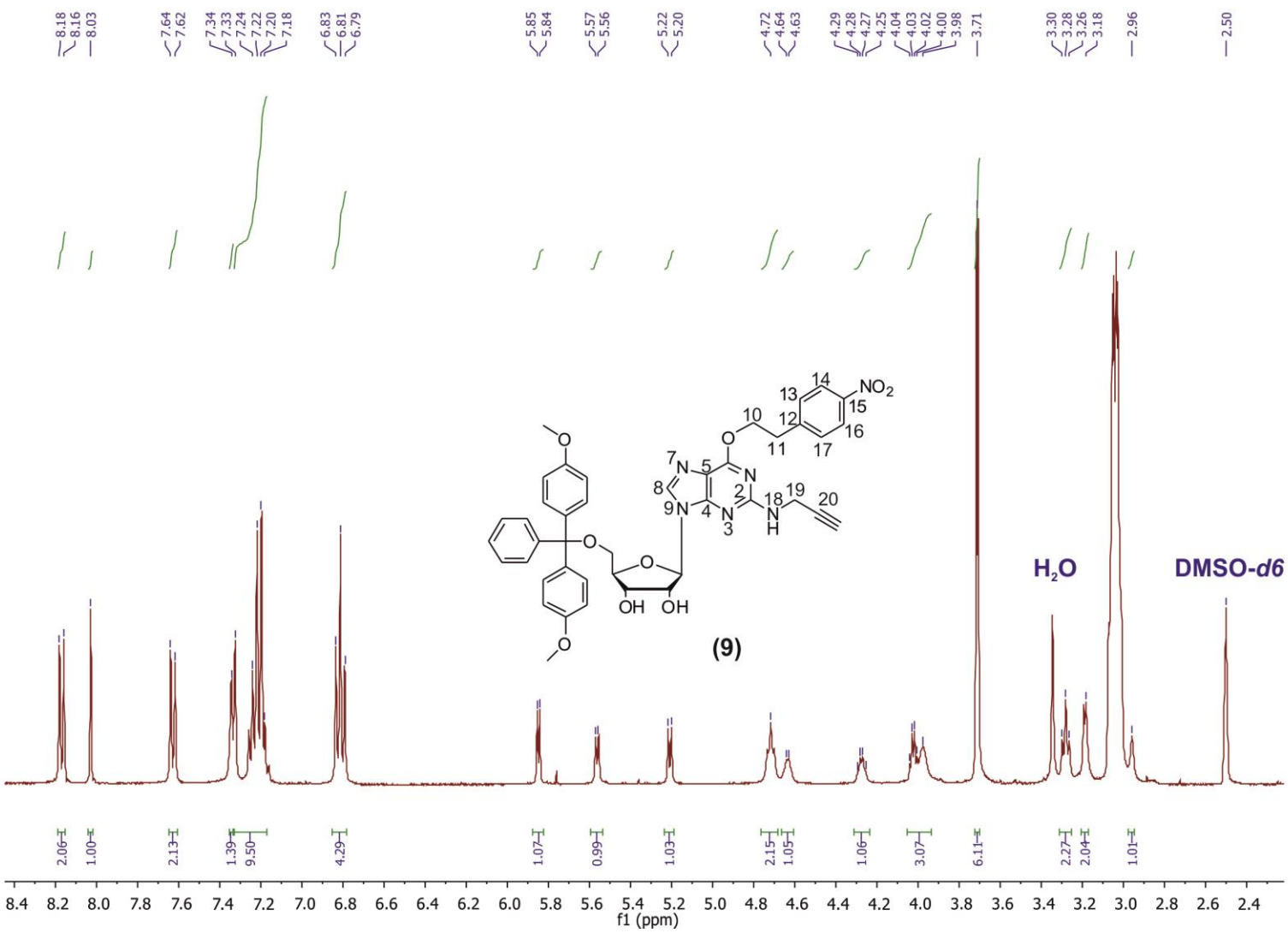
8.18
8.16
8.03
7.64
7.62
7.34
7.33
7.24
7.22
7.20
7.18
6.83
6.81
6.79
5.85
5.84
5.57
5.56
5.22
5.20
4.72
4.64
4.63
4.29
4.28
4.27
4.25
4.04
4.03
4.02
4.00
3.98
3.71
3.30
3.28
3.26
3.18
2.96
2.50
H2O
DMSO-d6
(9)
2.06
1.00
2.13
1.39
9.50
4.29
1.07
0.99
1.03
2.15
1.05
1.06
3.07
6.11
2.27
2.04
1.01
f1 (ppm)

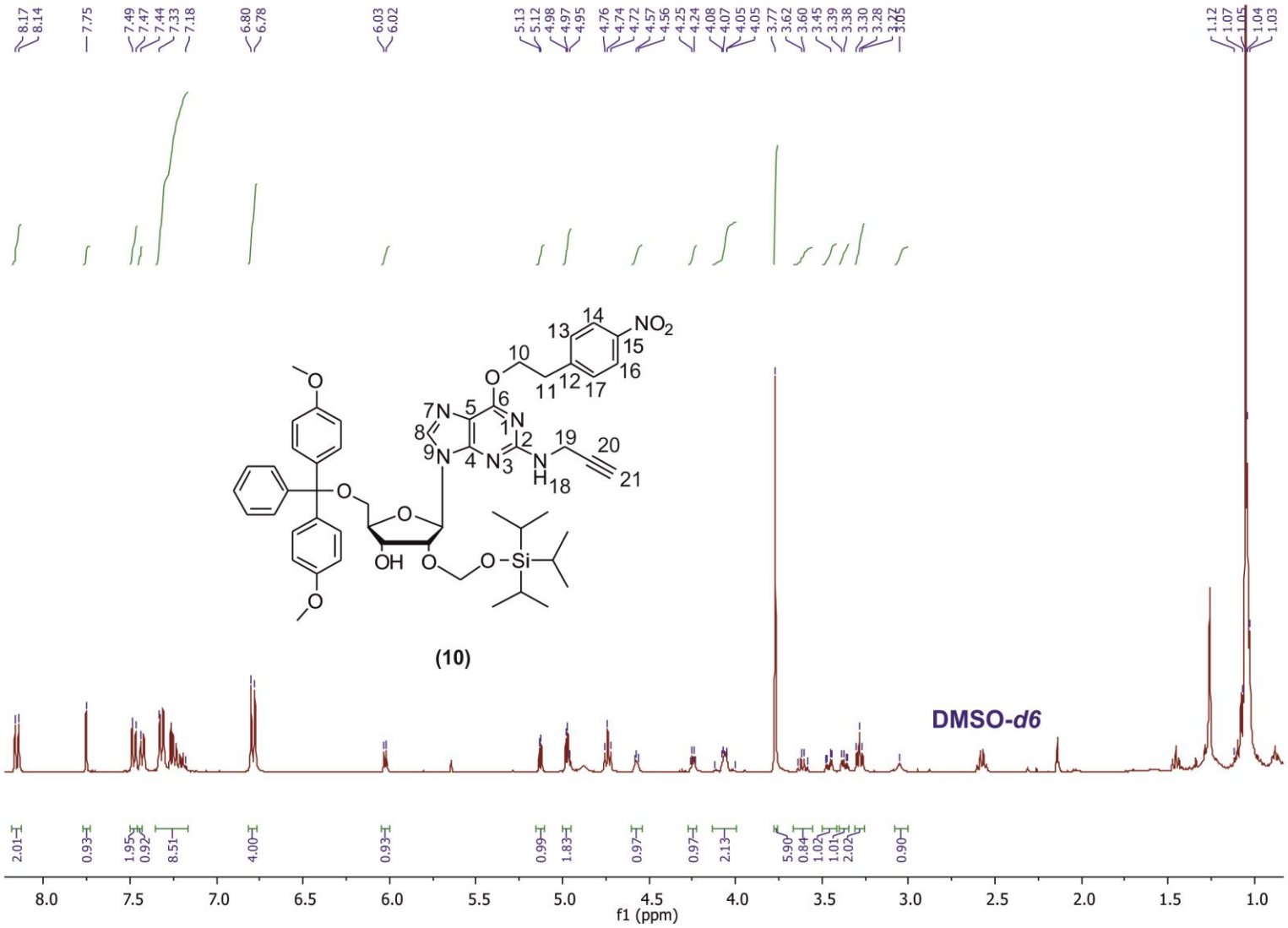
8.17
8.14
7.75
7.49
7.47
7.44
7.33
7.18
6.80
6.78
6.03
6.02
5.13
5.12
4.98
4.97
4.95
4.76
4.74
4.72
4.57
4.56
4.25
4.24
4.08
4.07
4.05
4.05
3.77
3.62
3.60
3.45
3.39
3.38
3.30
3.28
1.12
1.07
1.05
1.04
1.03
DMSO-d6
2.01
0.93
1.95
0.92
8.51
4.00
0.93
0.99
1.83
0.97
0.97
2.13
5.90
0.84
1.02
1.01
2.02
0.90
8.0
7.5
7.0
6.5
6.0
5.5
5.0
4.5
4.0
3.5
3.0
2.5
2.0
1.5
1.0
f1 (ppm)

(10)

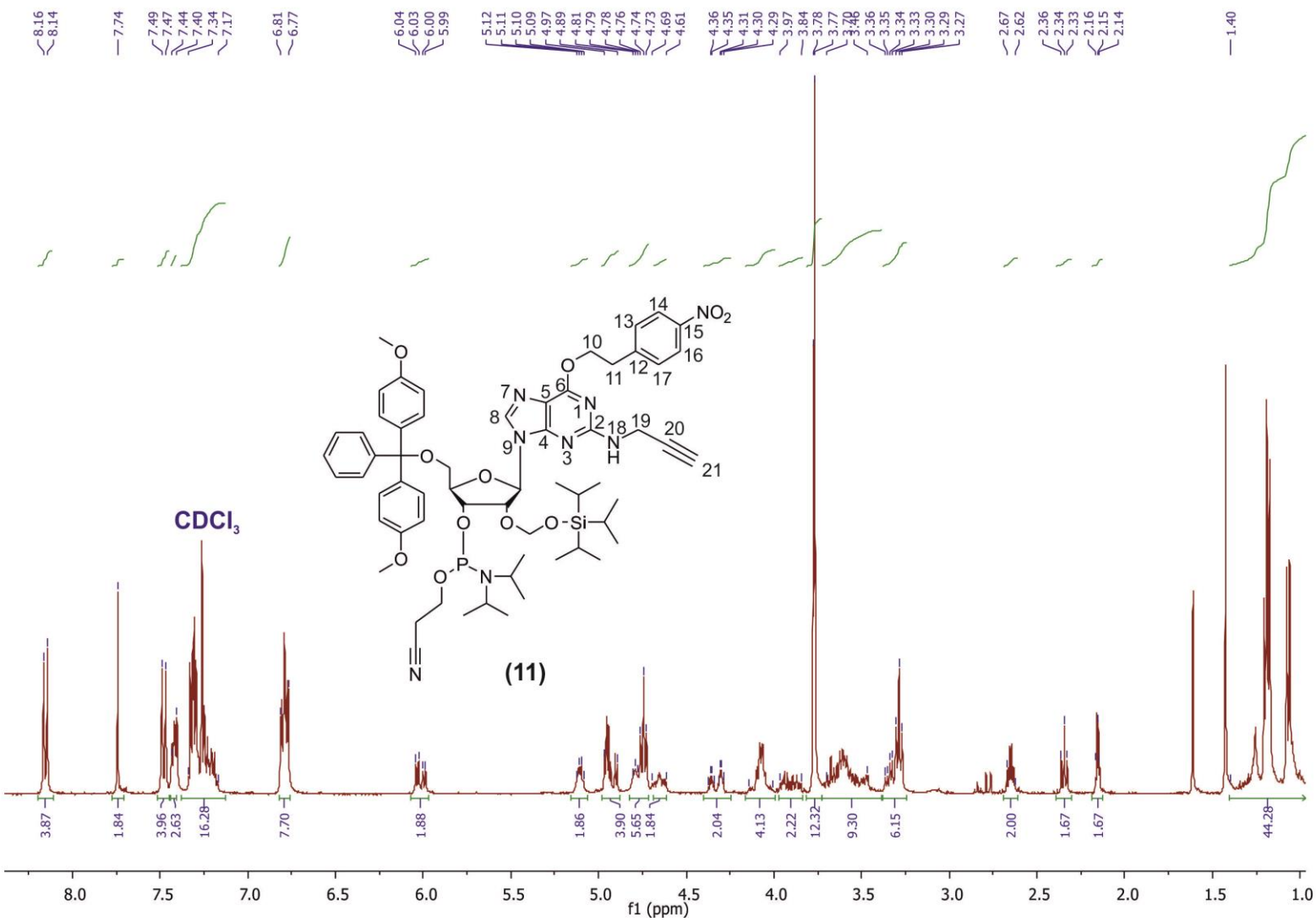
CDCl3
(11)
f1 (ppm)

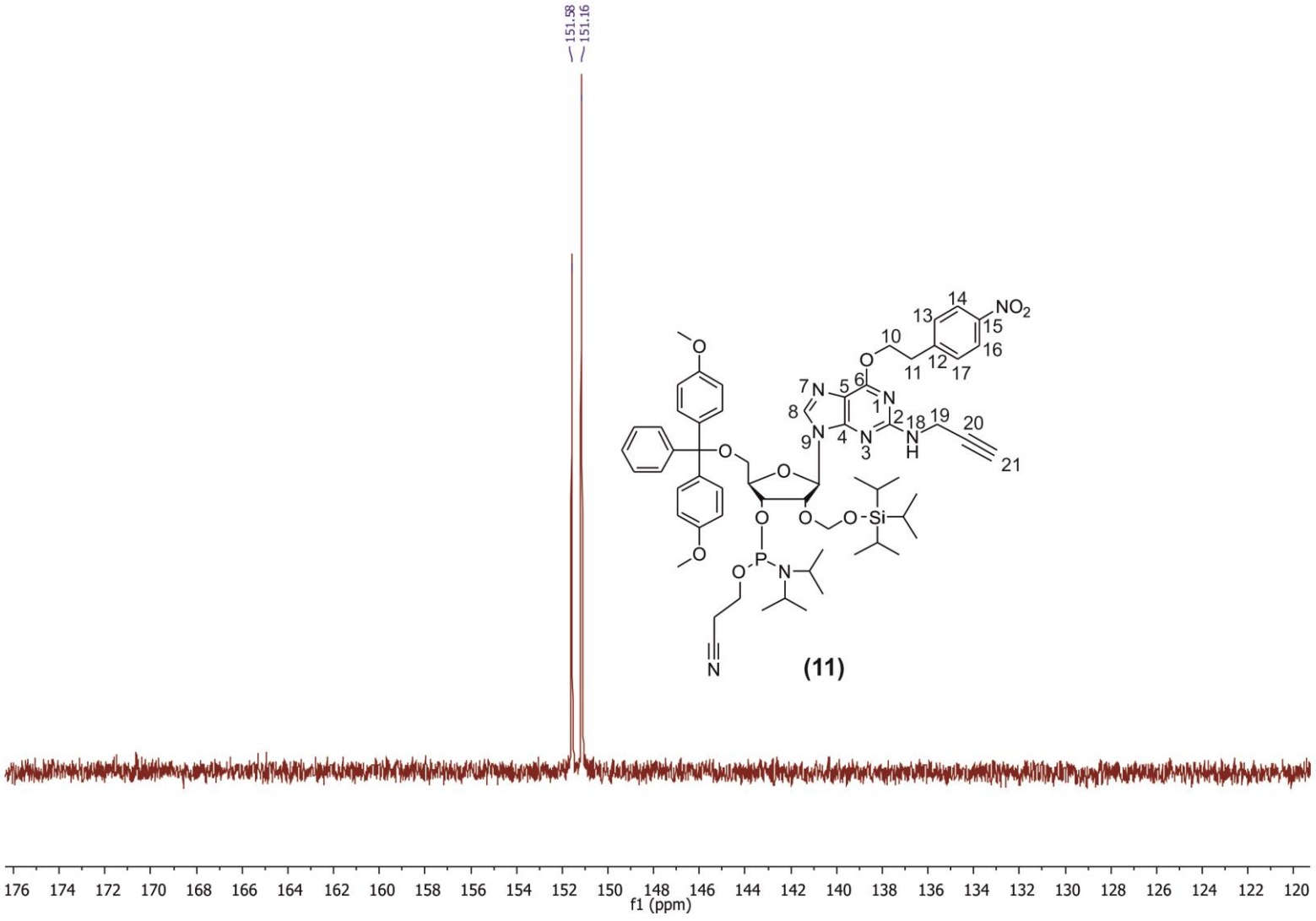
151.58
151.16
(11)
176 174 172 170 168 166 164 162 160 158 156 154 152 150 148 146 144 142 140 138 136 134 132 130 128 126 124 122 120
f1 (ppm)

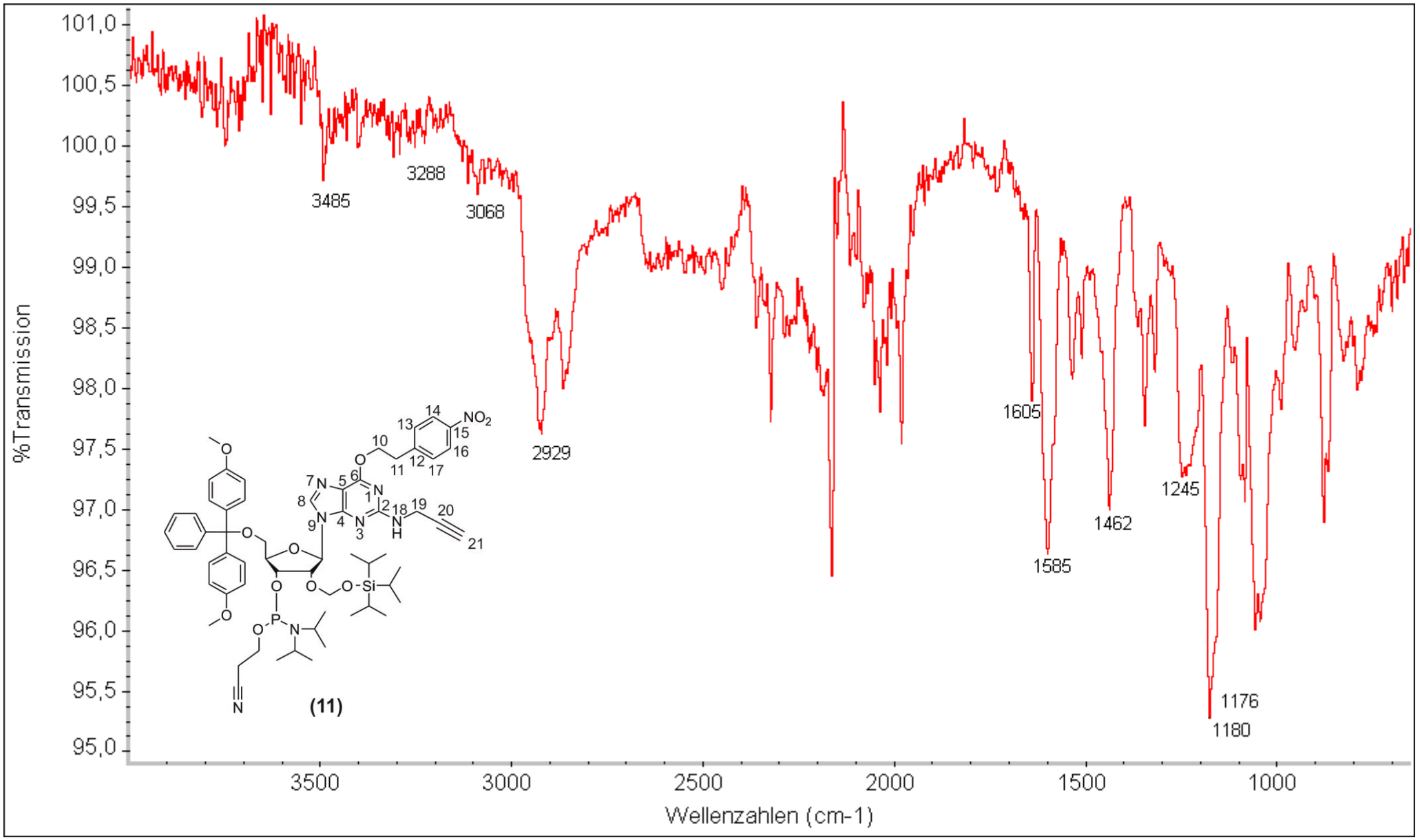
%Transmission
101,0
100,5
100,0
99,5
99,0
98,5
98,0
97,5
97,0
96,5
96,0
95,5
95,0
3500
3000
2500
2000
1500
1000
Wellenzahlen (cm-1)
3485
3288
3068
2929
1605
1585
1462
1245
1176
1180
(11)

XX

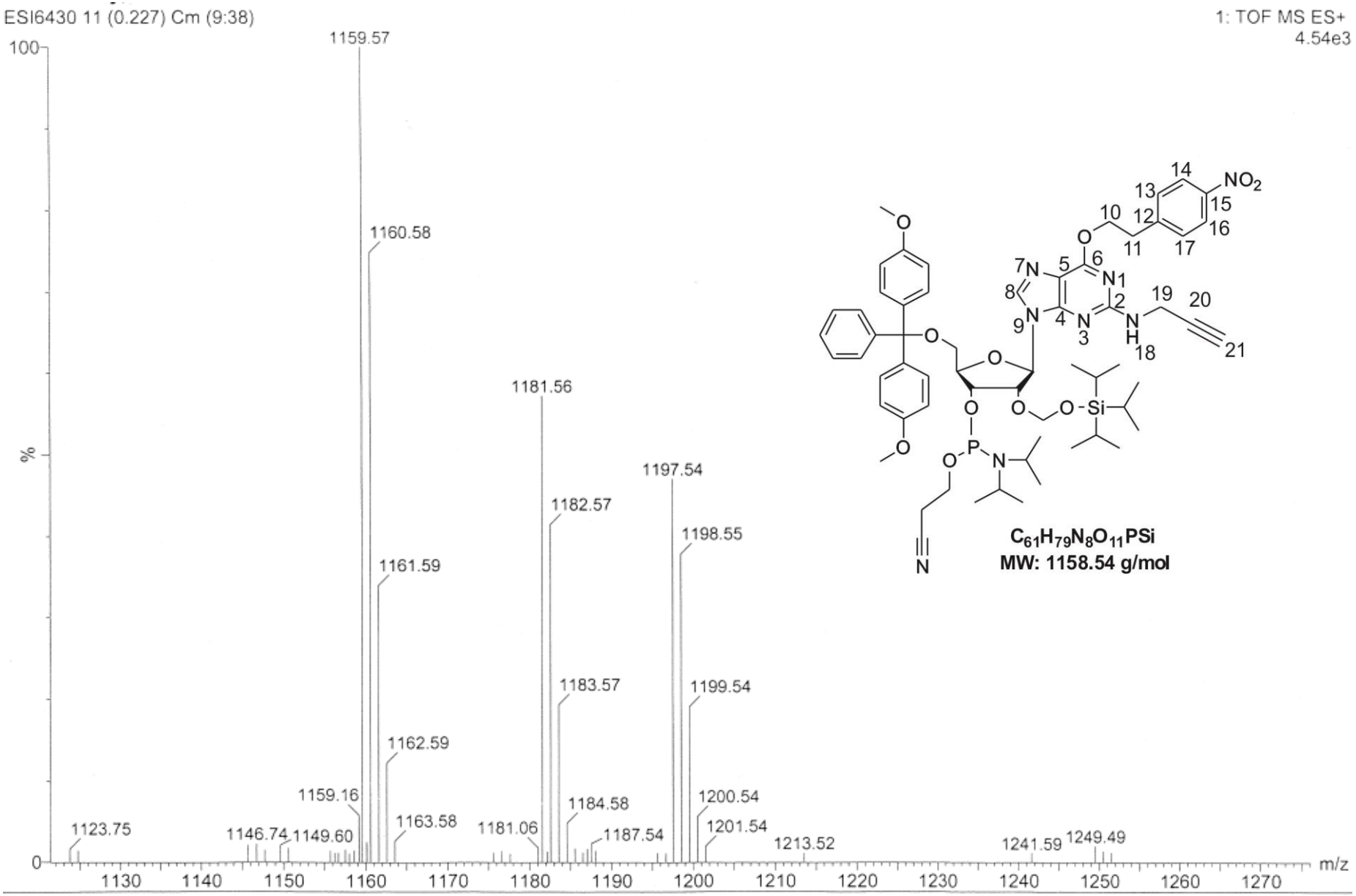
ESI6430 11 (0.227) Cm (9:38)
1: TOF MS ES+
4.54e3
100
%
0
1159.57
1160.58
1161.59
1162.59
1163.58
1181.56
1182.57
1183.57
1184.58
1187.54
1197.54
1198.55
1199.54
1200.54
1201.54
1159.16
1123.75
1146.74
1149.60
1181.06
1213.52
1241.59
1249.49
1130
1140
1150
1160
1170
1180
1190
1200
1210
1220
1230
1240
1250
1260
1270
m/z
C61H79N8O11PSi
MW: 1158.54 g/mol

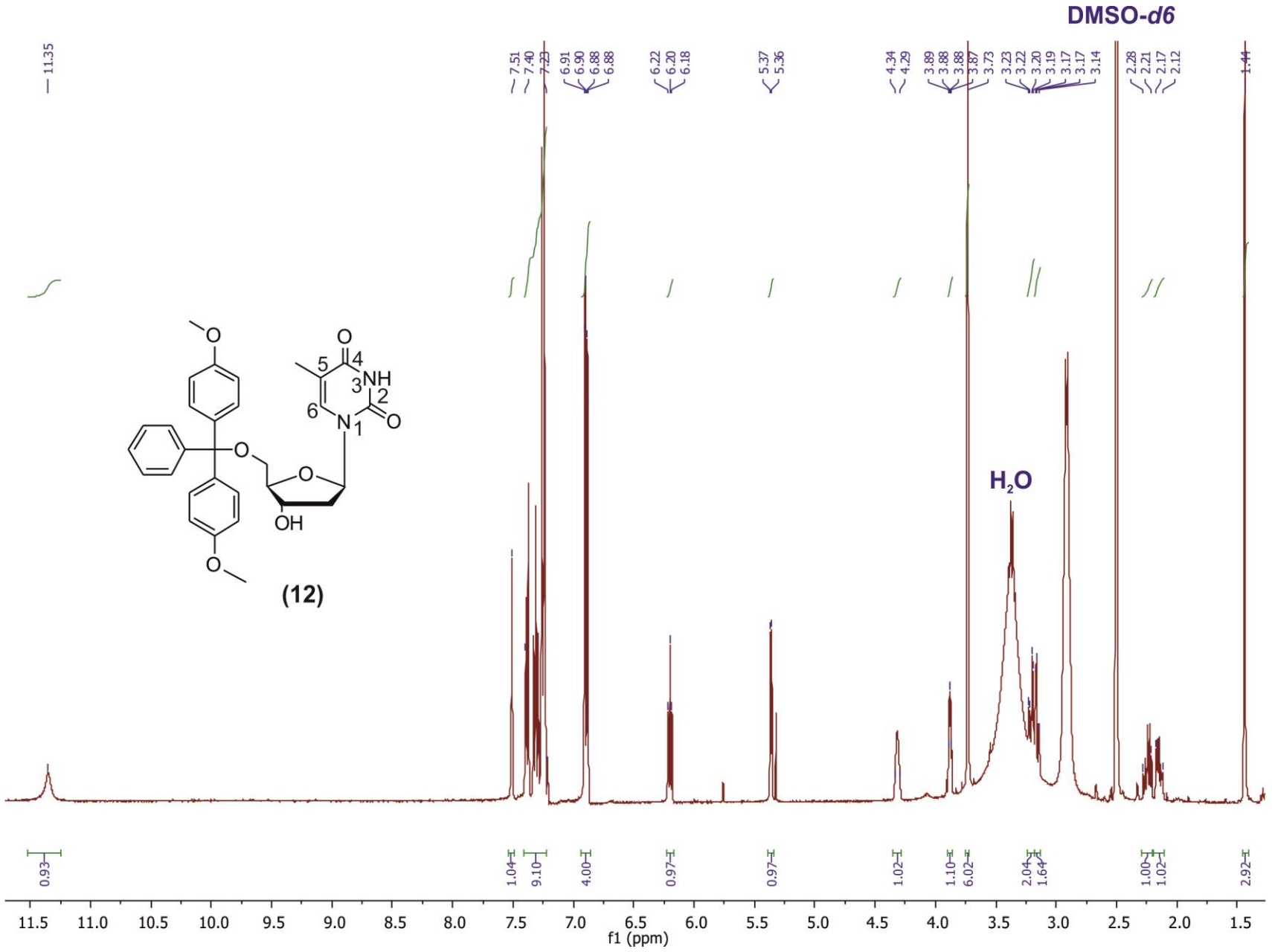
DMSO-d6
11.35
7.51
7.40
7.23
6.91
6.90
6.88
6.88
6.22
6.20
6.18
5.37
5.36
4.34
4.29
3.89
3.88
3.88
3.87
3.73
3.23
3.22
3.20
3.19
3.17
3.17
3.14
2.28
2.21
2.17
2.12
1.44
H2O
(12)
0.93
1.04
9.10
4.00
0.97
0.97
1.02
1.10
6.02
2.04
1.64
1.00
1.02
2.92
11.5
11.0
10.5
10.0
9.5
9.0
8.5
8.0
7.5
7.0
6.5
6.0
5.5
5.0
4.5
4.0
3.5
3.0
2.5
2.0
1.5
f1 (ppm)

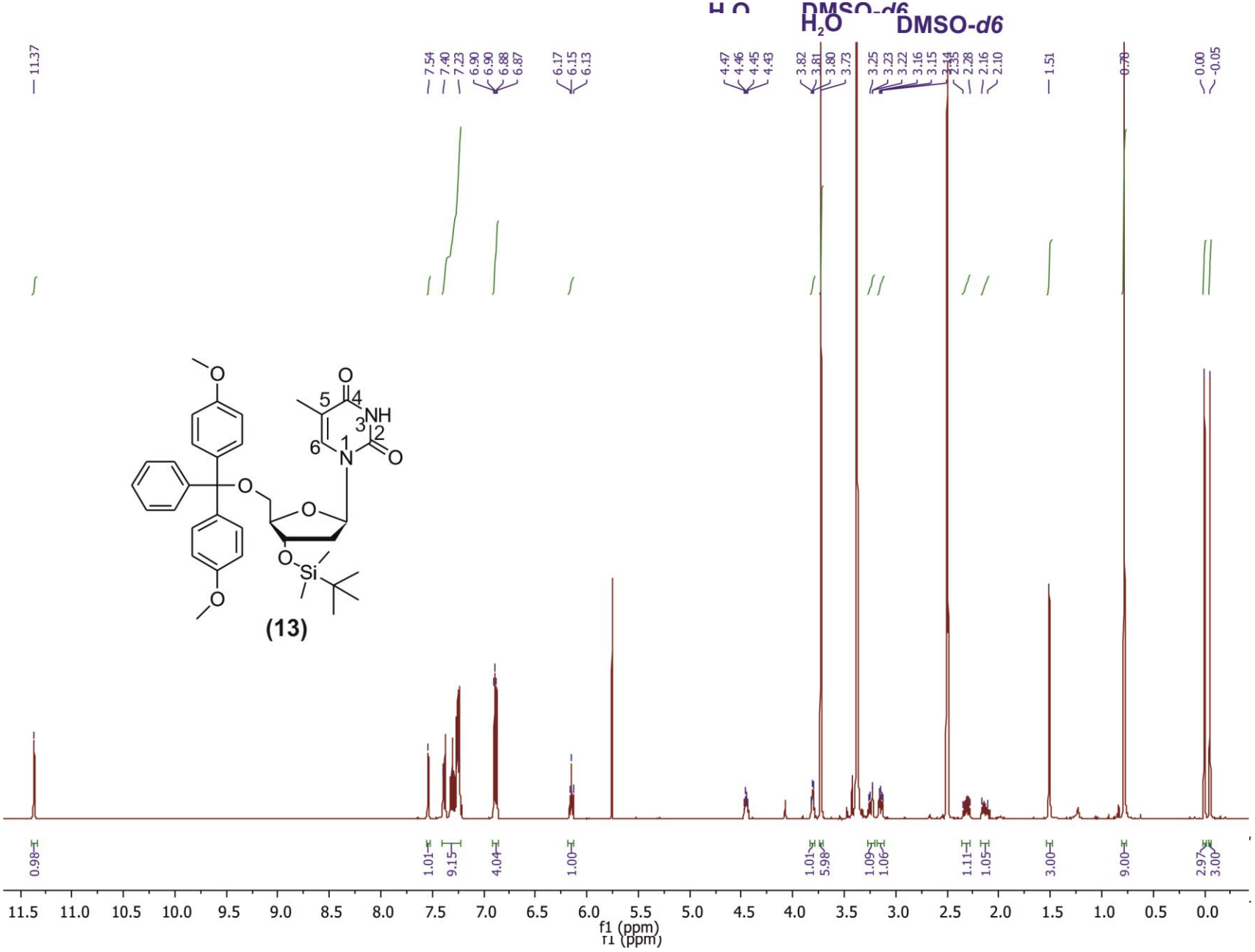
H2O
DMSO-d6
(13)
f1 (ppm)

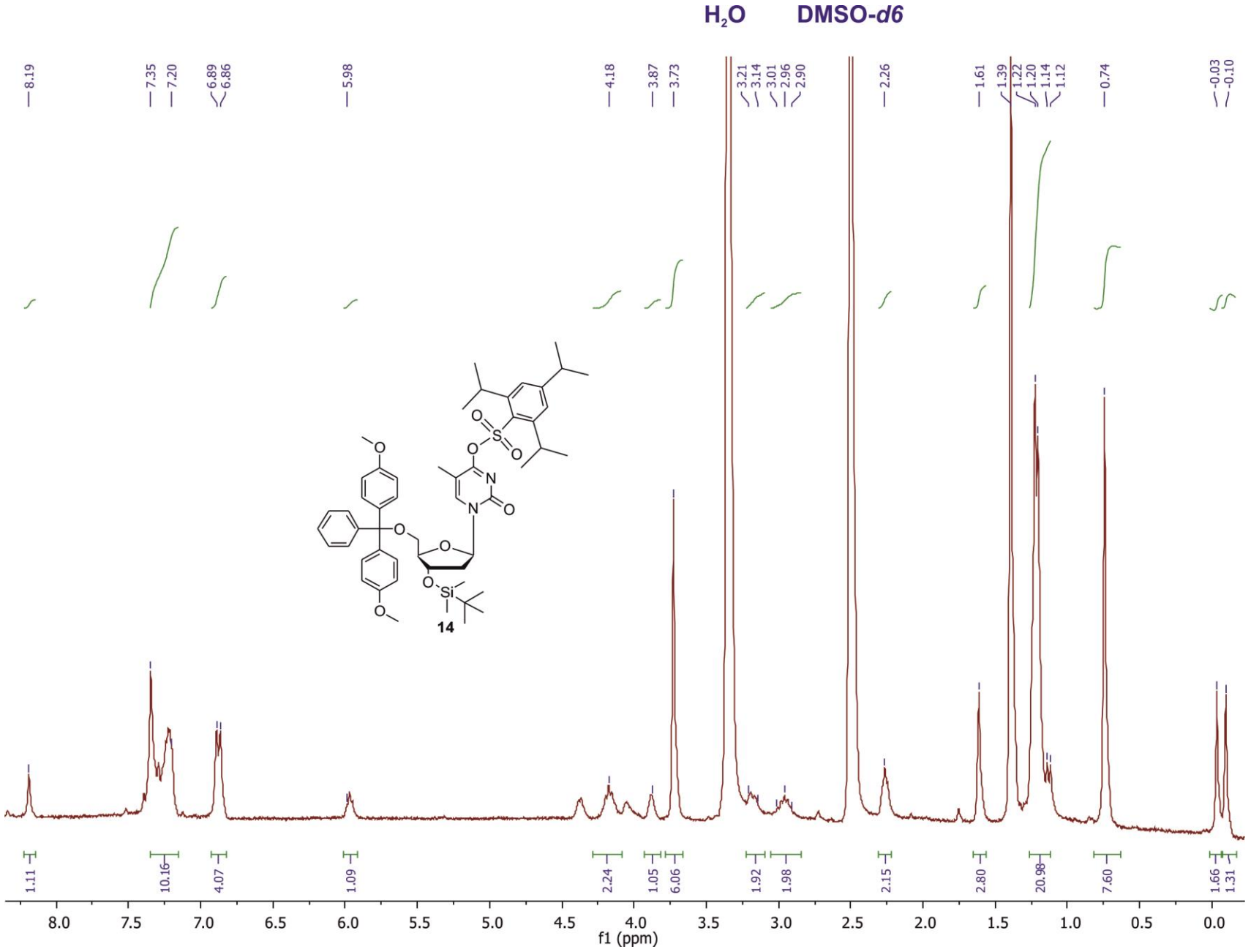
H2O
DMSO-d6
8.19
7.35
7.20
6.89
6.86
5.98
4.18
3.87
3.73
3.21
3.14
3.01
2.96
2.90
2.26
1.61
1.39
1.22
1.20
1.14
1.12
0.74
-0.03
-0.10
14
1.11
10.16
4.07
1.09
2.24
1.05
6.06
1.92
1.98
2.15
2.80
20.98
7.60
1.66
1.31
8.0
7.5
7.0
6.5
6.0
5.5
5.0
4.5
4.0
3.5
3.0
2.5
2.0
1.5
1.0
0.5
0.0
f1 (ppm)

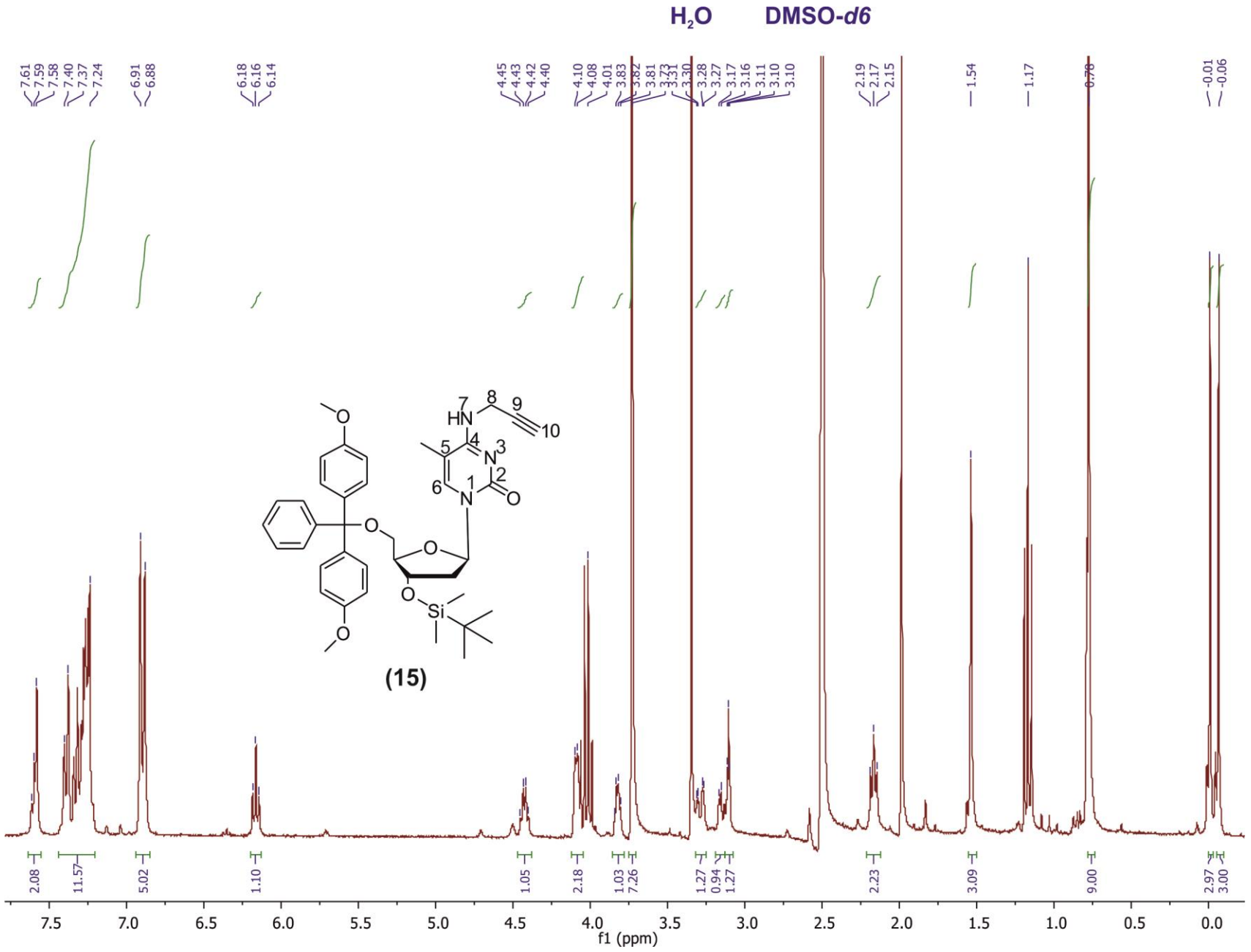
H2O
DMSO-d6
(15)
f1 (ppm)

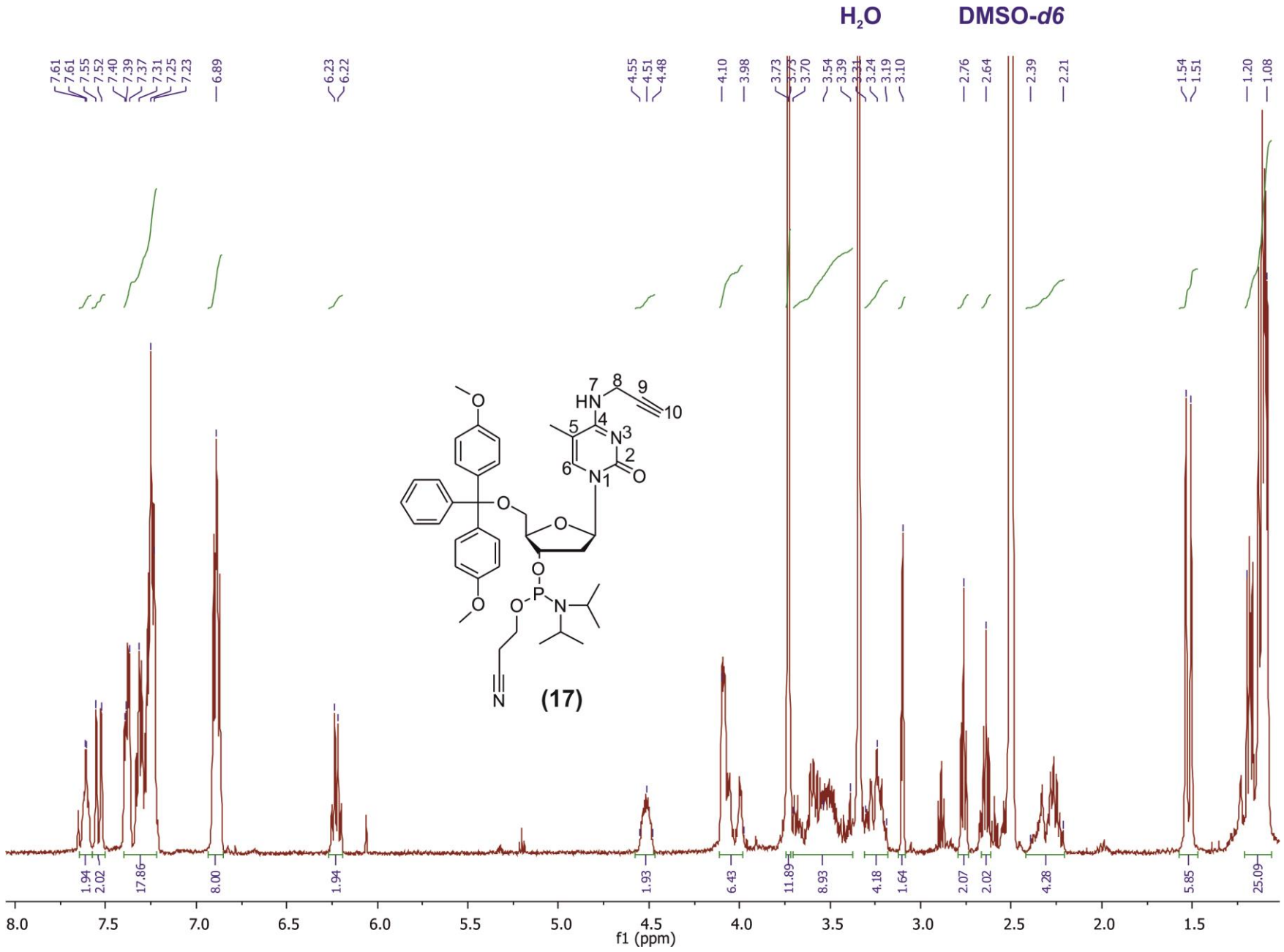
H2O
DMSO-d6
7.61
7.61
7.55
7.52
7.40
7.39
7.37
7.31
7.25
7.23
6.89
6.23
6.22
4.55
4.51
4.48
4.10
3.98
3.73
3.70
3.54
3.39
3.31
3.24
3.19
3.10
2.76
2.64
2.39
2.21
1.54
1.51
1.20
1.08
1.94
2.02
17.86
8.00
1.94
1.93
6.43
11.89
8.93
4.18
1.64
2.07
2.02
4.28
5.85
25.09
8.0
7.5
7.0
6.5
6.0
5.5
5.0
4.5
4.0
3.5
3.0
2.5
2.0
1.5
f1 (ppm)
(17)

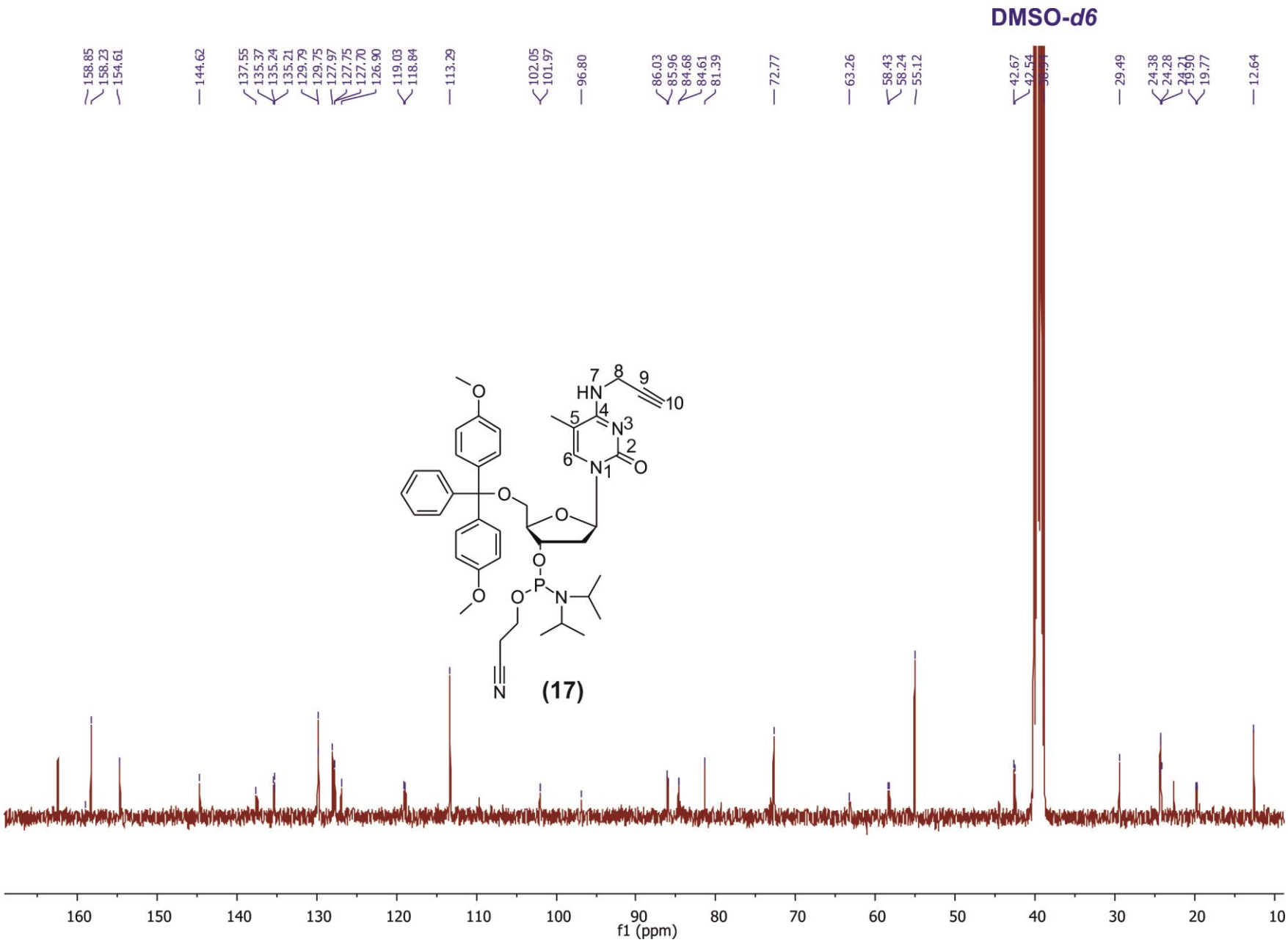
DMSO-d6
158.85
158.23
154.61
144.62
137.55
135.37
135.24
135.21
129.79
129.75
127.97
127.75
127.70
126.90
119.03
118.84
113.29
102.05
101.97
96.80
86.03
85.96
84.68
84.61
81.39
72.77
63.26
58.43
58.24
55.12
42.67
42.54
29.49
24.38
24.28
19.77
12.64
(17)
f1 (ppm)

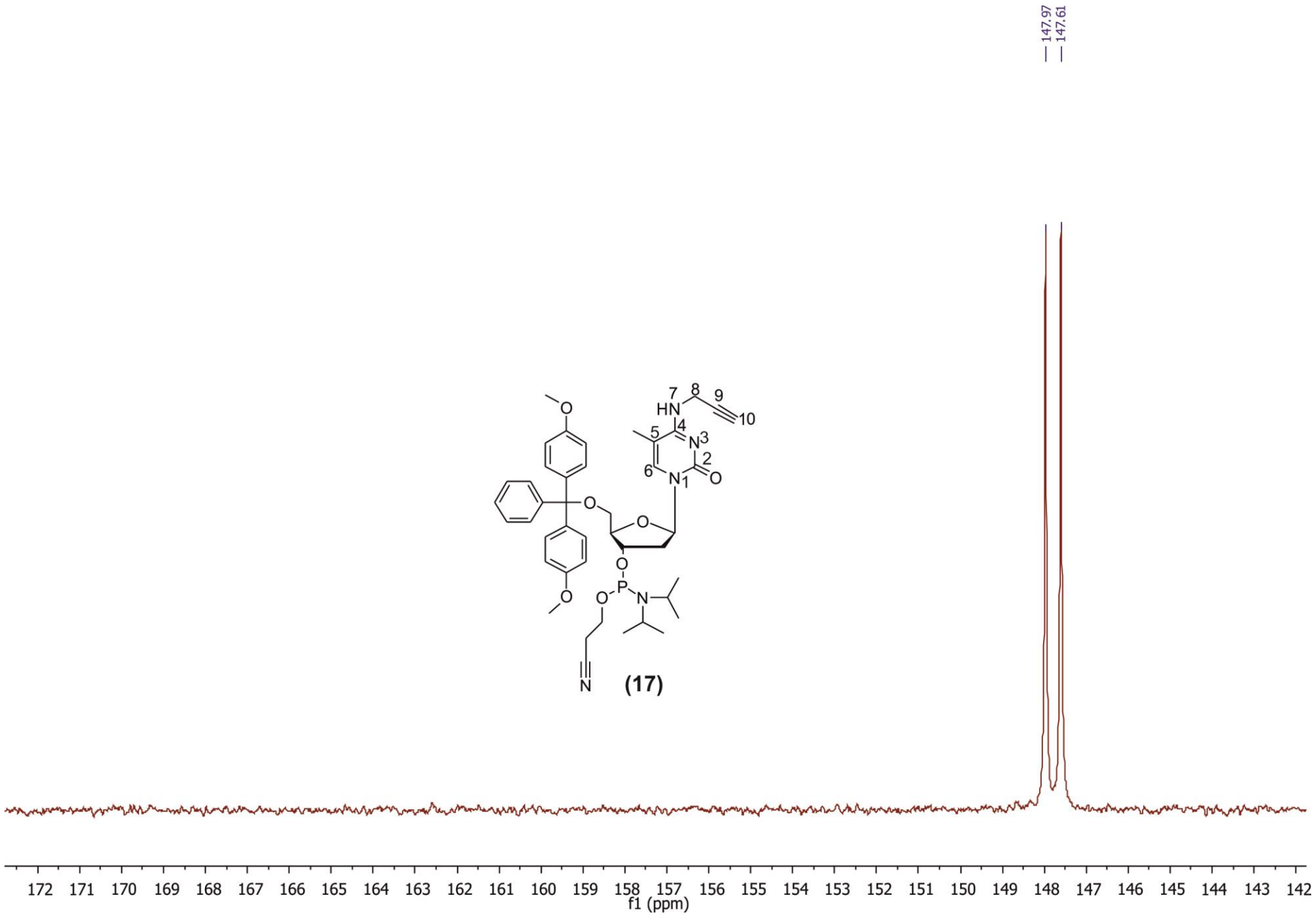
147.97
147.61
(17)
172 171 170 169 168 167 166 165 164 163 162 161 160 159 158 157 156 155 154 153 152 151 150 149 148 147 146 145 144 143 142
f1 (ppm)

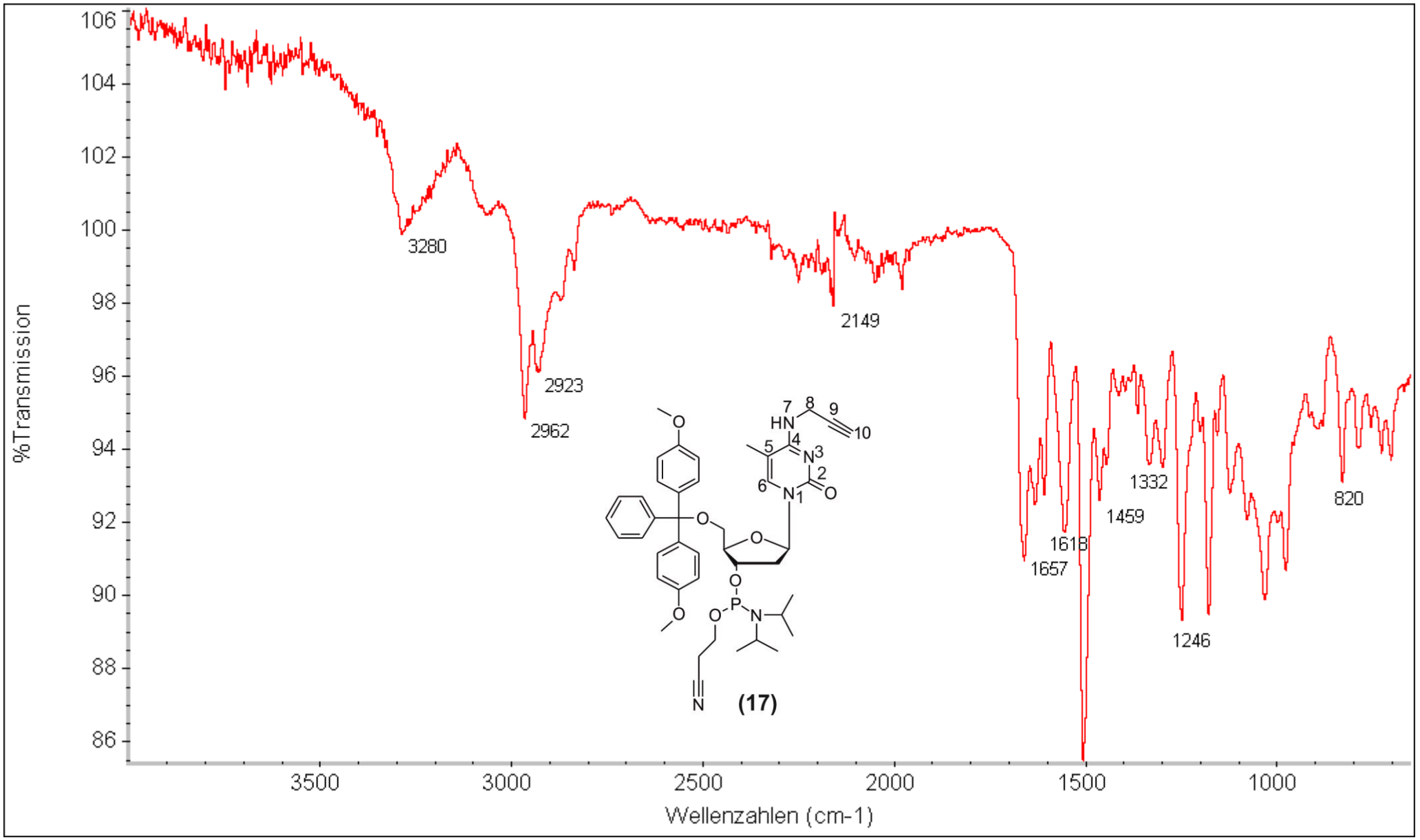
%Transmission
106
104
102
100
98
96
94
92
90
88
86
3500
3000
2500
2000
1500
1000
Wellenzahlen (cm-1)
3280
2962
2923
2149
1657
1618
1459
1332
1246
820
(17)

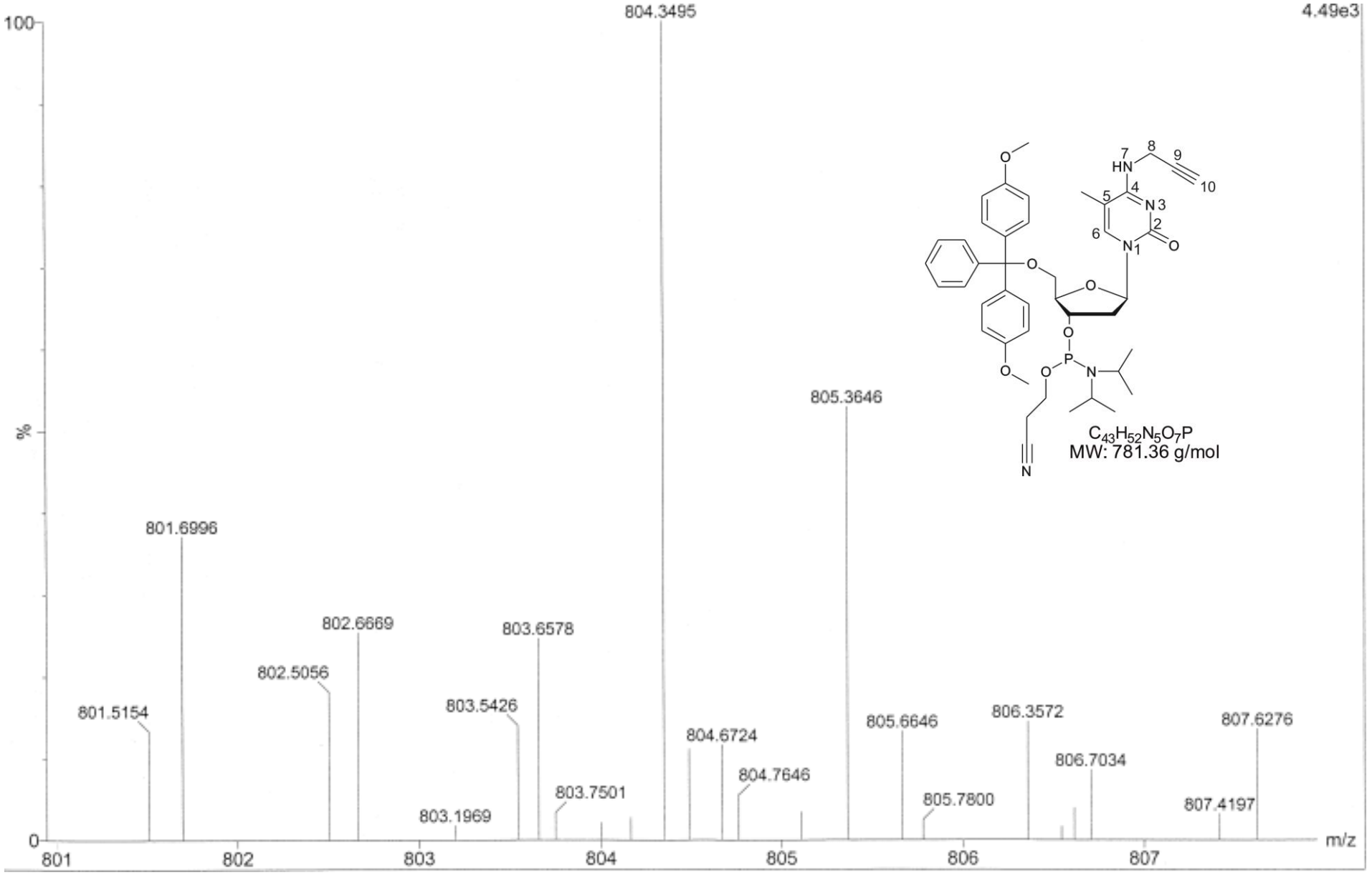
804.3495
4.49e3
100
%
0
801.6996
802.6669
803.6578
802.5056
801.5154
803.5426
804.6724
805.3646
805.6646
806.3572
807.6276
806.7034
804.7646
803.7501
805.7800
807.4197
803.1969
801
802
803
804
805
806
807
m/z
C43H52N5O7P
MW: 781.36 g/mol

XXX

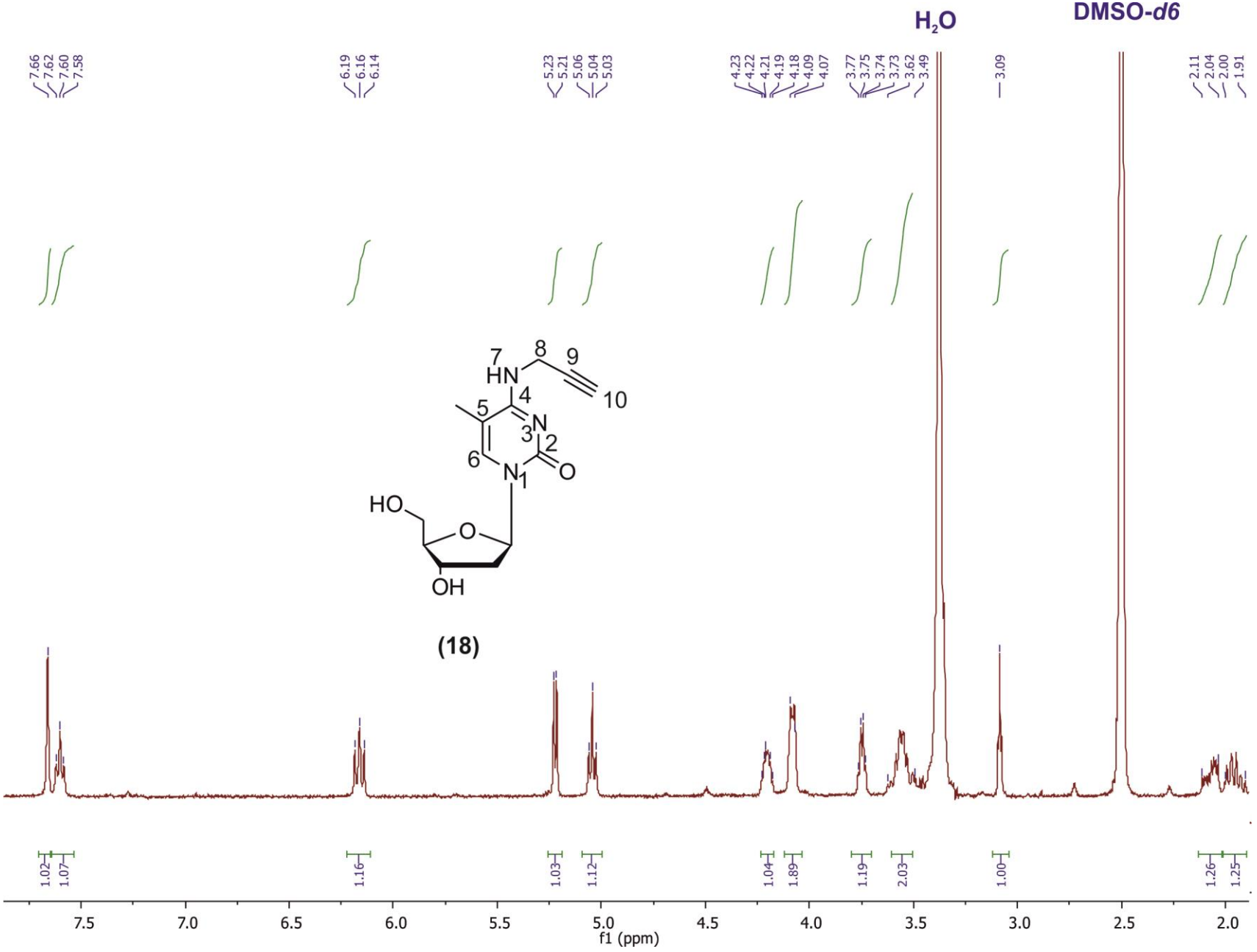
H2O
DMSO-d6
7.66
7.62
7.60
7.58
6.19
6.16
6.14
5.23
5.21
5.06
5.04
5.03
4.23
4.22
4.21
4.19
4.18
4.09
4.07
3.77
3.75
3.74
3.73
3.62
3.49
3.09
2.11
2.04
2.00
1.91
HO
O
OH
HN
N
O
1.02
1.07
1.16
1.03
1.12
1.04
1.89
1.19
2.03
1.00
1.26
1.25
7.5
7.0
6.5
6.0
5.5
5.0
4.5
4.0
3.5
3.0
2.5
2.0
f1 (ppm)

(18)

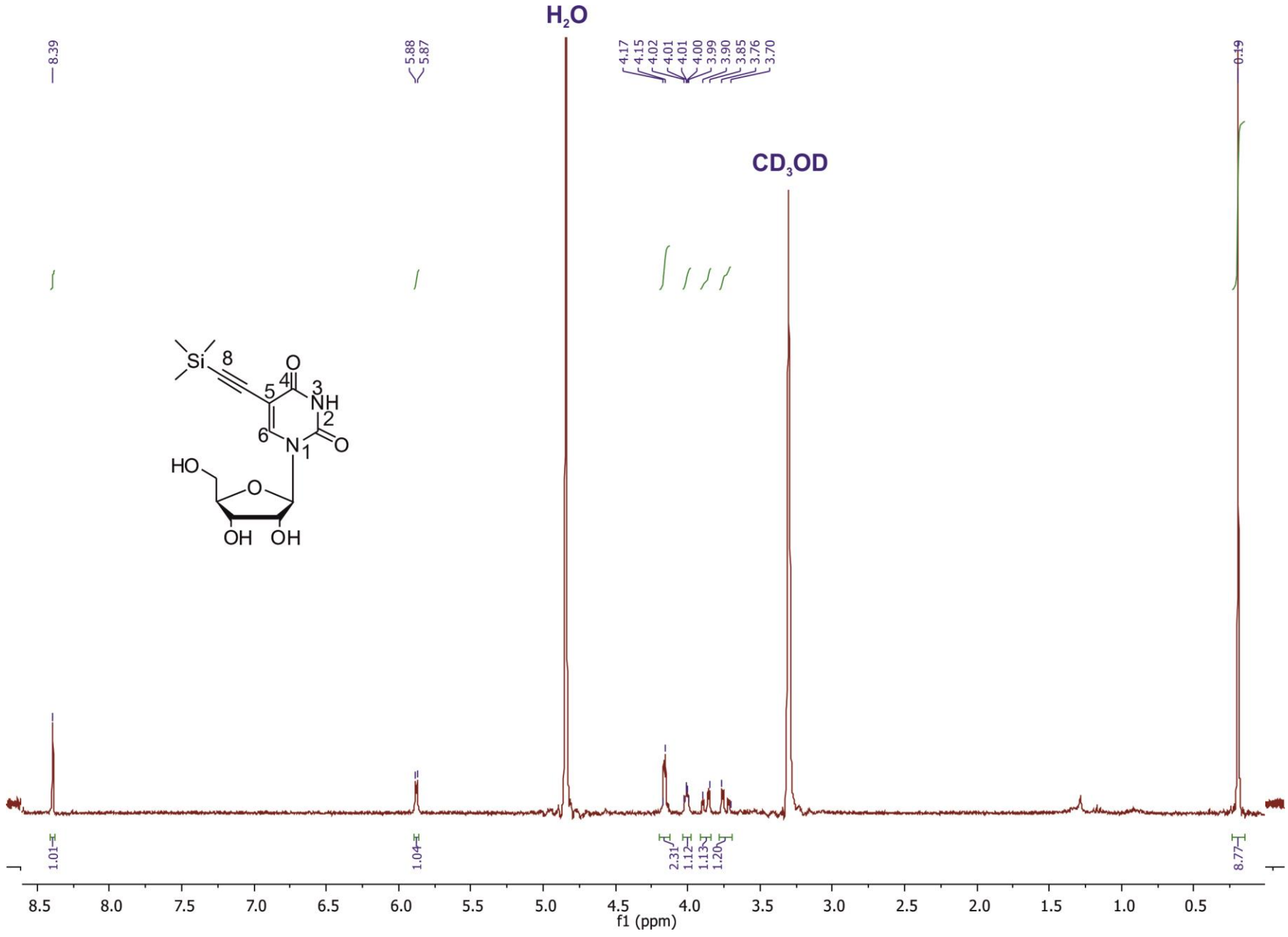
H2O
CD3OD
8.39
5.88
5.87
4.17
4.15
4.02
4.01
4.01
4.00
3.99
3.90
3.85
3.76
3.70
0.19
Si
8
O
4
5
3
NH
2
6
N
1
O
HO
O
OH
OH
1.01
1.04
2.31
1.12
1.13
1.20
8.77
8.5
8.0
7.5
7.0
6.5
6.0
5.5
5.0
4.5
4.0
3.5
3.0
2.5
2.0
1.5
1.0
0.5
f1 (ppm)

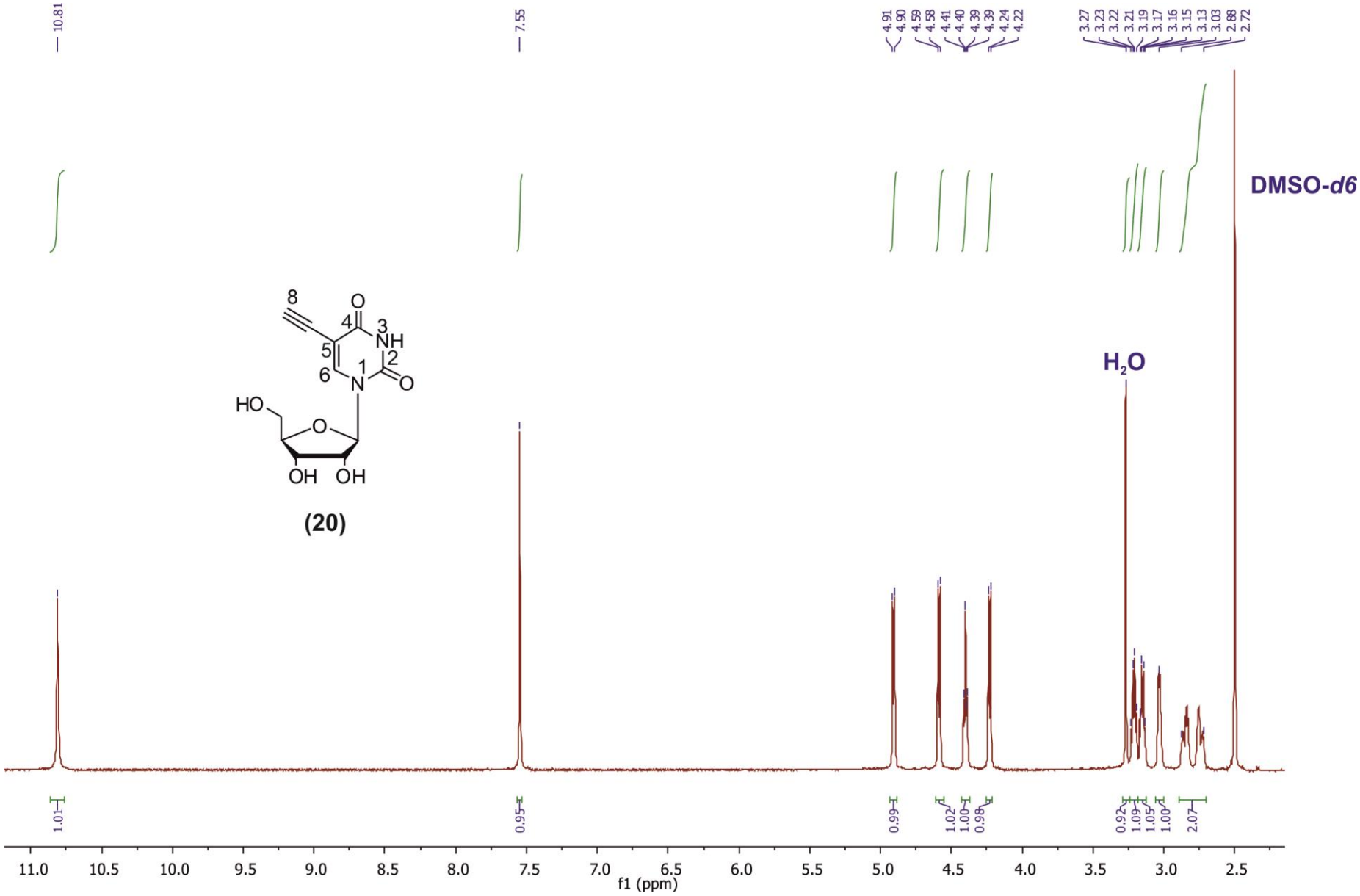
10.81
7.55
4.91
4.90
4.59
4.58
4.41
4.40
4.39
4.39
4.24
4.22
3.27
3.23
3.22
3.21
3.19
3.17
3.16
3.15
3.13
3.03
2.88
2.72
DMSO-d6
H2O
8
O
4
3
NH
5
2
6
1
N
O
HO
O
OH
OH
(20)
1.01
0.95
0.99
1.02
1.00
0.98
0.92
1.09
1.05
1.00
2.07
11.0
10.5
10.0
9.5
9.0
8.5
8.0
7.5
7.0
6.5
6.0
5.5
5.0
4.5
4.0
3.5
3.0
2.5
f1 (ppm)

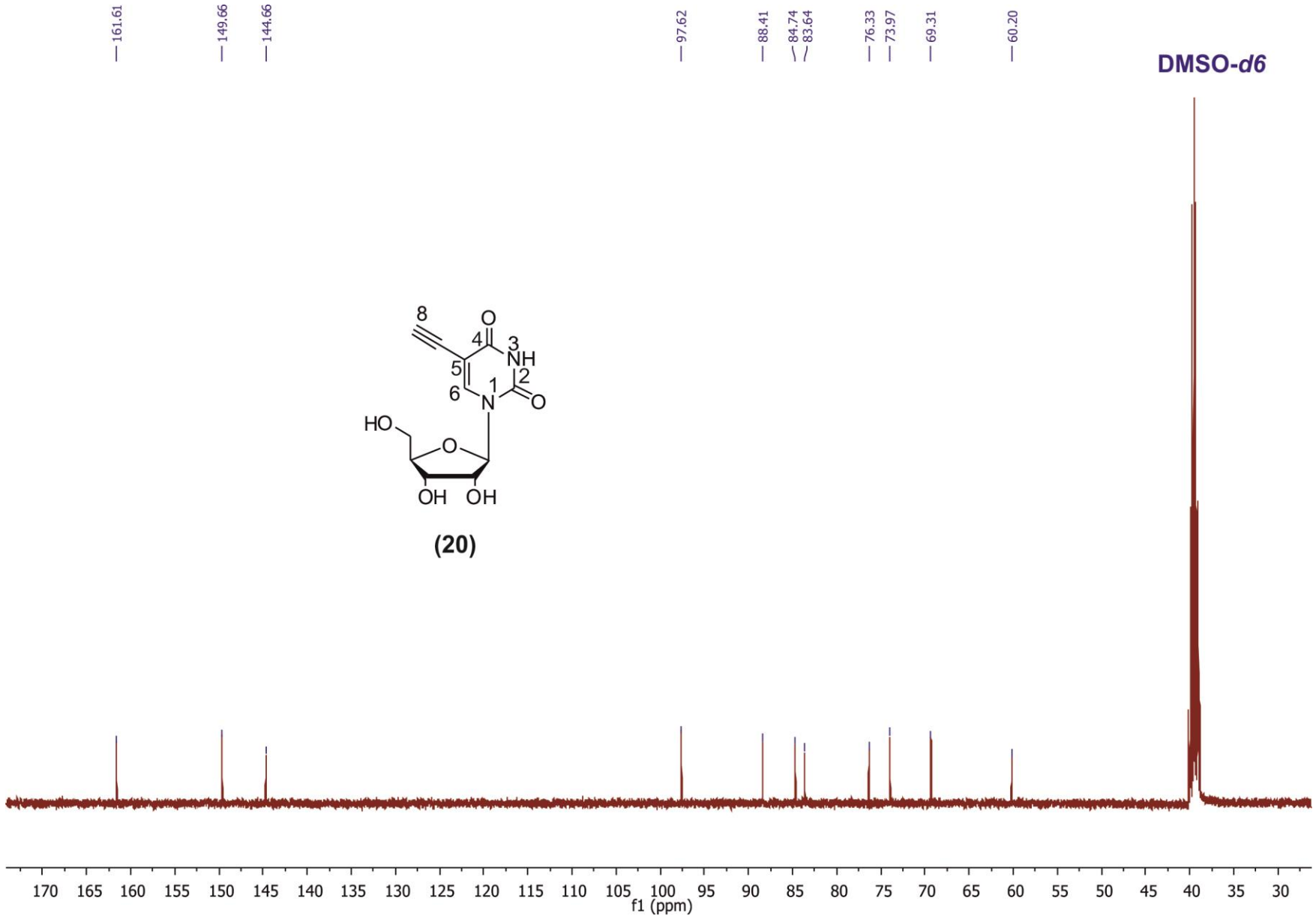
161.61
149.66
144.66
97.62
88.41
84.74
83.64
76.33
73.97
69.31
60.20
DMSO-d6
8
O
4
3
NH
5
2
6
1
N
O
HO
O
OH
OH
f1 (ppm)

(20)

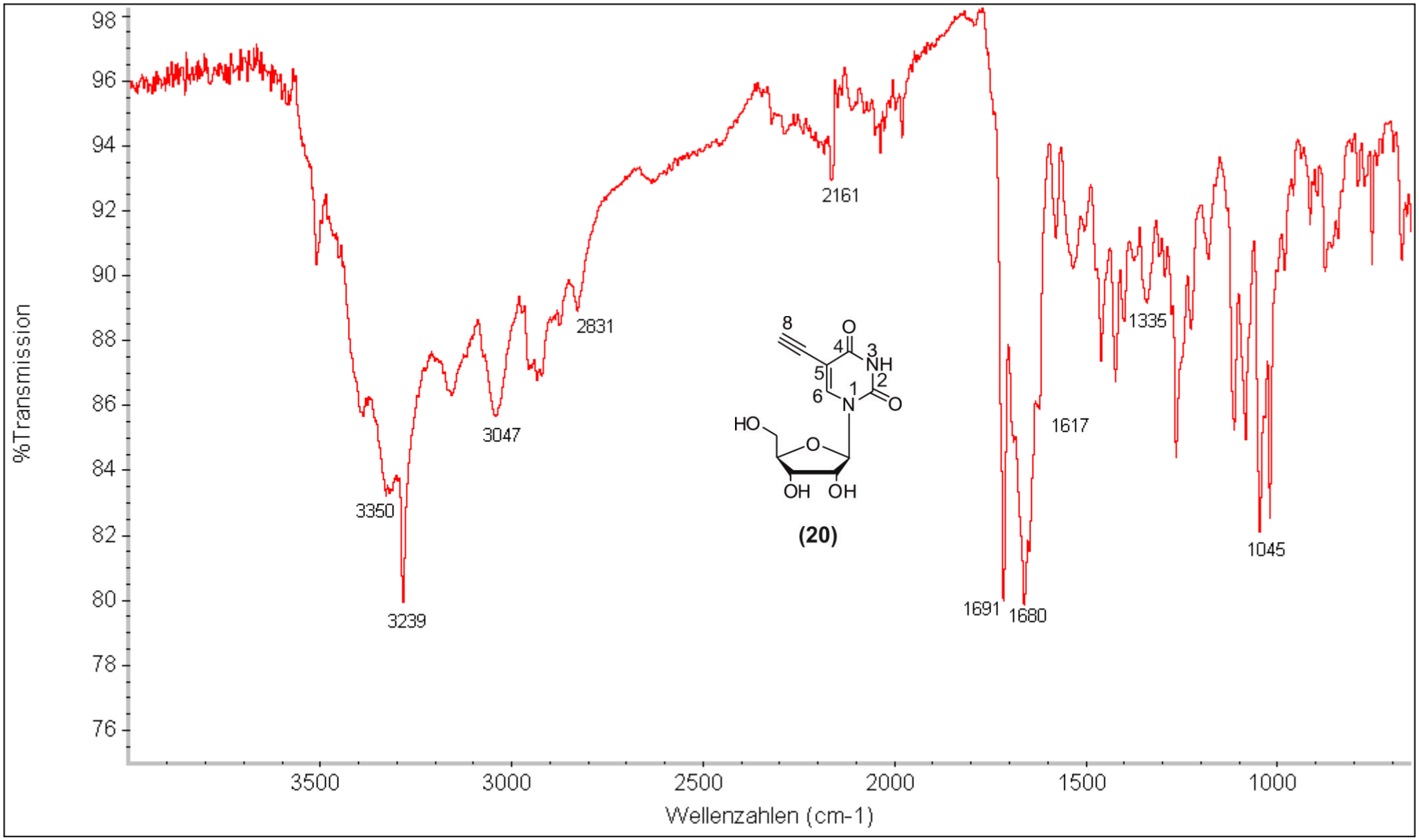
%Transmission
98
96
94
92
90
88
86
84
82
80
78
76
3500
3000
2500
2000
1500
1000
Wellenzahlen (cm-1)
3350
3239
3047
2831
2161
1691
1680
1617
1335
1045
8
O
4
3
NH
5
2
6
1
N
O
HO
O
OH
OH

(20)

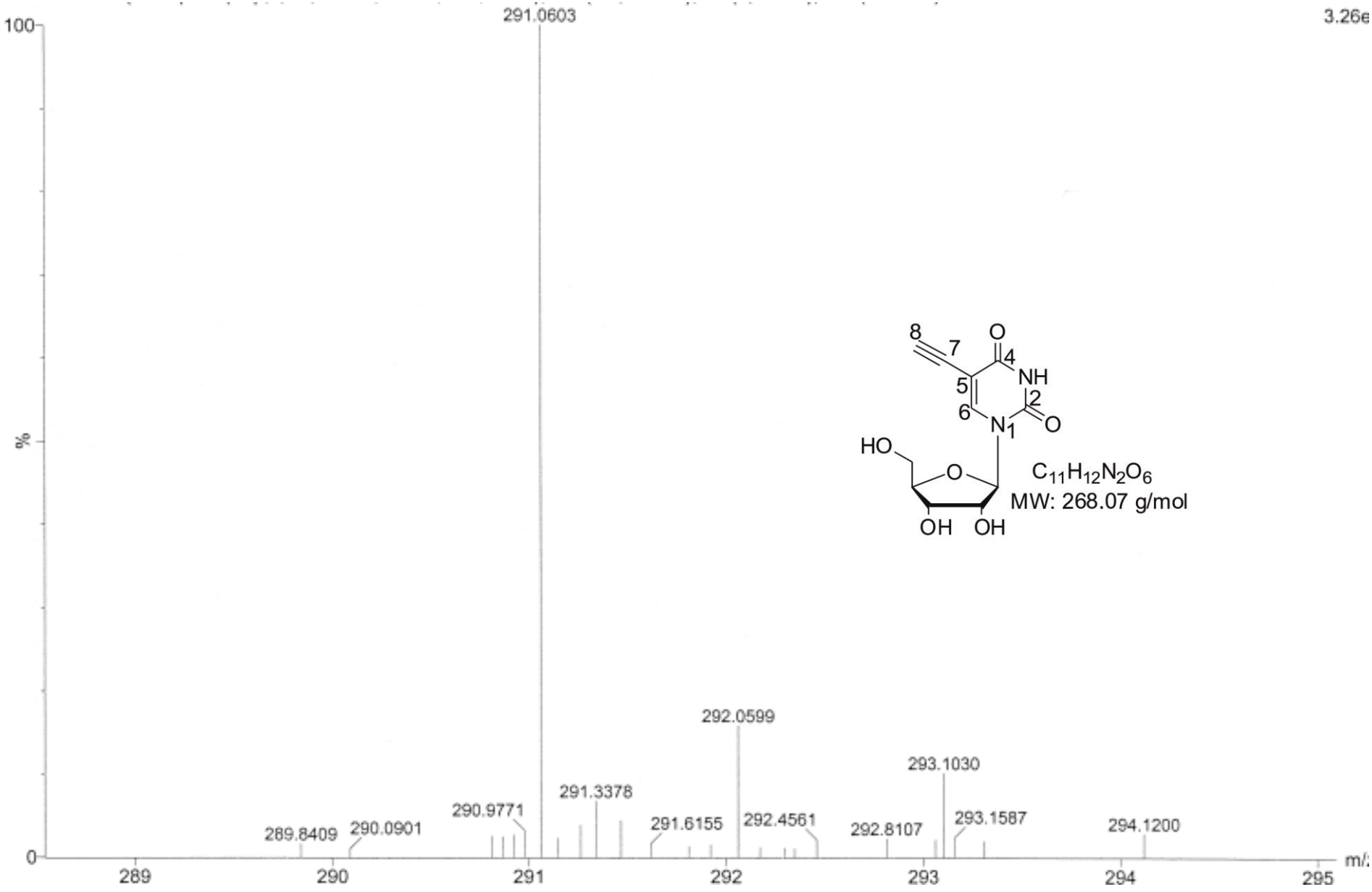
291.0603
3.26e
100
%
0
289.8409
290.0901
290.9771
291.3378
291.6155
292.0599
292.4561
292.8107
293.1030
293.1587
294.1200
289
290
291
292
293
294
295
m/
8
7
O
4
NH
5
2
6
N1
O
HO
O
OH
OH
C11H12N2O6
MW: 268.07 g/mol

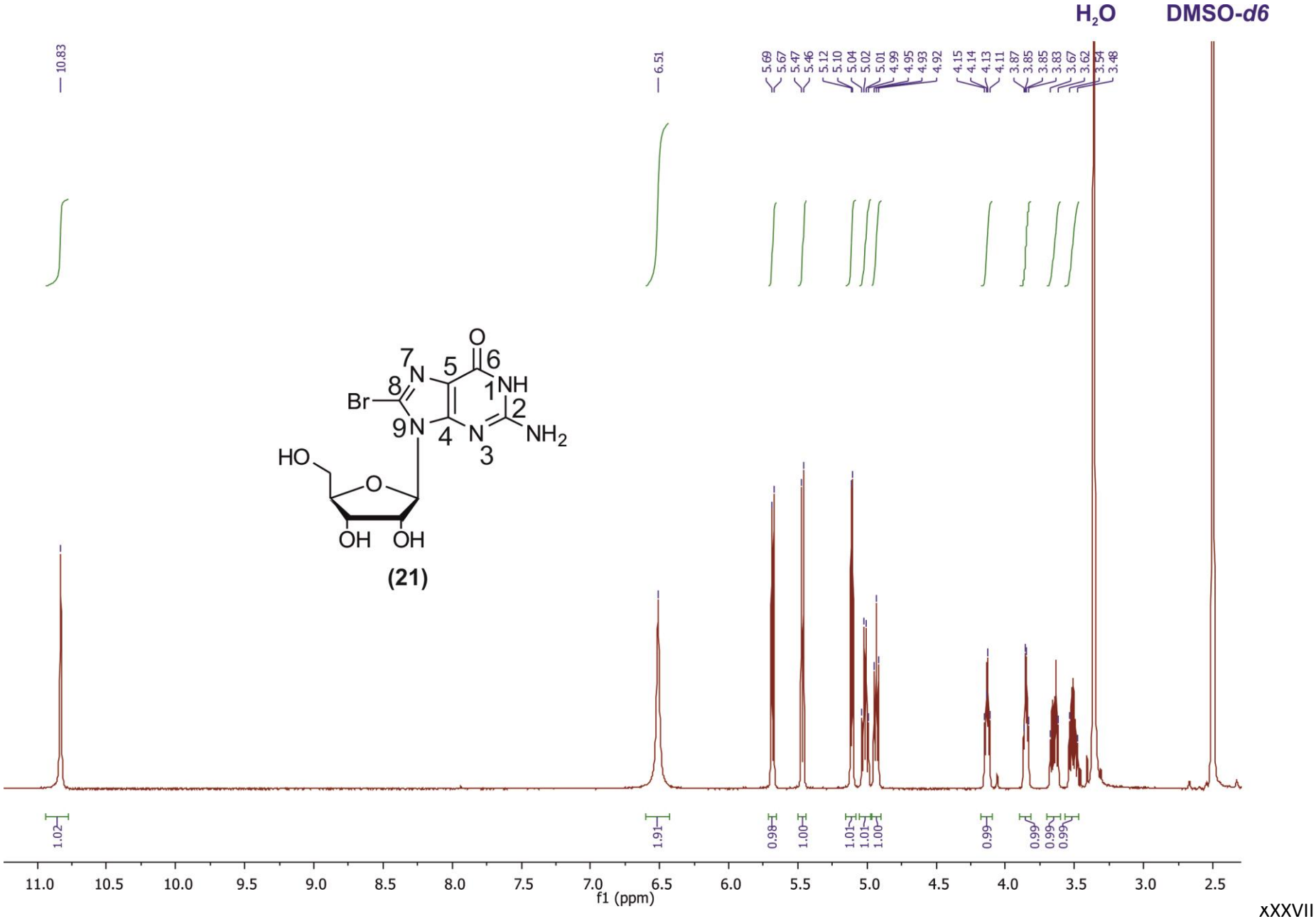
H2O
DMSO-d6
10.83
6.51
5.69
5.67
5.47
5.46
5.12
5.10
5.04
5.02
5.01
4.99
4.95
4.93
4.92
4.15
4.14
4.13
4.11
3.87
3.85
3.85
3.83
3.67
3.62
3.54
3.48
1.02
1.91
0.98
1.00
1.01
1.01
1.00
0.99
0.99
0.99
0.99
11.0
10.5
10.0
9.5
9.0
8.5
8.0
7.5
7.0
6.5
6.0
5.5
5.0
4.5
4.0
3.5
3.0
2.5
f1 (ppm)

(21)

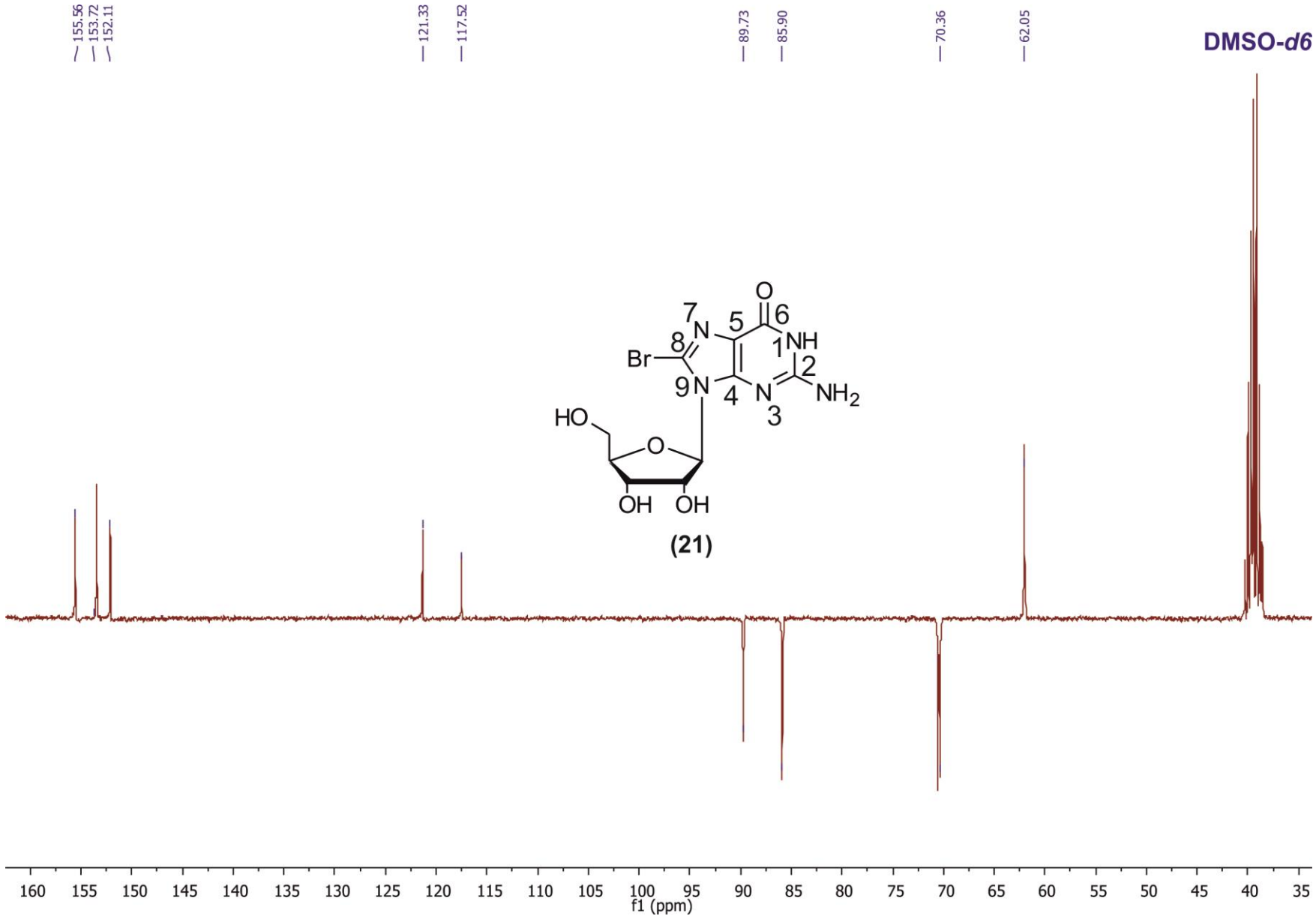
155.56
153.72
152.11
121.33
117.52
89.73
85.90
70.36
62.05
DMSO-d6
O
7
N
5
6
8
1NH
Br
2
9N
4
N
NH2
3
HO
O
OH
OH
(21)
160
155
150
145
140
135
130
125
120
115
110
105
100
95
90
85
80
75
70
65
60
55
50
45
40
35
f1 (ppm)

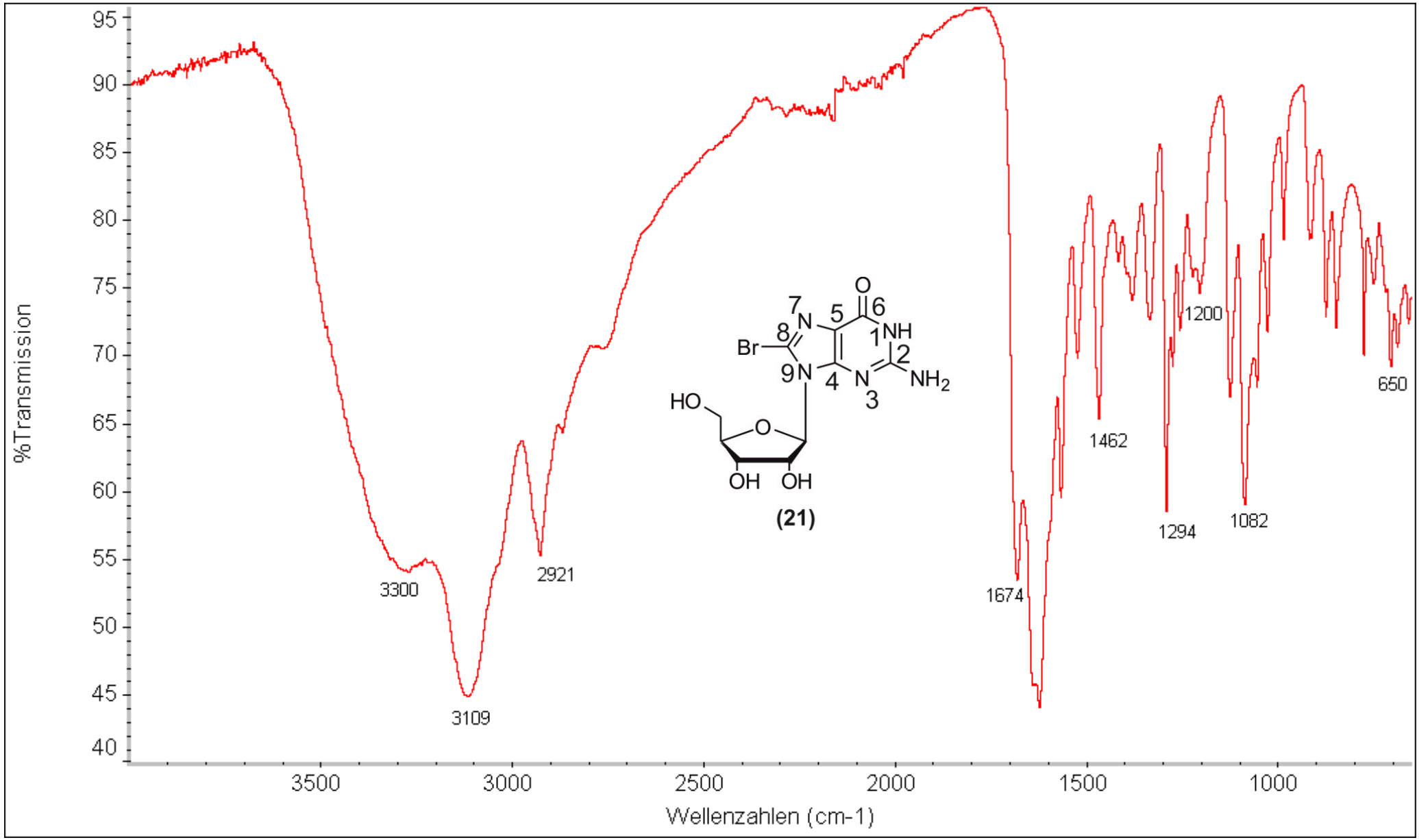
%Transmission
95
90
85
80
75
70
65
60
55
50
45
40
3500
3000
2500
2000
1500
1000
Wellenzahlen (cm-1)
3300
3109
2921
1674
1462
1294
1200
1082
650
Br
HO
OH
OH
NH
NH2
(21)

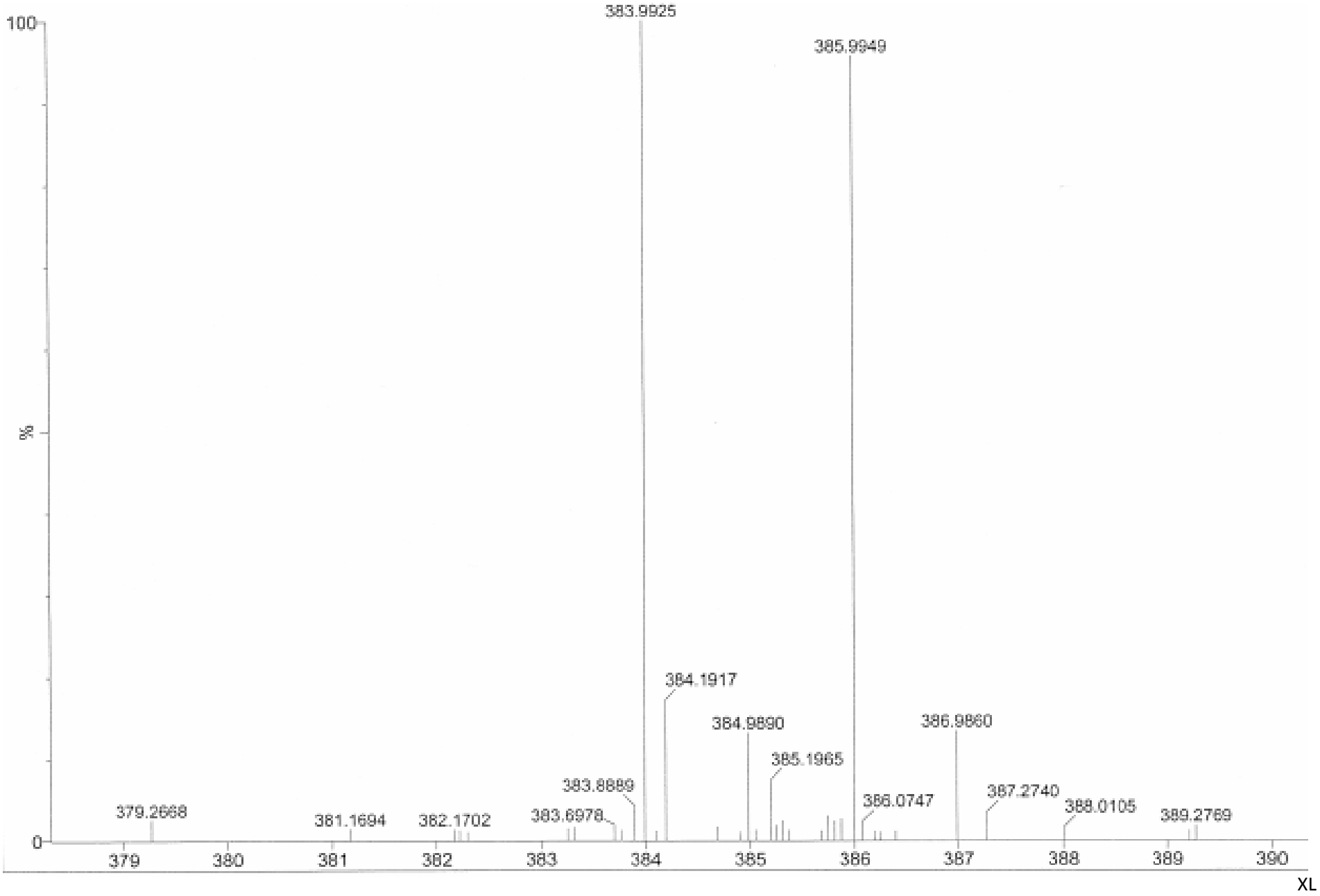
100
%
0
383.9925
385.9949
384.1917
384.9890
386.9860
385.1965
383.8889
387.2740
386.0747
388.0105
379.2668
381.1694
382.1702
383.6978
389.2769
379
380
381
382
383
384
385
386
387
388
389
390
XL